NELSON MANDELA UNIVERSITY

DEVELOPMENT AND CHARACTERISATION OF MICONAZOLE NITRATE LOADED SOLID LIPID NANOPARTICLES FOR INCORPORATION INTO A VAGINAL MUCOADHESIVE SYSTEM

BY

WIMANA ALEXIS GWIMO

SUBMITTED IN FULFILMENT OF THE REQUIREMENTS
FOR THE DEGREE OF

MASTER OF SCIENCE (General Health Sciences)

IN THE

FACULTY OF HEALTH SCIENCES

AT THE

NELSON MANDELA UNIVERSITY

APRIL 2019

SUPERVISOR: DR. GARETH KILIAN
CO-SUPERVISOR: MR. YAKUB ESMAIL KADERNANI

NELSON MANDELA UNIVERSITY

DECLARATION

NAME: Wimana Alexis Gwimo

STUDENT NUMBER: 212243314

QUALIFICATION: MASTER OF SCIENCE (General Health Sciences)

TITLE OF PROJECT: DEVELOPMENT AND CHARACTERISATION OF MICONAZOLE NITRATE LOADED SOLID LIPID NANOPARTICLES FOR INCORPORATION INTO A VAGINAL MUCOADHESIVE SYSTEM

In accordance with Rule G5.6.3, I hereby declare that the above-mentioned thesis is my own work and that it has not previously been submitted for assessment to another University or for another qualification.

…WA Gwimo……..

SIGNATURE

12/03/2019

……..

DATE

DEDICATION

This dissertation is dedicated to my family. Thank you for being my pillar of support, and for all your love, patience and guidance.

ACKNOWLEDGEMENTS

I would like to express my sincerest gratitude to the following people and institutions for their unwavering support:

- My supervisors, Dr Gareth Kilian and Mr Yakub Kadernani, thank you for your guidance, advice, input and patience.
- My parents, Alexis and Leah for all your love, sacrifice and patience.
- My sisters Nancy, Shimwe and Phoebe, thank you for being my biggest supporters. Your love and encouragement kept me going.
- My partner Hyacinthe, thank you for being a voice of reason and for your endless motivation.
- My friend, Nancy, thank you for walking alongside me on what seemed like a never-ending journey.
- My support system, Marcellah, Jaret and all my other friends. Thank you for the prayers and late night motivation.
- My fellow postgraduate students for the unforgettable times in the laboratory, constant motivation and advice.
- The staff members of the Department of Pharmacy, especially Mrs Jean van Jaarsveld and Mrs Arista van Jaarsveld for assisting me in the laboratory and ensuring that my environment was conducive for working.
- Mr Lukhanyo Bolo from the Department of Chemistry, for sharing your knowledge and expertise.
- The Nelson Mandela University Centre for High Resolution Transmission Electron Microscopy, for the assistance with microscopy work.
- The National Research Foundation, Dorhmel Cunningham Scholarship and the Nelson Mandela University Postgraduate Research Scholarship for their steadfast financial support.
- To the Almighty, it is by your love and strength that this work was achieved.

ABSTRACT

Purpose: Vulvovaginal candidiasis (VVC) is the second most common cause of vaginitis, affecting 75% of women of sexual maturity. The prescribed first line treatment involves the use of locally-acting imidazole creams. These conventional dosage forms possess limitations, such as leakage, messiness and low residence time at the site of application; all which promote poor patient adherence to pharmacotherapy. Poor adherence is then attributed to increased incidence of VVC reoccurrence and the emergence of *Candida* strains. It was, therefore, speculated that through the use of novel drug delivery systems (NDDS), the pharmacokinetic and antimicrobial characteristics of a model antifungal drug (miconazole nitrate [MNZ]) could be improved.

Primary aim: To develop, optimise and characterise a mucoadhesive hydrogel incorporated with MNZ loaded solid lipid nanoparticles (MNZ-SLNs) for the intended treatment of VVC.

Methodology: This study was conducted in three phases, *viz.* pre-formulation studies, development, optimisation and characterisation of MNZ-SLNs, and the development and characterisation of MNZ-SLN-loaded thermoresponsive hydrogel.

Results: An alternative method for the quantification of MNZ was developed through the use of an octyl stationary phase. The method was deemed suitable for its intended use with a linear equation of y = 811214x + 67958 and a respective limit of quantitation (LoQ) and detection of 0.015 mg/ml and 0.052 mg/ml. Differential scanning calorimetry (DSC) studies suggested that cholesterol showed great promise of facilitating high drug entrapment efficiency (EE). MNZ-SLNs were prepared by means of a novel melt-emulsification sonication and low temperature solidification method and optimised statistically by a 13-run-two-factor central composite rotatable design (CCRD). The predicted optimisation parameters were 4% m/v lipid concentration and 260.94 sonication time. Optimal MNZ-SLN formulations were prepared and characterised by means of photon correlation spectroscopy (PCS), transmission electron microscopy (TEM) and centrifugation. PCS revealed uniform particles with a narrow polydispersity index (PDI) and a mean hydrodynamic diameter (z-avg.) of 73.03 nm and zeta potential (ZP) of

38.43 mV. Percent EE was calculated via an indirect method as 75.24%. Furthermore, the MNZ -SLNs were incorporated into a mucoadhesive thermo-responsive hydrogel with a sol-gel transition temperature of 33.33 ± 2.82 °C. *In vitro* drug release testing (IVDRT) was undertaken with the aid of a Franz diffusion vertical cell (FDVC) apparatus. A % cumulative drug release of 27.94% and 15.87% was obtained for MNZ- SLNs and MNZ-SLN hydrogels, respectively, after eight hours. The resultant data was fitted into various kinetic models with the aid of DDSolver™ (Microsoft Excel® add-ins, 2016) to evaluate which model attained the highest correlation co-efficient (r^2). Both formulations attained high r^2 of 0.9941 and 0.9945, respectively, with the Korsmeyer- Peppas mathematical model. A high diffusional exponent (*n*) of >1 was observed, suggesting a super case II drug release mechanism. Finally, a modified Kirby-Bauer disc diffusion assay was used for ascertaining *Candida albicans* susceptibility to the developed formulations. Controls in the form of unloaded preparations and a commercially available cream were used. MNZ-SLNs and MNZ-hydrogel demonstrated superior antifungal activity to the commercially available cream.

Conclusion: These results indicate that the developed MNZ-SLNloaded hydrogel formulation with localised thermo-responsive effect may be a promising carrier for intravaginal delivery of MNZ in the treatment of VVC.

Keywords: Vulvovaginal Candidiasis (VVC), Solid lipid nanoparticles (SLN), Miconazole nitrate (MNZ), Mucoadhesive hydrogel, Controlled drug release, Thermoresponsive polymers, High performance liquid chromatography (HPLC), Central composite rotatable design (CCRD).

TABLE OF CONTENTS

CHAPTER 3

METHODOLOGY

CHAPTER 4

RESULTS AND DISCUSSIONS

LIST OF APPENDICES

LIST OF EQUATIONS

LIST OF FIGURES

LIST OF TABLES

LIST OF ABBREVIATIONS

µm:	micrometers
2D:	Two-dimensional
3D:	Three-dimensional
AIDS:	Acquired immunodeficiency syndrome
ANOVA:	Analysis of Variance
API:	Active Pharmaceutical Ingredient
AST:	Antimicrobial Susceptibility Testing
BCS:	Biopharmaceutics Classification System
BP:	British Pharmacopoeia
BPC:	British Pharmaceutical Codex
CCD:	Central Composite Design
CCS:	Colloidal carrier system
CFU:	Colony forming units
CI:	Confidence Interval
DoE:	Design of Experiments
DoH:	Department of Health
DSC:	Differential Scanning Calorimetry
FDA:	Food and Drug Administration
HIV:	Human immunodeficiency virus
HPLC:	High Performance Liquid Chromatography
HPMC:	Hydroxypropyl Methylcellulose
ICH:	International Conference on Harmonisation
IPI:	Inactive Pharmaceutical Ingredient
LOD:	Limit of Detection
LOQ:	Limit of Quantitation

mg:	milligrams
ml:	millilitres
MNZ:	Miconazole nitrate
nm:	nanometre
NDDS:	Novel drug delivery systems
NPI:	Non-pharmacological interventions
rpm:	rotations per minute
PDA:	Photodiode array
PCS:	Photon correlation spectroscopy
RCT:	Randomised control trials
RSD:	Relative Standard Deviation
RSM:	Response Surface Methodology
SD:	Standard Deviation
SLNs:	Solid lipid nanoparticles
spp:	Species
TLC:	Thin Layer Chromatography
$t_{½}$:	half-life
USP:	United States Pharmacopeia
UV:	Ultraviolet
VVC:	Vulvovaginal candidiasis
WHO:	World Health Organisation

CHAPTER 1

INTRODUCTION

1.1 BACKGROUND

Vulvovaginal candidiasis (VVC), commonly known as vaginal thrush, is an infection characterised by the overgrowth of *Candida* species on the vaginal mucosa (White and Vanthuyne, 2006). It is the second most common cause of vaginitis, following bacterial vaginosis. VVC affects approximately 70 to 75% of women of child-bearing age, half of which will experience multiple episodes of infection in their lifetime (Emeribe *et al.,* 2015; Nelson *et al.,* 2013). The highest prevalence of VVC is observed in women of sexual maturity between the ages of 20 to 40 years (Rathod *et al.,* 2012). Despite extensive research into the prevalence, aetiology and treatment of VVC, a global rise in the frequency of opportunistic infections has been observed in the past decade. Most notably, the growing trend in azole-resistant candidiasis and the alteration of pathogenic fungi, both of which exacerbate the VVC pandemic (Singh, 2001). Furthermore, *Candida* species account for 96% of all opportunistic mycoses (Bondaryk *et al.,* 2013). Due to *Candida* species being a vital cause of morbidity, superficial candidiasis of the mucosa is a major source of pain, irritation and disruption that, consequently, lowers a patient's quality of life (Adolfsson *et al.,* 2016). This serves as a strong motivation for the development of better treatment options.

Imidazole antifungals are a pharmacological class of antimycotic agents that have been formulated into locally-acting dosage forms. The World Health Organisation (WHO) (2017) and the South African National Department of Health (SANDoH) (2017) have approved the use of intravaginal imidazole creams, alone, as standard first line treatment regimens for VVC. When used correctly, imidazole creams demonstrate sufficient efficacy for the treatment of VVC. However, shortcomings, such as brief residence time at the site of infection and frequent need for application, render them impractical. Moreover, the lengthy treatment period of VVC accompanied with impractical pharmacotherapy promote a decline in patients' treatment adherence (Powell, 2010).

To mitigate such shortcomings and adherence failure, two key parameters for improvement could be to better the absorption of the active pharmaceutical ingredient

(API) at the site of infection and prolong drug release, thereby improving pharmacotherapy and subsequent treatment adherence. The availability of a mucosal formulation that combines controlled drug release and mucoadhesive characteristics is desirable (Nalungwe and Kilian, 2016).

Drug absorption is an important pharmacokinetic parameter that is guided by the physicochemical properties of the drug in question, the route of administration and the biological environment of the target site. For efficient drug delivery, the API must be absorbed at the site of application (Chillistone and Hardman, 2017). For systemically-acting dosage forms, the drug should ideally be absorbed consistently and completely at the site of application. In contrast, drugs intended for localised activity (i.e. the imidazole creams) should have minimal systemic absorption in order to prevent unwanted systemic exposure and adverse effects (Gerk *et al.,* 2016). Similar to other mucosal delivery routes, drug permeation across the vaginal membrane occurs through various mechanisms, such as (a) cell diffusion guided by a concentration gradient, (b) receptor-mediated transport and (c) diffusion across a tight junction of cells (Mirza *et al*., 2016). This varied delivery is due to the vaginal epithelium, which is about 200 to 300 µm thick and is protected by a thin fluid of film made up mixture of several biological components and enzymes. This fluid film plays a key role in drug absorption and dilution, as well as the rapid removal of dosage forms from the vagina (Ensign *et al.,* 2013). In addition, drug absorption from vaginal dosage forms is governed by the dissolution of the drug in the vaginal lumen and subsequent membrane penetration (Sahoo *et al.,* 2013). Successful drug delivery via the vagina remains a challenge owing to the poor absorption across the vaginal epithelium (Hussain and Ahsan, 2005).

Another approach for delivery may be to utilise nanotechnology. Nanotechnology is a multidisciplinary scientific field, applying engineering and manufacturing principles at a molecular level. By introducing nanotechnology to medicine, formulations have been created to mimic, alter or improve biological processes (Saini *et al.,* 2010). Innovations in pharmaceutics have led to the development of new formulations of existing drugs that are more beneficial to patients. Practical applications of nanotechnology in medicine include recent developments in dermatology, tissue engineering, biological assays and cancer therapy to improve the pharmacokinetic parameters of existing drug candidates (Nikalje, 2015). Novel approaches, such as nanoparticulate delivery systems, have been on the forefront of pharmaceutical research. And due to their small

size and large surface area, these drug delivery systems show improved solubility and enhanced bio-availability (Gunasekaran *et al.,* 2014). For example, it has been reported that particles in the size range of 100 nm demonstrated a 2.5-fold increased uptake at the site of absorption compared to 1 µm diameter particles, and a six-fold increased uptake than particles of 10 µm diameter (Desai *et al*., 1997; Rizvi and Saleh, 2018). This fact served as motivation for this study to investigate nanoparticulate drug delivery for their potential to improve drug absorption of imidazole antifungals through the vaginal mucosa.

However, novel approaches to drug delivery extend far beyond nanotechnology. Hence, the potential use of bioadhesive polymers to provide controlled release (CR) was also investigated for the purposes of this study. Mucoadhesive drug delivery systems are one of the most studied novel delivery systems. Numerous polymers demonstrate characteristics of mucoadhesion and have been employed in the formulation of conventional and novel drug delivery systems (NDDS) (Brahmbhatt, 2017). These formulations not only show an increase in local therapeutic activity but also in the residence time of the dosage form at the site of application (Kumar *et al.,* 2013); all of which would be beneficial in improving the current treatment option of VVC.

1.2 PROBLEM STATEMENT

The prescribed first line treatment regimen of VVC involves the use of a locally-acting imidazole cream (WHO, 2017; SANDoH, 2017). Imidazole antifungals represent one of two main classes of antifungal azole derivatives. However, the majority of these drugs are limited in their clinical use by their adverse effect profile, solubility, spectrum of activity and potency (Fromtling, 1988). Miconazole nitrate (MNZ) and clotrimazole are examples of a commonly used imidazole antifungals for localised VVC treatment (Johnson, 2018). The clinical efficacy of these two drugs is comparable, with no distinction in their curative or reoccurrence rates (Groll *et al.,* 1998; Leberhz *et al.*, 1983). The recommended directions for use state that the cream should be applied intravaginally at night, or, if needed, twice daily. The duration of treatment, however, varies from seven to 14 days, depending on the severity of the disease and the strength of the dosage form (Rossiter, 2017). Higher strengths require shorter durations, but the contrary is true for lower strength dosage forms (Centres for Disease Control and Prevention, 2015). Shorter durations of treatment are also not ideal, as they are

associated with less clinical efficacy and a higher incidence of reoccurrence when compared to longer treatment periods of seven to 14 days (Young and Jewell, 2001).

Furthermore, conventional vaginal drug delivery systems possess limitations, such as leakage, messiness and low residence time at the site of application. Current drug duration, dosage and delivery tend to promote poor patient compliance to pharmacotherapy (Bhat and Shivakumar, 2010). In addition, Jin *et al.,* (2008) stipulates that stopping pharmacotherapy too soon or decreasing dosing frequency can be a type of non-compliance that hinders favourable therapeutic outcomes. These two types of non-compliant behaviour are often observed in women undergoing treatment for VVC with locally-acting agents (Dobaria *et al.,* 2007). The unfortunate consequences of poor compliance include the increased incidence of VVC reoccurrence, emergence of resistant *Candida* strains and sub-therapeutic clinical outcomes that warrant the use of systemic antifungal therapy (Powell, 2010). The use of systemic therapy is discouraged due to its strong association with a greater side-effect profile and increased possibility of drug-to-drug interactions (Faro, 1994).

It was, therefore, speculated in this study that *in vitro* drug release and antimicrobial characteristics of locally-acting vaginal formulations could be improved through the use of NDDS. It was hypothesised that through the introduction of a thermoresponsive and mucoadhesive rate regulating polymer(s), the residence time of the dosage form within the vaginal tract could be prolonged. In addition, the study attempted to present that the reduction of the API particle size by means of a bio-friendly solid lipid nanoparticles (SLNs) could improve the absorption of the drug at the target site. This study, therefore, focussed on the development and characterisation of a MNZ formulation, which possesses poor solubility characteristics, into nanosized colloidal carrier systems (CCS) that allow for improved solubility and controlled drug release of MNZ. The study then further incorporated the carrier system into a thermoresponsive bioadhesive system in order to extend the drug residence time at the site of application. All of this was in an effort to enhance the absorption of MNZ at the target site and prolong its drug release, thereby, consequently, reducing the need for frequent applications.

1.3 AIM AND OBJECTIVES

The aim of this study was to develop, optimise and characterise a mucoadhesive hydrogel incorporated with MNZ loaded solid lipid nanoparticles (MNZ-SLNs) for the intended treatment of VVC.

Based on this aim, the following objectives were defined:

1. To conduct pre-formulation studies on MNZ by means of high performance liquid chromatography (HPLC) and differential scanning calorimetry (DSC);
2. To develop and optimise MNZ-SLNs by means of high-speed ultrasonication and response surface methodology (RSM);
3. To characterise the developed MNZ-SLNs by determining particle size (z-avg.), zeta potential (ZP), polydispersity index (PDI), stability and entrapment efficiency (%EE);
4. To develop a mucoadhesive hydrogel incorporated with MNZ-SLNs by means of a cold mechanical method;
5. To characterise the formulated hydrogel by defining its organoleptic properties, rheology and *in vitro* drug release rate; and
6. To determine the *in vitro* efficacy of the MNZ-SLN loaded hydrogel against *Candida albicans* by means of a modified Kirby-Bauer disc diffusion assay.

CHAPTER 2

LITERATURE REVIEW

2.1 INTRODUCTION

VVC affects 70 to 75% of the total global female population, and South Africa is no exception (Denning *et al.,* 2018; Govind, 2016). Of those affected, up to 50% will experience multiple episodes of infection in their lifetime (Rathod and Buffler, 2014). Treatment factors, such as lengthy treatment duration and frequent need for application have contributed significantly to the lack of patient adherence to the current prescribed pharmacotherapy (Bhat and Shivakumar, 2010; Dobaria *et al.,* 2007). It is, therefore, imperative to make improvements to the current treatment options in order to offer dosage forms with more favourable dosing regimens and clinical outcomes.

In this chapter, the aetiology and treatment of VVC and the use of NDDS (such as SLNs and mucoadhesive systems) for the improvement of drug delivery are discussed.

2.2 VULVOVAGINAL CANDIDIASIS (VVC)

VVC, more commonly known as vulvovaginitis or vaginal thrush, is caused by an overgrowth of *Candida* on the vaginal mucosa. The species, *Candida albicans,* accounts for 80 to 92% of all symptomatic VVC infections (Dresser and Brown, 2014). This disease is characterised by a thick 'cottage cheese'-like discharge, severe pruritus, swelling and redness of the vulvar that is accompanied by an acidic vaginal pH of less than 4.5 (Bitew and Abebaw, 2018).

2.2.1 Classification and pathophysiology

Candida forms part of the normal vaginal microflora, along with other microorganisms, in a controlled balance of healthy, non-symptomatic women. VVC is then brought about due to an imbalance between the colonising microflora and yeasts, resulting in the excessive proliferation and pathogenicity of *Candida* (Zeng *et al.,* 2018).

VVC begins with the mucosal surface colonisation by *Candida spp*., whereby surface molecules permit adherence of yeast to biological structures *viz*. human cells, proteases and phospholipids (Johal *et al.,* 2016). These surface molecules lead to the penetration and damage of cell envelopes that allow for the colonisation of *Candida*.

Candida spp. contain virulence factors that contribute to its disease causing ability. Moreover, an additional virulence factor, known as phenotypic switching, allows for the yeast to convert to its hyphal form, thus promoting pathogenicity and endorsing of resistant traits (Hildago and Vazquez, 2018). *Candida albicans* is the most common pathogen, followed by *Candida glabrata*, which is isolated in six to 16% of all cases (Turner and Butler, 2014). Figure 2.1 illustrates the pathophysiology of VVC.

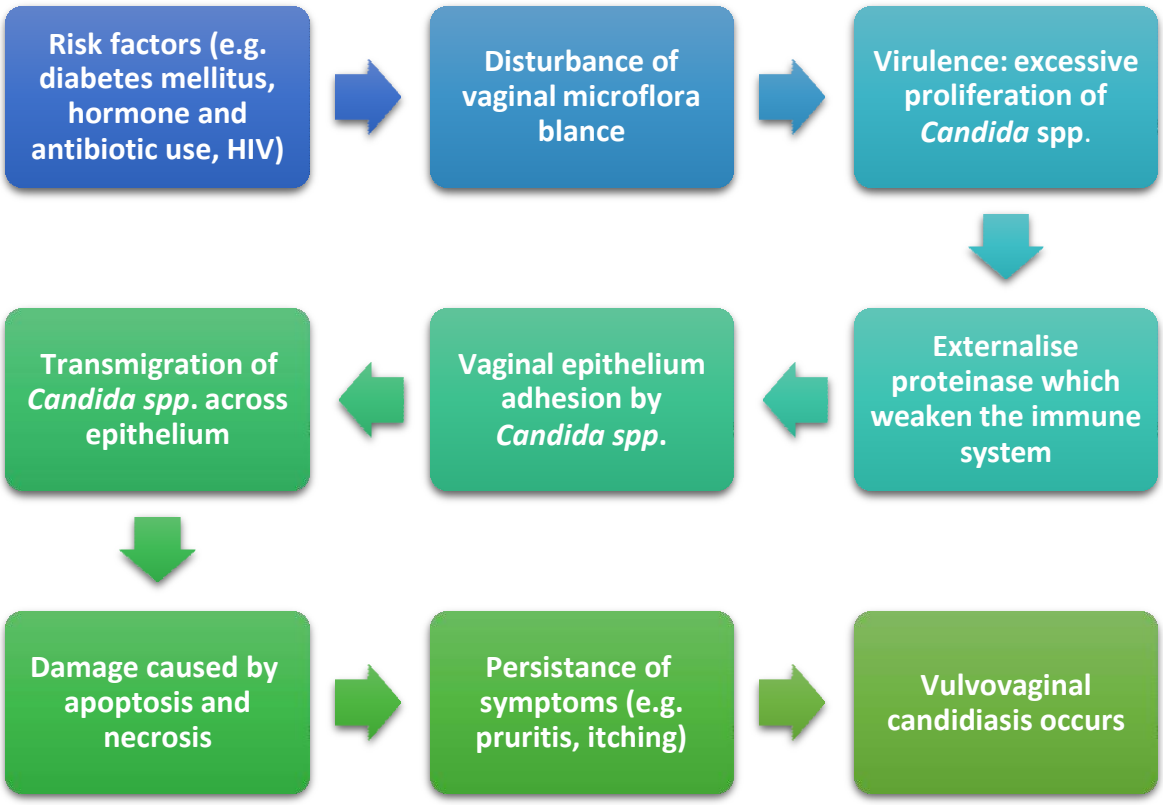

Figure 2.1: Pathophysiology of vulvovaginal candidiasis (VVC) (adapted from Johal *et al.*, 2016)

Symptomatic VVC infections are classified as 'complicated' or 'uncomplicated', depending on the clinical presentation, host factors, microbiology, response to pharmacotherapy and/or the severity or complexity of the infection (Centres for Disease Control and Prevention, 2015). Uncomplicated infections include sporadic and infrequent *Candida albicans* infections in non-pregnant women. Conversely, complicated infections encompass all chronic and recurrent infections (Owen and Clenney, 2004).

It is imperative that a healthcare professional makes a clear distinction between the various types of VVC infections in order to facilitate appropriate disease management strategies. Uncomplicated VVC is characterised by mild to moderate symptoms, visible hyphae or pseudo-hyphae under microscopic investigations and fewer than four episodes of infection in a year (Sobel, 2007). Complicated infections are characterised by moderate to severe symptoms, the visibility of budding yeast under microscopic examination, four or more episodes of infection in one year and the presence of adverse host factors, such as diabetes mellitus, pregnancy and immunosuppression (Rossiter, 2017). In addition, multitudes of non-*albicans* organisms are identified in complicated infections (Hainer and Gibson, 2011).

2.2.2 Epidemiology

Global statistics indicate that about 70 to 75% of all immunocompetent women will experience at least one episode of infection during their lifetime (Emeribe *et al.,* 2015). The highest rate of infection is observed in females of sexual maturity, between the ages of 20 to 40 years. Of this age group, nearly half will experience multiple episodes (Sobel, 2007; Rathod and Buffler, 2014).

Moreover, the incidence of infection in women of African origin compared to other ethnic groups is significantly higher (Sobel, 2017). However, updated and reliable data on the prevalence of VVC infections in South Africa is almost non-existent (Apalata *et al.,* 2014; Bongomin *et al.,* 2017). This can be attributed to the fact that VVC is not a notifiable disease and, therefore, all statistics and estimations are dependent on self-reported cases. Furthermore, these statistics are based on patient recollection or physician diagnoses (Sobel *et al.,* 1998). It should be noted that 50% of all cases may be mistaken for another vaginal condition, which, without microscopic examination, may deem the diagnosis inconclusive (Sobel *et al.,* 1998).

Factors, such as prolonged antimicrobial or hormonal therapy, pregnancy, HIV and AIDS infection, diabetes mellitus or any other immunocompromised status can contribute to the increased observance of VVC. These factors do so through different mechanisms, such as promoting biochemical changes in the vaginal tract and, consequently, increasing the likelihood of infection and re-infection (Sobel, 2017)

2.2.3 Diagnosis and treatment

Many treatment options are available to patients, but aspects like cost, availability, preference, tolerance and allergies all play a role in the selection of treatment for each individual patient (Nurbhai *et al.,* 2009; Rossiter, 2016). This section of the study focusses on the current pharmacological and non-pharmacological therapies available for the treatment of complicated and uncomplicated VVC infection. Furthermore, the limitations of these treatment options are discussed.

2.2.3.1 Pharmacological treatment options

Pharmacotherapy is the treatment of disease by the administration of drugs (Sanii *et al.,* 2016). For the purpose of this discussion, the current pharmacological treatment options have been divided into two major classes, namely systemic and locally-acting antifungals. Table 2.1 summarises the systemic pharmacotherapies available for the treatment of VVC.

Table 2.1: Current systemic pharmacotherapies for vulvovaginal candidiasis (VVC) (adapted from Rossiter, 2016; Krapf, 2018).

Active ingredient	Strength and dose	Comments
Ketoconazole	400 mg, orally daily for five days	Pharmacological class: Imidazole Drug interactions accredited to cyto-chrome P450 inhibition. Least effective and most toxic systemic antifungal therapy.
Fluconazole	150 mg, single oral dose	Pharmacological class: Triazole Attributed to numerous drug-to-drug interactions. Most implicated in antimicrobial resistance. Teratogenic effects.
Itraconazole	200 mg, orally daily for three days	Pharmacological class: Triazole Drug interactions accredited to cyto-chrome 3A4 inhibition.

Azole antifungals represent a class of drugs used for the treatment of various Candida infections (Rossiter, 2016). Ketoconazole, an imidazole antifungal, demonstrates *in vitro* activity against numerous fungi species including *Candida* (Bisschop *et al.,* 1979). Ketoconazole was introduced in 1972 by Jansen Pharmaceutica Research Facilities and is currently still in use. Since then, slow but gradual progresses have led to further developments of newer azole derivatives *viz*. fluconazole and itraconazole. These developments display favourable pharmacological characteristics, such as decreased toxicity and improved clinical efficacy which limit the use of ketoconazole (Fromtling, 1988; Khoza *et al.,* 2017).

However, the use of systemic therapies is limited to complicated infections, with the exception of fluconazole. Longer treatment periods with fluconazole, for up to six months, are required for the management of complicated infections (Rossiter, 2016; Krapf, 2018). Although the literature suggests that the efficacy of systemic therapies is comparable to that of local treatments, locally-acting agents are still preferred (Faro, 1994).

Furthermore, systemic therapies show a greater potential for teratogenicity and drug-drug interactions with drugs, such as oral hypoglycaemic and contraceptive tablets (Rossiter, 2016). The prescriber is also compelled to expend great efforts to monitor the patient during such treatment. This not only deters healthcare professionals from performing other duties, but also places an added financial burden on the patient (Pappas *et al.,* 2004). Table 2.2 provides a summary of current locally-acting pharmacotherapies for complicated VVC.

Table 2.2: Current locally-acting therapies for complicated vulvovaginal candidiasis (VVC (adapted from Krapf, 2018; Rossiter, 2016).

Active ingredient	Dosage form	Route of administration and dose
Clotrimazole		Pharmacological class: Imidazole
100 mg	Tablet	One tablet inserted vaginally for six to 12 nights
10 mg/g	Cream	One applicator dose inserted vaginally for six to 12 nights, repeated twice a day if necessary.
Miconazole	Cream	Pharmacological class: imidazole
20 mg/g		One applicator dose inserted vaginally for seven nights. Prolonged treatment necessary for severe infections.
Nystatin	Tablet	Pharmacological class: Polyene antifungal
10 000 IU		One tablet inserted vaginally once or twice daily for two weeks.

Localised treatment for complicated VVC with imidazole antifungals requires shorter durations (± seven days) and is more effective but can be pricier than nystatin. Furthermore, nystatin is not absorbed systemically from the vaginal mucosa and its use is considered safe in pregnancy and lactation (Rossiter, 2016). As for miconazole and clotrimazole, their safety in pregnancy has not been established and they are only deemed acceptable for use in cases of infection that are not responsive to nystatin. For recurrent VVC, longer durations of 10 to 14 days of induction therapy with a topical agent is required; followed by fluconazole 150 mg weekly for six months (Pappas *et al.,* 2016). Current locally-acting pharmacotherapies for uncomplicated VVC are discussed in Table 2.3.

Table 2.3: Current locally-acting therapies for uncomplicated (VVC) (adapted from Krapf, 2018; Rossiter, 2016; Schneider *et al.,* 2018).

Active ingredient	Dosage form	Route of administration and dose
Butoconazole		Pharmacological class: Imidazole
2% m/m	Sustained release cream	One single-dose intravaginal application
2% m/m	Cream	One applicator dose inserted vaginally for three nights
Clotrimazole		Pharmacological class: imidazole.
500 mg	Tablet/cream	Single-dose vaginal application at night
10 mg	Tablet	Two tablets inserted vaginally for three nights
Econazole		Pharmacological class: imidazole
150 mg	Depot ovule	Single-dose vaginal insertion at night
150 mg	Ovule	One ovule inserted vaginally for three nights
1000 mg/100 g	Cream	One applicator dose inserted vaginally for 14 nights
Fenticonazole		Pharmacological class: Imidazole
200 mg	Ovule	One ovule inserted vaginally for three nights
600 mg	Ovule	Single-dose vaginal insertion at night
100 mg/5 g	Cream	One applicator dose inserted vaginally twice a day for three days
Miconazole		Pharmacological class: Imidazole
400 mg	Capsule	One capsule inserted vaginally for three nights, accompanied by a 20 mg/g cream for external use
Ticonazole		Pharmacological class: Imidazole
6.5% m/m	Ointment	Single-dose vaginal insertion at night
Terconazole		Pharmacological class: Imidazole derivative
0.4% m/m	Cream	One applicator dose inserted vaginally for seven nights
0.8% m/m	Cream	One applicator dose inserted vaginally for three nights

Table 2.3 Current locally-acting therapies for uncomplicated VVC (adapted from Krapf, 2018; Rossiter, 2016; Schneider *et al.,* 2018) (Continued)…

Active ingredient	Dosage form	Route of administration and dose
Methylrosanilinium chloride (Gentian violet)	Solution	Pharmacological class: miscellaneous anti-infective 0.5 to 1% v/v solution inserted vaginally by means of a tampon twice a day. Caution note: may stain clothing.
Povidone-iodine 100 mg/g 100 mg/mL	Gel Douche	Pharmacological class: miscellaneous anti-infective One applicator dose inserted vaginally for 14 nights Dilute 30 ml with 1 L of water (H_20) for daily douching
Diiodohydroxyquinoline 1-2%	Gel	Pharmacological class: Quinoline derivatives 4 ml inserted vaginally in the morning and evening for five days, then 2 ml inserted vaginally at night. Note: Available in combination with other anti-infectives

All agents in the imidazole group display equal clinical efficacy in the treatment of VVC caused by *Candida albicans* and other *Candida spp*. (Groll *et al.,* 1998). In addition to demonstrating activity against Gram-positive microbes, such as *Staphylococcus* and *Streptococcus spp*., cross-resistance amongst different agents of this class occurs (Khoza *et al.,* 2017). Agents with unrestricted antifungal and bacterial activities, such as gentian violet, may be employed as second-line agents following the failure or unavailability of conventional therapies. These alternative agents provide cheaper and efficacious means of treatment. Finally, semisolid preparations, such as creams and gels, are useful for the treatment of a *Candida vulvitis* and a sexual partner (Rossiter, 2016).

2.2.3.2 Non-pharmacological treatment options

Non-pharmacological interventions (NPI) are literature- and scientific-based non-invasive interventions for human health. They aim is to prevent, care and cure ailments.

They are not limited to products but encompass methods or programmes for their users (Nguyen *et al.,* 2016). It is beneficial for healthcare professionals to be aware of all treatment options available to patients, whether conventional or unconventional. The most commonly used NPI are summarised in Table 2.4.

Table 2.4: Non-Pharmacological interventions (NPIs) for VVC (adapted from Sobel and Sobel, 2018).

Ingredient	Dose	Therapeutic benefit	Comments
Lactobacillus capsules or yoghurt	Five to 10 billion colony forming units (CFUs) orally, daily	Maintenance of immunity and vaginal microflora	No supporting evidence on efficacy from randomised control trials (RCT)
Boric acid	600 mg capsule inserted vaginally for seven to 10 nights	Relief of symptoms in recurrent VVC	Intravaginal capsule may cause burning or itchy sensation upon insertion which promotes poor compliance
Douche	Douching with 1% v/v hydrogen peroxide and 1% v/v acetic acid solution twice a day	Cleansing of the vaginal tract	Irritation to the vaginal mucosa. Increased risk of pelvic inflammatory disease, endometriosis and ectopic pregnancy.
Tea tree oil	Three to five drops every one to four hours until symptoms are alleviated	Alleviation of symptoms and discomfort	No supporting evidence of efficacy from RCT
Garlic	Standard extract of 400 mg (or one clove) inserted vaginally two to three times a day	Possible antifungal and immune stimulating activity	No supporting evidence of efficacy from RCT. Possible drug-to-drug interactions (e.g. warfarin).

Lactobacillus supplementation (or probiotics) through oral consumption or topical application is the most commonly used NIP for the treatment of chronic VVC (Xie *et al.,* 2013). Although 40% of women use alternative products, such as probiotics and 7% will seek advice from a complementary and alternative health specialist, there is limited literature on the use and efficacy NIP for the aforementioned NPI of VVC

(Morgan *et al.,* 2009). In addition to the recommended therapies, a healthcare professional could further advise a patient on supplementary precautions to promote favourable therapeutic outcomes. Table 2.5 provides a brief summary of such examples.

Table 2.5: Supplementary precautions for vulvovaginal candidiasis (VVC) management (adapted from Powell, 2010)

Precaution	Comments
Avoid excess sweating, keep vaginal area dry	Moist environment promotes excessive *Candida* proliferation
Avoid sexual intercourse until symptoms have cleared and treatment has been completed	VVC is not considered to be a sexually transmitted disease (STD), however, asymptomatic *Candida* colonisation of male genitalia is four times more likely in sexual partners of infected females (Centres for Disease Control and Prevention, 2015) Antifungal creams interfere with the barrier method of contraception, and sexual activity can decrease the residence time of locally-acting treatments
Take showers instead of baths and use unscented feminine hygiene products	Scented soaps may upset the natural flora balance or pH of the vaginal milieu, thus causing irritation or exacerbation of symptoms
Wear cotton underwear and loose-fitting clothes	Allows for the evaporation of excess moisture. Tight-fitting clothes promote friction and maceration, thereby increasing local acidity

Lifestyle habits play a key role in the introduction of microbes to the vaginal area and the changing of the normal microflora therein. Such changes can promote the pathogenicity of *Candida*. (Zeng *et al.,* 2018). Therefore, by promoting good hygiene practices frequent or persistent infections are reduced (Parsapure *et al.,* 2016).

2.2.3.3 Limitations of current treatment options

Uncomplicated VVC is the only vaginitis infection for which over-the-counter (OTC) treatments are readily available, and which allows women the liberty to self-diagnose and treat their ailment. It is critical, therefore, that patients are able to make a clear distinction between VVC and other vaginal infections so that appropriate treatment is not delayed. Topical azole formulations are available OTC and have been shown to have up to 90% clinical efficacy for the treatment of uncomplicated infection. These

products are considered safe, even though some patients have complained about a burning sensation (Angotti *et al.,* 2007). Short-course or single-dose treatments are the preferred dosing regimen, since they promote patient compliance. However, these preparations are closely linked to the rise in incidences of non-*Candida albicans* infections and cross-resistance amongst azole antifungals (Faro *et al.,* 1997).

Factors, such as cost, length of treatment, dosage form, ease of use and convenience, play a significant role in product selection and adherence to pharmacotherapy (Rossiter, 2016). Ideally, vaginal creams should be used at night with a sanitary pad to aid with the absorption of any leakage. Furthermore, sufficient patient counselling on the correct use and cleaning of the applicator device should be given in order to promote good hygiene practices and correct dose measurements (Vail *et al.,* 2004). Other drawbacks of locally applied treatments include their short residence time at the site of infection and the frequent and lengthy treatment periods; all of which promote poor adherence to pharmacotherapy (Dobaria *et al.,* 2007).

Patients should also be alerted to the fact that oil-based formulations, such as creams, weaken latex condoms and diaphragms, subsequently reducing the efficacy of contraceptive device (Meyboom *et al.,* 1995). Furthermore, locally-acting tablets and ovules are a more attractive form of treatment because they are not limited to nocturnal use, since their potential for leakage is diminished. However, they do not provide the benefit of vulvar application in cases of severe pruritus; yet, they do exhibit a greater extent of systemic absorption. Therefore, their potential for drug-interactions should be monitored carefully (Ringdahl, 2000).

With the exception of fluconazole, oral therapy is reserved for complicated VVC with moderate to severe symptoms. As previously stated, systemic treatments are not preferred over local therapies owing to their close association with drug-drug interactions and adverse systemic effects (Faro 1994; Rossiter, 2016). Furthermore, itraconazole and ketoconazole inhibit cyto-chrome 3A4 and P450, respectively; hence their implication in numerous drug interactions. Apart from its teratogenic effects and unsolicited systemic side-effects, fluconazole is the most implicated agent in the emergence of resistant fungi strains (Kaplan *et al.,* 2015; Whaley *et al.,* 2017).

2.3 INTRAVAGINAL DRUG DELIVERY

The route of administration for drugs is the path wherein the drug enters the body (Verma *et al.,* 2010). The vagina, as a means of drug delivery, offers many benefits, such as easy access, self-administration, systemic and localised drug delivery and the avoidance of the first-pass hepatic metabolism. Moreover, its large surface area promotes the absorption of various locally-acting agents with minimal side-effects (Andrade *et al.,* 2014).

The intravaginal route of administration also possesses some drawbacks, such as its self-cleaning nature which, in turn, reduces the residence time of conventional dosage forms at the site of application. Other drawbacks can occur in relation to hormonal fluctuations resulting from menopause or menstruation which bring about changes in vaginal characteristics (Sahoo *et al.,* 2013). These changes have a direct effect on conditions, such as pH and fluid volumes, which then affect the rate and extent of drug absorption (Khan and Saha. 2015). Factors that affect drug delivery from the vaginal mucosa, such as its anatomy and physiology, and variations in dosage formulations are discussed in more detail later in this chapter.

2.3.1 Anatomy and physiology of the vagina

The human vagina is a fibromuscular tube that connects the uterus to the exterior. It forms part of the female reproductive system, along with the fallopian tubes, ovaries, uterus, vulva and mammary glands (Amati *et al.,* 2003). Figure 2.2 illustrates the anatomical structure and location of the vagina.

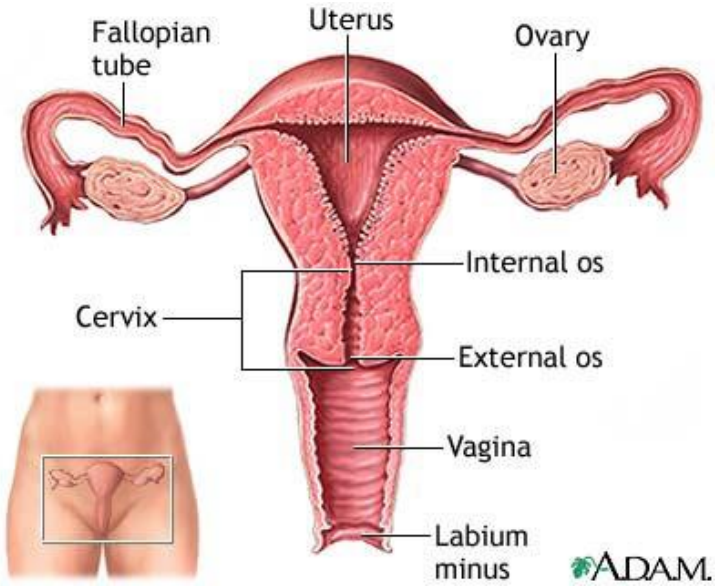

Figure 2.2: Anatomical structure of the human vagina (Microbewiki, 2016).

The vagina is made up of three distinct layers, namely the epithelial layer, *lamina propria* or *tunica adventia* and a muscular coat. The epithelial membrane layer lining the vaginal tract extends from the uterine cervix to the exterior genitalia and is covered with mucous. This membrane is comprised of stratified squamous cells that lie in sequential folds that increase its surface area. Although the surface lacks goblet cells and direct release of mucous, it is still considered a mucosal surface due to the fluid secreted by the cervix and uterus (Hussain and Hassan, 2005; Anderson *et al.,* 2014). Cervical and uterine secretions and transudation from blood vessels and desquamated vaginal cells and leucocytes constitute the vaginal mucous (Amati *et al.,* 2003).

Any alteration in the quantity, pH and constituents of fluid can affect the rate and extent of drug absorption. Similar to other mucosal surfaces, drug absorption via the vagina occurs transcellularly by means of concentration-dependent diffusion through cells; paracellularly by means of tight junctions; and via vesicularly- or receptor-mediated transport (Hussain and Ahsan, 2005). Moreover, the rate and extent of absorption is also influenced by factors like formulation type, vaginal physiology, menstrual cycle and patient age (Dodou, 2018).

2.3.2 Vaginal dosage forms

Conventional topical intravaginal systems have been used extensively to treat systemic and localised ailments. Ideally, intravaginal formulations should be non-toxic and non-irritating, and should possess wetting and emulsifying properties with adequate viscosity so as to avoid leakage. Mucoadhesive properties are also advantageous in

increasing the contact time between the formulation and site of application (Sahoo *et al.*, 2013). Table 2.6 presents examples of commonly used formulation systems intended for intravaginal delivery of various therapeutic agents.

Table 2.6: Formulation systems available for intravaginal drug delivery (adapted from Dodou, 2018).

Formulation type	Characteristics
Creams, gels, ointments	Semi-solid preparations utilised for localised or systemic drug delivery
Capsules	Single-dose, solid preparations with a smooth surface for localised or systemic drug delivery
Tablets	Single-dose, solid preparations with a smooth surface for localised or systemic drug delivery
Pessary	Single-dose, solid preparation for vaginal insertion
Foams, sprays	Drug and propellant contained as a solution or suspension under pressure
Suspensions, solutions, emulsions	Liquid preparations intended for localised drug delivery. Suspensions and emulsions require agitation prior to use, as phase separation and sedimentation can occur.
Films	Thin sheets for CR of localised or system-intravaginal drug release
Rings	Flexible circular system with drug contained in a polymer network
Medicated tampons	Single-dose solid preparations inserted in the vagina for a limited time and then removed

Based on the information presented in Table 2.6, there are a wide array of dosage forms available for intravaginal drug delivery. The variation in dosage formulations is to ensure accurate drug delivery, confer protection of the API, delivery of the API to the targeted site for optimal pharmacological action and to ensure the desired vehicle is used for insoluble drugs (Chatterjee *et al.,* 2008).

Solid formulation systems include tablets and pessaries. Pessaries are formulated to melt or dissolve upon vaginal insertion. The term ‘pessaries’ encompasses formulations, such as capsules and vaginal suppositories. They are spherical, conical or globular; weighing about 5 g (Dodou, 2018). Pessaries have been used extensively for the delivery of antimicrobial and contraceptive agents, and their benefits include cost-effective and easy manufacturing processes as well as accurate dose delivery upon administration (Punitha *et al.,* 2018). However, drawbacks of pessaries include their lack of symptomatic relief of pruritis which can contribute to low patient acceptability. Moreover, they are not ideal for highly lipophilic drugs, such as MNZ, which poses an issue for drug absorption at the site of infection (Rahman and Ahmed, 2016).

Douches are aqueous solutions administered vaginally for cleansing purposes. Regular douching is associated with increased susceptibility to pelvic inflammatory disease and is, therefore, discouraged (Martino and Vermund, 2002).

Vaginal rings are polymeric devices comprised of elastomeric polymers, such as silicone. They provide extended drug release and do not interfere with coitus; hence, they do not require frequent dosing or administration. A drawback of vaginal rings is, however, that they hold the potential for poor biotolerability of the elastomeric polymer (Punitha *et al.,* 2018).

Vaginal foams are a fairly new method of intravaginal drug delivery derived from the concept of vaginal rings. These formulations are used to deliver antimicrobial or anaesthetic medications. Most foams are non-irritant to the vaginal mucosa, as they are made from soft polyurethane (Dodou, 2018).

Vaginal tampons are traditional intravaginal formulations that have been approved by the food and drug administration (FDA) (Pollard, 2005). This feminine hygiene product is made up of soft material incorporated with the drug for vaginal insertion. This formulation facilitates the insertion of medicines without messiness and leakage. However, its drawbacks include low patient acceptability owing to its discomfort (Alexander *et al.,* 2004).

Vaginal films are a fairly new approach to vaginal drug delivery. They are thin sheets made up of polymeric materials that offer controlled drug release for localised or systemic action. Furthermore, they offer favourable organoleptic characteristics and homogenous drug delivery, thus making this product a good candidate for vaginal drug delivery (Machado *et al.,* 2013).

Finally, semi-solid preparations have been investigated extensively for vaginal drug delivery. Semi-solid formulations include the likes of creams, ointments and gels. Ointments and creams are comprised of a H_2O and oil phase, while gels are aqueous-based formulations (Chen *et al.,* 2016). These formulations are non-toxic and non-irritating, with high patient acceptability. The drawbacks of such products include messiness and leakage which promote discomfort. In addition to discomfort, leakage also results in non-uniform drug delivery (Bharat *et al.,* 2011).

The majority of vaginal formulations require a plastic insertion device to facilitate easy application and accurate dose delivery. If used incorrectly by a patient, optimal pharmacological benefits are not achieved (Dodou, 2018). Therefore, the main cause of therapeutic failure with topical agents is poor patient compliance (Cardot *et al.,* 2004). In order to address this issue, great interest has been shown in the pharmaceutical industry to make improvements in relation to this shortcoming. This study may aid the industry in this endeavour.

2.4 NOVEL APPROACHES TO INTRAVAGINAL DRUG DELIVERY

A growing interest in the use NDDS to overcome the limitation of conventional dosage forms has been observed in the pharmaceutical industry. The development of newer intravaginal drug delivery formulations is mainly driven by the need to increase choice and, thereby, compliance by the wider female population (Sawant and Khan, 2017). To achieve desirable bioadhesion, distribution, formulation retention within the vaginal tract and CR characteristics, novel approaches for intravaginal drug delivery have also been explored (Kenechukwu *et al.,* 2018).

Mucoadhesive drug delivery systems have been on the forefront of such pharmaceutical novel developments. Owing to their hydrating nature and good binding capacity to mucosal tissue for a considerable amount of time, these delivery systems

are investigated further in this research. This is because they offer an extended and predictable delivery rate of the API from the formulation, thus reducing the need for frequent application. Furthermore, a 25% reduction in the treatment time was reported for mucoadhesive formulations versus conventional treatments (Sahoo *et al.,* 2013).

Similarly, phase-transitioning polymers that respond to external stimuli, such as temperature and pH, are also drawing a lot of attention in pharmaceutical research. They can be formulated to undergo a sol-gel transition around a temperature range of interest. Furthermore, the combination of a mucoadhesive and phase-transitioning polymer allows for prolonged residence of the dosage form at the site of action (Baloglu *et al.,* 2009; Rencber *et al.,* 2016).

Effervescent vaginal tablets are also a recent development that allows for quick absorption of the API at the application site. They demonstrate a greater efficacy in antifungal delivery when compared to conventional solid formulations (Patel and Patel, 2010). Another distinct but equally exciting field of NDDS explored for intravaginal drug delivery is CCS. These systems include the likes of polymeric, micellar, liposomal and solid lipid nanoparticles. They focus on the improvement of API delivery and absorption at the application site through a reduction in particle size and targeted drug delivery (Mudshinge *et al.,* 2011).

The following factors should be taken into consideration when formulating any intravaginal formulation: (a) the maintenance of a desirable pH on the epithelial surface, (b) ease of application, considerable drug retention in the vaginal tract and (c) even drug distribution (Ibanga, 2012). Desirable formulation characteristics, such as compatibility with co-administered drugs, safety, efficacy, aesthetics, cost-effectiveness and acceptability by regulatory authorities promote patient use and compliance (Bharat *et al.,* 2011).

2.4.1 Colloidal carrier systems

CCS are particulate or vesicular formulations in the nanometre range size, ranging from 10 to 1000 nm (Mudshinge *et al.,* 2011; Sharma *et al.,* 2009). CCS were introduced to the pharmaceutical industry with the aim of improving the therapeutic index of many active compounds, either through the reduction of API's toxicity profile or through the improvement of its pharmacological efficacy (Tiwari *et al.,* 2012). CCS facilitate the protection, transportation and preservation of an API prior to delivering it

to the targeted site (Chashoo *et al.,* 2012).

There are many advantages of employing CCS in drug delivery, such as targeted delivery, the reduction of API size to facilitate better absorption and reduction in the amount of API required in various dosage forms; all of which minimise the potential for adverse effects and possible drug-drug interactions (Mudshinge *et al.,* 2011). Furthermore, CCS allow for the incorporation of compounds with poor aqueous solubility into particulate systems. These systems can then be formulated in a manner that facilitates sustained drug release, thereby reducing the dosing frequency and, consequently, promoting patient adherence (Gelperina *et al.,* 2005).

2.4.1.1 Comparison of colloidal carrier systems (CCSs)

CCS encompass a vast number of NDDS *viz*. nanoemulsions, mixed micelles and SLNs. Table 2.7 provides a brief summary of various CCS.

Table 2.7: Characteristics of various colloidal carrier systems (CCS)

Colloidal system	Size range	Characteristics	Applications
Non-ionic micelles	10 to 1000 nm	Biodegradable, complete API protection	Good candidate for sustained drug delivery. Passive or active drug delivery achieved with modifications.
Solid lipid nanoparti cles	50 to 1000 nm	Biocompatibility, biodegradable, sustained drug release	Provides good encapsulation of poor hydrophilic compounds
Nano-crystal quantum dots	2 to 9.5 nm	Semi-conducting material synthesised from II-IV and III-V column elements. Bright fluorescence with narrow emission and high photo-stability.	Long-term colour imaging of hepatic cells. DNA hybridisation, immunoassay, labelling of breast cancer cells.

Table 2.7: Characteristics of various colloidal carrier systems (CCS) (continued)

Colloidal system	Size range	Characteristics	Applications
Carbon nanotubes	0.5 to 3 nm (diameter) 20 to 1000 nm (length)	Possess incredible strength and distinctive electrical properties. Third allotropic crystalline form of carbon sheets as a single or multiple layer.	Carrier for peptide and gene delivery
Dendrimer	<10 nm	Highly branched, mono-dispersed polymer system produced through controlled polymerisation	Controlled and targeted delivery of bio-actives. Macrophage hepatic targeting.
Metallic nanoparticles	<100 nm	Gold/silver colloidal systems with high surface area	Drug/gene delivery, diagnostic assay, thermal ablation, enhancement of radiotherapy
Polymeric micelles	10 to 100 nm	Amphiphilic polymer micelles with high drug entrapment, payload and stability	Long circulatory, target specific delivery and diagnostics
Liposomes	50 to 100 nm	Phospholipid vesicles, biocompatibility and fair entrapment efficiency	Long circulatory, passive and active delivery of gene, peptides and other drug candidates
Iron oxide nanocrystals	4 to 5 nm with a hydrodynamic radius of 15 to 25 nm	Supraparamagnetism	Magnetic resonance imaging
Silica nanoparticles	10 nm to 50 µm	Coated by oligonucleotide and observed by florescence	Nucleic acid hybridisation Detection of DNA nanobiosensor

Based on the summary provided in Table 2.7, CCS are divided into two distinct groups, namely microparticulate and vesicular systems. Nanoparticulate systems include the likes of micelles, nanocapsules, magnetic and albumin microspheres, quantum dots and fullerenes. Vesicular systems include liposomes, niosomes, pharmacosomes, virosomes and immunoliposomes (Bhardwaj and Kumar, 2011).

Nanoparticulate systems comprise of synthetic or semi-synthetic polymers. They contain drugs embedded within a matrix or absorbed on the surface. Nanospheres are solid core spherical particulates, nanocapsules systems contain an API encapsulated within a central volume surrounded by an embryonic polymeric sheath and, finally, nanocrystals contain drugs that are encapsulated in a solution (Bhardwaj and Kumar, 2011). Some key advantages of nanoparticulate systems include their high stability and carrier capacity; their feasibility of variable routes of administration (ROA); and their incorporation of both hydrophilic and lipophilic drugs. In addition, they are designed to be able to facilitate controlled drug release from their matrices (Khadka *et al.,* 2014). In spite of these advantages, nanoparticulate systems possess some limitations, such as particle-particle aggregation, which makes physical handling difficult (Jawahar and Meyyanathan, 2012). The cytotoxicity of nanoparticulate systems or their degradation products remain a major concern for drug delivery in human and animal subjects (Tiwari *et al.,* 2012).

Vesicular CCS are highly ordered assemblies comprising of one or more concentric bilayers formed from the self-assembly of amphiphilic building blocks in the presence of H_20. They are particularly useful for targeted drug delivery due to their ability of localising drug activity at the site of action (Jain *et al.,* 2014). Vesicular CCS offer many advantages, such as the incorporation of lipophilic and hydrophilic drugs, the improvement of bio-availability of API at the targeted site, the prolonging of the circulation time of drugs in the body and the resolution of stability and issues of labile drugs (Jadhav *et al.,* 2011). Liposomes, in particular, have gained great interest in the past decade for targeted drug delivery. These lipid structures comprise of an aqueous compartment enclosed in a bilayer membrane (Hirai *et al.,* 2013). Yet, despite offering many advantages of vesicular CCS, liposomes also possess drawbacks, such as premature drug release, poor encapsulation efficiency of hydrophilic drugs and a short life span (Biju *et al.,* 2006). Improvements in biocompatibility, drug loading (DL) and release are a major concern for future research.

SLNs are novel carrier systems derived from liposomes and were introduced in 1991 for the delivery of cosmetic and pharmaceutical ingredients (Ekambaram *et al.,* 2011). They are spherical structures with a lipid core that solubilises lipophilic molecules (see Figure 2.2) (Ramteke *et al.,* 2012). Their long-term physical stability, biodegradability, protection of API and the absence of organic solvents in their formulation make them ideal pharmaceutical carriers. SLNs combine the benefits of various colloidal systems whilst avoiding their drawbacks (Swain and Babu, 2015); therefore, this study limits itself to the investigation of SLNs as potential drug carriers in facilitating favourable intravaginal drug delivery.

2.4.1.2 Solid lipid nanoparticles (SLNs)

SLNs comprise a solid lipid core matrix that is stabilised in an aqueous solution by emulsifiers (Lin *et al.,* 2017). Their generic structure is illustrated in Figure 2.3, where the core contains the API dispersed or dissolved in the lipid matrix. This matrix offers protection of APIs against chemical degradation whist providing sustained drug release. The hydrophobic portions of the surfactant layer are embedded into the lipid matrix and are responsible for the transportation of lipophilic and/or hydrophilic drugs or diagnostics (Bagul *et al.,* 2018).

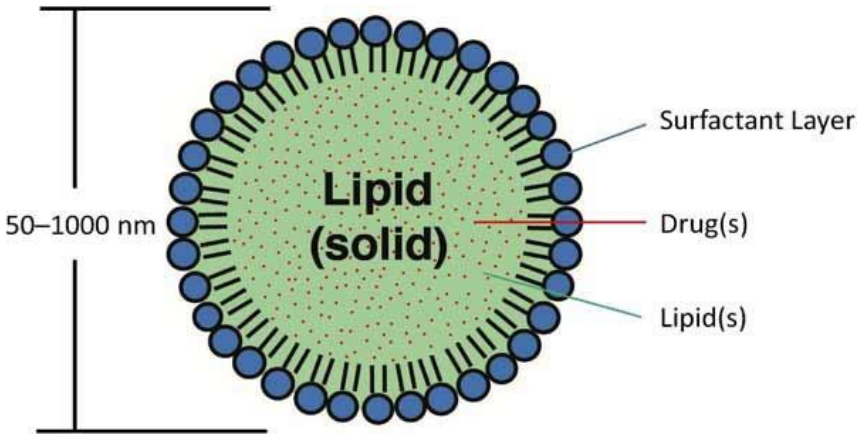

Figure 2.3: Generic structure of a solid lipid nanoparticle (SLN) (Khatak and Dureja, 2015).

SLNs utilise biodegradable lipids in their production that minimise the risk of toxicity to the mucosal tissue (Ekambaram *et al.,* 2011). They offer improved bio-availability of drugs that possess poor aqueous solubility and enhance the permeation of topically administered drugs (Shah *et al.,* 2007). The various production methods allow for possible scaling up at an industrial level, whilst simultaneously offering good stability and safety for intravaginal drug administration (Garud *et al.,* 2012). Drawbacks of this

delivery system include poor DL capacity, drug expulsion upon storage and high H_20 content (Schwarz *et al.,* 1994).

i. Constituents of solid lipid nanoparticles (SLNs)

The performance of an SLN formulation is highly influenced by its structure and composition (Shah *et al.,* 2015). Lipids, surfactants, co-surfactants and API account for the four basic materials used in the formulation of SLNs (Khatak and Dureja, 2015). Lipids are organic compounds that contain long-chain aliphatic hydrocarbons. These chains may be cyclic or acyclic, with an attached acid, alcohol or aldehyde derivative (Gigg, 2018). Table 2.8 illustrates some examples of commonly used lipids in the formulation of SLNs. The lipid materials are usually solid at room temperature, and are well-tolerated in physiological conditions (with the exception of cetyl palmitate). These selected lipids also possess low toxicity profiles and are biocompatible (Lin *et al.,* 2017). Based on their structural diversity, these lipids have been classified into fatty acids, alcohols, esters, triglycerides, partial glycerides and waxes (Shah *et al.,* 2015).

Table 2.8: Commonly used lipids in the formulation of solid lipid nanoparticles (SLNs) (adapted from Shah *et al.,* 2015).

Lipid group	Examples
Monoglycerides	Glyceryl monostearate
Triglycerides	Glyceryl tristearate, glyceryl palmitate, glyceryl trimyristate, glyceryl trioleate, medium chain triglycerides
Free fatty acids	Behenic acid, stearic acid, palmitic acid, myristic acid, oleic acid
Free fatty alcohols	Stearyl alcohol, cetyl alcohol, myristyl alcohol, lauryl alcohol
Waxes	Cetyl palmitate, beeswax, carnauba wax
Miscellaneous	Castor oil, hydrogenated castor oil, hydrogenated palm oil, cacao butter, goat fat, anhydrous milk fat
Mixtures	Glyceryl behenate, glyceryl palmitostearate, witepsol

Lipid compositions demonstrate the greatest effect on the overall quality of SLN formulation by influencing the API loading capacity, ZP and retardation of crystallisation processes (Pardeshi *et al.,* 2012). The solubility of the API candidate in the lipid matrix is pivotal, as it influences the drug encapsulation and loading efficiencies and,

consequently, the pharmacodynamics and pharmacokinetic parameters of the dosage form (Kasongo *et al.,* 2011).

Lipid polymorphisms are additional factors that affect the properties of an SLN formulation. The presence of multiple crystalline forms is beneficial in providing structural defects in which drugs molecules can be lodged (Schoenitz *et al.,* 2014). Complex mixtures of lipids are desirable, owing to variations in chain lengths which, in turn, produce less perfect crystals, thereby providing more space to accommodate drugs and decrease the likelihood of drug expulsion upon storage (Parhi and Suresh, 2010; Shah *et al.,* 2015).

Surface active agents, more commonly known as surfactants, are amphiphilic compounds that adsorb an interface in order to form orientated monolayers that aid in the reduction of surface tension between two immiscible media (Uner *et al.,* 2004). When a surfactant is placed in close contact with a polar medium (e.g. an aqueous solution) and a non-polar medium (e.g. a lipid), one section of the surfactant molecule will have an affinity for the non-polar medium and the other will orientate towards the polar component (Shi *et al.,* 2011).

SNLs can be categorised into three main groups, based on their respective charges (Naseri *et al.,* 2015; Shah *et al.,* 2015). For example, ionic surfactants are thought to impart electrostatic stability, whereas non-ionic surfactants infer steric repulsion stability. Similarly, amphoteric surfactants, such as phosphatidylcholines, possess both negatively- and positively-charged functional groups. They display features of cationic and anionic surfactant at high and low pH. Furthermore, non-ionic surfactants, such as poloxamer 470 or 188 are preferred for drug delivery, as they are less toxic and non-irritant than ionic surfactants (Uner *et al.,* 2004). They also do not alter the pH of a solution and they possess a higher critical micellar concentration (CMC), thus allowing the use of more surfactant in the SLN formulation without the risk of generating unwanted micelles (Shi *et al.,* 2011). A list of commonly used surfactants in the production of SLNs is provided in Table 2.9.

Table 2.9: Commonly used surfactants in the formulation of solid lipid nanoparticles (SLNs) (adapted from Shah *et al.*, 2015).

Surfactant group	Examples
Non-ionic	Polyoxyethylene (PEO) sorbitan fatty esters: polysorbate 20, 60, 80, 85
	PEO alkyl/aryl ethers: PEO(20)cetyl ether, polyexyethylene(20)isohecadecyl ether, polyethylene(20)oleyl ether, PEO(20)stearyl ether, tyloxapol
	Ethoxylated castor oils: Polyethylene glycol (PEG) 35, castor oil, PEG 40, hydrogenated castor oil
	Poloxamers: 188, 407
	Miscellaneous: PEO-glycerine monosterate, macrogol(15)hydroxystearate, PEG caprylic/capric triglycerides, polyglyceryl-3-methylglucose disterate
Anionic	Sodium dehydrocholate, sodium taurocholate, sodium glycocholate, sodium cholate, sodium lauryl sulphate
Cationic	Cetrimonium bromide, DOTAP, DPTMA, chlorhexidine salts, dimethyldiocta-decylammonium bromide
Amphoteric	L-α-phosphatidyl-choline, soya lecithin, egg lecithin
Co-surfactants	1-Butanol, low molecular weight PEG, diethylene glycol, monoethyl ether, propylene glycol, ethanol, sorbitan monostearate

Surfactants used in the preparation of SLN formulation play two distinct roles. Firstly, they disperse the lipid-melt in the aqueous phase during the production process. Secondly, they stabilise the particles in the dispersion upon cooling (Uner *et al.,* 2004). The selection of an ideal surfactant for a given formulation is dependent on the intended route of administration, effect on particle size and lipid modification, *in vivo* degradation of material and hydrophilic lipophilic balance (HLB) value of the surfactant. The combination of two or more surfactants is encouraged for promoting particle stability by preventing agglomeration more effectively (Mukherjee *et al.,* 2009, Shah *et al.,* 2015).

2.4.1.3 Preparation techniques of solid lipid nanoparticles (SLNs)

The preparation of SLNs commences with the selection of an appropriate lipid base and surfactant (emulsifier), followed by the selection of an appropriate method of production (Naseri *et al.,* 2015). Selecting a good method of production is critical for obtaining favourable formulation characteristics, such as particle size, scalability and stability (Mukherjee *et al.,* 2009). Various formulation techniques are discussed in this section.

High pressure homogenisation (HPH) is the most commonly used technique for SLN preparation (Yadav *et al.,* 2014). The mechanism of nanoparticle formation begins with pushing a coarse dispersion under high pressure (100 to 200 bars) through a micron size gap. The pressure causes rapid acceleration of the liquid, reaching speeds of greater than 1000 km/h and resulting in the breakdown of particles by shear cavitation forces (Kokardekar and Mody, 2011). This well-established technique may be conducted at elevated or lowered ambient temperature. Elevated temperatures are referred to as hot homogenisation, while lowered temperatures are referred to as cold homogenisation (Parhi and Suresh, 2012). Figure 2.4 illustrates the process of both hot and cold homogenisation techniques. Both of these processes work on the same concept of mixing drugs into the bulk of the lipids above their melting points.

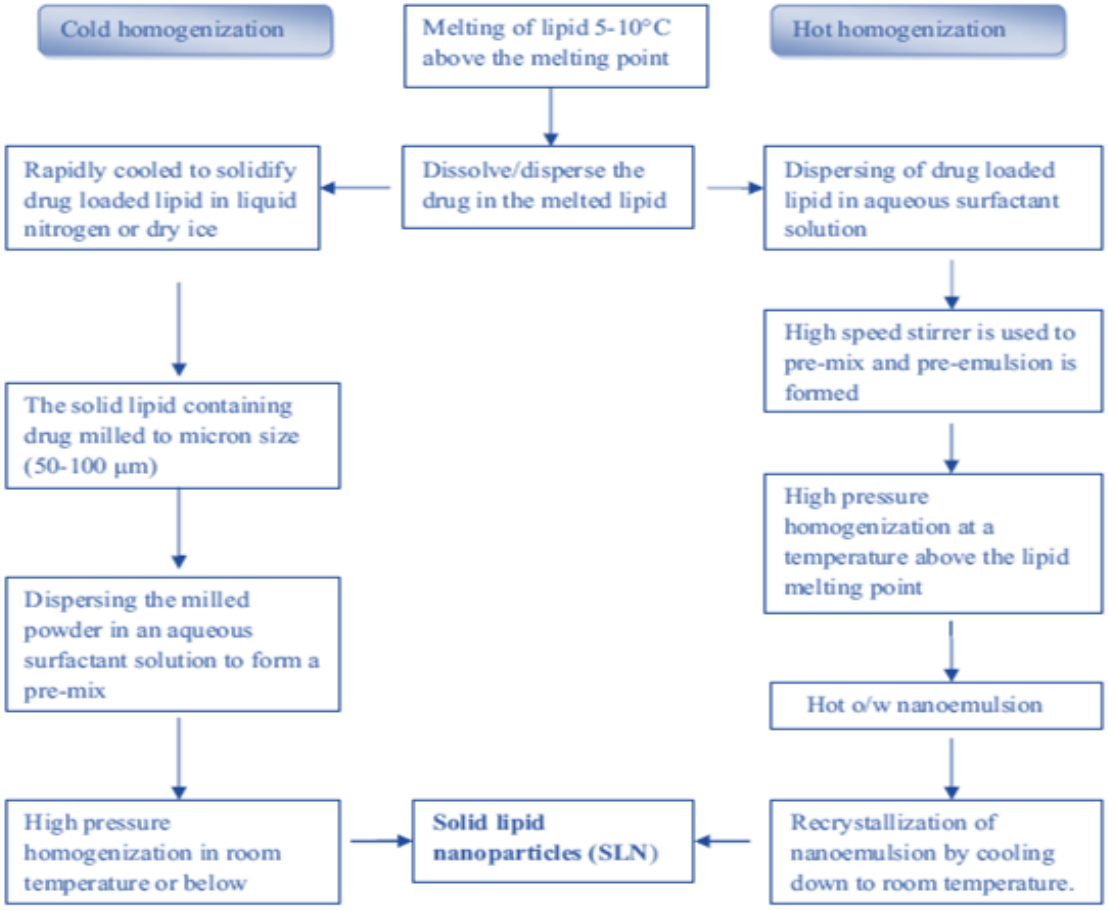

Figure 2.4: Schematic representation of high pressure homogenistaion (HPH) techniques for solid lipid nanoparticle (SLN) preparation (Parhi and Suresh, 2012).

High speed homogenisation (HSH) is a preparation technique employed in the preparation of SLNs by means of high speed stirring followed by sonication (Yadav *et al.,* 2014). High speed rates followed by ultrasound sonication are used to obtain a nanodispersion of melted lipids in a warm aqueous surfactant (Lason and Ogonowski, 2011). Figure 2.5 illustrates the formation of a solid lipid nanodispersion by means of high speed stirring and a bath sonication device. It should be noted that the energy input for the sonication step can be supplied through a bath or probe-tip ultrasonication (PUS) device. This high-energy input facilitates the breakdown of particles in the dispersion to nanosized particles (Ganesan and Narayanasamy, 2017).

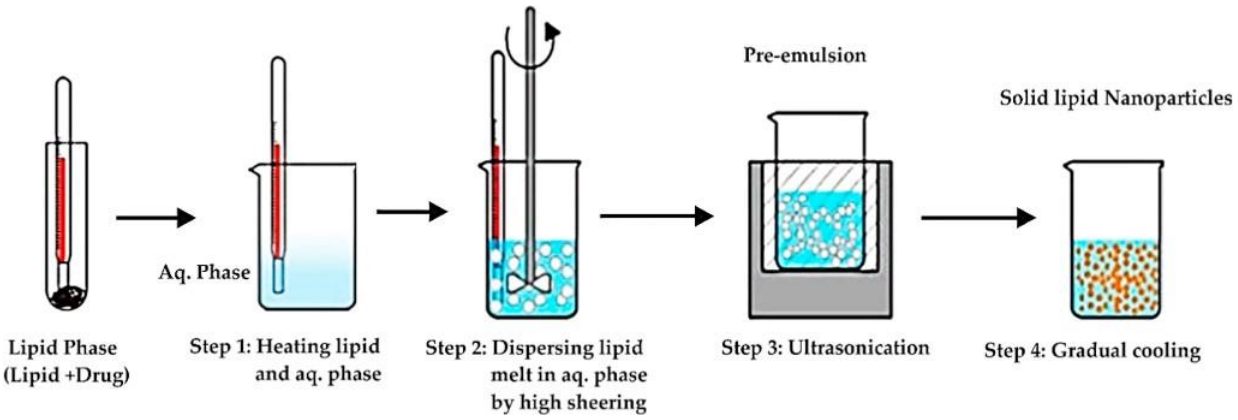

Figure 2.5: Schematic representation of High Speed Homogenisation (HSH) technique for solid lipid nanodispersion formation by means of a bath sonication device (Ganesan and Narayanasamy, 2017).

Solvent emulsification, also referred to as the solvent-emulsification-diffusion method, is a technique that involves the solubilisation of lipids in partially water-miscible solvents so as to yield an oil-in-water emulsion (o/w). The resultant emulsion is then passed through water under continuous stirring in order to solidify the lipid phase as a consequence of organic phase diffusion (Li *et al.,* 2017). Figure 2.6 provides a simple illustration of this preparatory technique.

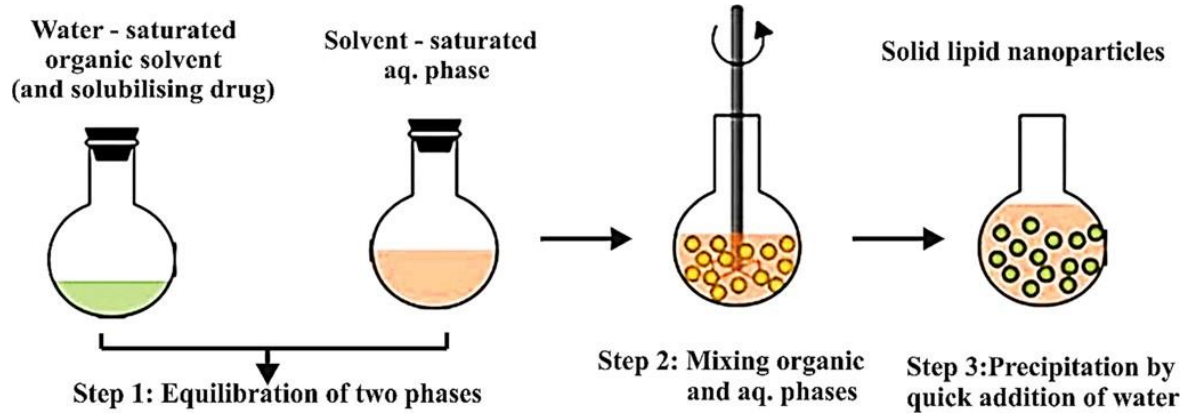

Figure 2.6: Schematic representation of solid lipid nanoparticle (SLN) preparation by solvent emulsification technique (Ganesan and Narayasamy, 2017).

The microemulsion technique is a low-energy input technique employed for the preparation of SLNs (see Figure 2.7). A hot micro-emulsion of lipids and surfactants is prepared by dispersing them in cold water (Mao *et al.,* 2003). This process leads to the precipitation of the lipid phase that results in the formation of fine particles. The excess water is then removed by means of lyophilisation to form SLNs (Parhi and Suresh,

2012).

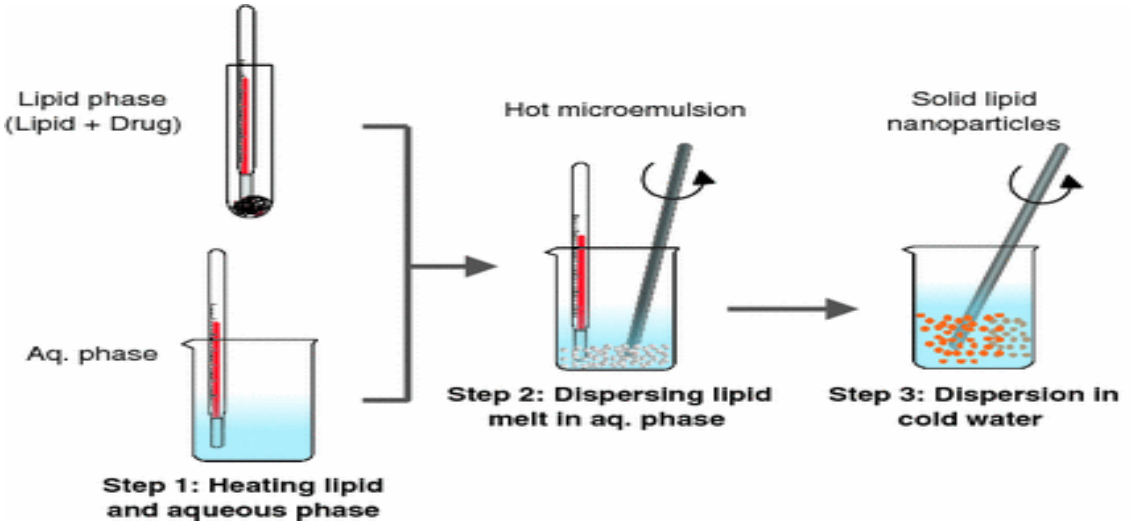

Figure 2.7: Schematic representation of the microemulsion based technique for solid lipid nanoparticle (SLN) preparation (Shah *et al.,* 2014).

Another low-energy approach to SLN preparation is the double-emulsion method. This method is derived from the aforementioned solvent-emulsification method. It entails the formation of two emulsions; the drug is encapsulated within a stabiliser to prevent the partitioning of the drug into the external aqueous phase during solvent evaporation (Nandini *et al.,* 2013). Figure 2.8 illustrates the process of SLN preparation by means of the double-emulsion method.

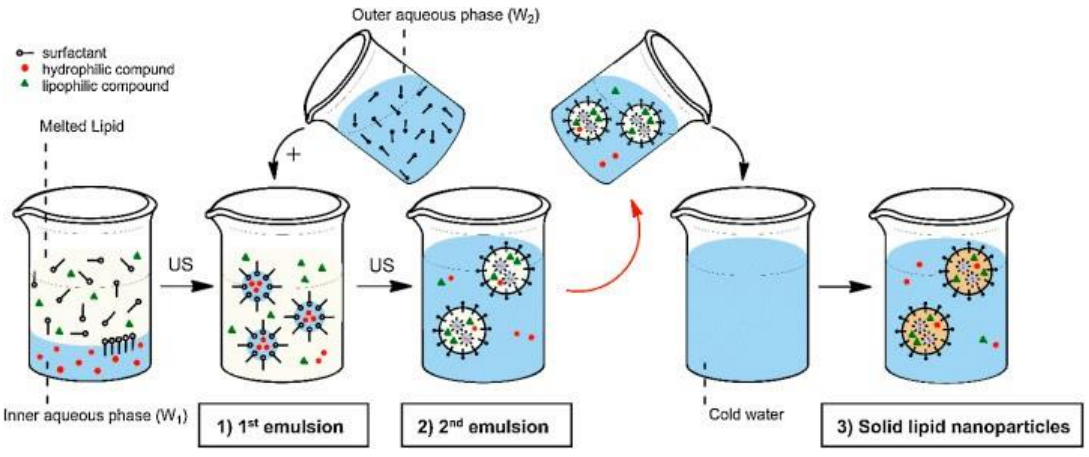

Figure 2.8: Schematic representation of the double emulsion technique for solid lipid nanoparticle (SLN) preparation (Peres *et al.,* 2016).

The solvent evaporation technique is a method of preparation that utilises organic solvents (see Figure 2.9). This process commences with the dissolution of the lipid in a water-immiscible organic solvent (Lason and Ogonowski, 2011). The mixture then undergoes emulsification in an aqueous phase prior to the evaporation of solvent. The final step results in lipid precipitation that forms nanoparticles (Ganesan and Narayanasamy, 2017).

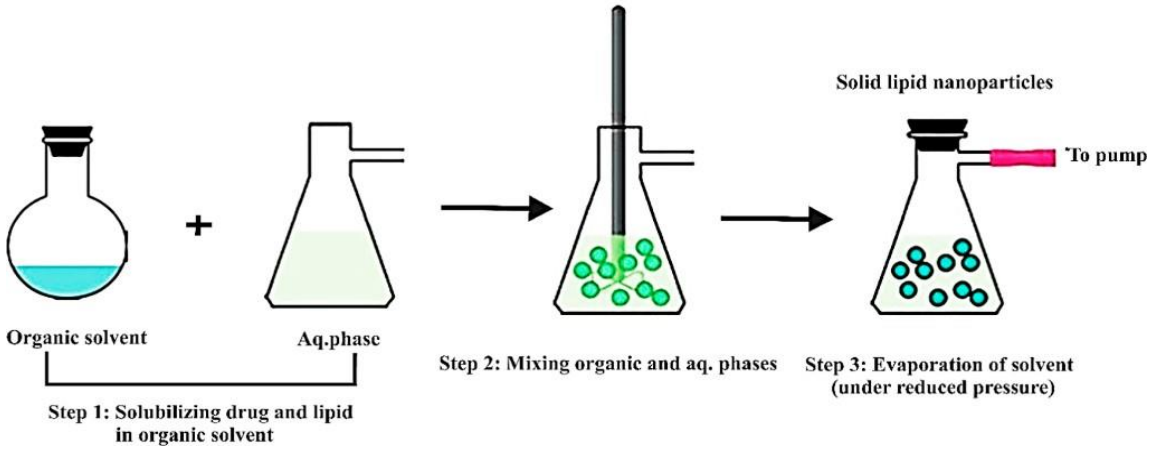

Figure 2.9: Schematic representation of solvent evaporation technique for solid lipid nanoparticle (SLN) preparation (Ganesan and Narayanasamy, 2017).

Another preparation technique that utilises organic solvents in the preparation of SLNs is the supercritical fluid (SCF) process. SCF is defined as a substance at a temperature and pressure above its critical point. The physiochemical properties of such fluids assume intermediate values of liquid and gasses which improve their solvent power (Noyori, 1999). Processes, such as rapid expansion of supercritical solution (RESS), particles from gas saturated solutions (PGSS), aerosol solvent extraction solvent (ASES) and supercritical fluid extraction of emulsions (SFEE) have been employed for nano-particle formation (Kankala *et al.,* 2017).

RESS, in particular, has been investigated extensively for the preparation of SLNs (Santo *et al.,* 2013). The process involves the dissolution of a nanodispersion product in a SCF. The resultant solution expands rapidly through the sprayer and causes rapid deposition of micro- and nanoparticles of the product. Figure 2.10 illustrates a simplified version of nanoparticle formation via RESS.

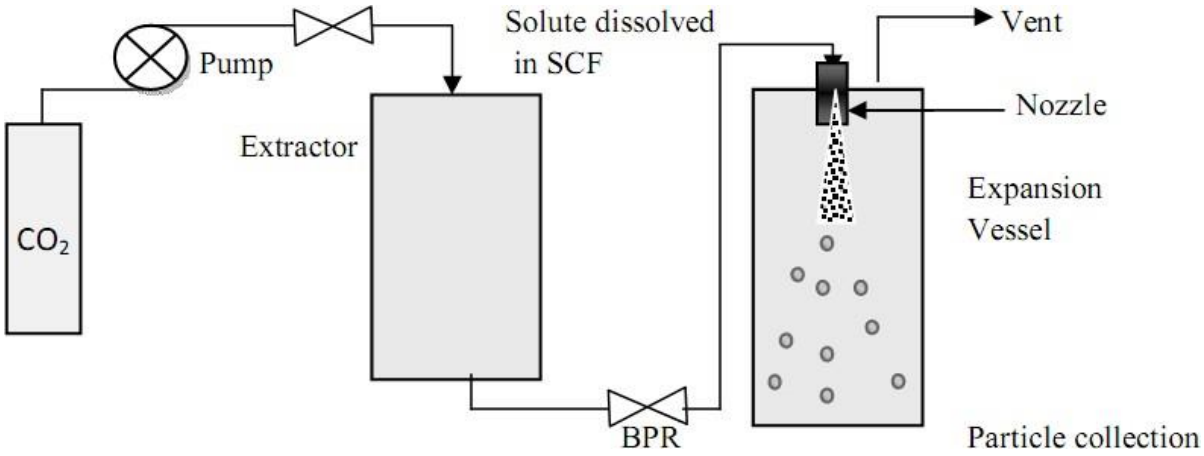

Figure 2.10: Diagrammatic layout of rapid expansion supercritical fluid (SCF) solution system for nanoparticle preparation (SLN) (Parhi and Suresh, 2012).

Finally, there are two emerging techniques related to SLN preparation, namely film ultrasound and spray drying. Spray drying is a novel technique that is employed to improve long-term storage stability of SLNs (Xia *et al.,* 2016). It is an alternative method to lyophilisation for converting liquid nanodispersions to a desiccated system which, consequently, promotes thermal stability and facilitates easy handling. Lipids with a melting point of greater than 70 °C are advised for spray drying (Pardeshi *et al.*, 2012).

Similarly, another fairly new technique is film ultrasound, in which lipids and drugs are dissolved in an appropriate organic solvent that then undergoes decompression, rotation and evaporation in order to yield a lipid film. An aqueous phase is then added, and a PUS device is used to provide high-energy input for the formation of mono-dispersed nanoparticles (Patel *et al.,* 2013).

i. Summary of solid lipid nanoparticle (SLN) preparation techniques

Table 2.10 provides a concise summary of the advantages and disadvantages of the most commonly used preparation techniques for SLNs. As noted previously, even though SLNs provide many advantages over other colloidal systems, many of their issues and limitations are attributed to their preparation process, where some processes are implicated in drug-induced degradation owing to high temperatures or pressure use, lipid crystallisation, low drug-loading capacity or the co-existence of multiple colloidal species (Yadav *et al.,* 2014).

Table 2.10: Summary of advantages and disadvantages of commonly used solid lipid nanoparticle (SLN) preparation techniques (adapted from Battaglia *et al*., 2015; Kesharwani *et al.*, 2013).

Process	Advantages	Disadvantages
Hot homogenisation	Commercially available, likelihood of scalability	Increased rate of drug and carrier degradation, burst release effect for hydrophilic drugs, polydisperse distribution, energy intensive
Cold homogenisation	Ideal for thermolabile and hydrophilic drugs, less poly-dispersion and more stable dispersions obtained compared to HHT	High pressure-induced degradation, energy intensive
Bath sonication	Availability of equipment, cost-effective, reduced shear stress	Poly-dispersed particle distribution, large particle size, instability of particles, agglomeration of particles
Probe sonication	Availability of equipment, cost-effective, reduced shear stress	Contamination by metal particles, physical instability upon storage, overheating
Solvent emulsification	Small particle size, low-energy input, ideal for thermolabile drugs, large-scale production	Use of organic solvents, emulsion instability
Micro-emulsion	Low-energy input, stability	Labour-intensive, sensitivity of method, lipid crystallisation, low nano-particle concentration
SCF process	Absence of organic solvent, mild temperature, particles obtained as dry powder	Novel and costly method
Spray drying	Dry particles for long-term stability	Particle aggregation, high temperature and shear required
Double emulsion	Not ideal for lipophilic drugs	Large particles obtained
Solvent evaporation	Small mono-dispersed nano-particles, high encapsulation efficiency, ideal for large scale production	Use of organic solvent, increased likelihood of bio-toxicity
Film ultrasound	Uniform particle size	Limited research

With a wide array of experimental procedures available for the preparation of SLNs (see Figure 2.11) and no stringent guidelines, operators can often feel confused about selecting the most suitable method. Factors, such as the availability of equipment, time-constraints, cost and the physicochemical properties of the drug and excipients were investigated and considered prior to the selection of a formulation method for this study. Due to limitations in equipment availability for this study, high-energy approaches (i.e. bath and probe-tip sonication) were investigated.

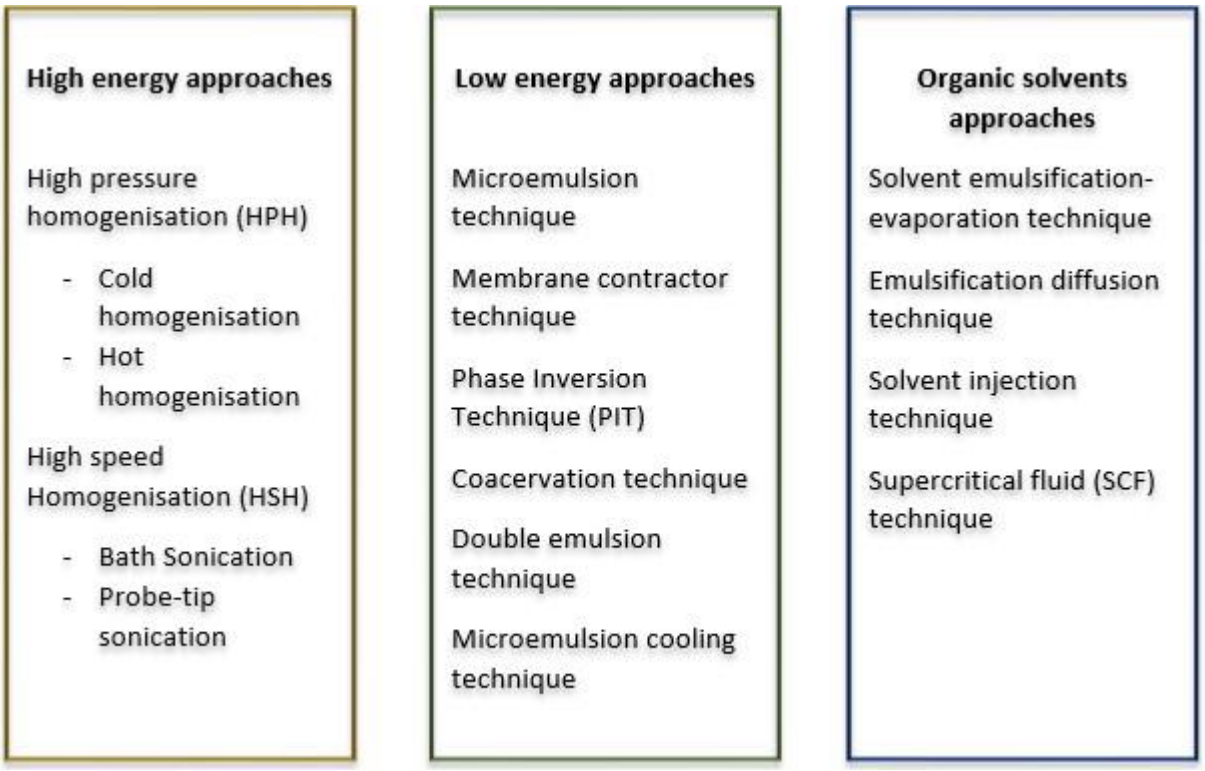

Figure 2.11: Summary of solid lipid nanoparticle (SLN) preparation techniques.

2.4.2 Mucoadhesive drug delivery systems

Mucoadhesion is defined as the adhesion between two materials, one of which is a mucosal surface (Shaikh *et al.,* 2011). This novel approach to drug delivery has received much attention, owing to its potential for improving drug delivery. Mucoadhesive formulations are designed to provide a controlled rate of drug release and prolong the retention of the dosage form at the site of application, thereby improving therapeutic outcomes (Shaikh *et al.,* 2011). Moreover, these formulations provide intimate contact between the dosage form and mucosa, which can cause high drug flux at the site of application (Boddupalli *et al.,* 2010).

As stipulated in Section 2.3, a major disadvantage of vaginal drug delivery is the short residence time of conventional formulations within the vaginal tract (Cardot *et al.,* 2004). Therefore, mucoadhesive systems for vaginal drug delivery have been extensively studied in order to remedy this issue. Mucoadhesive vaginal formulations prolong dosage form retention within the vaginal tract through the formation of physical and chemical bonds with the mucosa (Kaur *et al.,* 2016).

The initial step in the mechanism of mucoadhesion involves a contact phase in which hydration, wetting and spreading are pivotal steps. Upon completion of the contact phase, a consolidation phase follows, which includes the strengthening of polymer chains into the mucous layer and the formation of polymer-mucin bonding by means of electrostatic interactions or weak van der Waals forces (Caramella *et al.,* 2015). These dosage forms are put into various categories, such as gels, tablets, films, emulsions or pessaries. The focus of this study was, however, limited only to gels, owing to their ease of manufacture, superiority in patient preference and favourable pharmacokinetic profiles, such as sol-gel transition and controlled drug release (Acarturk, 2009).

2.4.2.1 Gels

A gel is defined as a semi-solid three dimensional (3D) polymer matrix made up of small quantities of solid material dispersed in large amounts of fluids (Rogovina *et al.,* 2008). The 3D polymeric network structure is responsible for the gel's viscoelastic properties that resist deformation. The classification of gels is dependent on the nature of the solvent. Two groups are available *viz.* organogels and hydrogels (Bhoyar *et al.,* 2012). Table 2.11 summarises the general characteristics of these two groups.

Table 2.11: General characteristics of organogels and hydrogels (adapted from Nabi *et al.*, 2016).

ORGANOGELS	HYDROGELS
Also known as oleaginous gels Non-polar solvent phase Consist of up to 35% H_2O Cross-linking prevents flow of external polar phase, thus increasing hydrophobicity and reducing drug release rate	Consist of a polar solvent and a polymer Consist of up to 90% H_2O Polymers assemble to form 3D network which retains significant amounts of H_2O

Organogels are regarded as bicontinuous systems comprised of gelators and organic solvents (Vintiloiu and Leroux, 2008). They are distinguished from hydrogels by their predominantly organic continuous phase. Furthermore, they are categorised as polymeric- or low-molecular weight organogelators (Swati *et al.,* 2014). In the pharmaceutical industry, they have been investigated for their potential in vaccine and lipophilic drug delivery (Vintiloiu and Leroux, 2008). Their ease of preparation, incorporation of lipophilic drugs and enhanced topical performance versus conventional dosage forms make organogels a vehicle of choice for topical drug administration (Fetih, 2010). However, their limitations, such as poor stability at elevated temperatures and greasiness (which reduces patient acceptability), make them unsuitable for vaginal drug delivery (Swati *et al.,* 2014).

2.4.2.2 Hydrogels

Hydrogels are polymer-based semi-solid dosage forms investigated for their potential in controlled drug release. The popularity of this novel dosage form has increased drastically owing to its flexibility, high water content and biocompatibility (Graham and McNeill, 1984). A visual representation of the 3D network structure formed by the cross-linking of polymers is illustrated in Figure 2.12.

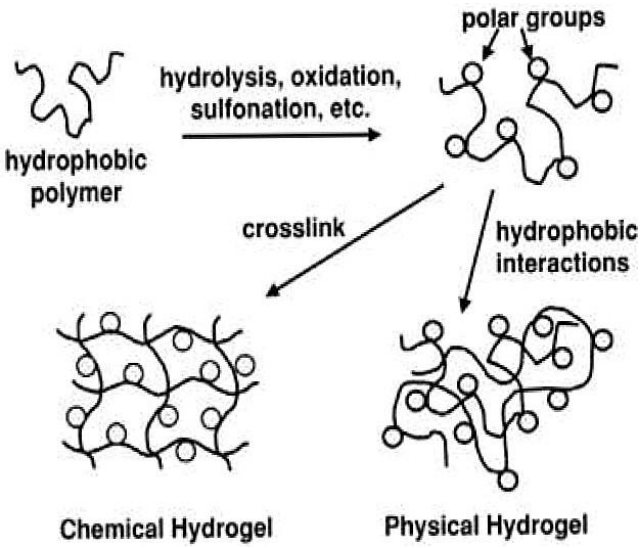

Figure 2.12: 3D polymeric structure of physical and chemical cross-linked hydrogels (Chirani *et al.,* 2015)

These cross-linked polymer networks display good swelling characteristics by absorbing large amounts of fluids (Chirani *et al.,* 2015). The mechanism of swelling begins with the primary bound water that is first absorbed by the hydrophilic groups of a dry hydrogel. Once the hydrophilic groups are hydrated, the network swells, causing hydrophobic groups to be exposed. These groups interact further with the fluid, leading to secondary bound water (Yang *et al,* 2012).

Once the hydrophobic and hydrophilic sites have interacted with the water molecules, the network absorbs additional water as a result of the osmotic driving force of the polymers towards infinite dilution. Infinite dilution is, however, opposed by physical or chemical cross-linking which causes the hydrogel to reach an equilibrium swelling level and prevents gel deformation (Yahia *et al.,* 2015). Cross-linking refers to the bonds that link one polymer molecule to another, thus changing a polymer to a solid or gel by restricting its mobility. The nature of cross-links varies, and the extent of cross-linking correlates with hydrogel characteristics, such as viscosity, elasticity and solubility. By controlling the degree of cross-linking, it is possible to exploit and optimise polymers for different applications (Maitra and Shukla, 2014).

The various types of hydrogels are classified as conventional or stimuli-responsive gels. The former absorbs water or fluid in the presence of an aqueous environment and shows no change in response to the change in the surrounding environment. The latter, also known as smart hydrogels, displays a change in swelling behaviour in response to a change in the surrounding environment (Chaterji *et al.,* 2007). Stimuli-responsive hydrogels were explored in this study, as they provide reversible phase transitions which are particularly useful for intravaginal drug delivery by maintaining the dosage form *in situ* (Dorraj and Moghimi, 2015). Figure 2.13 illustrates the reversible stimuli-responsive nature of these stimuli-responsive hydrogels' polymer chains.

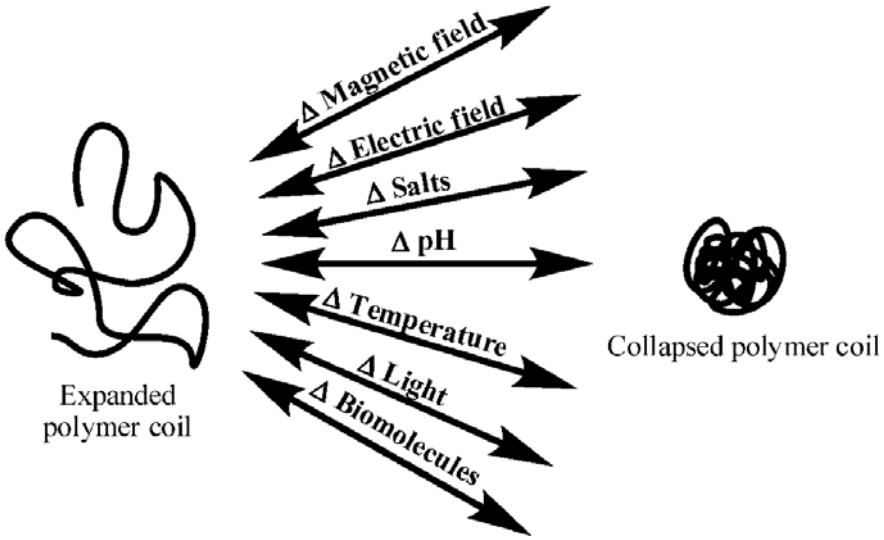

Figure 2.13: Stimuli responsive nature of polymer chains in smart hydrogels (Deen and Lab, 2018)

The type of stimuli responsible for inducing changes in a polymer network can be categorised into three groups, *viz*. physical, biological or chemical (Gandra, 2013). Examples of physical stimuli include magnetic and electric fields, temperature, pressure, light exposure and ultrasound. Biological stimuli include ligands, enzymes, antibodies or antigens. Chemical stimuli include the likes of pH and ionic strength (Almeida *et al.,* 2012). Thermo- and pH-responsive hydrogels account for the most commonly used systems in polymer-based drug delivery systems (Echeverria *et al.*, 2018). The use of stimuli-responsive hydrogels to circumvent issues of rapid drug release, fluctuations in API concentrations at the site of application, adverse effects, stability of APIs with short half-life and poor patient adherence as a result of frequent

dosing were investigated extensively in preparation of this study's literature review but, for the purposes of this study, thermosensitive hydrogels were the only ones considered for further research.

Thermosensitive, also referred to as thermoresponsive hydrogels are comprised of materials that facilitate a sol-gel transition in response to changes in temperature. Depending on the mechanism of response, they are classified as positive or negative polymers (Gandra, 2013). The majority of these polymers belong, however, to the former group and are characterised by swelling when temperatures increase above their critical temperature point. Simply stated, positive polymers solidify with increasing temperatures (Taylor *et al.,* 2017). They offer many advantages, such as site specificity, biotolerability and sustained release, a simple method of formulation and ease of administration for patients. Moreover, they do not make use of organic solvents or cross-linking agents in their preparations, which further deems them as biotolerable (de Souza-Ferreira *et al.,* 2015).

Gel formation occurs in response to the temperature difference between ambient and physiological temperature. In terms of intravaginal administration, thermoresponsive gels are characterised by easy application, owing to the low viscosity of their formulation which allows for complete spreading on the vaginal mucosa (Taurin *et al.,* 2018). Conversely, the formation of a gel following application overcomes the removal of the dosage form via mucocillary clearance, thus favouring the longevity of the loaded drug at the site of application (Caramella *et al.,* 2015).

Favourable characteristics attributed to hydrogels include their non-greasy and easily washable nature; their formation of a hydrating and protective layer at the site of application; and their incorporation of both hydrophilic and lipophilic drugs. Moreover, they can be formulated to provide intimate contact with the vaginal mucosal and establish controlled drug release (Andrade *et al.,* 2014; Fan *et al.,* 2016).

i. Polymers as materials for thermo-sensitive hydrogels

Polymers used in the preparation of thermoresponsive hydrogels are derived from natural or synthetic sources (Taylor *et al.,* 2017). Due to their availability in the study's laboratory, poloxamers and cellulose derivatives were investigated for their potential in thermoresponsive drug delivery.

Poloxamers, also referred to as Pluronic®, Kolliphor®, Tetronic® or Synpersonic® (Almeida *et al.,* 2018), are a class of block co-polymers synthesised from polyethylene oxide (PEO) and polyoxypropylene (PPO) in a tri-block structural arrangement (see Figure 2.14; Bodratti and Alexandridis, 2018).

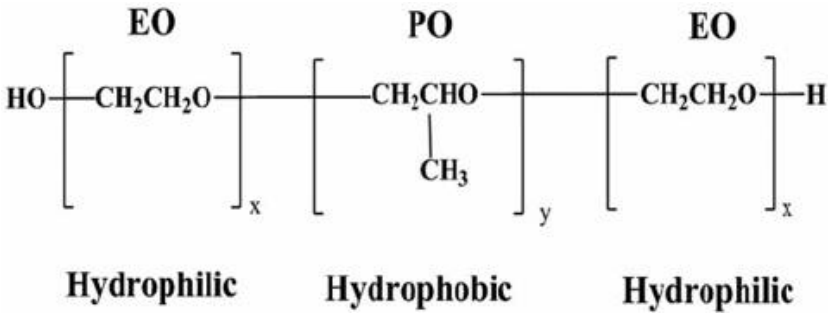

Figure 2.14: Generic structural arrangement of poloxamers (Shubhra *et al.*, 2014)

The x-y-x tri-block structure is formed by polymer chains of ethyleneoxide (EO) and propyleneoxide (PO) (Almeida *et al.,* 2018). This structure is responsible for defining surfactant characteristics. Through the modifications of various parameters, such as size, hydrophilicity and lipophilicity, the polymer can be altered (Yapar and Inal, 2012). Poloxamer solutions display temperature-dependent gelling and self-assembling behaviour that present great interest in optimising drug formulations (Shubhra *et al.,* 2014).

All poloxamers possess similar chemical structures, but have different molecular weights and compositions of EO and PO blocks (Bodratti and Alexandridis, 2018). The two most commonly used poloxamers are 188 and 407 (Patel *et al.,* 2009). A nomenclature system was established in 1950 in order to aid with the identification of each poloxamer type (Devi *et al.,* 2013). The naming of poloxamers includes three letters, *viz.* F, P or L that describe the physical state of the polymer at room temperature where solid flakes (F), liquids (L) or pastes (P) are represented (Bodratti and Alexandridis, 2018). This is then followed by two or three numerical figures which represent a code relating to the particular type's structural parameter. The first two (or one) digit translates to the molecular mass of the PPO multiplied by 300. The last digit translates to the hydrophilic content multiplied by 10 in order to yield the % of PEO content (Almeida *et al.,* 2018; Ban *et al.,* 2017).

Poloxamers possess high solubility capacity for many drugs and excellent compatibility with various pharmaceutical excipients (Almeida *et al.,* 2018). They are also soluble in most solvents (organic and inorganic) and extremely stable in the presence of metal ions, acids and alkalis. Due to these properties, poloxamers have established themselves as the preferred polymers for many formulations (Hurler *et al.,* 2012). They are used extensively in the preparation of thermoresponsive hydrogels, owing to their gel-forming abilities at elevated temperatures (Guiliano *et al.,* 2018). The use of poloxamers in isolation is, however, not encouraged, because of their weak mechanical strength which, consequently, promotes rapid erosion of the dosage form at the application site (Gandra, 2013). Rather, the blending of poloxamers with an additional co-polymer, such as HPMC, is recommended (Varshosaz *et al.,* 2008), as it not only improves the mechanical strength of the hydrogel, but also improves mucosal surface interactions. Thus, this approach prolongs dosage from retention at the site of application (Deshkar *et al.,* 2015).

Cellulose derivatives include, amongst others, HPMC, sodium carboxymethylcellulose (NaCMC) and methylcellulose (Granstrom, 2009). Cellulose is a linear homopolymer polysaccharide that is insoluble in aqueous solvents. It is comprised of D-anhydro-glucopyronase units joined by β-1.4-glycosidic bonds (Marks, 2015). Its aqueous insolubility results from extensive inter- and intramolecular hydrogen bonding. Figure 2.15 illustrates the chemical structure of cellulose with two β-1.4-glycosidic bonds.

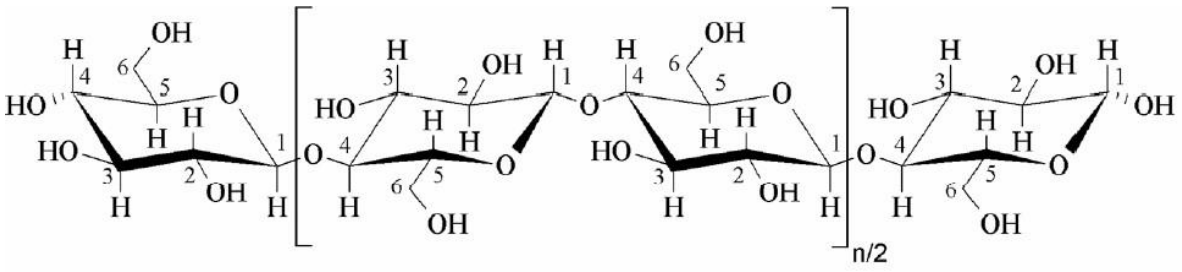

Figure 2.15: Chemical structure of cellulose with two β-1.4-glycosidic bonds (Marques-Marinho and Vianna-Soares, 2013)

Cellulose derivatives are amongst the excipients commonly used in pharmaceutical products (Marques-Marinho and Vianna-Soares, 2014). They are employed in a wide array of formulations, such as viscosity enhancers for topical dosage forms, suspending agents in liquid oral preparations, binding agents in tablet manufacturing processes and rate-controlling matrices for sustained release preparations (Jain *et al.,* 2013). Furthermore, favourable characteristics attributed to cellulose derivatives include low costs, reproducibility, recyclability and bio-compatibility, which make them ideal excipients for pharmaceutical formulations (Chambin *et al.,* 2004)).

In addition to their use in many pharmaceutical preparations, they possess mucoadhesive characteristics that allow for strong hydrogen bonding with the mucin present on the mucosal surface (Roy *et al.,* 2009). The mechanism of bonding includes the formation of hydrogen bonds between the carboxylic acid group of the polymer and glycoprotein of mucin (Almeida *et al.,* 2018). HPMC, in particular, is used extensively to facilitate controlled drug release (Chatterjee *et al.,* 2017).

Most natural polymers, such as chitosan, gelatine and polysaccharides exhibit thermo-gelation characteristics upon temperature decreases (Curcio *et al.,* 2010). However, aqueous solutions of some cellulose derivatives (see Table 2.12) exhibit reverse thermogelation (Jain *et al.,* 2013).

Table 2.12: Examples of thermo-gelling cellulose ether derivatives (adapted from Jain *et al.*, 2013)

Cellulose derivative	Chemical structure	Gelling temperature range	Concentration
Methyl cellulose	$-CH_3$	25-50°C	1-5%
Hydroxypropyl cellulose	$-CH_2CH_2CH_2OH$	46°C	2%
Hydroxypropyl methylcellulose	$-CH_3$ or $-CH_2CH(OH)CH_3$	75-90°C	1-5%
Hydroxylethyl cellulose	$-CH_2CH_2OH$	75°C	1-5%
Ethylhydroxyethyl cellulose	$-C_2H_5$ or $-CH_2CH_2OH$	30-40°C	1-5%

When the compounds presented in Table 2.12 have an optimum balance of hydrophilic and hydrophobic moieties, they undergo a sol-to-gel transition in H_20 (Kim and Matsunaga, 2017). This transition is actually dependent on the substitution of the hydroxy group. H_20 then becomes a poorer solvent, with increasing temperatures, and polymer-to-polymer interactions become dominant at higher temperatures which result in a gel (Desbrieres *et al.,* 2000; Jain *et al.,* 2013).

ii. Preparation methods of temperature-responsive hydrogels

Hydrogels are prepared through a wide range of methods and precursors that allow for the alteration of properties, such as pore size, mechanical strength, degradability and rate of degradation (Sosnik and Seremeta, 2017). The process of hydrogel preparation is segregated into two major categories, namely physical and chemical cross-linking (Gandra, 2013). The former involves the preparation of a hydrogel through the growth of physically-connected aggregates (i.e. hydrophobic or electrostatic interactions or chain entanglements), whist the latter is achieved by permanent covalent bonding (Ahn *et al.,* 2007). Physical cross-linking is more advantageous because physical junctions within the polymer display reversible transition behaviours in varying environmental conditions (Parhi, 2017). Further benefits of physical cross-linking include the absence of cross-linking agents, no organic solvents, and no heat and photo irradiation; all of which diminish toxicity and promote API stability (Gong *et al.,* 2013).

Physically cross-linked hydrogels are developed by crystallisation, ionic or protein interaction, stereo-complex formation, hydrophobised polysaccharides and hydrogen bonding (Maitra and Shukla, 2014). Table 2.13 provides a brief discussion of these methods.

Table 2.13: Mechanisms of physical cross-linking of hydrogels (adapted from Maitra and Shukla, 2014; Akhtar et al., 2016).

Mechanism	Comments
Ionic interactions	Gentle cross-linking conditions including ambient temperature and physiological pH Example(s): Alginate, chitosan
Crystallisation	Involves thawing and freezing processes to form highly elastic gel Example(s): Polyvinyl alcohol (PVA)
Stereo-complex formation	A hydrogel is formed via cross-linking that is produced between lactic acid oligomers of reverse chirality Example(s): enantiomeric lactic acid
Hydrogen bonding (H-bonding)	H-bonding between polymer chains can also lead to hydrogel formation. H-bond is produced by connecting an electron-deficient hydrogen atom and a functional group of high electronegativity. Example(s): Polyacrylic acid (PAAc)
Protein interactions	This method involves co-polymers that contain the repetition of silk-like and elastine-like blocks called ProLastins. These ProLastins are fluid solutions that occur in H_20 and can undergo a transformation from solution to gel under physiological conditions because of the crystallisation of the silk-like domains. Example(s): natural and synthetic amino acids
Hydrophobised polysaccharides	Hydrophobic interactions result in polymer swelling and, subsequently, take up H_20 to form the hydrogel Examples: Dextran, pullulan and carboxymethyl curdlan

The preparation of cellulose-based hydrogels normally consists of two steps. Firstly, there is the solubilisation of cellulose fibres or powder (Akhtar *et al.,* 2016). Secondly, there is the chemical and/or physical cross-linking in order to obtain a 3D network of hydrophilic polymer chains, which are able to absorb and retain a significant amount of water (Yahia *et al.,* 2015). Through the modification of the cross-linker and polymer concentrations, it is possible to optimise the hydrogel swelling capabilities and mechanical properties of the polymers (Navarra *et al.,* 2015). For the purposes of this study, only physical cross-linking methods have been investigated.

2.5 SUMMARY

As outlined in this chapter, poor patient adherence due to the shortcomings of conventional VVC dosage forms contributes to reinfection or poor therapeutic outcomes in the treatment of VVC (Cardot *et al.,* 2004; Dobaria *et al.,* 2007). While determining effective therapeutic strategies, it would be logical to optimise existing dosage forms in order to circumvent issues of poor adherence to VVC pharmacotherapy. Novel pharmaceutical drug delivery devices show the potential of optimising localised drug delivery by (a) improving drug absorption, (b) controlling the rate of drug release or (c) prolonging intimate contact of the dosage form at the site of application (Kenechukwu *et al.,* 2018). Any of these three solutions could aid in promoting better patient compliance in order to facilitate effective treatment outcomes.

By combining the advantages of SLNs with thermogelling mucoadhesive systems, the pharmacokinetic and pharmacodynamics parameters of locally-acting imidazole formulations could be improved; thereby potentially providing an alternative means of VVC treatment. The following chapter focuses on the methodology for the development and characterisation of a MNZ formulation into SLNs. The study then further incorporated the carrier system into a thermoresponsive bioadhesive system in order to extend the drug residence time at the site of application.

CHAPTER 3

METHODOLOGY

3.1 INTRODUCTION

For this study, various formulations of MNZ-SLNs were prepared by means of a novel low-temperature emulsification and ultrasonication method. The resultant formulations were optimised statistically through response-surface methodologies. Characteristics of the optimal formulation were determined by means of transmission electron microscopy (TEM), photon correlation spectroscopy (PCS), and HPLC. Upon preparation of the MNZ-SLNs, the optimal formulation displaying maximum entrapment efficiency and minimal particle size was chosen for incorporation into various mucoadhesive hydrogel preparations. The resultant hydrogel formulations were assessed for drug content uniformity and rheology. Formulations which displayed favourable sol-transitions were further characterised for *in vitro* drug release and antimicrobial susceptibility. The development, optimisation and characterisation of the NDDS are discussed in this chapter, along with formulation issues encountered during this process.

3.2 INSTRUMENTATION

3.2.1 High Performance Liquid Chromatography (HPLC)

Chromatography is an analytical technique that separates components in a mixture, based on their differences in distribution between two phases (Coskun, 2016). It currently serves as the strongest analytical tool available to modern scientists, hence its extensive use in analytical method development and validation (Prathap and Nishat, 2013; Chauhan *et al.,* 2015). HPLC evolved from classic column chromatographic (CCC) techniques. When compared to CCC, HPLC provides higher resolution, faster analysis, small reusable columns, controlled flow of mobile phase (MP) and the detection of minute sample amounts (Gupta *et al.,* 2012). Figure 3.1 illustrates a simplified layout of a modern-day reversed phase HPLC (RP-HPLC) apparatus that was utilised in this study to obtain chromatographic profiles of MNZ in bulk and complex pharmaceutical preparations.

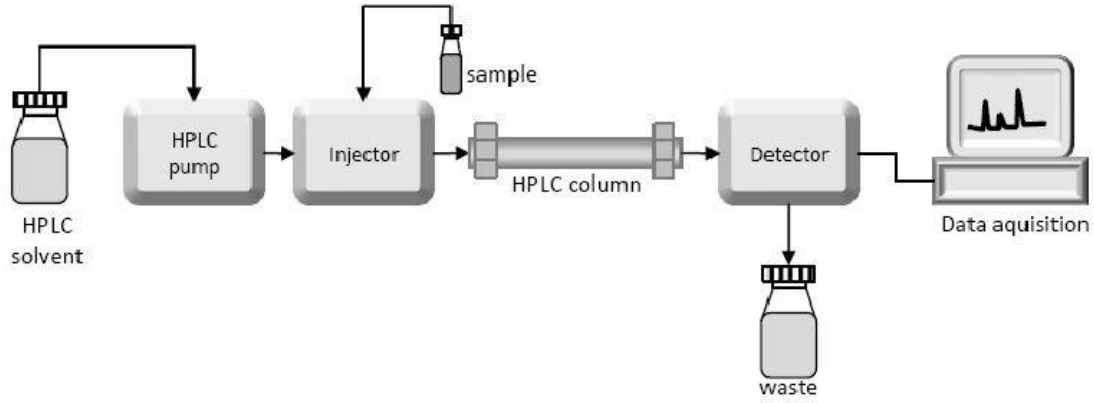

Figure 3.1: Layout of a modern day RP-HPLC apparatus (Czaplicki, 2014).

Chromatographic profiles MNZ in bulk and complex formulations were recorded and translated on a HPLC apparatus (Shimadzu™, Kyoto, Japan) and fitted with a SIL-20AFT autosampler, LC-20AB prominence solvent delivery module and CTO-20A prominence column oven. The solvent reservoir comprised the contents of the mobile phase (MP), where two individual containers holding the respective solvents were employed and mixed online. Liquefied samples for chromatographic analysis were placed inside the injector and pushed through the column under high pressure. The column was employed to effect a separation of sample components, after which it was translated into a chromatographic profile by the detector. Data acquisition was the final step and was achieved through the use of LCSolutions™ software (Shimadzu™, Kyoto, Japan).

3.2.2 Differential Scanning Calorimetry (DSC)

DSC is a thermal analytical technique utilising controlled resistance heaters to individually heat a sample and a reference compound at a predetermined rate (Gill *et al.,* 2014). The change in heat flow between the sample and reference compound are monitored against time and temperature so as to determine drug-excipient compatibility (Mazurek-Waldolkowska *et al.,* 2013).

A thermal analysis of the MNZ microcrystalline powder, excipient and MNZ-excipient mix was conducted by simultaneous thermo-gravemetric analysis (TGA) and DSC using a SDT Q600 (TA instrument™, Utah, USA).

3.2.3 Probe-tip ultrasound sonication (PUS)

Ultrasound sonication involves the use of ultrasonic frequencies (>20 KHz) to agitate particles (Majumdar and Devi, 2010). A probe-tip sonication device (Bandelin Sonoplus™, Berlin, Germany) was used in the preparation of SLNs. Optimal parameters for PUS were established through RSM.

3.2.4 Photon Correlation Spectroscopy (PCS)

Photon correlation spectroscopy (PCS), also known as dynamic light scattering (DLS), utilises a laser of known wavelengths which pass through a dilute sample solution; the intensity of the scattered light is collected by detectors in order to establish particle distribution characteristics (Tscharnuter, 2000). For this study, SLN characteristics of size, ZP and PDI were determined using a Malvern Zetasizer Nano-ZS particle analyser (Malvern Instruments™, United Kingdom).

3.2.5 Centrifugation

A centrifuge apparatus causes the separation of compounds in a mixture, based on differences in sedimentation velocities of components within a given mixture. The apparatus comprises a rotor to grip tubes containing the liquid mixture. This rotor is mounted on a drive shaft which rotates when powered by the motor (Majekodunmi, 2015). An indirect method using centrifugation apparatus (Hermle™ Z300, Germany) was used in the determination of drug entrapment efficiency of the prepared nanoparticles in this study.

3.2.6 Transmission Electron Microscopy (TEM)

Particle size and surface morphology assessments were done through a JEOL JEM 2100 LaB6 (JOEL Limited [Ltd]™, Japan) transmission electron microscope. TEM works by bombarding the sample with a stream of electrons and, consequently, monitoring the resultant transmission in order to produce detailed images of nano- or microscopic samples (Winey *et al.,* 2014).

3.2.7 Rheometer

Rheology is a branch of science concerned with the study of the deformation and flow of matter (Rueda *et al.,* 2017). For this study, a rheometer (Anton Paar™ MCR 72, Austria) was used to assess the viscosity and rheological properties of the prepared hydrogel formulations.

3.2.8 pH meter

A measure of the hydrogen ion concentration in a solution yields a pH value (Bates, 1948). pH measurements of developed hydrogel formulations were determined using pH instrumentation (Metrohm™, Herisau, Switzerland).

3.2.9 Franz vertical diffusion cells (FVDC)

Franz diffusion vertical cells (FDVC) provide a reliable and reproducible means of *in vitro* drug release-testing (IVDRT) for various dosage forms (Kanfer *et al.,* 2017). Vertical diffusion cells (VDC) have been investigated extensively for their use in IVDRT in hydrogels (Naik *et al.,* 2016). An illustration of the FVDC apparatus utilised in this study is given in Figure 3.2.

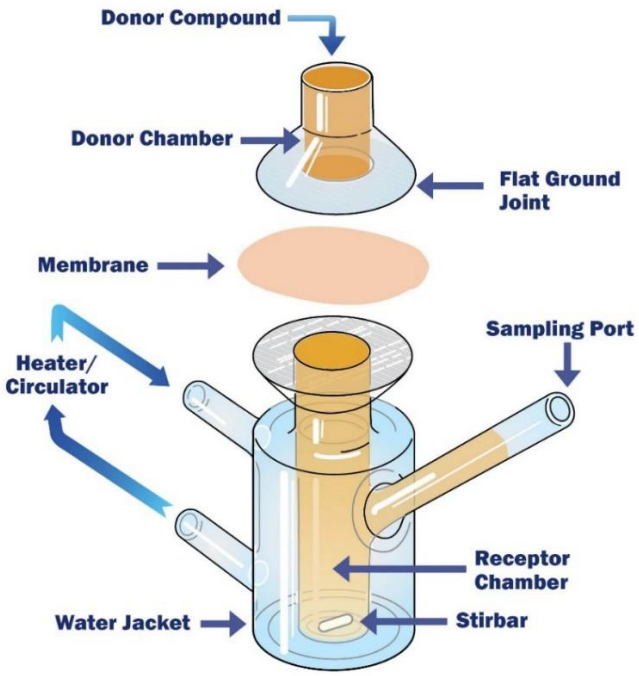

Figure 3.2: Illustration of Franz vertical diffusion cell (FVDC) apparatus (Dandamudi, 2017).

IVDRT, by means of FVDC, requires minute sample amounts (Cabral *et al.,* 2014). The sample is placed on the membrane surface on the donor component side. The sample is then allowed to permeate through the membrane into the receptor fluid, after which aliquots are withdrawn for assay (Naik *et al.,* 2016). Additional parts of the FVDC include, amongst others, a receptor chamber filled with a receptor fluid, sampling ports and water jacket. The donor chamber comprises a donor compound and a flat ground

joint resting on the membrane, which connect to the receptor chamber (Dandamudi, 2017).

The membrane used may be synthetic or natural, depending on the nature of the sample and the study. The receptor chamber is filled with a suitable medium that is maintained at a fixed temperature by a circulating water jacket (Kanfer *et al.,* 2017).

The selection of a receptor medium is dependent of the type of cell used and the nature and solubility of the drug. An ideal medium should mimic *in vivo* environmental conditions for the intended use (Salamanca *et al.,* 2018). Mediums, such as phosphate-buffered saline (PBS) are first-choice agents for IVDRT, since they closely resemble physiological fluids (Modi and Shah, 2016). The stir bar is located inside the filled receptor chamber and is responsible for providing mechanical agitation so as to ensure even distribution of the donor compound within the cell. The recommended IVDRT temperature for intravaginal mucosal drug delivery systems is 37 °C (Dandamudi, 2017)

3.3 MATERIALS

3.3.1 Miconazole Nitrate (MNZ)

MNZ (Acros Organics™, ThermoFischer Scientific™, Massachusetts, USA) is an antimycotic drug belonging in the pharmacological class of imidazole antifungals. The members of this class (e.g. clotrimazole, ketoconazole, etc.) are structurally related and have comparable physicochemical properties and mechanisms of action (Ghannoum and Rice, 1999). For the purposes of this study, MNZ was selected as the API of choice. This choice was based on its availability in the study laboratory and the fact that MNZ is listed as an essential medicine by both the WHO and South African DoH (SANDoH, 2017; WHO Expert committee, 2017).

3.3.1.1 Pharmacological action and uses

MNZ elicits its pharmacological action by causing a disruption of ergosterol (a vital fungal cell component) synthesis (Sud and Feingold, 1981). The disruption occurs through the inhibition of the enzyme cytochrome p450 14-alpha demethylase, which results in an accumulation of ergosterol precursors and peroxides that, in turn, cause cytolysis. Additional mechanisms of action include the inhibition of oxidative and peroxidative enzymes by influencing triglyceride and fatty acid synthesis, thereby increasing the amount of reactive oxygen species in susceptible yeast (Francois *et al.,* 2006).

MNZ possesses both antifungal and antibacterial activities with its spectrum extending to dermatophytes, gram-positive cocci, gram-positive bacilli and *Candida spp*. (Cope, 1980). In the treatment of VVC, MNZ is formulated into solid or semi-solid dosage forms that are administered intravaginally for localised effect (Rossiter, 2016). The side-effect profile of these dosage forms includes local irritation, sensitisation and rashes. If absorbed systemically diarrhoea, gastric pain, fever, drowsiness and flushing may ensue (Francois *et al.,* 2006). Adverse effects of pharmacotherapy often influence a patient's adherence to treatment (Roose, 2009). Therefore, through the use of biotolerable excipients, this study aims to lessen the potential of such effects. The excipients employed in the preparation of this novel formulation include physiological lipids with low acute and chronic toxicity with minimal mucosal irritation (Das and Chaudhury, 2011).

3.3.1.2 Pharmacokinetic profile of miconazole nitrate (MNZ)

Pharmacokinetic parameters describe the process by which the body handles a specific drug (de Campos *et al.,* 2014). By being aware of and modifying pharmacokinetic parameters, developers can select an appropriate route of administration and optimise therapeutic efficiency of a drug (Tiwari *et al.,* 2012). The pharmacokinetic profile of MNZ is summarised in Table 3.1.

Table 3.1: Pharmacokinetic profile of miconazole nitrate (MNZ) (adapted from Pershing *et al.,* 1994; Stevens *et al.,* 2013).

Pharmacokinetic parameter	MNZ
Absorption (A)	Vaginal: 1.4% absorption following a single-dose insertion of a 1200 mg vaginal capsule Oral: 25-30% absorption Topical: <0.013% absorption
Distribution (D)	90-93% protein bound with an intravenous (IV) volume of distribution of 1400 L in normal patients and 800 L in renal-impaired patients
Metabolism (M)	Undergoes extensive hepatic metabolism upon oral administration so as to yield metabolites 2.4-dichlorophenyl-1-H imidazole ethanol and 2.4-dichloromandelic acid
Elimination (E)	Undergoes three phases of elimination, which are centred, fast and slow, with respective elimination half-lives of 0.4, 2.1 and 24.1 hours. Heamodialysis does not affect its half-life.
Excretion (E)	Mostly excreted as unchanged drug with about 50% faecal excretion and 1% renal excretion
Vaginal drug concentration	Time to peak concentration: 18.4 hours after administration of 1200 mg intravaginal capsule. 10.72-12 ng/mL was noted in the blood. Area under the curve: 329-338 × hrs/mL from zero to 48 hours after a single dose of 1200 mg

MNZ is metabolised by the liver in order to yield inactive metabolites that are excreted via the faecal and renal routes (Pershing *et al.,* 1994). The distribution of vaginal-administered MNZ is unknown (Stevens *et al.,* 2013). Finally, MNZ displays a terminal half-life of about 24 hours, with triphasic elimination.

Systemic absorption of MNZ is minimal (<1%), which suggests that the majority of the drug remains localised (Daneshmend, 1986; Merkatz *et al.,* 2017). This is ideal for reducing drug interactions and adverse effects. Effective pharmacotherapy of topical disease, however, requires that the API is delivered to the site of infection in sufficient concentrations in order to produce a pharmacological effect (Pershing *et al.,* 1994). In

the case of VVC, where the pathogen resides on or within the vaginal mucosa, the antifungal agent must be delivered in adequate concentrations and maintain intimate contact with the mucosa for maximal periods so as to inhibit the growth of the fungal pathogen (Daneshmend, 1986).

3.3.1.3 Physicochemical properties of miconazole nitrate (MNZ)

Physicochemical properties describe the chemistry and physical attributes of a compound. They are useful in advising developers of possible optimisation strategies for a pharmaceutical compound and its dosage form (Shah *et al.,* 2014). A comparative analysis of miconazole versus salt and MNZ is shown in Table 3.2.

Table 3.2: Comparative analysis of miconazole and miconazole nitrate (MNZ) (adapted from The Pharmaceutical Society of Great Britain. 1979).

Physicochemical property	Miconazole	Miconazole nitrate (MNZ)
Chemical structure	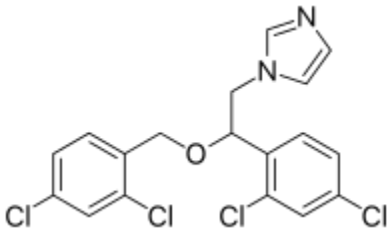	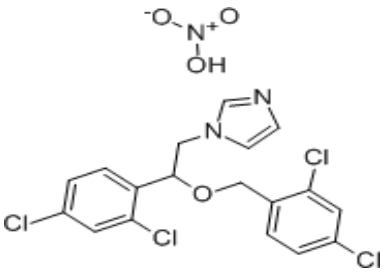
Chemical formula	$C_{18}H_{14}Cl_4N_2O$	$C_{18}H_{15}Cl_4N_3O_4$
Molecular mass	416.127 g/mol	479.135 g/mol
Elemental analysis	C 51.96%; Cl 34.08%; N 6.73%; O 3.84%	C 45.12%; Cl 29.59%; N 8.77%; O 13.36%
Appearance	White to pale cream, crystalline powder	Odourless white, microcrystalline powder
Route of administration	Oral and intravenous	Topical and vaginal
Melting point	178 to 184 °C	78 to 82 °C
Solubility	Less soluble than MNZ. Freely soluble in ethanol, chloroform, acetone, dimethylformamide, isopropanol, methanol (MeOH) and propylene glycol	Slightly soluble in H_20, soluble in 140 parts of alcohol, very slightly soluble in ether, hot chloroform, dimethylformamide and dimethylsulfoxide
Partition co-efficient (pKa)	6.7	
Storage conditions	Powder should be stored in an airtight container away from direct light in order to avoid photochemical degradation.	

MNZ is a nitrate salt form of miconazole, designed to improve the aqueous solubility profile of antifungal drugs and, consequently, improve their absorption (Singh *et al.,* 2014). As depicted in Table 3.2, the melting point of miconazole was reduced greatly through the formation of a salt base; furthermore, its solubility was enhanced but the

pKa remained constant. The discussion of this study is limited to the MNZ and its solubility.

The International Union of Pure and Applied Chemistry (IUPAC) defines solubility as the analytical composition of a saturated solution, expressed in terms of the proportion of a designated solvent (IUPAC, 1997). Solubility is a critical parameter for achieving desirable drug concentrations at the site of action (Singh *et al.,* 2014). It has a direct effect on the bioavailability of an active ingredient and, consequently, its therapeutic response; therefore, an increase in solubility is accompanied by an increased therapeutic response (Kadam *et al.,* 2013).

MNZ is a BCS class II drug, which indicates high permeability characteristics accompanied by low solubility (Singh *et al.,* 2014). The biopharmaceutics classification system (BCS) is a structure that is employed in segregating and classifying drugs, based on their solubility and permeability. MNZ's poor aqueous solubility of less than 1 µg/mL contributes to its less-than-ideal therapeutic efficacy (El-Garhy, 2013). Therefore, particle size reduction and lipid carrier encapsulation by means of SLN preparation was investigated in this study as a means of improving absorption properties of this BCS II drug.

3.3.2 Inactive pharmaceutical ingredients (IPIs)

IPIs, better known as excipients, are inert components of a drug product that do not add to or affect the intended action of therapeutically-active ingredients (Haywood and Glass, 2011). These ingredients are included in pharmaceutical formulations for a variety of reasons, including long-term stabilisation, bulking agents and lubricants. Table 3.3 provides a concise summary of all IPIs used in this study.

Table 3.3: Summary of excipients used in this study

Ingredient	Source	Function
Cholesterol	AppliChem™, GmbH, Darmstadt, Germany	Lipid for SLN preparation
Soy lecithin	AppliChem™, GmbH, Darmstadt, Germany	Co-emulsifier for SLN preparation
Polysorbate 80	Sigma-Aldrich™, Steinheim, Germany	Emulsifier for SLN preparation
Poloxamer 188	Sigma-Aldrich™, Steinheim, Germany	Emulsifier for SLN preparation, thermo-responsive polymer for hydrogel preparation
Hydroxylpropyl methylcellulose (HPMC)	Aspen Pharmacare™, Port Elizabeth, South Africa	Mucoadhesive and thermoresponsive polymer for hydrogel preparation
Methylcellulose 450	Aspen Pharmacare™, Port Elizabeth, South Africa	Mucoadhesive and thermoresponsive polymer for hydrogel preparation

An ideal excipient should be multifunctional so as to reduce manufacturing costs (Good and Wu, 2017). It should also be suitable for the intended dosage form, should enhance patient experience with great organoleptic properties, should be easy to source and should adhere to pharmacopeial regulations (Quijano, 2017). All of the selected excipients for this study were freely available in the laboratory, with good toxicity profiles. As a result, poloxamer 188, HPMC and methylcellulose 450 served dual functions. Poloxamer 188 was used as an emulsifier in the preparation of SLNs and as a thermogelling polymer in the preparation of the hydrogel. HPMC and methylcellulose 450 both served as mucoadhesive and thermo-gelling agents in the preparation of the hydrogel.

3.3.3 Solvents

Solvents account for more than half of the materials used in the manufacturing process of pharmaceutical products (Welton, 2015). Solvents are chemical substances that dissolve, suspend or extract materials without altering the chemistry of the material in question or the solvent itself. In pharmaceutical manufacturing, solvents provide a reaction medium, or can be used for the extraction or purification of compounds (Grodowska and Parczewski, 2010).

Unless otherwise stated, all solvents and reagents were obtained from Sigma Aldrich™ (Steinheim, Germany) or Merck™ (Dramstadt, Germany) and were of analytical grade. Filtration of all solvents by means of a vacuum filter was done prior to use. All waters used underwent reverse osmosis purification (Purite™ Select Analyst, Camlab, United Kingdom).

3.4 ANALYTICAL METHOD DEVELOPMENT

3.4.1 Introduction

In the field of pharmaceutical drug development, analytical method development is a process of selecting and assaying for the determination of constituents within a formulation. This process comprises the development and validation of an assay method that can successfully identify, quantify and separate active ingredient(s) within a complex mixture (Chauhan *et al.,* 2015). Analytical method development and validation run parallel to the evolution of the dosage form. The initial phase of method development focusses on the chemical behaviour of an active ingredient(s) in order to generate a model that supports stability, pre-clinical and toxicity evaluations (Ahmad *et al.,* 2018).

There are countless techniques used to generate this initial model, such as HPLC, gas chromatography, capillary electrophoresis and proton nuclear magnetic resonance (NMR) that have been employed for the quantification of MNZ in bulk or complex pharmaceutical mixtures (Belal and Haggag, 2012). However, these methods are rarely utilised due to their high costs, complexity or rarity of equipment in most standard laboratories. Therefore, techniques which promote simplicity, selectivity and rapidity are considered more ideal (Paczkowska *et al.,* 2014). Thus, HPLC with PDA detection

was selected as the instrumentation of choice for this study, owing to its availability in the laboratory facility, simplicity and frequent use in published literature (see Section 3.21). This choice was also made based on how HPLC demonstrates high sensitivity and selectivity when compared with traditional chromatographic techniques (Guillarme *et al.,* 2010).

3.4.2 Principles of high performance liquid chromatography (HPLC)

3.4.2.1 Separation of analyte

Analyte separation by means of chromatography is reliant on molecular size, net charge of molecule and the affinity of the analyte for the organic solvent at high pressure (Coskun, 2016). Several methods, such as ion-exchange, size-exclusion and normal (NP-HPLC) or reverse phase (RP-HPLC) chromatography are used as separation techniques (Thammana, 2016). Characteristics of the various separation techniques are summarised in Table 3.4.

Table 3.4: Characteristics of high performance liquid chromatography (HPLC) separation techniques (adapted from Thammana, 2016)

Separation technique	Mobile phase (MP)	Stationary phase	Analyte characteristics
Normal phase	Non-polar solvent	Polar	Longer retention of polar compounds
Reversed phase	Polar solvent	Non-polar	Quick elution of polar compounds
Ion exchange/Ion pair	Aqueous buffer	Ionic groups	Suitable for charged molecules only
Affinity	Multi-component MP	Gel matrix (e.g. cellulose beads)	For isolation of proteins, enzymes and antibodies
Size exclusion	Organic solvent	Porous silica/gel	Large molecules undergo rapid elution

Normal- and reversed-phase techniques are characterised by the polarity of mobile and stationary phases, respectively (Ačanski *et al.,* 2003). In NP-HPLC, the stationary phase (e.g. silica gel) is polar with a non-polar MP that causes prolonged retention of polar samples within the column packing. Conversely, RP-HPLC utilises non-polar stationary material with a polar MP in order to prolong the elution of non-polar materials (Jandera, 2002). Furthermore, the elution polarity allows for additional classification into isocratic or gradient elution. In isocratic elution, the MP composition is kept constant for the entire analysis, whilst the latter requires a variation of the MP throughout a single analysis (Schellinger and Carr, 2006).

Ion-exchange chromatography comprises of a charged surface stationary phase which interacts with sample ions that carry the opposing charge. This technique is suitable for ionic or ionisable analytes (Moustafa and Morsi, 2013). The strength of the charge determines the extent of affinity of the analyte to the surface. The MP is an aqueous buffer where pH and ionic strength can be manipulated to vary the retention times of the analyte (Kunin and McGarvey, 1962).

For the purposes of this study, RP-HPLC was selected as the analytical method of choice for the quantification of MNZ. This choice was based on how RP-HPLC represents the most common analytical method of separation in the pharmaceutical, biomedical and food industries (Prathap and Nishat, 2013). It is also useful in the separation of many compounds, and can employ a wide a range of stationary phases and MPs so as to alter the retention and sensitivity of a given analyte (Sabir *et al.,* 2013).

3.4.2.2 Method of detection

HPLC detectors obtain spectral profiles of a compound. To facilitate adequate detection, the analyte absorbance of light should exceed that of the matrix at the given wavelength (Swartz, 2010). The selection of the correct detector type is dependent on the physicochemical properties of the analyte, its limit of detection (LoD), cost and availability of equipment (Wittrig, 2003).

Ultraviolet (UV)/visible (VIS) detectors are able to measure compounds in the absorption spectrum of the UV and VIS region. These detectors employ a deuterium (D_2) lamp as a light source, with a wavelength range of 190 to 300 nm. For analytes

requiring detector wavelengths of greater than 380 nm, a tungsten (W) lamp is used (Swartz, 2010). The detection of MNZ is conducted at a lower wavelength (UV) since it lacks strong chromophore groups (Patel *et al.,* 2016).

Single UV/VIS detectors generate information at a single wavelength, which can be impractical and time-consuming in the development of new analytical methods. To optimise practicality and method efficiency, the use of multiple diode array detectors (DADs) is encouraged (Swartz, 2010). DADs facilitate the generation of information over a wide range of wavelengths, concurrently. Furthermore, photodiode array DADs offer rapid, low-noise analysis (Martono *et al.,* 2017) that deemed this detection method the appropriate choice for the purposes of this study.

3.4.2.3 Column selection

HPLC columns are responsible for the separation of compounds in a mixture into their various components. These columns constitute the stationary phase in HPLC (Ncube *et al.,* 2016). RP-HPLC columns are comprised of non-polar hydrophobic packing materials. Modern columns derived from silica packing material contain hydrophobic coatings that ensure the rapid elution of hydrophobic compounds. Various matrices, such as silica, polymers and alumina are also available for use (Kazakevich and Lobrutto, 2007).

Great emphasis is placed on column selection during method development as this demonstrates a direct effect on the selectivity and efficiency of a method (Taylor, 2016). Silica columns are used in abundance in related literature, due to their strength, easy derivatisation and manufacturing. In addition, the minimum compression of packing materials occurs under high pressure, which results in negligible deformation of the column (Young and Weigang, 2002). For analyses requiring a pH of greater than seven, standard silica columns are not ideal (Kirkland *et al.,* 1997). Table 3.5 provides a review of several RP-HPLC column types.

Table 3.5: Comparison of RP-HPLC column types showing compounds in order of increasing polarity and decreasing retention of non-polar compounds (adapted from Claessens, 1999; Cledera *et al.*, 2007).

Column type	Structure	Polarity	Retention of non-polar compounds
C_{18} (octadecyl) – $C_{18}H_{37}$	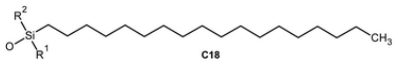	↓	↑
C_8 (octyl)	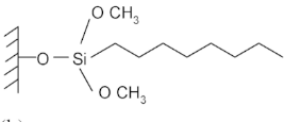		
C_4 (butyl)	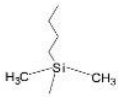		
Cyano – $(CH_2)_3CN$	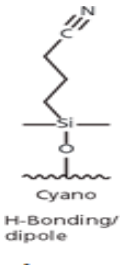		
Phenyl – $C_6H_5(-C_{12}H_9)$	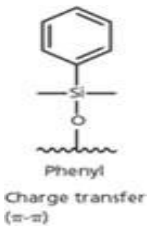		
Amino – $(CH_2)_3NH_2$	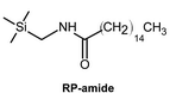		

The most commonly used columns in RP-HPLC are silica-based gels in which octadecyl chains are covalently bound in order to free hydroxyl groups (Kazakevich and Lobrutto, 2007). These columns are referred to as the C_{18} phase. The silica particles contained within the column contain unreacted silanol groups that may form secondary polar interactions with the analyte, which can result in peak broadening and is considered to be disadvantageous (Claessens, 1999). Modification of silica gels with increasing polarity, such as the C_8 phase, can be used at higher pressures and across a wider pH range of 2-8.5 (Nagy and Vekey, 2008).

Although an existing pharmacopeia method is available for the quantification of MNZ by means of RP-HPLC which utilises a C_{18} phase, its limited availability in the study's laboratory and time constraints for delivery warranted the use of a C_8 column for the purposes of this research. This column was ideal due to its particle size and porosity that aid in the separation of compounds. Furthermore, its inert nature minimises interactions with other materials in the sample phase or MP (Claessens, 1999). The retention of compounds occurs by means of apolar interactions between the stationary phase and the analyte (Jandera and Hajek, 2017).

3.4.3 Experimental

3.4.3.1 Sample preparation

Sample preparation is a critical step of method development (Ravisankar *et al.,* 2015). Therefore, the following points need to be taken into consideration prior to the preparation of each sample:

1. The stability of the analyte in solution. This ensures that the solution does not undergo rapid degradation under laboratory or storage conditions;
2. For RP-HPLC, the solubility of the analyte. This needs to be in an appropriate polar organic solvent, such as methanol. It is of great importance to ensure the absence of precipitation materials during analysis, as precipitated materials often lead to blockages of columns and HPLC lines that can lead in poor results or damage to the apparatus; and
3. The filtration of samples prior to analysis. This is done by means of suitable micron pore filters and is adequate for the removal of particles in the solution.

In addition, filtration functions as a preventative maintenance tool for the apparatus (Smith, 2011).

Based on these aforementioned considerations, a stock solution was prepared by dissolving 20 mg of accurately-weighed (Mettler Toledo^{TM} XP205, Ohio, USA) MNZ in 8.5 ml of methanol. The resultant solution was agitated mechanically to facilitate adequate dissolution of MNZ, after which water was added to yield a final volume of 10 ml. The stock solution was prepared freshly prior to use in order to ensure that no degradation of the sample occurred prior to analysis. This stock solution would undergo necessary dilution with a premixed solution of methanol, namely water (85:15) in order to yield the required concentration for a specific experimental run. Proper

3.4.3.2 Mobile phase (MP) optimisation

MP composition demonstrates the greatest influence on sample retention times and separation characteristics (Guillaume and Peyrin, 2000). As a result, the selectivity of a method can be manipulated through the alteration of the quantity of the organic modifier or the pH (in cases where a buffer is utilised) (Crawford Scientific, 2017). Some of the most commonly used solvents in RP-HPLC are illustrated in Figure 3.3.

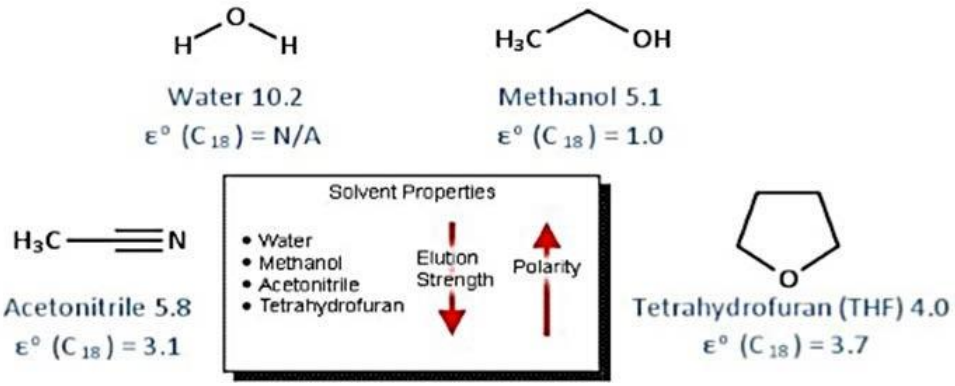

Figure 3.3: Commonly used solvents for RP-HPLC (Crawford Scientific, 2017).

An ideal solvent should be water miscible, have favourable solubility properties, be chemically inert and possess low viscosity and UV detection absorbance (Crawford Scientific, 2017).

i. Selection of organic phase ratio

Hermawan and colleagues (2017) proposed an RP-HPLC method for the quantification of miconazole using a C_8 column. Up to the date of their publication, the authors had not come across any other published literature that had successfully used a C_8 column for the quantification of MNZ by means of RP-HPLC (Hermawan *et al*., 2017). The outcomes of their research resulted in highly sensitive and reproducible results, however, due to limited information provided by the authors regarding the chromatographic conditions, the method could not be replicated. Yet, the Hermawan *et al.* (2017) study served as a template for the selection of the MP composition used in this current study.

Specifically, MeOH and H_2O were utilised for the MP in various ratios. MeOH provides excellent retention characteristics and allows for sufficient solubility of MNZ (Cavrini *et al.,* 1989). MeOH is also an organic solvent that has been employed in the RP-HPLC analysis of many compounds. It is readily available in many standard laboratories, is cost-effective and has demonstrated sufficient compatibility with MNZ (Crawford Scientific, 2017). H_2O is considered chromatographically weak due to its polarity, as it repels hydrophobic analytes into the stationary phase which results in the extension of analyte retention. The addition of the organic modifier (i.e. MeOH) to the H_2O results in rapid elution of the analyte as a result of the decreased polarity of the MP (Gillar *et al.,* 2014).

Additionally, in this study, a 0.25 mg/ml standard solution was prepared by the dilution of stock solution with a premix solution of H_2O and MeOH (15:85). The solution was agitated mechanically to facilitate adequate mixing, after which it was filtered using a 0.45 µm, polyvinylidene fluoride (PVDF) filter (Sartorius™, Goettingen, Germany) to remove any suspended particles. One millilitre of the resultant solution was transferred into three respective 1.5 ml (32 × 11.6 mm) sample vials (LaPha-Pack™, ThermoFischer Scientific™, Massachusetts, USA) for assay. The influence of the organic modifier was investigated by varying its composition at predetermined concentration levels, at a fixed temperature and flow rate. Analytical grade MeOH and vacuum-filtered reverse osmosis H_2O were then placed in separate containers and were mixed online.

ii. Use of buffers

Buffers are aqueous systems that facilitate the resistance of pH changes when small quantities of acid or base are added. They are comprised of a weak acid and a conjugate base, or vice versa (Heinisch and Rocca, 2004). Buffers function by minimising changes in hydrogen ion concentration, thus stabilising the pH within a narrow range. Their potential for use to control the ionisation state of analytes in RP-HPLC has been explored extensively (Lupo and Kahler, 2017).

For the purposes of this study, the use of buffers within the MP was investigated so as to ascertain whether or not its use resulted in better selectivity and retention of MNZ when compared to the proposed organic phase and water mixture. Preliminary investigations and literature reviews conducted suggested that an ammonium acetate buffer (pH 4) was the most suited for RP-HPLC analysis of MNZ (Sahoo and Jain, 2016). The alteration of MP pH can change the extent to which compounds like MNZ are ionised, thus influencing their hydrophobicity. Consequently, such alteration can affect their interaction with the stationary phase and elicit a change in selectivity and elution (Dayyih *et al.,* 2012).

For the preparation of a 0.2 M ammonium acetate buffer solution (pH 4), ammonium acetate salt (15.42 g) was weighed accurately and dissolved in 1000 ml of vacuum-filtered reverse osmosis water and stirred using a magnetic stirrer to facilitate adequate dissolution. The pH of the resultant solution was later adjusted through the dropwise addition of glacial acetic acid (Merck™, Germany) until a final pH of 4 was obtained. The final solution was vacuum-filtered prior to use.

Sample preparation involved the dilution of stock solution with a premix solution of H_20 and MeOH (15:85) to yield a standard concentration of 0.25 mg/ml. The solution was agitated mechanically to facilitate adequate mixing, after which it was filtered using a 0.45 µm, PVDF filter (Sartorius™, Goettingen. Germany) to remove any suspended particles. One millilitre of the resultant solution was transferred into three respective 1.5 ml (32 × 11.6 mm) sample vials (LaPha-Pack™, ThermoFischer Scientific™, Massachusetts, USA) for assay. The use of H_2O in the MP was replaced with an ammonium acetate buffer (pH 4). The mixing of the MP occurred online at predetermined concentration levels. All other chromatographic conditions remained unchanged.

iii. Flow rate optimisation

The volume of MP passing through the column per unit time is known as the flow rate (IUPAC, 1997) and is expressed in ml/min. Adjustments to flow rate demonstrate a direct effect on peak symmetry and analyte elution time. The effect of flow rate is minor when compared to other chromatographic variables; therefore, it is only utilised to fine-tune separation (Crawford Scientific, 2017). Its effect on the developed method was investigated in this study to ensure that a highly sensitive yet rapid method was established. Through a review of the literature it was found that an increase in flow rate results in shorter retention times (Keunchkarian *et al.,* 2006). However, this is not always ideal, as it may cause poor separation of peaks that elute closely. In addition, caution should be taken when working at high rates to ensure that the pressure limit of the apparatus is not exceeded so as to maintain apparatus integrity (McCalley, 2000).

Sample preparation in this study involved the dilution of stock solution with a premix solution of H_2O and MeOH (15:85) to yield a standard concentration of 0.25 mg/ml. The solution was agitated mechanically to facilitate adequate mixing, after which it was filtered using a 0.45 µm, PVDF filter (Sartorius™, Goettingen, Germany) to remove any suspended particles. One millilitre of the resultant solution was transferred into three respective 1.5 ml (32 × 11.6 mm) sample vials (LaPha-Pack™, ThermoFischer Scientific™, Massachusetts, USA) for assay. The prepared samples were analysed in triplicates at each flow rate level, as demonstrated in Table 3.6. Great caution was taken to ensure that the resultant pressure was maintained below 2000 psi.

Table 3.6: Flow rate specifications for optimisation of mobile phase (MP) parameters.

Run	MNZ concentration	Flow rate
1	0.25 mg/ml	0.8 ml/min
2	0.25 mg/ml	1.0 ml/min
3	0.25 mg/ml	1.2 ml/min
4	0.25 mg/ml	1.5 ml/min
5	0.25 mg/ml	2.0 ml/min

3.4.3.3 Injection volume optimisation

Column overloading, poor retention times and asymmetrical peaks are issues associated with poor selection of injection volume. This is due to an increase in the diffusion process time when a sample is loaded on the column (Kazakevich and Lobrutto, 2007). Large injections volumes promote the generation of asymmetrical peaks, which take longer to elute, and, conversely, smaller injection volumes may result in the loss of response (Keunchkarian *et al.,* 2006). The effect of the injection volume on the quantification of MNZ by means of RP-HPLC was investigated in this study to ensure that symmetrical peaks with sufficient purity and clarity were obtained.

The sample preparation process was similar to that of Section 3.4.3.2. Where, sample preparation involved the dilution of stock solution with a premix solution of H_2O and MeOH (15:85) to yield a concentration of 0.25 mg/ml. The solution was agitated mechanically to facilitate adequate mixing, after which it was filtered using a 0.45 µm, PVDF filter (SartoriusTM, Goettingen. Germany) to remove any suspended particles. One millilitre of the resultant solution was transferred into three respective 1.5 ml (32 × 11.6 mm) sample vials (LaPha-Pack™, ThermoFischer Scientific™, Massachusetts, USA) for assay. The prepared sample was analysed in triplicates, whist varying the injection volume with each run. All other chromatographic conditions were kept constant.

3.5 ANALYTICAL METHOD VALIDATION

3.5.1 Introduction

The conduction of method validation is pivotal in proving that the developed method in a study is, indeed, suitable for its intended use. This process assesses the quality, reliability and consistency of analytical results (Ravisankar *et al.,* 2015). The application of method validation is required before the initial use of a method in routine testing, when process is transferred to another laboratory or when conditions or parameters of a method have been altered (Huber, 2007). Figure 3.4 illustrates the International Conference of Harmonisation (ICH) guideline for validation parameters which are discussed in detail in Section 3.5 (*ICH Harmonised Tripartite Guideline* Q2 (R1), 1994). For the purposes of this study, the following validation parameters have been discussed in the methodology: peak symmetry, specificity, linearity, accuracy, intra- and inter-day precision, limit of quantitation (LoQ) and LoD.

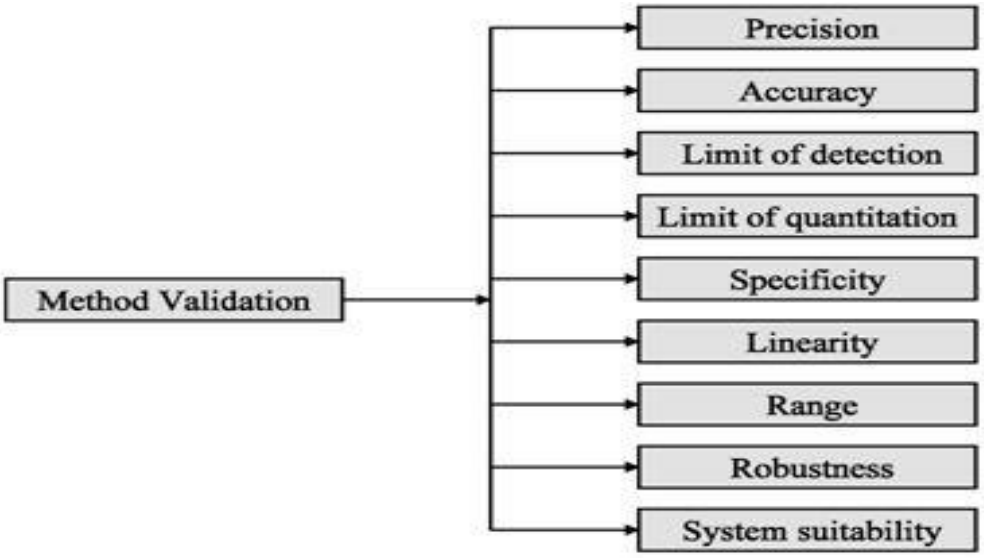

Figure 3.4: International Conference of Harmonisation (ICH) (2005) method validation parameters.

3.5.2 Experimental

3.5.2.1 Peak analysis

A chromatogram is a graphical depiction of the separation of compounds that has occurred in the HPLC system; each observed peak is a representative of the detector response for each analyte (Stoll, 2007). The analysis and optimisation of peak shape and symmetry is vital for ensuring good resolution and the accurate quantification of the analyte (Ravisankar *et al.,* 2015).

The sample preparation process in this part of the study was replicated from Section 3.4.3.2. Where, sample preparation involved the dilution of stock solution with a premix solution of H_2O and MeOH (15:85) to yield a standard concentration of 0.5 mg/ml. The solution was agitated mechanically to facilitate adequate mixing, after which it was filtered using a 0.45 µm, PVDF filter (Sartorius™, Goettingen. Germany) to remove any suspended particles. The freshly-prepared samples were analysed in accordance with the optimised chromatographic conditions (see Section 4.1.2) to yield peak models. With the aid of Equation 3.1, the symmetry of the MNZ peak was calculated. CorelDRAW™ software was employed for the generation of peak dimensions, where information of *a* and *b* values were obtained. Where A_s is the symmetry factor, *a* is the peak width before the centre at baseline and *b* represents the peak width after peak centre at 10% of peak height.

$$A_s = {}^{b}/_{a}$$

Equation 3.1: Calculation of chromatographic peak asymmetry factor (Wahab *et al.,* 2017)

3.5.2.2 Linearity

In method validation, linearity is the process of evaluating an analytical procedure within a particular range in order to obtain a response that is directly proportional to the concentration of an analyte in a given sample (Kazusaki *et al.,* 2012). It is expressed as the confidence limit around the slope of a linear regression line (*ICH Harmonised Tripartite Guideline* Q2 (R1), 1994).

In this study, a freshly-prepared stock solution underwent serial dilution with a MeOH:H_2O (85:15) mixture so as to yield concentrations of 0.25, 0.4, 0.5, 0.6, 1 and

1.5 mg/ml, respectively. Commencing with the most dilute concentration, seven samples (*n*=7) at each concentration level were prepared in three clear glass 1.5 ml (32 × 11.6 mm) short-thread vials (La-Pha-Pack™, ThermoFischer Scientific™. USA). Each sample was then analysed in triplicates by means of RP-HPLC under the optimised conditions.

Data of the peak area was generated, and the corresponding concentration was calculated. The resultant data was analysed on Microsoft Excel® (2016) software in order to generate a graph of the observed signal response as a function of analyte concentration. In addition, relative standard deviation (RSD) values of the mean peak area, assessment values and % RSD were determined. The significance of the plot, as illustrated by Equation 3.2, was also determined.

$$Assessment\ value\ (z) = \frac{y - intercept}{50\%\ of\ measured\ response} \times 100$$

Equation 3.2: Calculation of linearity assessment value (z).

3.5.2.3 Accuracy

Accuracy, also referred to as recovery, is the expression of the closeness of agreement of data between an experimental value and its theoretical value (Paithankar, 2013). It is reported as the % recovery of known amounts of analytes and is expressed in Equation 3.3.

$$\%\ Recovery = \frac{experimental\ yield}{theoretical\ yield} \times 100$$

Equation 3.3: Calculation of % recovery.

A freshly-prepared stock solution was prepared, as previously described in Section 3.4.3.1. Where, sample preparation involved the dilution of stock solution with a premix solution of H_2O and MeOH (15:85) to yield a standard concentration of 0.5 mg/ml. The solution was agitated mechanically to facilitate adequate mixing, after which it was filtered using a 0.45 µm, PVDF filter (Sartorius™, Goettingen. Germany) to remove any suspended particles. This solution underwent further dilution with a MeOH:H_2O (85:15) mix so as to yield concentrations of 0.5 and 1.0 mg/ml, respectively. Commencing with

the most dilute concentration, each solution was filtered into six (*n*=6) clear short-thread vials (La-Pha-Pack™, Thermofischer Scientific™, USA). Each sample was then analysed under optimised chromatographic conditions in triplicates, where the consequent data of peak area was gathered. This information was later used to calculate % recovery with the aid of the linear regression equation of the MNZ calibration curve.

3.5.2.4 Precision

Precision, also termed repeatability, is the measurement of variation experienced by a single analyst on a given instrument (Paithankar, 2013). Unfortunately, the determination of precision does not distinguish system variations from other variations experienced during the sample process. It does, however, assume that all variables remain constant for each analysis (Betz *et al.,* 2011).

Six samples (*n*=6) were prepared by diluting a freshly-prepared stock solution (see Section 3.4.3.1) with an 85:15 mix of MeOH and H_2O so as to yield a concentration of 1.5 mg/ml. One millilitre of the resultant solution was filtered into clear short-thread vials and analysed by means of RP-HPLC in triplicates. All samples were analysed under the predetermined chromatographic conditions. The mean % recoveries and respective % RSD of each sample were determined.

i. Intermediate precision

Intermediate precision focusses on the influence of variations within a laboratory as well as on the overall recovery of the analyte in a sample (Betz *et al.,* 2011). Factors for assessment in this section include the variation of machinery, working days or operator (Tiwari and Tiwari, 2010). For the purposes of this study, machinery, chromatographic conditions and operating personnel were kept constant, whilst the days of operation were varied.

Six samples (*n*=6) were prepared by diluting a freshly-prepared stock solution (see Section 3.4.3.1) with an 85:15 mix of MeOH and H_2O so as to yield a concentration of 1.5 mg/ml. One millilitre of the resultant solution was filtered into clear vials and analysed by means of HPLC in triplicates. The % recovery and RSD were calculated accordingly. This process was then repeated on day three and seven after the initial run by keeping all variables constant.

3.5.2.5 Limit of detection (LoD)

The LoD of a sample is defined as the smallest quantity that can be detected by a given method above the noise level of a system (Armbruster and Pry, 2008). The simple approach to determining the LoD is based on the signal-to-noise ratio in which measured signals from samples of known concentration are compared to those of blank samples (Sengul, 2016). An alternative approach to LoD determination is based on the standard deviation (SD) of the response and slope, as expressed by Equation 3.4, where σ is the SD of the slope and *S* is the gradient of the calibration curve.

$$Limit\ of\ detection\ (LoD) = \frac{3.3\sigma}{S}$$

Equation 3.4: Calculating limit of detection (LoD).

A further alternative approach to LoD determination is based on the visual assessment method. This method entails the definition of LoD through the analysis of various samples of known concentration and the establishment of the minimum level at which the analyte can be reliably detected (Sengul, 2016). Piano and Moore (1999) suggest that any of the aforementioned methods are favourable for the determination of LoD. Therefore, the final choice of technique is governed by the operator. Owing to the simplicity of the method, the LoD approach was determined best for the purposed of this study, with the aid of the aforementioned equation.

3.5.2.6 Limit of quantitation (LoQ)

The lowest amount of analyte that can be reliably quantified is known as the LoQ (Armbruster and Pry, 2008). Detector sensitivity and appropriate sample preparation techniques are the main influencers of LoQ data reliability (Paithankar, 2013). It is critical, therefore, that the operator ensures that the preparation of samples is conducted with the outmost accuracy and that the apparatus is well-maintained (Smith, 2011).

Additionally, the technique for the establishment of LoQ is left to the discretion of the operator (Piano and Moore, 1999). For the purposes of this study, LoQ was determined through from the signal-to-noise ratio, where the LoQ corresponds to 10 times the noise level (see Equation 3.5), and where σ represents the SD of the linear calibration curve and *S* is the slope of the regression line (Shrivastava and Gupta, 2011).

$$Limit\ of\ quantitation\ (LoQ) = \frac{10\sigma}{S}$$

Equation 3.5: Calculation of limit of quantitation (LoQ).

3.5.2.7 Specificity

The ability to distinguish an analyte in a complex mixture without interference from other components is referred to as the specificity of an analytical method (McPollin, 2009). Various tests need to be conducted to ascertain specificity. Firstly, identification tests are employed to establish the identity of the analyte being investigated. This process comprises qualitative data in which the ability to discern between compounds of closely linked structures or comparisons of reference material is demonstrated (Ravisankar *et al.,* 2015). These identification tests are run concurrently to the assays that assist in the quantification of the analyte, where content or potency of the analyte are established (Betz *et al.,* 2011). Secondly, samples are spiked in order to illustrate that the method results are unbothered in the presence of impurities, excipients or degradants. Lastly, purity tests are carried out so as to ensure that the developed method allows for accurate statements of impurity content that could result from the contamination of organic solvents in the MP or degradants from stress testing (McPollin, 2009).

When it is impossible to demonstrate specificity by spiking the sample, the operator can opt to compare their results with a well-characterised procedure, or include results of samples obtained under appropriate stress conditions (Swartz, 2006). For the purposes of this study the sample was not spiked with an internal standard to ascertain specificity. Rather, the samples underwent forced degradation studies under predetermined stress conditions.

Forced degradation studies, also referred to as stress testing, are procedures that subject an API or drug product to severe and accelerated conditions so as to generate degradation products, which are, in turn, used to establish the stability of the molecule

(Iram *et al.,* 2016). The chosen stability-indicating method used for the quantification of the API should be able to detect the loss of content and subsequent increase in degradation compounds (Bajaj *et al.,* 2012). The information generated from these forced degradation studies aided the selection of the appropriate dosage forms for the API, storage conditions and primary or secondary packaging of the API or the final drug product in this study.

i. Selecting experimental conditions

The ICH has developed and adopted a set of guidelines for forced degradation studies which are alluded to in general terms for commercialisation purposes (*ICH Harmonised Tripartite Guidelines* Q1A, 2003; *ICH Harmonised Tripartite Guidelines* Q1B, 1996). However, these guidelines can also be applied to the development of stability-indicating methods during the developmental phase (Venkataraman and Manasa, 2018). Due to the very general conditions stated by the ICH and the structural diversity of analytes, there is a wide array of experimental conditions available for the conduction of stability-indicating studies. For established molecules, such as MNZ, the stability-indicating studies are defined by previous work in well-documented literature to facilitate consistency throughout development (Hicks, 2012).

General experimental conditions include acid/alkali hydrolysis, oxidation, photolysis and thermal degradation (Venkataraman and Manasa, 2018). Striking a balance between experimental conditions with regard to temperature, extent of degradation or duration of experiment is vital because if minimal stress is applied, some degradation pathways may not be apparent, which can result in partial detection of the API and its degradant products. Conversely, if excessive force is applied, then unrealistic results may be obtained, which could deem the method unsuitable for use. It is, therefore, suggested that careful consideration of API physicochemical properties and degradation under typical conditions, use and storage be taken into account when selecting these experimental conditions (Reynolds *et al.,* 2002).

ii. Identification and characterisation of drug products

Conventional methods, such as liquid chromatography (LC), mass spectrometry (MS) and NMR spectroscopy can be used in the identification and quantification of drug products. RP-HPLC, however, remains the preferred method of quantification for

stability-indicating assays (Khoshk and Afshar, 2014; Bisht *et al.,* 2017). Advantages of RP-HPLC include its compatibility with numerous organic solvents, precision, sensitivity and ability to detect polar compounds (Amanolahi *et al.,* 2017). Therefore, RP-HPLC was selected as the method of choice for this study, where the optimised chromatographic conditions were applied for the quantification of MNZ and separation of peaks.

iii. Acid/alkali hydrolysis

Hydrolysis is the decomposition of a compound by its reaction with H_20. Acids or alkali catalyse the hydrolysis of ionisable functional groups that are present in the analyte (Iram *et al.,* 2016). Degradation happens when an interaction between an analyte and acid/base occurs and produces primary degradants within a desirable range (Rao *et al.,* 2015).

Strong acids, such as hydrochloric acid or sulphuric acid, in the concentration range of 0.1 to 1 M are employed for acidic hydrolysis tests. Sodium or potassium hydroxide, in the concentration range of 0.1 to 1 M is employed for basic hydrolysis testing (Blessy *et al.,* 2014). For the acid and alkali stress testing that took place in this study, two separate 10 ml solutions (0.5 mg/ml MNZ) were prepared and equal amounts of 1 M of HCL and 1 M of NaOH, respectively, were added. Each solution was then refluxed for 120 minutes at 80 °C. Upon completion, all solutions were neutralised prior to assay in order to maintain system integrity. The resultant solutions were filtered and transferred to sample vials and analysed by means of RP-HPLC under optimised chromatographic conditions.

iv. Oxidation

Many drugs have the potential to undergo autoxidation as a consequence of long-term storage conditions. This process involves a free-radical reaction that requires an initiator to facilitate a chain reaction. Hydrogen peroxide, metal ions or minute levels of impurities can act as potential initiators for autoxidation (Rawat and Pandey, 2015). For stability-indicating methods, hydrogen peroxide (H_2O_2) is a commonly used oxidant that produces degradants during long-term stability studies of pharmaceutical formulations (Sharma and Murugesan, 2017). It is used at concentrations of three to 30% at temperatures below 40 °C for a maximum of eight days.

In this study, equal amounts of a 3% v/v H_2O_2 solution were added to 10 ml of a 0.5 mg/ml MNZ solution. The resultant solution was transferred into a round bottom flask and refluxed at 80 °C for 120 minutes. The solution was then allowed to cool to room temperature and filtered into clear short-thread vials and analysed by means of RP-HPLC.

v. Photolytic degradation

Photolytic stress studies investigate the potential of light to produce degradants within pharmaceutical ingredients and preparations. The rate of degradation is often directly proportional to the light intensity and the amount of light absorbed by a sample (Venkataraman and Manasa, 2018). This kind of investigation can be carried out by exposing a drug product to a combination of VIS and UV light in the range of 300 to 800 nm (Iram *et al.,* 2016).

Photolytic degradation occurs through oxidative or non-oxidative degradation (Shinde *et al.,* 2013). Isomerisation, cyclisation, dimerisation, decarboxylation and haemolytic cleavage of X-C bonds, rearrangement, dealkylation and deamination all constitute as non-oxidative reactions. Furthermore, oxidative reactions occur through singlet oxygen or triplet oxygen mechanisms. Oxidative reactions assume that light can act as a catalyst for oxidation reactions (Rawat and Pandey, 2015).

In this study, a 0.5 mg/ml MNZ solution was prepared by diluting the stock solution with the MP (MeOH 85% v/v and H_2O 15% v/v). The resultant solution was filtered and transferred to a stoppered glass vial and placed in an incubation chamber (Binder™, Tuttlingen, Germany). The sample was then stored for 48 hours at ambient conditions at 1.6-ICH compliant UV-A Illumination (ICH Harmonised Tripartite Guidelines Q1B, 1996), after which the sample was analysed by means of RP-HPLC in triplicates. An additional control sample was prepared and placed in a ‘dark-room’; after 48 hours this control sample was also analysed by means of RP-HPLC.

vi. Thermal degradation

Temperature has a direct effect on the rate of a chemical reaction, where its increase directly results in an increase of the reaction rate. Hence, the analyte and formulation of a sample are susceptible to degradation when exposed to higher temperatures (Kaul

et al., 2005). The mechanism of thermal degradation involves hydrolytic, pyrolysis, isomerisation, decarboxylation, rearrangement and polymerisation reactions. Temperatures exceeding 80 °C result in sporadic outcomes that are not indicative of the analyte's pathway of decomposition (Rawat and Pandey, 2015).

For the purposes of this study, a 0.5 mg/ml solution was prepared by diluting the stock solution with the MP (MeOH 85% v/v and H_2O 15% v/v). The resultant solution was filtered and separated into three stoppered vials. Each vial was then either placed in a 25, 60, or 80 °C incubation chamber. Withdrawal of sample solutions from each vial for RP-HPLC analysis at 60 minutes, 24, 72 and 120 hours was done in triplicate.

3.6 DRUG-EXCIPIENT COMPATIBILITY STUDIES

3.6.1 Introduction

It is of great importance that the compatibility of excipients with the APIs are investigated prior to the formulation of a dosage form. This kind of investigation ensures that the excipients' interaction do not lead to instability or the formation of new chemical entities that possess alternative physiochemical or pharmacological properties. Investigative methods, such as thermal, chromatographic or spectroscopic analysis have been employed for compatibility studies (Patel *et al.,* 2015; Ozioko, 2017).
This study determined that thermal analysis comprises numerous techniques that aid with the monitoring of physical and chemical changes of a sample that occur when the temperature is varied (Radic, 2017). Techniques, such as DSC or differential thermal analysis (DTA), are used to determine sample purity, polymorphism, heat of solvation, thermal degradation of API or excipients, as well as the glass transition temperature of polymers. All these techniques allow for the determination of drug-excipient compatibility. However, DSC provides rapid identification of the physicochemical interactions (Deangelis and Papariello, 1968), and was, therefore, chosen for the purposes of this study.

3.6.2 Differential scanning calorimetry (DSC)

DSC is a thermal analytical technique that utilises controlled resistance heaters to individually heat a sample and a reference compound at a predetermined rate (Gill *et al.,* 2010). The change in heat flow between the sample and reference compound are monitored against time and temperature when the substances undergo a thermal event, such as melting or crystallisation. Probable interactions between components

are noted according to their change in corresponding enthalpy, appearance or disappearance of shift in endo- or exothermic peaks (Steinmann *et al.,* 2013). DSC is ideal for the purposes of this study as it operates over a wide range of temperature changes, produces rapid results and consumes miniscule sample quantities. Furthermore, the results obtained from DSC studies correlate with those of stability tests (Navartilova *et al.,* 2014). Thus, it was deemed to be the ideal method for the prediction of pharmaceutical product stability in this study.

It should be noted, however, that some limitations of DSC include the poor detection of samples upon long-term storage, high sensitivity, the inability to effectively monitor minute sample changes and possible misinterpretation of data by the operator. The observation of interactions at high temperatures is also not guaranteed upon storage of a product at ambient temperature (Deangelis and Papariello, 1968).

3.6.3 Experimental

3.6.3.1 Thermal analysis

For this study, thermal analysis of MNZ microcrystalline powder, cholesterol and MNZ-cholesterol mix was conducted using simultaneous thermogravemetric analysis (TGA) and DSC utilising a SDT Q600 (TA instrument™, Utah, USA). An empty aluminium pan was used as a reference. DSC scans were recorded at a flow rate of 100 ml/min and a heating rate of 10 °C/min in the temperature range of 25 to 350 °C.

Sample preparation consisted of the accurate weighing of MNZ and cholesterol, respectively, onto the sample pan and analysing the compounds individually. For the preparation of an MNZ-cholesterol mix, a ratio between lipid and API for the solid lipid nanoparticles (SLNs) was proposed. This ratio was then utilised to formulate a binary mix of MNZ and cholesterol. The two compounds were dissolved in 10 ml of a 1:1 mixture of chloroform and methanol. The solvent was then removed by means of a rotary evaporator (Buchi-210 Rotavapor™, Switzerland). The resultant solid was weighed and placed on the DSC sample pan for analysis. Further details regarding the findings of this process will be presented in the following chapter.

3.7 DEVELOPMENT AND OPTIMISATION OF MNZ-LOADED SOLID NANOPARTICLES (MNZ-SLNs)

3.7.1 Introduction

The development of novel pharmaceutical dosage forms, such as SLNs, follows a process of combining various chemicals and compounds with the API to form a final dosage form (Patel *et al.,* 2015). For the purposes of this study, SLNs functioned as a carrier for the API. This carrier was later incorporated into a semi-solid dosage form for its intended clinical use.

Optimisation is a method of improving the performance of a process, system or product in order to gain maximal benefit. Pharmaceutical optimisation is achieved by realising conditions that yield the best response (Garg and Singhvi, 2015). Formerly, optimisation involved the monitoring of the influence of one factor at a time for a specific experimental response. This way of thinking resulted in lengthy processes that yielded no information on the interactive effect between the studied factors. Consequently, it also resulted in increasing expenses owing to the consumption of more materials (Vakilinezhad *et al.,* 2018). To overcome these shortcomings, multivariate statistical techniques, such as response surface methodology RSM were adapted into the optimisation of analytical processes (Bezerra *et al.,* 2008). Figure 3.5 illustrates a simple flow chart of an ideal optimisation process.

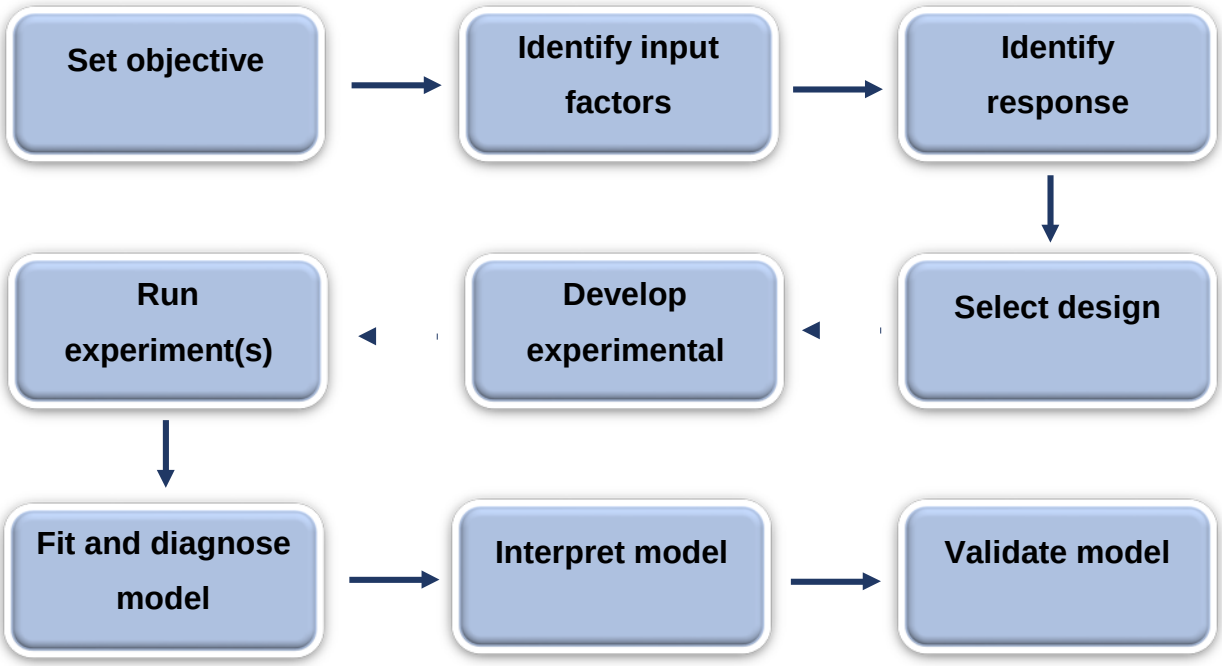

Figure 3.5: Flow chart of pharmaceutical optimisation process (SixSigma, 2018)

Prior to the application of RSM, it is vital that objectives, input variables and expected responses (i.e. output variables) are defined in order to serve as a guide for the experimental procedure (Garg and Singhvi, 2015). Once these variables have been identified, a statistical design should be selected in order to generate an experimental run sheet for the operator. Upon the completion of the experiments, the findings are used to fit and diagnose a model, after which the model is interpreted and validated.

3.7.1.1 Response surface methodology (RSM)

RSM is a statistical tool that is used to empirically derive a functional relationship between an input variable and an experimental response so as to aid with the development, improvement and optimisation of processes. RSM is used extensively in the industrial field to identify input variables that can potentially influence the performance or quality of a product (Behera *et al.,* 2018). It was employed in this study to optimise formulation parameters and identify possible interactive effects between the selected variables.

The term ‘response’ implies the measurement of performance or product characteristics. A variable is a feature or characteristic that is altered during an experiment (Garg and Singhvi, 2015). During RSM, the operator is responsible for the control of input variables, which are also commonly referred to as independent variables. Output variables, also known as dependent variables, are measured responses or characteristics (Schneider *et al.,* 2010). The operator should be mindful when selecting these variables, because an increase in the number of output factors can result in a more complex optimisation process. A response surface can only be generated once a relationship between input and output variables have been established (Raissi and Eslami-Farsani, 2009).

The improvement of statistical methods through the introduction of RSM has allowed for the simultaneous consideration of possible interacting factors, thereby saving time and finances within pharmaceutical developmental processes. In addition, RSM also enables the detection of faults in the process since a trial and error method is not used (Bezerra *et al.,* 2008). RSM also accounts for interactions between many variables and maximises the generation of information through minimal experimental runs (Spall, 2010). When compared to conventional statistical methods, RSM offers a greater amount of data and is a more economical approach since a small number of

experiments are performed for monitoring the interaction of the independent variables on the response (Wani *et al.,* 2012), hence was selected as the method of choice for the purposes of this study.

i. Mathematical modelling

Empirical mathematical models are employed in RSM for the estimation of process performance and the generation of approximation models which are, in turn, used for the prediction of a response in a given process (Chhabra and Singh, 2011). Once an appropriate model has been identified, an approximated surface is produced. The gathered data of the approximated surface is then used for the optimisation of process conditions (Malakar *et al.,* 2012). Equations 3.6, 3.7 and 3.8 demonstrate the most commonly used mathematical models, respectively.

$$y = \beta_0 + \beta_1 x_1 + \beta_2 x_2 + \cdots + \varepsilon$$

Equation 3.6: 1st order empirical model.

$$y = \beta_0 + \beta_1 x_1 + \beta_2 x_2 + \beta_{12} x_1 x_2 + \cdots + \varepsilon$$

Equation 3.7: Screening response model.

$$y = \beta_0 + \beta_1 x_1 + \beta_2 x_2 + \beta_{12} x_1 x_2 + \beta_{11} {x_1}^2 + \beta_{22} {x_2}^2 + \cdots + \varepsilon$$

Equation 3.8: 2nd order empirical model.

In each of these equations, *y* is the estimated response, *xi* represents the input factors, β_0 is the intercept constant, β_i is the first-order co-efficient, β_{ii} is the co-efficient of the second-order terms and β_{ij} is the co-efficient of the second-order interaction terms.

The first-order empirical model is appropriate when an operator is investigating the true response surface over a small region of the input variable in a linear location of the function (Myers *et al.,* 2009). If there are any notable interactions between the variable (xi), the addition of the interaction term (see Equation 3.7) introduces a curvature. For situations where the interaction term is inadequate for producing linearity in the response function, a second-order model (see Equation 3.8) is employed. This model is commonly used in RSM due to its flexibility, where it can take on a wide array of functional forms and the least squares are easily used to estimate co-efficient parameters (β) (Carley *et al.,* 2004). The pharmaceutical industry employs second-

order empirical modelling extensively, thus allowing operators to establish a relationship between input variables and a response; determine the significance of input factors; and define optimum values for these variables over a region of interest (Peasura, 2015).

ii. Experimental design

Within an experimental design, the introduction of statistical analysis during the initial stages of research and not in the final product is implemented to ensure that quality is built into the product (Politis *et al.,* 2017). For the purposes of this research, statistical design of experiments (DoE) by means of a central composite rotatable design (CCRD) was investigated for establishing a relationship between process input factors and the generated response.

CCRD, also referred to as a Box-Wilson design, is a systematic statistical method (Dutka *et al.,* 2015). This method incorporates five levels, coded –α, -1, 0, +1 and +α. It is the largest factorial design for three factors and the smallest for ≥ 5 factors. CCRD comprises axial and factorial points around a centre point using second-order statistics where 2 ≤ n ≤ 6 (Muriithi *et al.,* 2017). A graphical representation of a two-factor CCRD is illustrated in Figure 3.6.

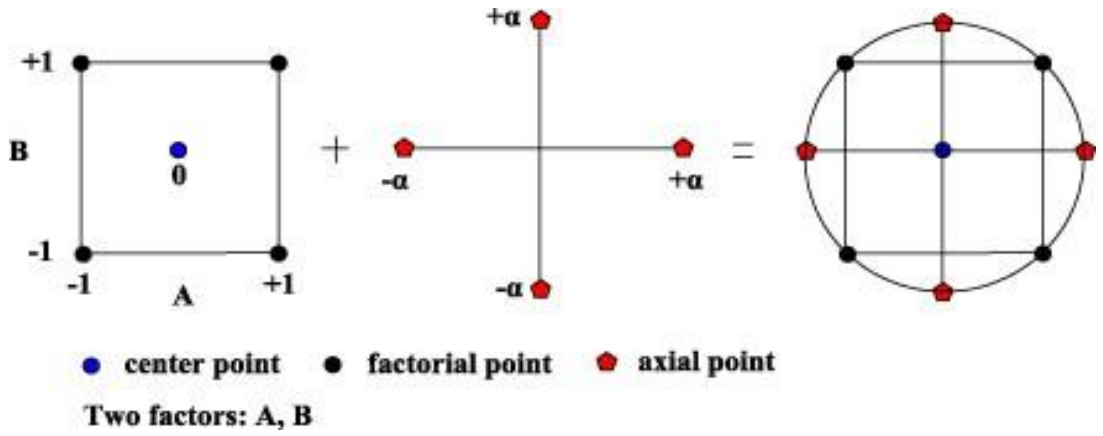

Figure 3.6: Two-factor central composite rotatable design (CCRD) (Salehi *et al.,* 2012).

Equation 3.9 defines the total number of points in a CCRD, where n is equal to the total number of design points and *k* represents the number of input variables.

$$n = 2^k + 2k + n_0$$

Equation 3.9: Number of design points in a central composite rotatable design (CCRD).

The axial consists of 2^k points arranged in a star; the two points lie on the axis of each control variable at a distance of α (see Equation 3.10) from the design centre, where the distance from the centre to any point is always alpha (i.e. axial or factorial points are always alpha units away from the centre, and are, therefore, rotatable) (Salehi *et al.,* 2012). CCRDs are rotatable in a manner that all points are equidistant from the centre. Rotatability denotes the variance of the response function. A rotatable design exists when there is an equal prediction variance for all points at a fixed distance from the centre (Pennsylvania State University, 2018).The factorials then form a cube around the centre using coded levels of -1 and +1, respectively.

$$\alpha = \sqrt{n}$$

Equation 3.10: Defining alpha (α) in central composite rotatable designs (CCRDs).

3.7.2 Experimental

3.7.2.1 Formulation of MNZ-loaded solid lipid nanoparticles (MNZ-SLNs)

For this study, MNZ-SLNs were prepared by means of a novel melt-emulsion ultrasonication and low-temperature solidification method. A lipid phase was first prepared by dissolving a weighed amount of MNZ, cholesterol and soy lecithin in 10 ml of a 1:1 MeOH and chloroform mixture. The organic phase was then removed by means of a rotary evaporator (Buchi210, Rotavapor™, Switzerland) at 70 ± 2 °C for 20 minutes. Meanwhile, an aqueous phase was prepared concurrently by dissolving equal amounts of surfactant (2% v/v polysorbate 80 and 2% m/v poloxamer 188 solution) in H_20 so as to yield a clear solution. The aqueous phase was maintained at 70 ± 2 °C in a warm bath over a hot plate.

Upon complete evaporation of the organic phase, 20 ml of the aqueous phase was added to the lipid phase (under mechanical agitation) in order to yield an opaque white

coarse emulsion. The resultant emulsion was split into two equal parts, where one part underwent PUS and the other underwent bath sonication.

For PUS, the emulsion was placed in an open McCartney glass jar over a warm bath (70 ± 2 °C) and sonicated at 40% power for four minutes. The remainder of the emulsion was poured into a McCartney jar, which was later sealed and placed inside a warm bath sonicator (70 ± 2 °C) for four minutes. The respective nanodispersions were rapidly cooled in an ice bath immediately after sonication so as to facilitate the solidification of the nanoparticles. PCS was then employed for size and dispersion stability characterisation.

3.7.2.2 Design of Experiments (DoE)

A CCRD generated by DesignExpert® software (Version 7.0 StatEase™, Minneapolis, USA) was used to investigate the influence of lipid concentration and sonication time on MNZ-SLNs formulation characteristics. Preliminary studies (drug excipient compatibility studies) assisted with the selection of lipid type, concentration range and sonication time parameters in this study. The investigated input variables and their respective ranges are recorded in Table 3.7.

Table 3.7: Level of factors in central composite rotatable design (CCRD) for the preparation of MNZ-solid lipid nanoparticles (MNZ-SLNs).

Parameters	Levels		Alpha	
	-1	+1	-α	+α
X_A – Lipid conc. (% m/v)	3	4	2.79289	4.20711
X_B – Sonication time (sec.)	240	200	227.574	312.426

DoE involves the planning of experiments to ensure that relevant data is extracted and analysed statistically (Weissman and Anderson, 2015). A 13-run, two-factor and five-level CCRD was generated for the optimisation process within this study. Table 3.8 illustrates the values of lipid concentration and sonication time for each individual run.

Table 3.*8*: Design of Experiments (DoE) for the evaluation of MNZ loaded solid lipid nanoparticles (MNZ-SLNs).

Run	Constants				Variables			
	API	Co-emulsi-fier	Surfactants		Lipid conc.		Sonication time (sec.)	
	MNZ % m/v	Soy lecith. % m/v	Tween 80% v/v	Kolliphor 188% m/v	Level	% m/v	Level	Sec.
1	2	3	2	2	-1	3.0000	+1	300.00
2	2	3	2	2	-α	2.7900	0	270.00
3	2	3	2	2	0	3.5000	0	270.00
4	2	3	2	2	+α	4.2100	0	270.00
5	2	3	2	2	0	3.5000	-α	227.57
6	2	3	2	2	-1	3.0000	-1	240.00
7	2	3	2	2	0	3.5000	0	270.00
8	2	3	2	2	+1	4.0000	+1	300.00
9	2	3	2	2	0	3.5000	0	270.00
10	2	3	2	2	+1	4.0000	-1	240.00
11	2	3	2	2	0	3.5000	0	270.00
12	2	3	2	2	0	3.5000	0	270.00
13	2	3	2	2	0	3.5000	+α	312.43

Thirteen MNZ-SLN formulations were prepared through PUS, as described in Section 3.7.2.1. The lipid and sonication time parameters were varied for each run in accordance with the DoE set out in Table 3.8. The total volume and concentration of the API and surfactant within each formulation was kept constant for each run. Each resultant formulation was split into two, where one part was stored at room temperature (25 ± 2 °C) and the other in a refrigerator (4 ± 2 °C). The resultant formulations were analysed in triplicates for particle size, ZP, PDI and drug content characteristics on days zero, 14 and 28.

3.8 CHARACTERISATION OF OPTIMISED MNZ LOADED SOLID NANOPARTICLES (MNZ-SLNs)

3.8.1 Introduction

Solid lipids are dispersed in an aqueous medium to form SLNs (Mukherjee *et al.,* 2009). Although many advantages, such as bio-tolerability, are attributed to them, SLNs exhibit low DL capacity and drug expulsion upon storage as a result of crystalline transition (Attama *et al.,* 2007). Therefore, characterisation testing is conducted on pharmaceutical formulations to gain insight on SLNs' physical and chemical properties. These properties can demonstrate a direct impact on formulation performance, appearance and stability (Liu, 2005). Characterisation testing can also be conducted on raw and intermediate materials, as well as on the finished product (Anacleto *et al.,* 2018). Various tests and methodologies for the characterisation of SLNs are discussed in this section.

3.8.2 Micro-structure analysis

The determination of particle characteristics is critical for controlling the quality of dispersion and to provide confirmation that the formulated product is indeed within the nanometre range (Singh and Lillard, 2009). PCS, coulter counter (CC), laser diffraction (LD), photosensitive intensity diffraction (PIDS), atomic force microscopy (AFM), field flow fractionation (FFF), transmission or scanning electron microscopy (SEM) and cyrofield scanning microscopy are some techniques that are employed for particle size determination in novel pharmaceutical systems (Akbari *et al.,* 2010).

For the purposes of this study, PCS was employed as the technique of choice, owing to the availability of equipment and simplicity of the method. This commonly used method works by measuring the fluctuation of the intensity of scattered light caused by particle kinetics. The resultant measurement yields a mean diameter (z-avg.) of the bulk population of the particles (Tscharnuter, 2000). In this study, the size measurements obtained from PCS were later validated by means of TEM.

Advantages of PCS include its simple experimental set-up, high-speed analysis, use of low sample volumes, repeatability, reliability and cost-effectiveness. Its use is, however, limited to particles within the nano- to micrometre range (Brar and Verma, 2011).

Particle size (z-avg.), PDI and ZP are additional parameters for demonstrating the production quality and stability of a solid lipid nanodispersion (Akbari *et al.,* 2010). Altogether, these parameters can have a direct effect on the release kinetics and clearance of nanoparticles (Gaumet *et al.,* 2008).

3.8.2.1 Polydispersity index (PDI)

As noted previously, the PDI is a vital parameter that is also defined through PCS. This ratio gives an indication of size distribution within a dispersed system and is defined by Equation 3.11.

$$Polydispersity\ Index\ (PDI) = {}^{M_w}/_{M_n}$$

Equation 3.11: Polydispersity index (PDI) ratio

In this equation, M_n and M_w represent the mean number of molar mass and weight, respectively (Rane, 2005). The numerical values of PDI can range from 0.0 (perfect uniform sample) to 1.0 (highly poly-dispersed sample with multiple size populations). Although pharmaceutical quality standards do not specify criteria for an acceptable PDI of nanodispersions, values below 0.2 are acceptable for polymer-based colloidal systems. As for lipid-based carrier systems, a PDI of <0.3 is acceptable for indicating homogeneity (Danaei *et al.,* 2018).

3.8.2.2 Zeta potential (ZP)

Virtually all particles that come in contact with a liquid acquire an electric charge on their surface. This electrical potential at the shear plane is referred to as the ZP (Khoshnevisan and Barkhi, 2015). ZP is defined as the electrical potential that is created by the presence of a charge on the particle surface, which expresses a degree of repulsion between similarly charged particles. It is quantified from the mean electrophoretic mobility of particles and expressed in millivolts (mV). Depending on the chemistry and the nature of the particle, ZP may have a negative or a positive value

(Ostolska and Wiśniewska, 2014). Figure 3.5 illustrates the schematic distribution of ions around a charged particle.

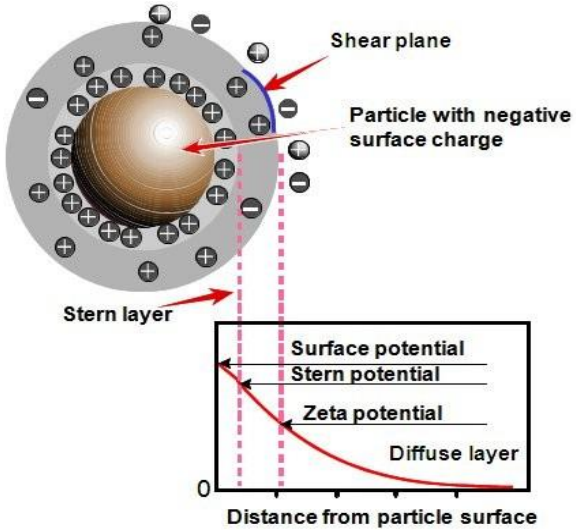

Figure 3.7: Distribution of ions around a charged particle (Malvern™ Instruments, 2018).

This parameter is a useful indicator of surface charge and, consequently, serves as a predictor of dispersion stability by offering insight on the aggregation ability of colloidal systems. Variables, such as pH and temperature, can affect ZP measurements (Emami *et al.,* 2015).

ZP values of ± 0 to 10 mV are characteristic of highly unstable systems, ± 10 to 20 mV point to relatively stable systems, ± 20 to 30 mV indicate moderately stable systems and the highest stability is expressed by a ZP value of ± 30 mV (Bhattacharjee, 2016).

3.8.2.3 Particle morphology

Particle morphology plays a vital role in validating the reliability of routine sizing techniques like PCS. It is responsible for generating detailed nano- and microscopic images for the visualisation of surface morphology and dimensions (Jain *et al.,* 2009) Although a vast number of imaging techniques are available, micro-structure analysis by means of TEM or SEM have proved to be the most popular techniques (Das and Chaudhury, 2011).

Electron microscopy produces detailed images of nano- or microscopic samples (Voutou and Stefanaki, 2008). It works by bombarding the sample with a stream of electrons and, consequently, monitoring the resultant transmission (TEM) or scattering

(SEM) effects. The scattered or transmitted electrons are then detected and converted into enlarged images (Johari, 1968). Furthermore, image analysis software (e.g. ImageJ®, National Institute of Health [NIH], Maryland, USA) utilises this information to generate data on the morphology and dimensions of each individual particle within the nanodispersion.

The primary difference between the two imaging techniques is their data output. SEM produces 3D imaging, whilst TEM produces two-dimensional (2D) imaging (Stadtlander, 2007). The former method is preferred for morphological characterisation of nanoparticles. However vacuum drying utilised in the sample preparation process causes shrinkage in size SLN size. The latter renders better resolution and derives internal composition details within the nanoparticle, such as lattice structures (Pardeshi *et al.,* 2012). Therefore, it was selected as the method of choice for microstructure analysis of the developed SLNs in this study.

3.8.3 Drug entrapment efficiency (%EE)

Entrapment efficiency (%EE) is the expression of the amount of drug incorporated into the nanoparticle and is commonly defined as the % of drug bound to a nanoparticle relative to the total amount of drug in the dispersion (Ekambaram *et al.,* 2011). Determining the %EE is pivotal to the performance of SLNs, since it has a direct influence on the rate and extent of drug release which, in turn, affects therapeutic outcomes (Emami *et al.,* 2015).

To facilitate the improvement of drug encapsulation, operators should aim for high DL capacity with minimal nominal DL. Theoretically, %EE is directly proportional to DL until saturation of the carrier occurs, where the maximum loading capacity is reached, and further DL can have a negative impact on efficiency (Lecaroz *et al.,* 2006). The physicochemical properties of the API and the extent of interactions between the drug, carrier matrix and surrounding environment have a direct effect on DL and entrapment efficiency. Therefore, to obtain high drug entrapment, it is beneficial for the API to interact preferentially with the carrier system rather than with the surrounding environment (Rana *et al.,* 2013).

Methods of %EE determination include gel filtration, dialysis bag diffusion, ultrafiltration and ultracentrifugation. Presently, there is overwhelming literature available related to the use of dialysis or ultracentrifugation for the determination of %EE in SLNs

(Andanova and Peneva, 2017; Uner, 2006). The use of the dialysis bag method is, however, time-consuming and impractical for drugs like MNZ, which possess poor aqueous solubility (D'Souza, 2014). Alternatively, centrifugation offers rapid analysis and was, therefore, chosen as the method used for the purposes of this study.

3.8.3.1 Principles of centrifugation

A centrifuge apparatus causes the separation of compounds in a mixture, based on the difference of sedimentation velocities of components within that mixture (Majekodunmi, 2015). The apparatus comprises a rotor to grip tubes containing the liquid mixture. This rotor is mounted on a driveshaft which rotates when powered by the motor. The centrifugal forces generated by this rotary motion cause particles of higher densities to sediment to the bottom, whilst the lighter particles float to the top (Roberts *et al.,* 1999). The basic principle of sedimentation is explained in Equation 3.12, where *F* is the relative centrifugal force (RCF), *M* represents the mass of the particles, *r* is the distance of particles from the axis of rotation and ω is the mean angular velocity expressed as radians/sec.

$$F = M\omega^2 r$$

Equation 3.12: Basic principle of sedimentation.

Many centrifuge apparatus have settings of revolutions per minute (rpm) and it is, therefore, necessary to use Equation 3.13 to convert and express this setting in units of gravitation time (Pierce Biotechnology™, 2005), where the RCF is denoted by *g*, *R* is the radius of the rotor (cm) and *S* is the rotary speed (rpm).

$$g = (1.118 \times 10^{-5})RS^2$$

Equation 3.13: Conversion formula for RCF and RPM (Pierce Biotechnology™, 2005)

For the centrifugation of lipid nanodispersions, following the initial formation of a fatty layer (where most oil droplets are deposited and compressed), an aqueous phase of free-oil is then observed on top of the tube (Laouini *et al.,* 2012). It should also be noted that the breakdown of an emulsion reaches a threshold with prolonged centrifugation, which causes redistribution of the API into the supernatant.

This can be a cause for concern when employing ultracentrifugation as a method of choice for %EE determination (Hao *et al.,* 2011).

3.8.3.2 Calculating entrapment efficiency (%EE)

In this study, the amount of encapsulated drug per unit weight was determined after separating the lipid phase from the aqueous phase by means of centrifugation. The supernatant obtained after this process was then analysed by means of HPLC or spectrometry to determine the quantity of free drug. The loading capacity and %EE of the SLNs are expressed by equations 3.14and 3.15, respectively.

$$\%\ DL = \left(\frac{W_{initial\ compound} - W_{free\ compound}}{W_{lipid}}\right) \times 100$$

Equation 3.14: Calculating % drug loading (%DL) of SLNs.

$$\%\ EE = \left(\frac{W_{initial\ compound} - W_{free\ compound}}{W_{initial\ compound}}\right) \times 100$$

Equation 3.15: Calculating % entrapment efficiency (%EE) of SLNs.

In these equations, $W_{initial\ compound}$ is the total mass of MNZ assayed in the nanodispersion, or the theoretical mass loaded in nanodispersion; W_{lipid} represents the mass of lipids added to the nanodispersion; and the W_{free} compound is the mass of MNZ assayed in the clear supernatant after centrifugation of the nanodispersion (Pardeshi *et al.,* 2012). For the purposes of this study on %EE has been discussed.

3.8.4 Accelerated stability testing

Inappropriate storage conditions can lead to the physical and chemical deterioration of pharmaceutical products, which can result in the reduced activity and formation of toxic by-products (Shafaat *et al.,* 2013). Due to the potential for chemical reactions taking place between excipients and APIs, dosage forms are more susceptible to degradation

than bulk or pure drug products (WHO, 1997). External factors, such as high temperature, humidity and exposure to light have all also demonstrated their potential to induce degradation (Bajaj *et al.,* 2012).

Accelerated stability tests offer a way of comparing the stability of alternative formulas, effect of packaging materials and manufacturing processes during the developmental phase (Arunachalam and Shankar, 2013). The WHO classification of climatic regions lists South Africa under the zone IVA (WHO, 2009) for the purposes of stability testing of pharmaceutical products (see Table 3.9). Long-term stability studies conducted at zone IVA and IVB conditions, instead of, or in addition to, zone II, is also acceptable (Hela, 2012).

Table 3.9: WHO climatic classification for stability testing of pharmaceutical products (Hela, 2012).

Climatic zone	Definition	Criteria Mean annual temperature measured in open/ Mean annual partial water vapour pressure	Long-term Testing conditions
I	Temperate climate	≤15 °C/≤11 hPa	21 °C/45% RH
II	Subtropical & Mediterranean climate	>15 to 20 °C/11 to 18 hPa	25 °C/60% RH
III	Hot and dry climate	>22 °C/≤ 15 hPa	30 °C/35% RH
IVA	Hot and humid climate	>22 °C/>15 to 27 hPa	30 °C/65% RH
IVB	Hot and very humid climate	>22 °C/>27 hPa	30 °C/75% RH

For accelerated studies, a minimum of three intervals, inclusive of the initial and final time points, from a six-month study is recommended (WHO, 2009). Table 3.10 illustrates the general storage conditions of finished pharmaceutical products under refrigeration conditions.

Table 3.10: General storage conditions for finished pharmaceutical products (FPPs) under refrigeration conditions (Hela, 2012).

Study	Storage conditions	Minimum time period covered by data at submission
Long-term	5 ± 3 °C	12 months
Accelerated*	25 ± 2 °C / 60 ± 5% RH or 30 ± 2 °C / 65 ± 5% RH or 30 ± 2 °C / 75 ± 5% RH	Six months

**Whether accelerated stability studies are performed at 25 ± 2 °C / 60 ± 5% RH, 30 ± 2 °C / 65 ± 5% RH or 30 ± 2 °C / 75 ± % RH is based on a risk evaluation. Testing at more severe accelerated conditions can be an alternative to the storage condition at 25 °C / 60% RH or 30 °C / 65% RH (Hela, 2012).*

The WHO (1997) general request is that a stability report be established for internal use and registration purposes. The results within this report should propose appropriate storage conditions and shelf-life of the dosage form (WHO, 1997). The storage stability of SLNs can be simply assessed by monitoring the physical or chemical properties (i.e. the lipid and drug stability) of the SLNs upon storage (Bahari and Hamishehkar, 2016). Physical characteristics, such as ZP, drug content, particle size and organoleptic properties are examples of factors that were monitored during this course of this study.

3.8.5 Experimental

3.8.5.1 Photon correlation spectroscopy (PCS)

For the determination of particle characteristics (z-avg., ZP and PDI), PCS was employed in this study. Each formulation was analysed by dispersing 1 ml of the resultant suspension in 10 ml of reverse osmosis H_2O and vortexed (Gemmy Industrial Corporation™ VM300, Texas, USA) in order to yield a 10-fold diluted suspension. The diluted suspension was then filtered through a 0.45 µm micropore PVDF membrane filter (Satorius™, Germany) into clear disposable zeta cells. The samples were loaded onto and analysed by a Malvern Zetasizer Nano-ZS particle analyser (Malvern Instruments™, United Kingdom) at ambient conditions (25 ± 2 °C) in triplicates using

H_20 as the dispersant medium. The number of sub-runs and attenuator settings were automatically set by the instrument in accordance with the generated phase plot data.

3.8.5.2 Transmission electron microscopy (TEM)

TEM was selected as a visualisation aid in the microstructure analysis of the developed MNZ-SLNs in this study. Preliminary studies that were first conducted under a standard electron microscope indicated that the direct analysis of the developed MNZ-SLNs without dilution yielded clumpy, unclear images with no separation of the individual nanoparticles. Therefore, MNZ-SLNs samples were prepared by adding 4 ml of reverse osmosis H_2O to a 1 ml MNZ-SLN suspension. The prepared samples were agitated and vortexed at low speed to facilitate adequate mixing. Using a tweezer, a mesh carbon-coated copper grid was dipped into the sample. The grid was rapidly stained with phosphotungstic acid and the excess was removed using filtered paper and left to dry in a vacuum desiccator for 24 hours. The dried sample was then analysed by TEM (JOEL™ Ltd, Japan).

3.8.5.3 Calculating drug entrapment efficiency (%EE) of MNZ loaded solid lipid nanoparticles (MNZ-SLNs)

For this study, the drug entrapment efficient was determined through an indirect method by measuring the concentration of free drug in the dispersion medium. Firstly, the total amount of API (MNZ) in each formulation was determined by dissolving 1 ml of the suspension in 8.5 ml of methanol; the resultant solution was mechanically agitated and 1.5 ml of H_2O was then added to yield a final mixture. The resultant mixture underwent filtration (0.45 µm PVDF membrane filter, Sartorius™, Germany) into three (n=3) 1.5 ml (32 × 11.6 mm) clear glass short-thread vials (La-Pha Pack™ ThermoFischer Scientiific™, Massachusetts, USA). This mixture was then analysed by means of RP-HPLC in triplicates under the optimised chromatographic conditions. The peak area generated was used to calculate the concentration of MNZ in the solution, with the aid of the determined calibration curve of MNZ.

For the determination of free drug, 2 ml of each MNZ-SLN formulation was centrifuged (Hermle™ Z300, Gosheim, Germany) at 50 000 rpm for one hour so as to yield a clear supernatant liquid at the top of the test tube. Half a millilitre of the supernatant liquid was removed using a pipette (Eppendorf™, Germany) and transferred into a clear

glass test tube where 4.25 ml of MeOH and 0.75 ml of H_2O were subsequently added in order to yield a clear solution. The resultant solution was filtered and analysed by means of RP-HPLC in triplicates under the optimised chromatographic conditions. Equations 3.14 and 3.15 were used to calculate the % DL and %EE respectively.

3.8.5.4 Storage stability determination of MNZ loaded solid lipid nanoparticles (MNZ-SLNs)

In this study, the stability of the formulated nano-dispersion was determined by investigating the change in particle characteristics over a period of six months. Changes in z-avg., PDI and ZP were monitored by means of PCS. MNZ-SLNs were prepared in duplicates and stored at 4 ± 2 °C and 25 ± 2 °C, respectively; with the sample analysis occurring at predetermined time intervals at months zero, one, three and six.

3.9 DEVELOPMENT AND CHARACTERISATION OF *IN SITU* VAGINAL HYDROGEL

3.9.1 Introduction

NDDS are a rapidly developing field of study. This development has been strengthened by innovative developments in, amongst others, the fields of pharmaceutics, biotechnology, nanotechnology and chemistry (Rangasamy and Parthiban, 2010). Hydrogels have also recently become a key focus in the field of pharmaceutical drug delivery, owing to their versatility in terms of compositions and their adjustability to a variety of ROA (Sosnik and Seremeta, 2017). Thermoresponsive polymers, in particular, provide triggered drug release; hence, they have been exploited for pharmaceutical drug delivery (Taylor *et al.,* 2017). Because of its many uses, this current research limits its focus to localised vaginal drug delivery by means of thermoresponsive hydrogels.

The vaginal route is useful for both systemic and localised drug delivery, since first-pass hepatic metabolism is bypassed. Moreover, its dense vascularisation and high mucosal permeability allows for the administration of various classes of drugs, such as antifungals and hormones (Srikrishna and Cardozo, 2013). Systemic drug delivery is often associated with toxicity and increased manifestations of adverse effects (Faro,

1994). Localised drug delivery, on the other hand, allows for drug administration at lower doses and direct tissue targeting (Tiwari *et al.,* 2012).

Thus, *in situ* gels that respond to external thermal stimuli are ideal for intravaginal drug delivery. They have the ability to overcome limitations like messiness, leakage and the uneven spreading of dosage forms within the vaginal tract (Gandra, 2013). At room temperature, their sol state facilitates easy insertion and spreading. Once in the vaginal tract, the change in temperature from the external to internal environment causes a phase transition into a gel. The solid state of the gel ensures that the dosage form maintains intimate contact with the vaginal mucosa for prolonged periods (Taurin *et al.,* 2018).

3.9.2 Methods of thermoresponsive hydrogel preparation

There are three methods of gel preparation, *viz.* fusion, cold or dispersion. The fusion method employs waxy materials in non-polar media. The drug is then incorporated when the waxy material is melted by fusion until a gel is formed. The dispersion method, on the other hand, involves the dispersion of the gelling agent at high speeds (1 200 rpm) for 30 minutes. For this method, a non-aqueous solvent is required for API incorporation (Arun *et al.,* 2016). The cold method (CM) of gel production was investigated for the purposes of this study. This commonly used method allows for physical cross-linking between the chosen polymers in the absence of organic solvents. CM involves the dissolution of polymers at ambient temperature under vigorous stirring. The resultant formulation is then refrigerated (4 ± 2 °C) to facilitate complete cross-linking (Chakraborty *et al.,* 2014).

3.9.3 Characterisation of thermo-responsive hydrogels

For the purposes of this study, characterisation studies for the prepared hydrogels were limited to rheology, organoleptic properties, pH, drug content uniformity, sol-gel transition, *in vitro* drug release and antimicrobial susceptibility testing (AST).

3.9.3.1 Rheology

Rheology is a branch of science concerned with the study of deformation and flow of matter. An instrument used for the measurement of viscosity and rheology is called a rheometer (Korolczuk-Hejnak, 2014). The conduction of rheological studies on semi-

solid preparations is critical for demonstrating their flow properties that influence packaging, storage stability and ease of application of the dosage form (Sivaraman and Banga, 2015).

Rheometer should not be confused with a viscometer, which is only capable of conducting viscosity measurements. Viscosity defines a fluid's resistance to flow, and plays a vital role in rheology as it affects the flow of matter and materials (Malkin and Isayev, 2017). A rheometer works by determining the stress-deformation relationships of materials and is classified according to the flow type wherein material properties are investigated according to two main groups (Chen *et al.,* 2010).

The two groups comprise shear (rotational) and extensional rheometers. Extensional rheometry is, generally, not performed on low-viscous materials, such as suspensions or semi-solid preparations, and therefore, is not discussed in this study. Shear rheometers include the likes of rotational and capillary rheometers (Gandra, 2013). Extensional rheometers generate shear between fixed and moving surfaces, whilst shear rheometers are pressure-driven and generate shear through a pressure difference along the channel through which a material flows (Galindo-Rosales *et al.,* 2013). Rotational rheometers are ideal for measuring the complex flow and oscillatory properties of materials. They are also used for viscosity measurements where fluids cannot be defined by a single value of viscosity and offer greater measurements and parameters than viscometers (Brockel *et al.,* 2013). Equation 3.16 illustrates the mathematical relationship of viscosity, shear stress and shear rate.

$$\eta = \frac{F/A}{dv_x/dz}$$

Equation 3.16: Mathematical relationship between viscosity, shear rate and shear stress.

In the aforementioned equation, η denotes viscosity in millipascal second (mP·s), *F/A* is the force per unit area representing shear stress and dv_x/dz represents the shear rate. Factors like temperature, concentration, attractive forces and particle size can influence the flowability of materials (Likavcan *et al.,* 2014).

The flow properties of a substance are then determined by two methods known as controlled stress or rate mode (Gandra, 2013). In the former mode, a known amount of stress (torque) is applied to a material and its resultant strain (shear rate) is measured. For the latter mode, a defined shear rate is applied and the subsequent stress (torque) is measured (Janmey and Schilwa, 2010). The information generated from these two modes is used to obtain a shear stress versus shear rate plot (see Figure 3.8, which provides insight on the flow properties of the test material).

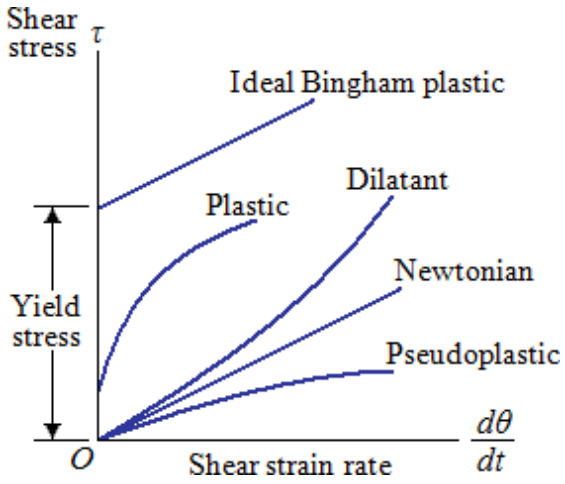

Figure 3.8: Flow curve of shear stress as a function of shear rate for various fluids (Kazemian *et al.,* 2012).

Material flow behaviour is classified into various groups, as depicted in Figure 3.8. The first group is Newtonian fluids which are characterised by a linear relationship between applied stress and shear rate. Examples of Newtonian fluids include cooking oil and corn syrup. The second group is known as Bingham bodies or non-Newtonian fluids and demonstrate a change in flow or viscosity under stress (Chharbra, 2010). Characteristic differences between Bingham bodies and non-Newtonian materials are that the former can maintain shapes or peak when no stress is applied, whilst the latter is a flat and featureless surface. Further classification of non-Newtonian material is dependent on their viscosity (Abegunrin *et al.,* 2016).

The third group is shear thinning (pseudoplastic) behaviour, which is characterised by a decrease in viscosity and an increase in shear stress (Chharbra, 2010). Conversely, shear thickening (dilatant) behaviour is characterised by an increase in viscosity with an increase in shear stress. The fourth group consists of Bingham plastic materials

that behave as rigid bodies at low stresses but begin to flow under high stress once the yield point has been surpassed (Barnes, 1999). Examples of such materials included clay suspensions and toothpaste. The final group is Bingham pseudoplastic behaviour, which comprises materials that require minimum stress application before they flow; after which any addition in strain results in reduced viscosity (Moller *et al.,* 2006).

Viscoelastic investigations determine the interactions between polymers and additives with great sensitivity. The flow characteristics of poloxamer-based solutions can be Newtonian or non-Newtonian, dependent of the temperature and concentration of the polymer (Chharbra, 2010). The flow characteristic of the prepared hydrogel formulations was investigated for the purposes of this study.

i. Plate geometry

The generic structure of a parallel plate measuring system was employed for the purposes of this study and is illustrated in Figure 3.9. The sample is loaded into the gap between the upper measuring plate and the temperature controller, thereafter shear flow is generated by rotation or oscillatory motion (Gandra, 2013). Generally, the type of measuring plate used is dependent on the sample being analysed. This plate may be a cone and plate or cylinder/parallel system (Khan *et al.,* 2009). The upper measuring plate is supported by a near-frictionless air-bearing beam and driven by an ultra-low inertia motor coupled with a high-position encoder. The temperature of the sample is maintained by the lower plate/temperature controller (i.e. the upper heated or Peltier plate) (Gandra, 2013; Mendez *et al.,* 2014).

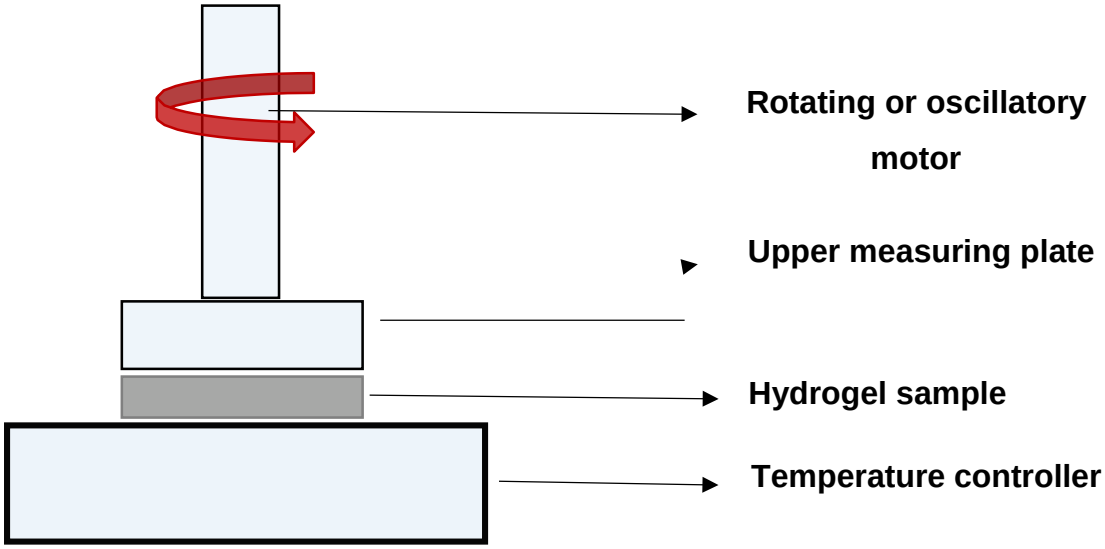

Figure 3.9: Generic diagram of a parallel plate measuring system.

The rheological characteristics of the prepared hydrogel can be determined by rotating or oscillatory motions or by applying a step-function within the measuring system. Common modes for rheometry include the rotational mode for the measurement of stress viscosity and the oscillatory mode for the measurement of dynamic material properties like phase angle and viscoelastic properties (Mendoza, 1998).

The oscillatory mode employs a motor oscillating shaft and a plate of varying frequencies that maintains constant shear. The material exerts a torque on the rheometer in response to applied stress (Kocen *et al.,* 2017). For viscoelastic materials, the torque is dependent on the applied frequency, as is the phase angle between the torque and shear. The loss modulus (G") is then calculated based on the phase, storage (G') and torque (Franck, 2016). In the rotational mode, the rheometer is maintained at a constant speed by the motor by using a torque detection system. When the suspended measuring plate is rotated, the flow resistance (viscosity) of the sample tries to twist the measuring plate. By determining the resultant 'twisting' force and knowing the stiffness of the plate, the torque may be obtained (Gandra, 2013). This method was employed for rheological testing of prepared hydrogel formulations in this study.

3.9.3.2 Organoleptic assessments

Organoleptic evaluations make use of sensory organs in the determination of product characteristics. They are applicable in cases where scientific testing is unavailable or

not yet established. The organoleptic properties of materials are determined through tactile, olfactory, visual and gustatory perceptions (Patil *et al.,* 2017). The information gathered from organoleptic evaluations correlate strongly with patient compliance and adherence. Unacceptable sensory properties, such as bad odour, taste or texture contribute to compromised pharmacotherapy adherence (Morrow *et al.,* 2015).

The physical properties of vaginal dosage forms, including the mode of application and organoleptic properties are strong determinants of patient acceptability and can influence patient adherence and, subsequently, therapeutic outcomes (Rosen *et al.,* 2015). Semi-solid preparations, such as gels, demonstrate the highest patient acceptability for intravaginal drug delivery (Ndesendo *et al.,* 2008; Rohan and Sassi, 2009; Sahoo *et al.,* 2013). A descriptive cross-sectional study conducted by Palmeira-de Oliviera and colleagues (2014) utilising a web-based survey concluded that odour was the most important sensory characteristic that influenced women's decisions on using intravaginal products. Odour was closely followed by colour and flavour, respectively. The majority of the respondents indicated that they preferred transparent products with little to no odour and taste, and which could be applied by means of an applicator. Sensory characteristics will be evaluated in this study.

3.9.3.3 pH assessment

pH is a measure of hydrogen ion concentration [H^+] in a solution (Bates, 1948). This term is expressed mathematically as the logarithmic (base 10) of the reciprocal of hydrogen ion concentration (see Equation 3.17).

$$pH = -\log[H^+]$$

Equation 3.17: Mathematical expression of pH (Munhoven, 2013).

An acidic pH is characterised by a low pH corresponding to a high value of hydrogen ion concentration. The contrary is applicable for a basic or alkaline pH, where the concentration of hydrogen ions in the solution is low with a high numerical pH value (Hamm *et al.,* 2015). Physiological pH ranges from one to eight, depending on the site or function of the organ, surrounding tissue or fluid. The vast pH range creates a basis for pharmaceutical dosage forms that ionise in response to the pH gradient (He *et al.,* 2003). For example, the pH of an API is governed by ionisation constants that affect

the lipophilicity and, consequently, the bioavailability of the API. If a particular drug does not contain a functional group that is ionisable in a given range, it adopts qualities of a non-electrolyte that remains unionised under physiological conditions (Kah and Brown, 2008). The control of pH is critical during dosage form development in order to minimise potential degradation of the API. Furthermore, dosage forms formulated within a pH range of the intended site of application create non-irritant products that can not only improve drug administration, but also patient compliance by improving the adverse effect profile (Wen *et al.,* 2015).

3.9.3.4 Drug content uniformity

Drug content uniformity is an analytical parameter of the quality control of pharmaceutical dosage forms. It ensures that a consistent dose of the active is maintained between batches so that the patient, in turn, receives the correct dose (Slew, 2018).

Mandatory product quality tests for semi-solid topical drug products include the determination of tube uniformity (Ueda *et al.,* 2009). The term ‘tube uniformity’ can be described as the degree of uniformity of the amount of API amongst tubes containing multiple doses of a given semi-solid dosage form (United States Pharmacopeial Convention, 2013). Ideally, this test should be conducted over a predetermined interval, as some products tend to show physical separation at accelerated storage temperatures due to the nature of the vehicle. The drug uniformity of the topical dosage form is demonstrated by assaying the top, middle and bottom of the sample (Ueda *et al.,* 2009). Drug content uniformity tests will be conducted to ascertain the uniformity of MNZ in the final formulation.

3.9.3.5 Sol-gel transition temperature

Thermoresponsive polymeric hydrogels have been investigated extensively for their potential in sustained drug release and surgical innovations (Bora *et al.,* 2014). The term ‘thermoresponsive’ implies a critical change due to temperature variation and not progressive thermosensitivity. This thermoresponsive phenomenon is defined by a transition temperature whereby a substance acquires loses due to distinct superconductive properties (Taylor *et al.,* 2017).

Thermoresponsive hydrogels undergo phase transition at temperatures above or below the critical solution temperature (CST). Depending on the mechanism of transition, hydrogels are further classified as positive or negative thermoresponsive polymers (Mah and Ghosh, 2013). Polymers belonging to the positive group swell in H_20, with an increase in temperature above the CST, and solidify above the upper critical solution temperature (UCST). A subsequent decrease in temperature below the UCST forms a free-flowing solution due to shrinkage of the polymer network (Gandra, 2013). The contrary applies to negative polymers, which demonstrate shrinkage with an increase in temperature above the CST (Klouda and Mikos, 2011).

For vaginally administered products, the sol state is an aqueous solution prior to administration that quickly transforms to a non-flowing gel upon administration in response to the vaginal milieu (Alves *et al.,* 2018). The sol-gel transition can be measured by means of rheology or qualitative assessments (Ponton *et al.,* 2005).

3.9.3.6 In vitro drug release studies

In vitro drug release testing (IVDRT) is a measure of the release of the API from the dosage form matrix in a controlled laboratory environment. It is a vital evaluation in drug development and quality control (Brown *et al.,* 2011). The process of IVDRT involves subjecting the dosage form to a set of conditions that could promote drug release, and quantifying the amount of drug released under predetermined conditions (Shen and Burgess, 2013).

For drug development, IVDRT is critical for modelling *in vivo* formulation behaviour and predicting the time-frame of drug release (Stillhart *et al.,* 2017). There are currently no approved compendial methods for the determination of IVDRT of topical products like gels, however, instrumentation, such as flow-through cell apparatus or VDC, have been investigated extensively for their use in the IVDRT of semi-solid preparations. VDCs comprising of FVDC also come highly recommended (Kanfer *et al.,* 2017; Naik *et al.,* 2016). Advantages of the FVDC systems include their simplicity and yield of reliable and reproducible results (Liebenberg *et al.,* 2003).

Pharmaceutical drug delivery systems play a key role in regulating the therapeutic efficacy of APIs by manipulating their toxicity profile, rate of drug release and duration of action at the target site (Upadhyay, 2014). The drug release profiles of various pharmaceutical dosage forms may be described in several ways, including: immediate

release formulations that are designed to allow the release of API instantaneously upon administration; or modified release (MR) formulations that encompass a group of novel pharmaceuticals that facilitate extended or delayed release of API. Examples of MR formulations include delayed, extended, pulsatile and CR dosage forms (Challener, 2018). The focus of this study is limited to CR semi-solid dosage forms.

Controlled release (CR) formulations are designed to maintain drug levels within a desirable range over a sustained period at a constant rate (Ummadi *et al.,* 2013). The main objective of CR formulations is to ensure safety, improve the therapeutic efficacy of many drugs and increase patient compliance by decreasing dosing frequency (Bhowmik *et al*., 2012; Jalwal *et al.,* 2018). CR formulations are not confined to a specific ROA; therefore, many dosage forms have been developed for, amongst others, transdermal, buccal and vaginal drug delivery (Siegel and Rathborne, 2012. The use of systemically-acting CR formulations are often associated with an increased manifestation of adverse effects and the potential for drug interactions, owing to drug accumulation in tissues not associated with the target site. As a countermeasure, regional or localised drug delivery permits drug administration at lower doses and drug tissue targeting, thereby limiting drug exposure to the affected site (Alomar, 2014)

i. Calculating drug release

IVDRT defines the liberation process of a drug from the dosage form. It is a complex process where, upon contact with an aqueous medium, H_20 penetrates into the dosage form matrix and dissolves the drug (Kakar *et al.,* 2014). The now dissolved drug consequently diffuses out of the matrix due to the presence of a concentration gradient. Moreover, the dosage form may undergo several changes, such as swelling or dissolution in the aqueous medium, thus further contributing to the overall process of drug release (Jug *et al.,* 2017). Once the drug has diffused out of the matrix and into the aqueous medium, minute samples of the medium are withdrawn for analytical quantification of the drug (Nounou *et al.,* 2006). The amount of drug quantified from the analytical assay is then used to determine the cumulative amount of API released per surface area of the membrane, as added by Equation 3.18.

$$Q = \{C_n V + \sum_{i=1}^{n-1} C_i S\}/A$$

Equation 3.18: Calculating cumulative amount (Q) of drug release for IVDRT (Thakker and Chern, 2003).

In the aforementioned equation, *Q* is the cumulative amount of API released per surface area of the membrane (µg/cm2), C_n defines the concentration of API at a predetermined sampling interval, *V* represents the receptor fluid volume in an individual cell, $\sum^{nn-1} CCii$ is the sum of concentrations of API (µg/ml) determined as n-1 of the sampling interval, *S* is the volume of sampling aliquot and *A* is the surface area of the sample well (Thakker and Chern, 2003). A plot of % cumulative drug release as a function of time is designed to illustrate the drug release kinetic profile over a predetermined period.

The final drug release kinetics from CR semi-solid preparations, such as hydrogels, commonly follow the Higuchi model (Brown *et al.,* 2011; Kanfer *et al.,* 2017). The Higuchi model for the rate of drug release from a matrix is based on the following assumptions:

1. The initial drug concentration in the dosage form matrix is much higher than the drug solubility;
2. Drug diffusion is one dimensional;
3. Drug particles are smaller than system thickness;
4. Drug diffusion is constant;
5. Matrix dissolution and swelling are negligible; and
6. Ideal sink conditions are always attained in the release environment (Dash *et al.,* 2010).

Equation 3.19 further explains the basic principles of the Higuchi model for drug release kinetics.

$$Q = A\sqrt{D(2C_0 - C_s)C_s t}$$

Equation 3.19: Basic Higuchi equation for modelling drug release kinetics.

In this equation, *Q* is the cumulative amount (µg/cm2) in time (*t*) per unit area (*A*). C_0 represents the initial drug concentration, C_s is the solubility of the drug in the matrix and *D* denotes the diffusion co-efficient of the drug in the matrix. This mathematical relationship holds true until total drug depletion from the dosage form occurs (Siepmann and Peppas, 2011). In order to study dissolution of dosage forms where drug release occurs through a porous system, the resultant equation is modified slightly (see Equation 3.20).

$$Q = A\sqrt{\left(\frac{D\delta}{\tau}\right)(2C - \delta C_s)C_s t}$$

Equation 3.20: Higuchi model equation for drug dissolution via a planar heterogeneous system.

Here, *D* is the diffusion co-efficient of API in the solvent, *δ* denotes the porosity of the matrix, *τ* is the tortuosity of the dosage form matrix, *A* and *t* and C_s are as per Equation 3.19's description. Equation 3.20can further be simplified to yield Equation 3.21.

$$Q = K_H \times t^{1/2}$$

Equation 3.21: Simplified Higuchi model equation for drug release kinetics

In this equation, the Higuchi constant is denoted by K_H. This final equation (see Equation 3.20) is normally used to define the drug release kinetics of several MR dosage forms.

However, for the purposes of this study various mathematical models, Including Higuchi, first order and Korsmeyer-Peppas, were investigated in the determination of release kinetics of MNZ-SLNs and MNZ-Hydrogels respectively.

3.9.4 Experimental

3.9.4.1 Preparation of unloaded hydrogels

For this study, unloaded hydrogels of various compositions were prepared and characterised for their pH and thermoresponsive potential. Table 3.11 gives an overview of the respective ingredient compositions within the given formulations. All formulations were prepared using the CM with minor variations in the process steps.

Table 3.11: Composition of unloaded hydrogel formulations.

Formulation code	Poloxamer 188 (% m/v)	HPMC (% m/v)	Methylcellulose 450 (% m/v)	Chitosan (% m/v)	MNZ (% m/v)
FG1	-	2.0	-	2.0	-
FG2	-	2.0	-	1.0	-
FG3	-	1.0	-	2.0	-
FG4	-	2.0	-	-	-
FG5	18	-	-	1.0	-
FG6	18	2.0	-	2.0	-
FG7	18	1.5	-	-	-

i. Preparation of formulation FG1 to FG4

Due to their likenesses in composition, formulations FG1 to FG4 were prepared in a similar manner. Sufficient quantities of a 2% m/v chitosan solution were prepared by dissolving low-molecular weight chitosan (Sigma-Aldrich™, Steinheim, Germany) in a 1% v/v glacial acetic acid solution (pH 4.5) (Merck™, Dramstadt, Germany) at room temperature under continuous stirring for 60 minutes. Sufficient quantities of a 2% m/v HMPC solution were also prepared concomitantly. HPMC powder (Aspen Pharmacare™, Port Elizabeth, South Africa) was weighed and added to sufficient quantities of H_20 at 80 °C and stirred continuously for 30 minutes in order to yield a transparent homogenous solution. The two individual solutions (chitosan 2% m/v and HPMC 2% m/v) were added together in equal amounts and agitated further under magnetic stirring for 30 minutes, after which the solutions were refrigerated for 24 hours.

ii. Preparation of formulation FG5 to FG7

For the preparation of FG5, sufficient quantities of poloxamer 188 were weighed and gradually dispersed in a 5% v/v glycerol solution. The solution was stirred for 30 minutes in order to yield a colourless and transparent solution that was then refrigerated (at 4 °C) for 24 hours. A 1% m/v chitosan solution was prepared separately by dispersing chitosan in a 1% v/v glacial acetic acid solution so as to yield a transparent, off-yellow solution with a pH of 4.5. The chitosan solution was then mixed proportionally with the poloxamer after 24 hours and refrigerated for a further 24 hours to allow for complete solubilisation.

The preparation of FG6 and FG7 was very similar to the aforementioned method used in FG5. However, here, the adequate quantities of poloxamer 188 were weighed and dispersed in a 5% v/v glycerol solution. Thereafter, individual chitosan solutions and HPMC were added to the poloxamer solution, where applicable.

3.9.4.2 Determination of optimal hydrogel formulation

i. Organoleptic assessments

Descriptive sensory tests for all formulations were undertaken to define the aroma, colour and texture of the hydrogels. For the appearance test, each formulation was assessed visually for colour and homogeneity at an ambient temperature (i.e. 25 ± 2 °C) and at an elevated temperature (i.e. 37 ± 2 °C). Five millilitres of each formulation was transferred to a clear glass tube and placed against a white background, where it was assessed by the operator.

For formulation homogeneity and texture evaluation, stickiness and grittiness assessments of the respective hydrogels were conducted at ambient and elevated temperatures, respectively. Small quantities of the gel were placed between the thumb and index finger and rubbed gently to feel for the presence of any particles.

The aroma test was conducted to define odour characteristics for each formulation. Parametric sensory measurements of each formulation were undertaken by employing the human nose as an odour detector so as to directly determine the properties of odours as experienced by humans (Bratolli *et al.,* 2011). A formulation was deemed ideal for patient use if it demonstrated favourable organoleptic characteristics, such as

colourlessness and odourless (see Section 3.9.3.2).

ii. pH measurements

pH measurements of all formulations were determined by means of a pH meter (MetrOhm™, Herisau, Switzerland). The pH meter was calibrated prior to use by standardised buffer solutions at pH 4, 7 and 9 (Merck™, Dramstadt, Germany). Five millilitres of each respective formulation was placed in a previously cleaned and dried test tube and readings were taken in succession by immersing the electrode in the sample. Each formulation was assessed at ambient and elevated temperatures in triplicates. The electrode tip was submerged in purified H_20 after each reading in order to clean it. A formulation was deemed ideal if its pH was found to be around that of the vaginal milieu (i.e. pH 4.5 ± 2). This process was repeated on the samples after a 12-week storage period at refrigeration temperature.

iii. Viscosity measurements

Temperature-dependent viscosity measurements of the prepared unloaded hydrogels were determined by means of a rheometer (Anton Paar™ MCR 72, Austria) that was equipped with a PP25 parallel plate. Data interpretation was conducted using RheoCompass® software (Anton Paar™ MCR 72, Austria). The shear rate was kept constant within a working temperature range of 25 to 40 °C and a gap width of 1mm. The viscosity properties of each formulation were measured in succession over a temperature range of 25 to 40 °C at a constant shear rate, with intermediate cleaning of the plate. Sufficient quantities of samples were applied carefully to the lower plate of the instrument and allowed to equilibrate for five minutes prior to each analysis. A formulation was deemed ideal if it demonstrated a rapid increase in viscosity over a temperature range of interest (i.e. 35 to 37 °C).

3.9.4.3 Incorporation of MNZ loaded solid lipid nanoparticles (MNZ-SLNs) into optimal hydrogel formulation

Due to limited resources, MNZ-SLNs could not be incorporated in all hydrogel formulations for testing. Therefore, unloaded hydrogels were first prepared for the characterisation of rheological, organoleptic and pH properties. The formulation that demonstrated the most favourable characteristics was then selected for MNZ-SLN incorporation. MNZ-SLNs were incorporated into a polymer solution containing a

mucoadhesive and thermoresponsive agent under vigorous stirring. The resultant gel was refrigerated for 24 hours in order to facilitate adequate cross-linking.

3.9.4.4 Characterisation of hydrogel incorporated with MNZ loaded solid lipid nanoparticles (MNZ-SLNs).

i. Measurement of sol-gel transition temperature

A qualitative test tube inversion method was used owing to its cost-efficiency, speed, convenience and simplicity. One millilitre of the prepared hydrogel formulation was placed in a clear glass vial (32 × 11.6 mm, LaPha-Pack™, ThermoFischer Scientific™, Massachusetts, USA). The loaded vial was then submerged in a water bath on a hot plate. The water was gradually heated over a working temperature range of 25 to 40 ± 2 °C. The contents of the tube were allowed to equilibrate over periodic intervals, after which the test tube was inverted and the ability of the gel to flow under its own weight was assessed. The temperature at which the gel would not flow was noted as the sol-gel transition temperature. If the gel continued to flow beyond 40 °C, it was considered that no sufficient gelation for vaginal drug delivery had occurred.

ii. Drug content uniformity

Drug content uniformity assessments of the prepared hydrogel were conducted in order to determine whether the prepared dosage units were within a narrow limit of the label claim. One millilitre (containing 0.2% m/v MNZ) of the prepared hydrogel was dissolved in 7.5 ml of a PBS (pH 4.5) and stirred continuously for five minutes. The resultant solution was transferred to a clean McCartney jar and sealed, where it was then allowed to equilibrate in a bath sonication device for 15 minutes at 37 °C. The final solution was filtered and quantified by means of RP-HPLC under the optimised chromatographic conditions.

iii. *In vitro* drug release testing (IVDRT)

IVDRT of MNZ from the hydrogel through a semi-permeable membrane was evaluated by means of the FVDC method. The FVDC set-up consisted of three replicate samples. A synthetic snake skin membrane (4cm^2, ThermoFischer™ Scientific, Massachusetts, USA) was hydrated in PBS (pH 4.5) for 30 minutes prior to its use, after which it was placed between the donor and receptor compartments. The receptor compartment contained 15 ml PBS (pH 4.5) under continuous magnetic stirring. The temperature of

the receptor cell was maintained at 37 ± 2 °C by a circulating water jacket. Three millilitres of the prepared hydrogel was carefully measured and placed on the membrane surface side of the donor compartment. Aliquots of 0.5 ml were drawn from the receptor compartment at periodic intervals over a 12-hour period. Equal amounts of fresh PBS were added after each withdrawal to maintain sink conditions. The withdrawn aliquots were diluted with MeOH and H_2O (85:15% v/v) for API quantification via RP-HPLC under optimised chromatographic conditions. The mean cumulative amount of drug permeation per unit surface area of the membrane was plotted versus time.

3.10 ANTIMICROBIAL SUSCEPTIBILITY TESTING (AST)

AST is a process of determining the vulnerability of a microbe to a test compound. Results obtained from AST are useful for the prediction of *in vivo* antimicrobial responses (Balouiri *et al.,* 2016). There are currently a vast majority of AST methods available, ranging from simple diffusion-based methods to more complex broth-based automated systems (Reller *et al.,* 2009). This study, however, limits itself to the investigation of the agar disc diffusion method, owing to its simplicity, low cost and flexible use for a wide spectrum of test compounds. Even though this method possesses many advantages, it does not allow for the differentiation between bactericidal and bacteriostatic test compounds (Mayrhofer *et al.,* 2008). Moreover, it does not provide a direct means for determining test compounds' minimum inhibitory concentrations (MICs) (Balouiri *et al.,* 2016; Luc *et al.,* 2015).

The agar disc diffusion method (commonly referred to as the Kirby-Bauer test) is employed for the testing of microbial susceptibility to antimicrobial agents. An overview of the test involves the inoculation of the agar surface with a test microbe, on which filter discs containing the antimicrobial agents are placed. The resultant sample undergoes incubation under desirable conditions in order to allow for the test compound to diffuse into the agar and inhibit microbial germination (Wheat, 2001; Jorgensen and Ferraro, 1998).

AST is preferred for AST of pharmaceutical products because rapid and reliable identification of microbial susceptibility is critical for optimal clinical efficiency of drug products and resource utilisation (Balouiri *et al.,* 2016). Table 3.12 details factors that influence the generation of accurate and reliable results via the Kirby-Bauer test.

Table 3.12: Factors influencing microbial sensitivity in Kirby-Bauer test (adapted from Lalitha, 2004).

Factor	Comment	Remedy
Moisture	Moisture present in medium counteracts accuracy of AST	Remove excess moisture by incubating (35 ± 2 °C) prior to use Use laminar flow at room temperature with lids ajar until evaporation of excess moisture occurs
pH	Low pH leads to loss of potency of the drugs (e.g. aminoglycosides and macrolides) and excessive activity in others (e.g. tetracycline). These issues are reversed following a high pH.	Test pH of agar to ensure that it is within 7.2 and 7.4 at ambient temperature after solidification
Medium components	Presence of high levels of thymidine or thymine in agar can reverse the effects of some drugs (e.g. sulfonamides) which can lead in inaccurate resistance results	Evaluate efficiency of MHA with *E.faecalis* using trimethoprim/sulfamethoxazole discs. A zone of inhibition of ≥20mm is indicative of low thymidine levels.
	Medium with excessive cationic content yields of small zones of inhibition. The converse applies for mediums with low-cation content.	Performance test with each match of MHA to be conducted
Types of strains	Certain strains do not germinate in MHA (e.g. *N gonorrhoeae, S. pneumonia*)	Supplementation of MHA required; or the selection of an alternative media that facilitates growth
Quantity	Amount of organism or antimicrobial concentration has a direct effect on AST	Use a standardised quantity of organisms with a predetermined antimicrobial concentration level

These factors were monitored carefully to ensure that reliable and reproducible results were obtained.

3.10.1 Experimental

3.10.1.1 Modified Kirby-Bauer disc diffusion assay

The AST of the prepared hydrogel, SLNs and controls were conducted by means of a modified Kirby-Bauer disc diffusion assay. This process followed three steps described in the following sub-sections, *viz.* preparation of agar, inoculum preparation and assay.

i. Preparation of Mueller-Hinton Agar (MHA)

MHA was selected as the most suitable medium to facilitate microbial growth, owing to its versatility in different microbes, high-accuracy results and reproducibility in microbiology (Jorgensen *et al.,* 1987). MHA (Merck™, Dramstadt, Germany) comprising of 0.5 g/L meat infusion, 17.5 g/L casein hydrolysate, 1.5 g/L soluble starch and 14.0 g/L agar was prepared in accordance with the manufacturer's instructions. A 1 L solution was prepared by dissolving 38 g of accurately-weighed MHA in purified water over a hot plate under continuous stirring. The resulting agar solution was sterilised in a vertical-type steam autoclave (AlreadyEnterprise Inc™, Model HL-340, Taiwan) at 121 °C for 15 minutes. The sterile agar was allowed to cool to 45 ± 2 °C and immediately transferred into six individual flat-bottomed petri dishes (100 × 20 mm, TPP™, Sigma Aldrich™, Steinheim, Germany) in order to yield uniform depths of ± 4 mm. The agar in the petri dishes was allowed to further cool to ambient temperature and, unless utilised on the same day, they were refrigerated (4 ± 2 °C).

ii. Preparation of inoculum

Candida albicans were utilised for the purposes of this study. The inoculum was prepared by selecting three to five distinct colonies of about 1 mm in diameter from a 24-hour-old culture. The fungal colonies were suspended in 5 ml of freshly-prepared normal saline and vortexed for 30 seconds. The turbidity of suspension was adjusted by the gradual addition of saline solution to a comparable turbidity of a 0.5 McFarland solution.

To inoculate *Candida albicans* onto the MHA test plates, a sterile cotton swab was dipped into the prepared suspension and streaked over the surface of the plates. The process was repeated twice, whilst rotating the plate at ± 60° to facilitate even distribution of the inoculum on the plate surface. The plates were left to dry for 10 minutes so as to remove excess moisture before introducing the test compounds.

iii. Disc diffusion assay

After the surface inoculation of the test plates, the agar was partitioned into six equal segments. Equal quantities of MNZ loaded hydrogels, blank hydrogels, MNZ loaded SLNs, unloaded SLNs and a commercially available MNZ cream were placed onto the surface. The last segment was left blank (i.e. formed the control). The test plates were covered and incubated at 37 ± 2 °C for 24 hours before assessing the respective zones of inhibition. All tests were conducted in triplicates and the mean values of the respective zones were calculated. The findings of this study will be discussed in Chapter 4.

3.11 ETHICAL CONSIDERATIONS

No animal or human subjects were used for the purposes of this study; therefore, no ethical approval was required.

3.12 SUMMARY

The methodology described in this chapter led to the development of a thermoresponsive hydrogel comprising of MNZ-SLNs, for the intended treatment of VVC. A brief overview of this chapter is given in Figure 3.10.

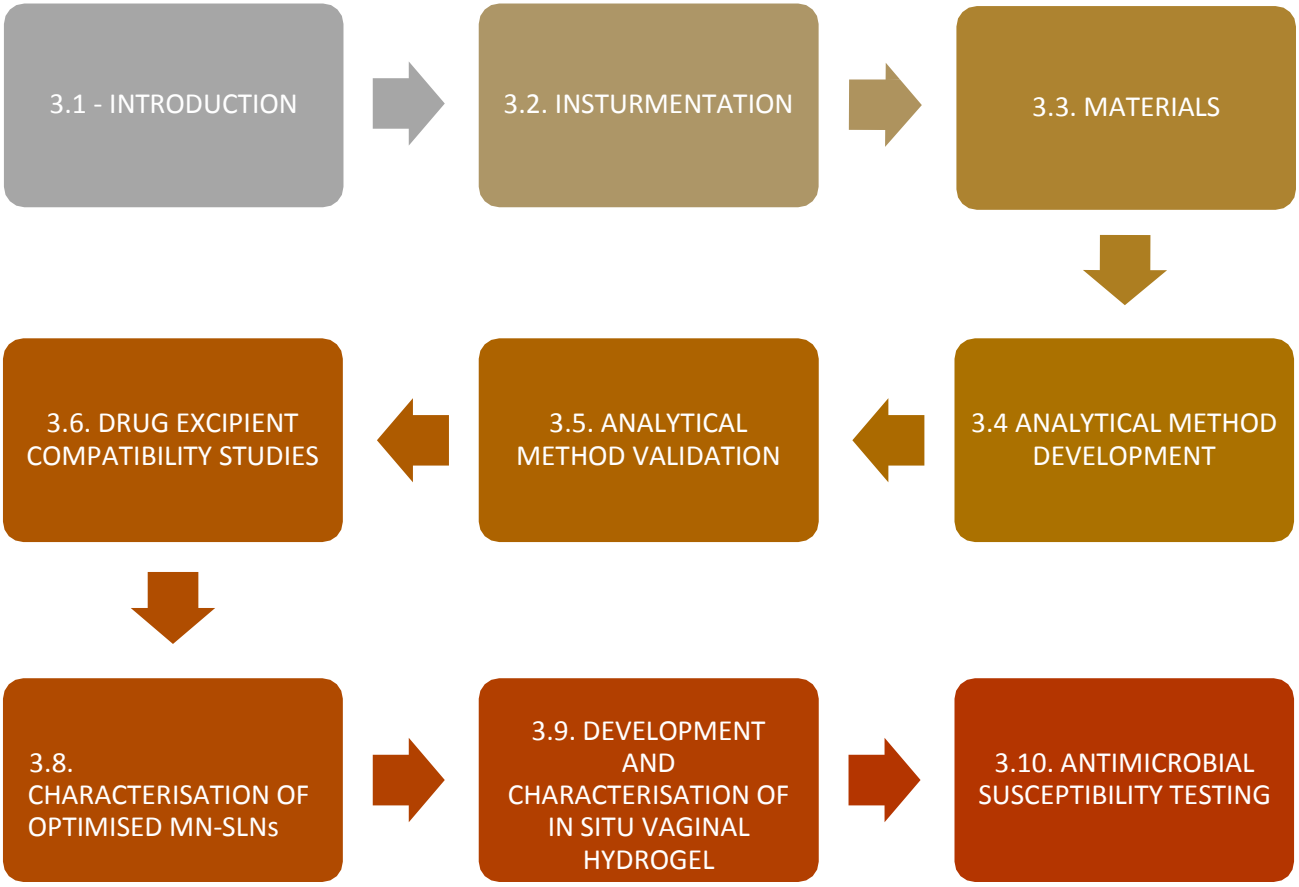

Figure 3.10: Summary of study methodology

The findings of all experimental tests discussed in this chapter will be presented in the following chapter.

CHAPTER 4

RESULTS AND DISCUSSIONS

4.1 INTRODUCTION

Various assessments were conducted for the preparation of the MNZ-SLN loaded vaginal hydrogel. The experimental findings of the development, optimisation and characterisation tests of this novel formulation are discussed in this chapter.

4.2 ANALYTICAL METHOD DEVELOPMENT

An alternative analytical method for the quantification of MNZ in a bulk or complex pharmaceutical product was developed through the use of RP-HPLC. HPLC is a highly selective analytical technique that is capable of identifying, quantifying and purifying isolated ingredients within a complex mixture (Hassan, 2012). It was employed as a means of quantification and subsequent purity assessment of MNZ for the purposes of this study, owing to its accuracy, speed and efficiency.

The use of an already-existing method is ideal, as it is less labour-intensive and time-consuming and is better at generating unbiased results from the operator. There are well-established and documented methods for the quantification of MNZ by means of RP-HPLC available (British Pharmacopeia Commision, 2014). Adopting these methods would have been ideal for this study, however, due to a lack of availability of some of the equipment as well as limited resources, a new method was developed.

4.2.1 Sample preparation

A 2 mg/ml MNZ stock solution was prepared by dissolving MNZ microcrystalline powder in 8.5 ml of MeOH, followed by the addition of H_2O in order to yield a final volume of 10 ml. The resultant solution was colourless and transparent, with a characteristic alcohol odour (see Figure 4.1). No precipitation was observed in the solution suggesting that the API had undergone sufficient dissolution in the solvent.

Figure 4.1: Miconazole nitrate (MNZ) 2 mg/ml stock solution for analytical method development.

Proper sample preparation technique is essential to maintaining RP-HPLC system integrity and to prevent unwarranted chromatographic interference (Moldoveanu, 2004). Furthermore, a homogenous solution that is free of suspended particles is desirable for maintaining RP-HPLC system integrity by preventing blockages and subsequent pressure increase (Shahtaheri *et al.,* 2005; Lim, 1988). Proper sample preparation and a homogenous solution was achieved in this study.

4.2.2 Mobile phase (MP) optimisation

The MP is responsible for the transportation of components in a sample through the column so as to facilitate separation (Kazakevich and Lobrutto, 2007). The quantity and type of organic phase used in a method has a direct influence on selectivity and resolution of the method. Owing to their practicality and availability, MeOH and H_2O were selected as MP components for the purposes of this study.

The experimental results noted in Section 3.4.3.2 are discussed in the following sub-sections. Most notably, there is a discussion on the effect of the organic phase composition and buffers as components of the MP that were investigated respectively. Various types of MPs and ratios were tested, and the results were compared.

4.2.2.1 Selection of organic phase ratio

Preliminary investigations deemed MeOH as the most favourable organic phase in the MP for the purposes of this study. A sample of 0.25 mg/ml MNZ was prepared by diluting the stock solution with a MeOH:H_2O (85:15) premixed solution. The sample was analysed by means of RP-HPLC under preliminary chromatographic conditions. All variables were kept constant with the exception of the quantity of MeOH in the MP. The MeOH to H_2O ratio in the MP was varied at predetermined ratios. The resultant analyte retention times (R_f) and MNZ peak symmetry factors (A_s) are shown in Table 4.1.

Table 4.1: Implications of varying organic modifier (methanol) in mobile phase (MP).

Sample	MNZ conc. (mg/ml)	H_2O (% v/v)	MeOH (% v/v)	Symmetry factor	Retention time (min)
1	0.25	15	85	0.95	5.57
2	0.25	20	80	0.97	6.01
3	0.25	25	75	1.04	8.86
4	0.25	30	70	1.05	10.13
5	0.25	50	50	-	-

As depicted in Table 4.1, MeOH concentration levels of 70 to 85% v/v yielded acceptable peak symmetry and rapid elution times (≤10.13 minutes). Figure 4.2 summarises the relationship between MeOH and retention time, where an increase in MeOH concentration caused a gradual decrease in retention time. Further increases in MeOH concentration above 85% v/v resulted in the subsequent loss of resolution, while MeOH concentrations below 70% v/v resulted in very poor resolution with an unstable baseline where no distinct peaks were observed. Minor deviations were noted in the peak symmetry factors, but all results obtained in the MeOH concentration range of 70 to 85% v/v where deemed favourable for method development. All MNZ peaks obtained were also pure, with purity values of ≥0.999.

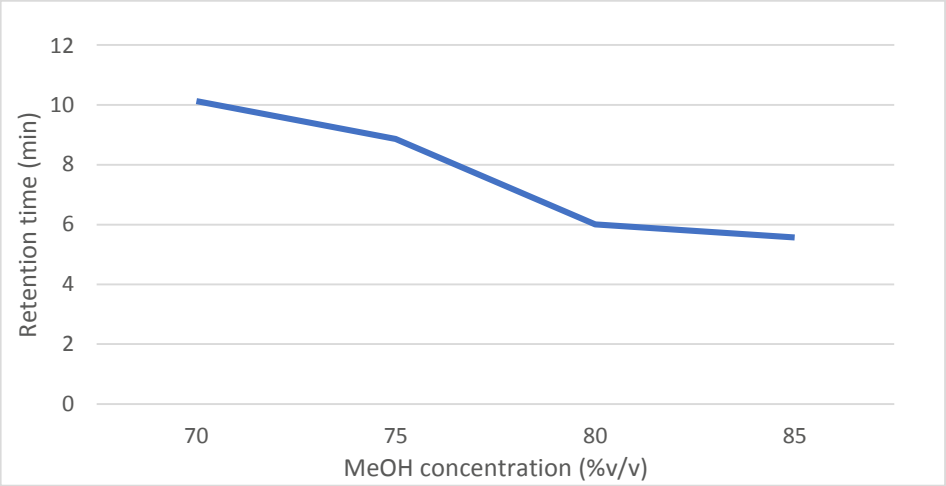

Figure 4.2: Plot of retention time as a function of MeOH concentration for the RP-HPLC analysis of a 0.25 mg/ml miconazole nitrate (MNZ) sample.

High H_2O content in the MP causes the repulsion of lipophilic analytes out of the MP and into the non-polar stationary phase where they remain until they partition into the MP again (Carr *et al.*, 1986). Therefore, the addition of an organic modifier lowers the polarity of H_2O and ensures that the analyte does not repel strongly into the stationary phase. This phenomenon suggests that the use of H_2O reduces the elution strength of the MP and causes a gradual increase of MNZ retention time for the developed method (Joshi *et al.,* 2015).

Through this process, it was also noted that a decrease in MeOH concentration (<70% v/v) led to poor resolution, unstable baselines and the presence of impurities in the MNZ peak. An increase in MP viscosity could possibly explain this phenomenon (Crawford Scientific™, 2017). Solvents of low viscosity are ideal for RP-HPLC, as they reduce the likelihood of dispersion and a build-up of system backpressure (Shalliker and Guichon, 2009). MeOH possesses a viscosity of 0.544 mPa•s at 20 °C, which produces a low-pressure drop at certain flow rates, thereby allowing for rapid analysis due to an increase in mass transfer. A binary mixture of MeOH (60% v/v) and H_2O (40% v/v) produces the maximal acceptable velocity at a pressure of 1.62 mPa•s but, in turn, significantly increases system backpressure (Crawford Scientific™, 2017). Furthermore, the rate of analyte mass transfer is reduced, and the operator runs the risk of system malfunction due to an increase in pressure of the system; therefore, the use of H_2O in the MP above 40% v/v was not advised for the purposes of this study.

Based on these established percentages, the final MP composition was selected at MeOH (85% v/v) and H_2O (15% v/v) because they produced the quickest method for achieving acceptable purity and peak symmetry required in this study.

4.2.2.2 The use of buffers in mobile phase (MP) composition

The potential of buffer use in RP-HPLC has been explored extensively in the literature (Roses *et al.,* 1996; Tindall and Dolan, 2003). For the purposes of this study, the buffer potential was investigated in order to determine whether its use resulted in more favourable selectivity and retention of MNZ when compared to a simple MeOH and H_2O binary mixture.

To that end, an ammonium acetate buffer (pH 4) was freshly prepared and used at 15% v/v (in place of H_2O) with respect to MeOH so as to yield a new MP. Figure 4.3 illustrates a chromatogram of a 0.25 mg/ml MNZ sample recorded at a flow rate of 1.2 ml/min and a temperature of 40 °C using a MeOH (85% v/v):H_2O (15% v/v) MP. Conversely, Figure 4.4 illustrates a chromatogram of a 0.25 mg/ml MNZ sample under similar chromatographic conditions with the exception of an 85% v/v MeOH and 15% v/v ammonium acetate buffer MP.

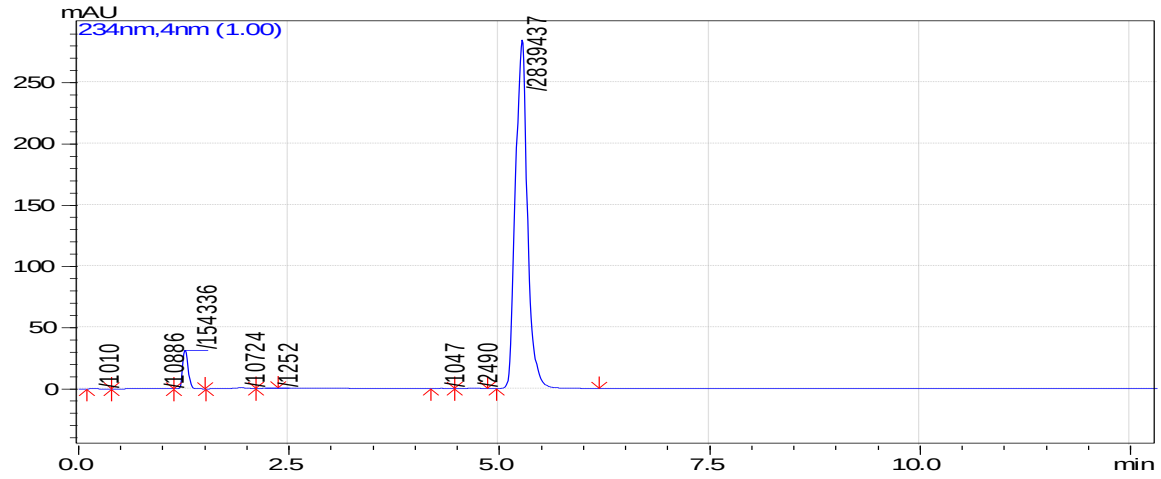

Figure 4.3: Chromatogram of 0.25 mg/ml miconazole nitrate (MNZ) sample at 234 nm (Temp: 40 °C, Flow rate: 1.2 ml/min, MP: MeOH 85% v/v and H_2O 15% v/v).

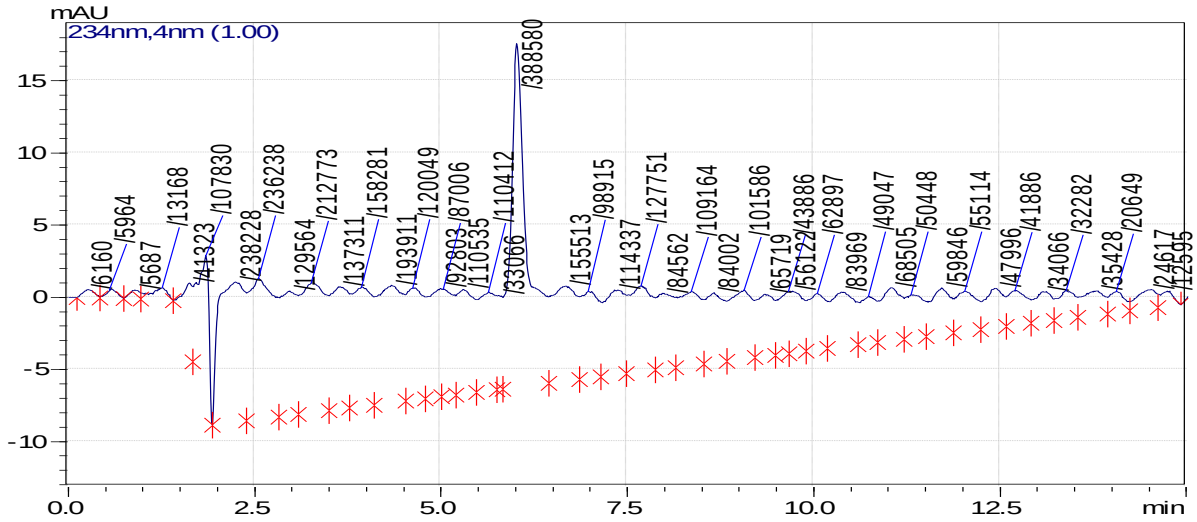

Figure 4.4: Chromatogram of 0.25 mg/ml miconazole nitrate (MNZ) sample at 234 nm (Temp: 40 °C, Flow rate 1.2 ml/min, MP: 85% v/v MeOH and 15% v/v ammonium acetate buffer).

Visual disparities were noted when the two chromatograms were compared. For example, the use of an ammonium acetate buffer resulted in the generation of a smaller miconazole peak, this is possibly attributed to interference by electrolytes from the buffer. Furthermore, a slight increase in retention times of peaks one and two by 30 seconds was observed, with peak one demonstrating a negative protrusion from the baseline.

For ionised compounds, such as MNZ, the use buffer solutions in the MP can improve the selectivity and reproducibility of the method (Roses *et al.,* 1996). It was observed, however, that for this study, the use of a H_20 instead of a buffer solution resulted in improved purity and stability of the baseline. In addition, the method was less time-consuming and more cost-efficient because fewer reagents and materials were consumed. For these reasons, MeOH and H_2O were selected as ideal solvents in the MP for the purposes of this study.

4.2.2.3 Mobile phase (MP) flow rate optimisation

Flow rate is defined as the volume of MP transported through a column per unit time (Bhardwaj *et al.,* 2015). It was believed that the alteration of MP flow rate would have a direct influence on elution time and peak symmetry. To optimise the current chromatographic conditions, the effect of flow rate was investigated. Table 4.2 depicts the measured peak symmetry and retention times of a 0.25 mg/ml MNZ sample at predetermined flow rates.

Table 4.2: Variation of flow rate in the RP-HPLC analysis of a 0.25 mg/ml miconazole nitrate (MNZ) sample at 234 nm (Temp: 40 °C).

Sample	MP MeOH:H_2O (% v/v)	MNZ conc. (mg/mL)	Flow rate (mL/min)	Symmetry factor	Retention time (min)
1	85:15	0.25	0.8	1.26	13.15
2	85:15	0.25	1.0	0.97	9.57
3	85:15	0.25	1.2	0.94	6.42
4	85:15	0.25	1.5	0.85	5.02
5	85:15	0.25	2.0	-	-

As depicted in Table 4.2, flow rates of 1.0 to 1.2 ml/min yielded chromatograms with acceptable peak symmetry and retention times. A decrease in flow rates below 1.0 ml/min resulted in lengthy retention times and excessive peak tailing, which were not ideal. Conversely, the gradual increase of flow rate resulted in faster elution of the analyte, which is ideal for producing rapid analytical methods.

However, extreme caution should be taken when increasing the flow rate in order to ensure that the system does not succumb to malfunction as a result of an increased pressure (Carr *et al.,* 2009). In addition, it was noted that subsequent increases in flow rate beyond 1.2 ml/min resulted in the fronting of chromatographic peaks, and a flow rate of ≥2 ml/min resulted in column leakages and system malfunction as a result of the excessive pressure build-up.

Figure 4.5 illustrates an indirect proportionality relationship between flow rate and retention time(s), where an increase in flow rate resulted in a decrease of retention time.

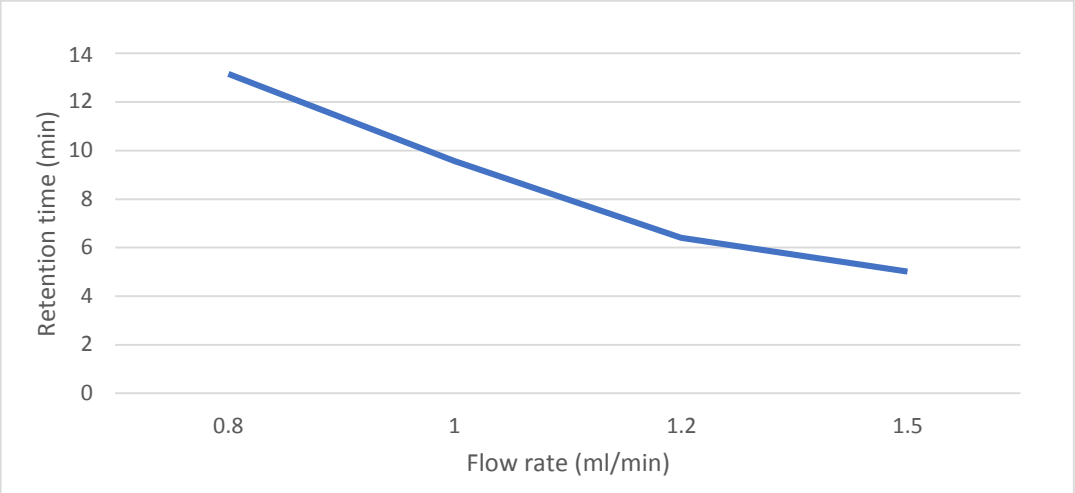

Figure 4.5: Plot of flow rate as a function of retention time for the RP-HPLC analysis of a 0.25 mg/ml miconazole nitrate (MNZ) sample.

Sufficient time must be given for the analyte to interact with the stationary phase; therefore, shorter separation times or rapid methods are not always ideal (Astefanei *et al.,* 2016). As a result, a flow rate of 1.0ml/min was selected because it allowed for sufficient time for the MNZ to interact with the column packing. It also provided sufficient opportunity to observe the generation of other degradants in the sample whilst producing a Gaussian peak. A reduction of flow rate (<1.0 ml/min) maintained similar peak areas because the concentration of the sample remained unchanged; however, the peaks observed became wider and shorter.

4.2.3 Sample injection volume optimisation

Column overloading, poor retention times and asymmetrical peaks are common issues associated with the poor selection of injection volume (Boonen *et al.,* 2013; Sailaja *et al.,* 2016). Therefore, the effect of the injection volume on the RP-HPLC method for the quantification of MNZ was investigated so as to ensure that symmetrical peaks with sufficient purity and clarity were obtained. Table 4.3 illustrates the values obtained for peak symmetry and retention times at each predetermined injection volume.

Table 4.3: Variation of injection volume for the RP-HPLC analysis of a 0.25 mg/ml miconazole nitrate (MNZ) sample.

Sample	MeOH:H_2O	MNZ conc. (mg/mL)	Flow rate (mL/min)	Injection Vol. (µL)	Symmetry factor	Retention Time (min)
1	85:15	0.25	1.0	1	0.98	9.55
2	85:15	0.25	1.0	2	0.98	9.57
3	85:15	0.25	1.0	5	0.97	9.72
4	85:15	0.25	1.0	10	1.03	10.03
5	85:15	0.25	1.0	20	-	-

Injection volumes below 10 µL produced satisfactory MNZ peak symmetry, while the retention times of all analyses remained fairly constant. An increase in injection volume was associated with an increase in the diffusion process time, which translated to more time being used to load the sample on the stationary phase. Larger volumes equated to wider peaks, which took longer to elute and led to significant tailing being observed. Fronting was expressed by a symmetry value (A_s) of <0.8, which indicated possible column overloading (Ornaf and Dong, 2005). As noted previously, the choice of injection solution can affect the retention time. However, in this case, the solution was similar to that of the MP, hence minimal deviations of the retention times were noted. These findings correlate with the findings of Ren and colleagues (2012).

Optimal injection volumes are directly related to the cylindrical volume of the column. The recommended injection volume for the column dimension (4.6 mm × 150 mm) utilised for this study are two to 10 µL. Volumes that exceed this range are only acceptable if the resultant peak is symmetrical (Silicycle, 2018). Based on these parameters, it was observed, experimentally, that volumes exceeding 10 µL produced asymmetrical peaks with significant fronting. Furthermore, an injection volume of 20 µL resulted in column leakage and system malfunction as a direct result of pressure build-up. This was not ideal for the maintenance of system integrity. Conversely, injection volumes of one to 10 µL produced satisfactory peak symmetry and retention times. It should be noted that too low injection volumes are closely linked to a loss of response, especially upon sample dilution (Swartz, 2010). Therefore, 10 µL was selected as the ideal volume for the rapid quantification of MNZ by means of RP-HPLC.

4.2.4 Summary of optimised chromatographic conditions

Carefully optimised chromatographic conditions result in high sensitivity of analyte detection (Montemurro *et al.,* 2016). Method sensitivity is dependent on MP composition and interface parameters, such as temperature and flow rate (McCalley, 2000; Ho and Kim, 2011). Table 4.4 provides a brief summary of optimal chromatographic conditions, as expressed in the British Pharmacopoeia (British Pharmacopeia Commission, 2014) and current literature (e.g. Hermawan *et al.,* 2017), where differences in each method are contrasted with the experimental conditions of this study.

Table 4.4: Summary of chromatographic conditions in the British Pharmacopoeia (British Pharmacopoeia Commission, 2004), current literature (Hermawan *et al.*, 2017) and the developed method for this study.

Chromatographic variable	British pharmacopoeia	Literature review (Hermawan *et al.*, 2017)	Experimental conditions
Analyte	MNZ	Miconazole	MNZ
Concentration	10 mg/1ml	0.05 mg/ml	0.25 mg/ml
Sample solvent	MP	MeOH	MP
Injection volume	10 µL	5 µL	10 µL
Column type	Octadecylsilyl C_{18} (100 × 4.6 mm, 3 µ)	Phenomenex C_8 Luna® (150 × 4.6 mm, 10 µ)	Phenomenex C_8 (150 × 4.6 mm, 5 µ)
Flow	Isocratic	Isocratic	Isocratic
Flow rate	2 ml/min	0.8 ml/min	1.0 ml/min
Temperature	30 °C	unspecified	40 °C
Wavelength	235 nm	220 nm	234 nm
Mobile phase (MP)	6.0 g ammonium acetate in 300 ml acetonitrile, 320 ml methanol, 380 ml H_2O	MeOH:H_2O (85:15% v/v)	MeOH:H_2O (85:15% v/v)

When compared to the existing pharmacopoeial method, this experimental method

provided comparable results with regard to resolution in the quantification of MNZ. The new method also resulted in the consumption of fewer reagents by simplifying the MP, thereby making it cost-effective. The current method proposed by Hermawan *et al.* (2017) provided faster quantification of MNZ, with a retention time of approximately seven minutes and a drifting baseline. The optimised method for this study, however, provided superior resolution and a steady baseline, with a slight increase in analyte retention time. Table 4.5 summarises the experimental findings for the optimised method in this study.

Table 4.5: Summary of experimental findings for the optimised method.

Parameter	Sample 1	Sample 2	Sample 3	Mean ± RSD
Peak area	2055001	2053998	2055063	2054687 ± 0.020
Peak symmetry	0.97000	0.98000	0.97000	0.97000 ± 0.048
Peak purity	0.99998	0.99999	0.99998	0.99998 ± 0.000
Retention time (min)	10.6600	10.6900	10.6900	10.6800 ± 1.253

The mean peak area for an assayed 0.25 mg/ml MNZ sample was 2 054 687 ± 0.020, with a mean peak symmetry of 0.97 ± 0.048, which suggested a Gaussian peak. A mean peak purity value of 0.999 suggested that there was no interference from other compounds in the sample. Finally, <15 minutes suggests that a rapid method was developed for the quantification of MNZ.

The benefits of updating existing analytical methods include providing enhanced sensitivity and resolution, rapid elution of the investigated analyte. Moreover, newer solvent-sparing methods provide a cost-effective analysis for resource-limited facilities (Dong and Guillarme, 2017). This study managed to achieve both.

4.3 ANALYTICAL METHOD VALIDATION

A successfully validated method demonstrates that the developed method is indeed suitable for its intended use (Varshosaz *et al.,* 2011). Validation parameters including peak analysis, linearity, precision, accuracy, LoD and LoQ were investigated and their outcomes are discussed in this section.

4.3.1 Peak analysis

The assessment of peak symmetry allows the operator an opportunity to discern the physicochemical process undertaken within the stationary phase (Papai and Pap, 2002). For this study, a chromatogram obtained from the analysis of a 0.5 mg/ml MNZ sample was assessed visually (see Figure 4.6) under the optimised chromatographic conditions, after which the symmetry factor was calculated. Morepver, Equation 4.1 expresses the mathematical calculation of the symmetry factor (A_s) depicted in Figure 4.6.

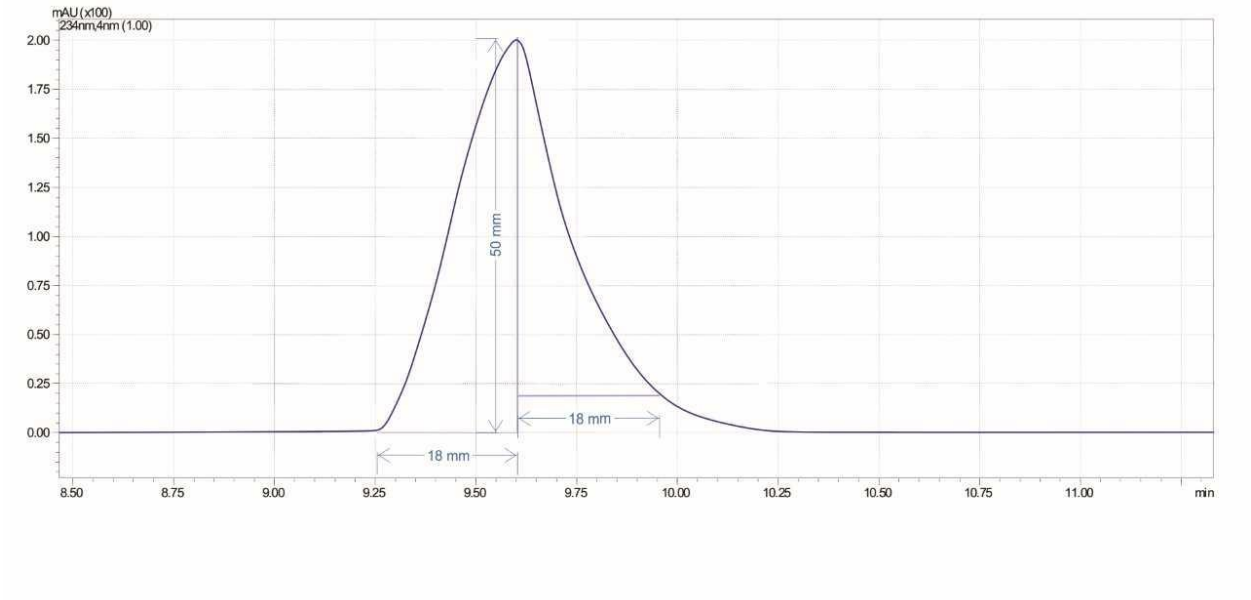

Figure 4.6: RP-HPLC chromatogram of 0.5 mg/ml miconazole nitrate (MNZ) sample (Temperature: 40 °C, Flow rate: 1 ml/min and MP:MeOH 85% v/v:H_2O 15% v/v).

$$A_s = \frac{b}{a} = 1$$

Equation 4.1: Symmetry factor calculation for 0.5 mg/ml miconazole peak under optimised RP-HPLC conditions.

An A_s value of 1 was obtained and was deemed acceptable since it was within the noted range of 0.9 to 1.2. An A_s value in the range of 0.9 to 1.2 is sufficient for indicating a Gaussian peak with negligible tailing or fronting (Kadjo *et al.,* 2017).

4.3.2 Linearity and range

The linearity of the experimental data was determined within a working range of 0.125

to 1.00 mg/ml. Seven (*n*=7) samples at predetermined concentration levels were assayed in triplicates and their experimental results are presented in Table 4.6.

Table 4.6: Calibration data for the quantification of miconazole nitrate (MNZ) in the range of 0.125 to 1.000 mg/ml under optimised chromatographic conditions.

Concentration (mg/ml)	% Target analyte	Peak area (mean of *n*=3)	Peak area % RSD
0.125	25	1110973.557	1.95
0.250	50	2054979.667	0.51
0.400	80	3312895.023	0.82
0.500	100	4164199.890	0.51
0.600	120	4935189.234	1.96
0.750	150	6093138.165	0.26
1.000	200	8210823.447	1.87
Linear regression equation: y = 811214x + 67958		r^2: 0.9998	

The mean peak values for each concentration level assayed in triplicate was calculated and utilised in order to generate a plot of mean peak area as a function of concentration. This function was referred to as the calibration curve of MNZ, as illustrated in Figure 4.7.

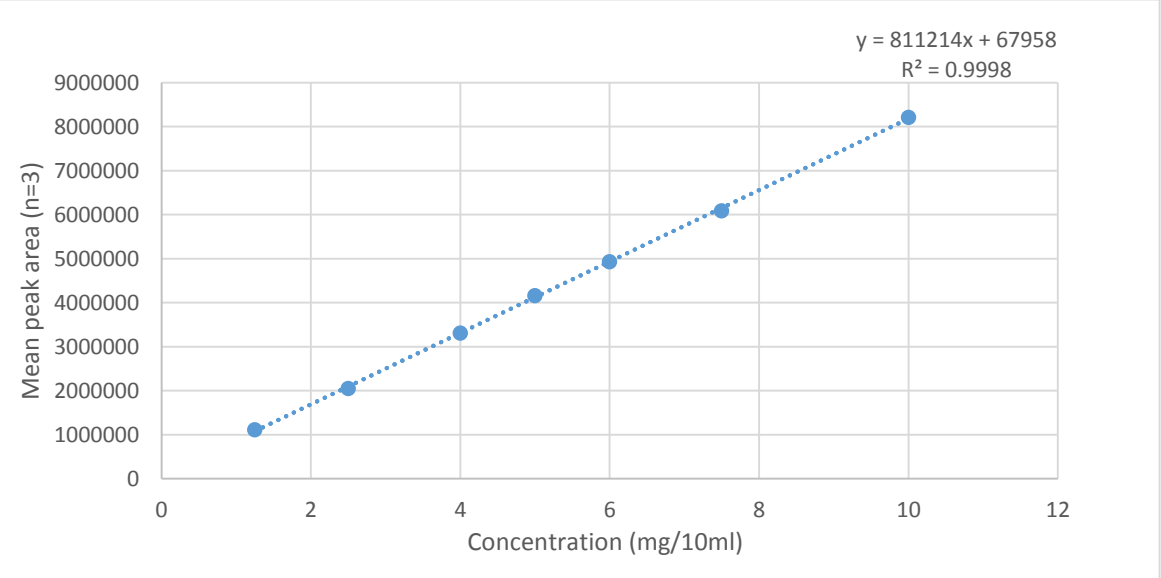

Figure 4.7: Calibration curve of miconazole nitrate (MNZ) in the working range of 0.125 to 1.00 mg/ml.

Data acceptability was judged from the assessment of the correlation co-efficient (r^2) of the regression line. An r^2 value of >0.999 with no curvature of the residual plot is sufficient for the declaration of a linear method (Bakshi *et al.,* 2017). A straight line was obtained with a linear regression equation of y = 811214x + 67958 and an r^2 value of 0.9998. Moreover, the % RSD of the mean peak areas was ≤2 (see Table 4.6). This indicated a directly proportional relationship between response and concentration, thus deeming the method linear.

The significance of the plot, also referred to as the assessment value (z), was investigated in order to determine whether the plot would cross the line of origin. A z value of -2≥ z ≥2 is deemed acceptable (Ghasemi and Zahediasi, 2012).

$$Assessment\ value\ (z) = \frac{67958}{4164199.890} \times 100$$

$$z = 1.63$$

Equation 4.2: Assessment value (z) for the calibration plot of miconazole nitrate (MNZ) in the working range of 0.125 to 1.00 mg/ml.

A z value of 1.63 was obtained, which suggested that there would be a high likelihood of the regression line intersecting at zero. This result was favourable.

4.3.3 Accuracy

An accurate method, as defined by the ICH, fulfils the following criteria: the % recovery of the analysed samples does not deviate by a value of ± 2% of the theoretical yield with a % RSD of ≤2% for the mean concentration (*ICH Harmonised Tripartite Guideline* Q2 (R1), 1994). Table 4.7 illustrates the % recovery and the mean concentration value obtained from the assay MNZ samples (n=5) in triplicates at five concentration levels within the working range.

Table 4.7: Method accuracy data for the quantification of miconazole nitrate (MNZ) within the working range under optimised chromatographic conditions.

Theoretical yield (mg/ml)	Actual yield (mg/ml)		% Recovery
	Mean (*n*=3)	% RSD	
0.250	0.254	1.76	101.60
0.400	0.402	0.52	100.50
0.500	0.511	1.62	102.00
0.600	0.611	1.90	101.83
1.000	0.983	1.97	98.350

All calculated % RSD were below the acceptance limit of 2% and the % recovery did not deviate more than 2% from theoretical value, thus deeming the method accurate.

4.3.4 Precision

The acceptance criteria for method precision (i.e. repeatability) is very similar to that of accuracy, where a deviation of ≤2% is acceptable for recovery and % RSD (*ICH Harmonised Tripartite Guideline* Q2 (R1), 1994). Table 4.8 illustrates the results obtained from the assay of six samples (n=6 in triplicate at a chosen concentration within the working range.

Table 4.8: Method precision data for the quantification of MNZ within the working range under optimised chromatographic conditions.

Theoretical yield (mg/mL)	Actual yield (mg/mL)		% Recovery
	Mean (*n*=3)	%RSD	
0.50	0.508	0.83	101.60
0.50	0.506	0.26	101.20
0.50	0.506	0.15	101.20
0.50	0.501	0.12	100.20
0.50	0.509	0.41	101.80
0.50	0.508	0.21	101.60

All calculated % RSD values were below the acceptance limit of 2% and the % recovery did not deviate more than 2% from theoretical value, thus deeming the method precise.

4.3.4.1 Intermediate precision

The acceptance criteria for intermediate precision is the same as that of repeatability (*ICH Harmonised Tripartite Guideline* Q2 (R1), 1994). The assay results obtained on the different working days should have a statistical significance of ≤2% RSD (Little, 2016). The findings of this study's assay of six samples (n=6) at 0.5 mg/ml in triplicates on two separate days by the same operator and on the same machine are depicted in Table 4.9.

Table 4.9: Intermediate precision data for the quantification of miconazole nitrate (MNZ) within the working range under optimised chromatographic conditions.

Theoretical yield (mg/mL)	Actual yield (mg/mL)					
	Day 1		Day 7		Day 1	Day 7
	Mean (*n*=3)	% RSD	Mean (*n*=3)	% RSD	% Recovery	
0.50	0.508	0.83	0.491	0.58	101.60	98.13
0.50	0.506	0.26	0.494	0.06	101.20	98.74
0.50	0.506	0.15	0.492	0.07	101.20	98.40
0.50	0.501	0.12	0.492	0.18	100.20	98.40
0.50	0.509	0.41	0.490	0.23	101.80	98.00
0.50	0.508	0.21	0.494	0.12	101.60	98.86

All calculated % RSD were below the acceptance limit of 2% and the % recovery did not deviate more than 2% from theoretical values, thus deeming the method precise. However, while the intermediate precision was deemed acceptable, a slight deviation in % recovery was observed. This deviation may have been as a result of human error during the preparatory steps, such as the weighing of the MNZ, dilution of the stock solution or transfer into the sample vials. This deviation was not deemed significant since all results were maintainied within the limit of acceptability.

4.3.5 Limit of detection (LoD)

A signal-to-noise ratio of 3:1 was considered as the LoD (Tamilsevan *et al.,* 2014; Sun *et al.,* 2012). Table 4.10 illustrates the calculated data for LoD for MNZ quantification under optimised chromatographic conditions.

Table 4.10: Limit of detection (LoD) data for the quantification of miconazole nitrate (MNZ) under optimised chromatographic conditions.

Sample no.	Active ingredient	Peak purity	Concentration (mg/ml)	Concentration (% w/v)	% RSD
1	MNN	0.9999	0.015	1.5	0.62
2	MNZ	0.9999	0.015	1.5	0.80
3	MNZ	0.9998	0.016	1.6	0.56

It was determined that the LoD was 0.015 mg/ml, where MNZ could be accurately detected under the optimised chromatographic conditions.

4.3.6 Limit of quantitation (LoQ)

A signal-to-noise ratio of 10:1 was considered as the LoQ (Tamilsevan *et al.,* 2014; Sun *et al.,* 2012). Table 4.11 illustrates the calculated data for LoQ for MNZ quantification under the optimised chromatographic conditions.

Table 4.11: Limit of quantitation (LoQ) data for the quantification of miconazole nitrate (MNZ) under optimised chromatographic conditions.

Sample no.	Active ingredient	Peak purity	Concentration (mg/mL)	Concentration (%w/v)	% RSD
1	MNZ	0.9999	0.052	5.2	0.96
2	MNZ	0.9999	0.052	5.2	0.80
3	MNZ	0.9999	0.052	5.2	0.83

The LoQ was determined to be 0.052 mg/ml, where MNZ could be accurately quantified under the optimised chromatographic conditions.

4.3.7 Specificity

Peak purity tests were conducted utilising PDA detection. These tests were useful in displaying that analyte responses were not associated with the presence of other components in the sample. Similarly, chromatograms were evaluated for the presence of compounds which may cause potential interference or co-elution with the MNZ peak.

Figure 4.8 depicts a chromatogram of a 0.5 mg/ml MNZ sample under optimised chromatographic conditions.

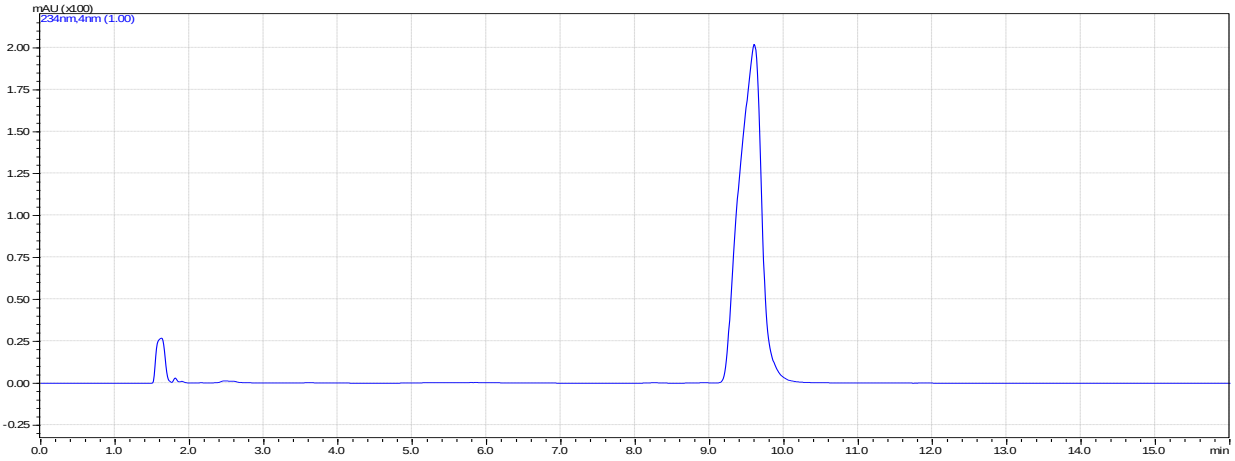

Figure 4.8: Chromatogram of a 0.5 mg/ml miconazole nitrate (MNZ) sample under optimised chromatographic conditions (Temperature: 40 °C, Flow rate: 1 ml/min and MP:MeOH 85% v/v:H_2O 15% v/v).

Two peaks were generated at 1.23 and 10.03 minutes, respectively, with good resolution and no obvious interference noted. Peak symmetry and baseline noise were satisfactory. The initial peak observed may be attributed to the partitioning of the nitrate ion upon dissolution in solvent. The second peak indicates the detection of miconazole at 0.9999 purity (see Figure 4.9).

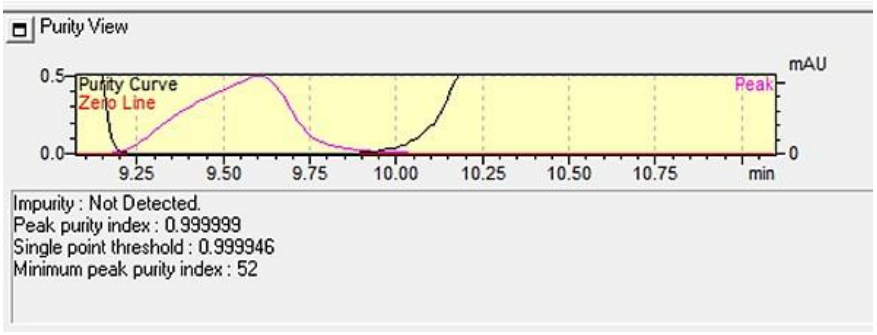

Figure 4.9: Peak purity profile of MNZ assayed under optimised chromatographic conditions (Temperature: 40 °C, Flow rate: 1 ml/min and MP:MeOH 85% v/v:H_2O 15% v/v).

A negative control in the form a blank injection of the MP was investigated under optimised chromatographic conditions (see Figure 4.10), where no obvious peaks that may cause potential interference with MNZ were observed. There was, however, a peak observed at ± 1.63 minutes. This may be attributed to the solvent front, which represents unretained material in the column.

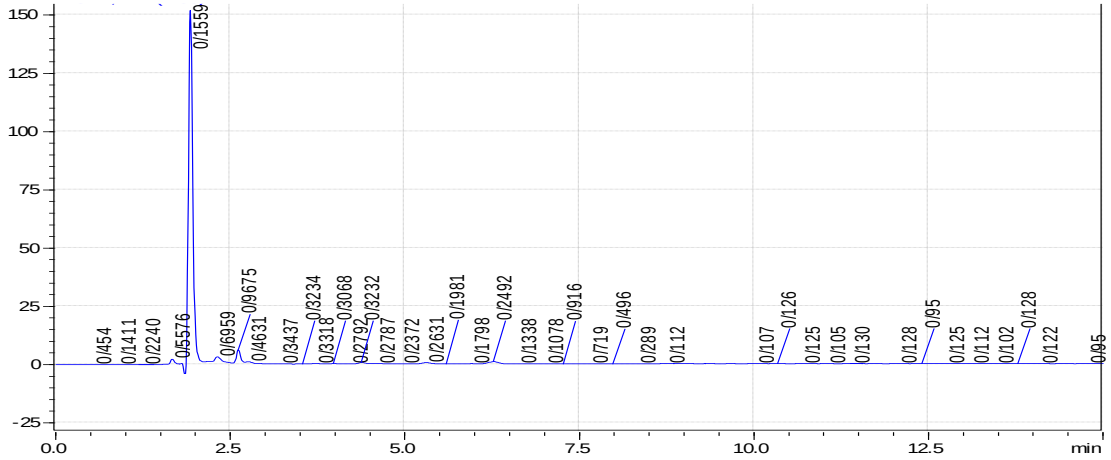

Figure 4.10: Blank injection of MP under optimised chromatographic conditions (Temperature: 40 °C, Flow rate: 1 ml/min and MP:MeOH 85% v/v:H_2O 15% v/v).

A positive control (in the form of a MNZ-SLNs) was investigated under the optimised conditions. Figure 4.11 depicts the generated chromatogram, where no additional peaks were observed. This lack of peaks suggested that the method was suitable for the analysis of MNZ in bulk, or within a complex pharmaceutical mixture. However, there was a noted shift in the retention time to 12.25 minutes. This shift could possibly be attributed to the complex composition of the MNZ-SLN formulation, such as the presence of lipids.

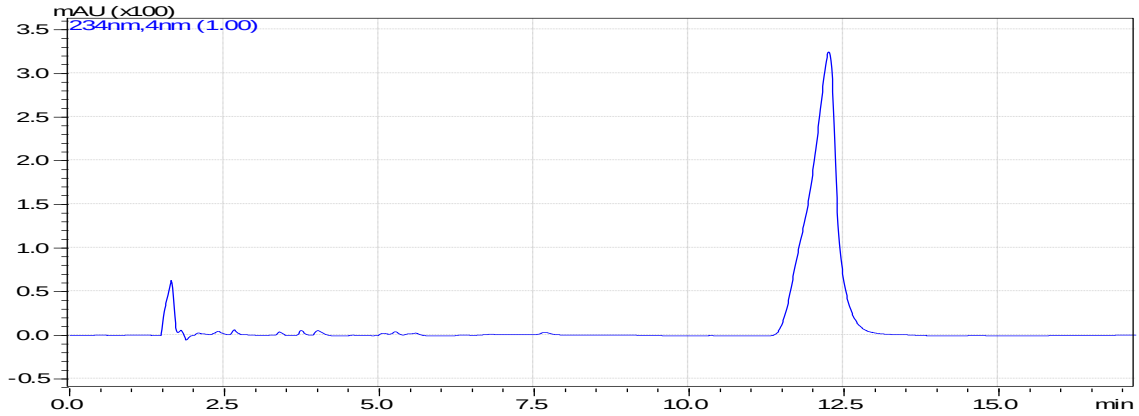

Figure 4.11: Chromatogram of 0.5 mg/ml MNZ-SLNs under the optimised conditions (Temperature: 40 °C, Flow rate: 1 ml/min and MP:MeOH 85% v/v:H_2O 15% v/v).

4.3.7.1 Acid/Alkali hydrolysis

Freshly-prepared samples were subjected to extreme acid/base conditions in order to generate chromatographic profiles of MNZ under these stress conditions. Figure 4.12 depicts a chromatogram of a 0.5 mg/ml MNZ sample under acidic stress conditions.

The peak area value, here, was significantly smaller than that found in Figure 4.8 (standard solution). This finding indicated that MNZ underwent significant degradation. Additional peaks were formed (marked 2 to 10 in Figure 4.12), which indicated the presence of degradation products within the sample.

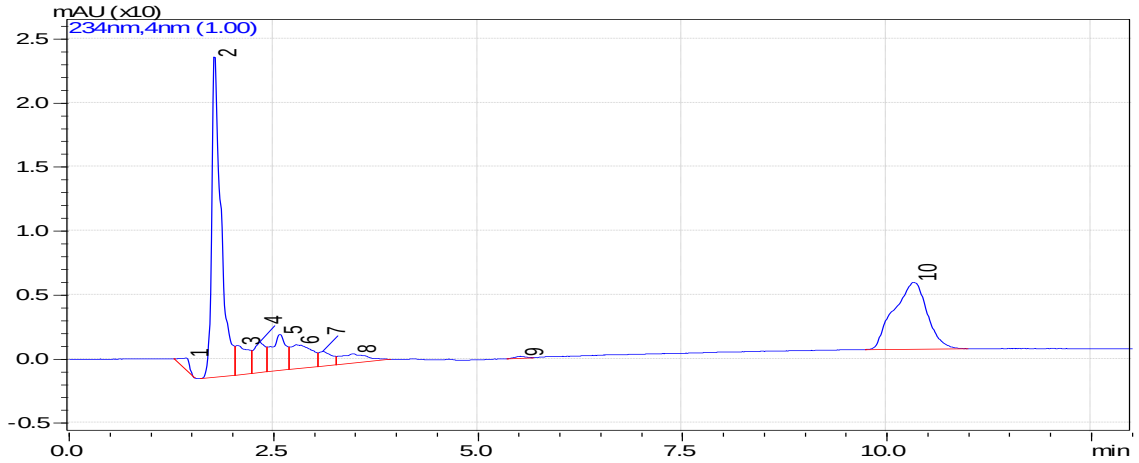

Figure 4.12: Chromatogram of a 0.5 mg/ml miconazole nitrate (MNZ) sample under acidic stress conditions.

The peak purity profile (depicted in Figure 4.13) was also assessed. It revealed a good factor of 0.999, which indicated that the detected analyte was, indeed, MNZ. The retention time of the analyte was consistent with that of the standard sample under the optimised conditions.

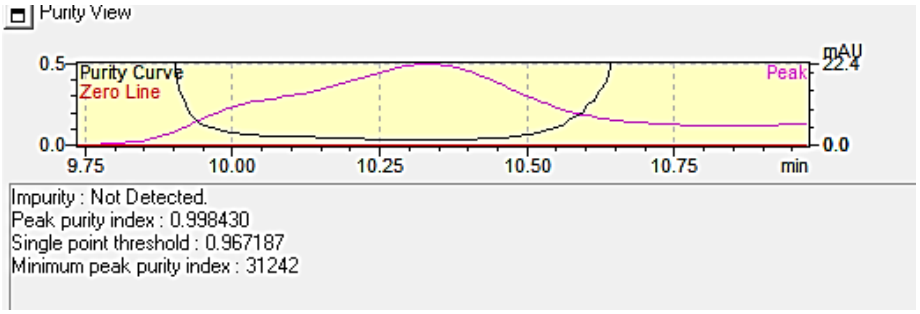

Figure 4.13: Peak purity profile of 0.5 mg/ml miconazole nitrate (MNZ) under acidic stress conditions.

The results from the alkali stress testing of a MNZ 0.5 mg/ml sample is depicted in Figure 4.14. The peak values obtained are much smaller than that of the standard solution, which indicated that significant degradation of the analyte took place. Additional peaks, labelled 2 to 9 in Figure 4.14, further indicated the presence of degradation products.

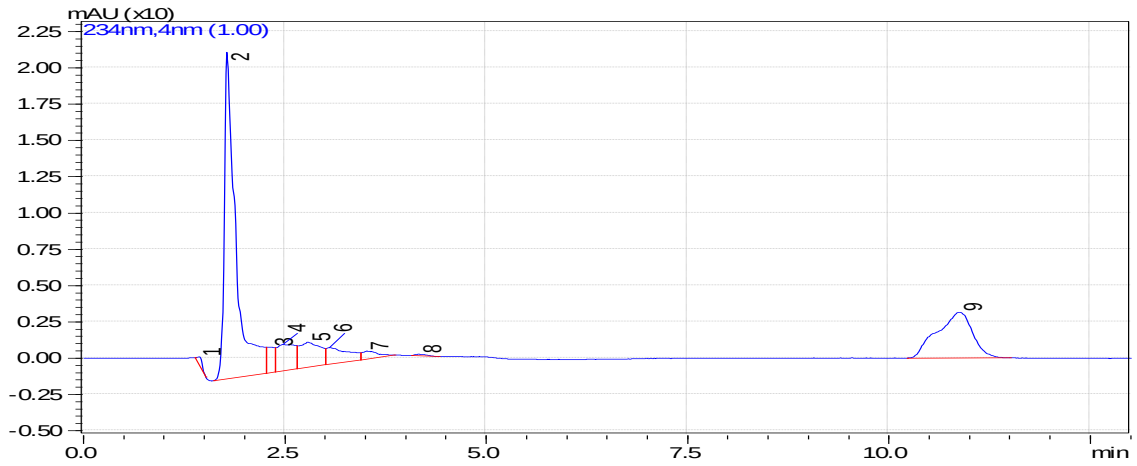

Figure 4.14: Chromatogram of a 0.5 mg/m miconazole (MNZ) sample under alkali stress conditions

The peak purity of the resultant MNZ peak was investigated (see Figure 4.15). A purity index of 0.9962 was obtained, which demonstrated the absence of other by-products at that elution time, and concluded that MNZ had eluted at 10.00 minutes.

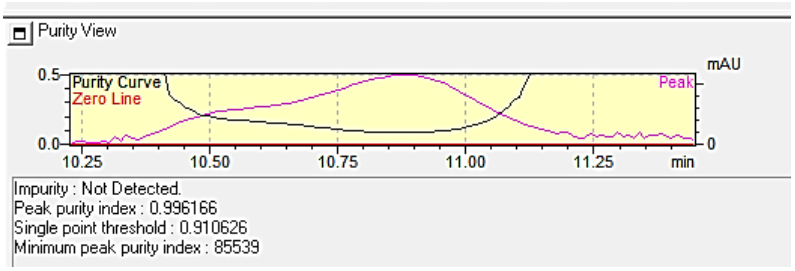

Figure 4.15: Peak purity profile of 0.5 mg/ml miconazole nitrate (MNZ) under alkali stress conditions.

An overview of the acid/alkali force degradation study is provided in Table 4.12. The rate of degradation under acidic conditions was much less than that of alkali conditions. MNZ was found to be labile under both hydrolytic conditions. The respective chromatograms indicated the presence of additional peaks, which correlated with degradation products and impurities. A reduction of peak height and the broadening of peak bases were observed, which indicated that MNZ underwent hydrolysis to degrade chromophoric groups.

Table 4.12: Overview of acidic/alkali stress testing of a 0.5 mg/ml miconazole nitrate (MNZ) sample.

	Acid hydrolysis			Alkali hydrolysis		
Sample	**1**	**2**	**3**	**1**	**2**	**3**
Purity profile	0.9989	0.9999	0.9999	0.9973	0.9972	0.9962
Peak area	147989	148101	148025	105760	105800	105782
Mean peak area (*n*=3) + SD	148038.3 ± 0.21			105780.7 ± 0.04		
Mean conc.	0.099 mg/ml			0.047 mg/ml		
Retention factor	10.75	10.70	10.71	10.82	10.79	10.80
Mean retention time	10.72 ± 0.03			10.80 ± 0.02		
% Degradation	80.2%			90.6%		

4.3.7.2 Oxidation

Freshly-prepared samples were subjected to extreme oxidative conditions so as to generate chromatographic profiles of MNZ under stress conditions. Figure 4.16 demonstrates a chromatogram of a 0.5 mg/ml MNZ sample under oxidative stress using a 3% H_2O_2 solution.

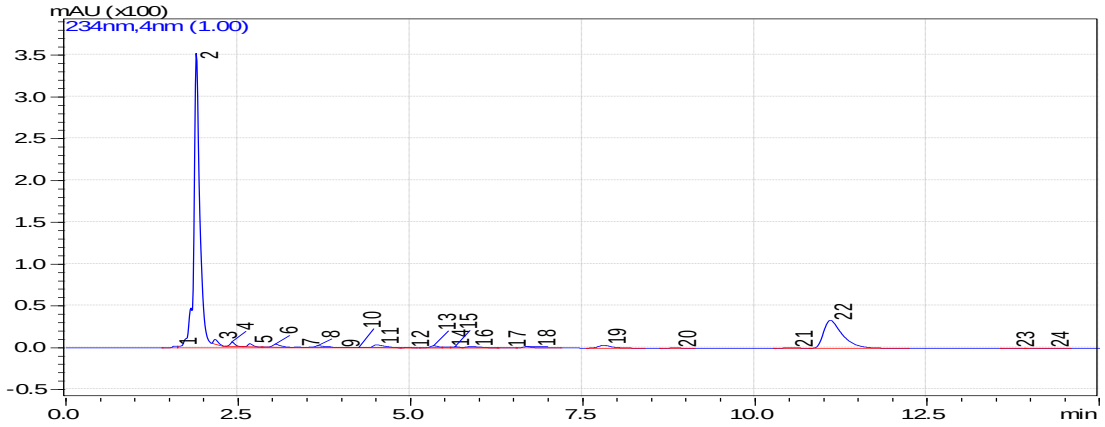

Figure 4.16: Chromatogram of 0.5mg/ml miconazole nitrate (MNZ) sample under oxidative stress conditions (3% hydrogen peroxide solution).

The MNZ peak values obtained were significantly smaller than those of the standard sample, which suggested that MNZ underwent oxidative degradation. Additional peaks, labelled 2 to 22 in the aforementioned figure, were observed, which further indicated the presence of degradation products. There was also a slight shift in retention time of the analyte.

A control in the form a blank sample (MeOH 85% v/v and H_2O 15% v/v) was also investigated under oxidative stress in order to determine whether there was the presence of degradation products as a result of the oxidising agent (see Figure 4.17). One peak was observed before two-and-a-half minutes; this represented the solvent front. The baseline was stable, with the presence of degradation products. Thus, the findings indicated that the presence of degradation product was due to the MNZ sample analysis and not due to the 3% H_2O_2 solution.

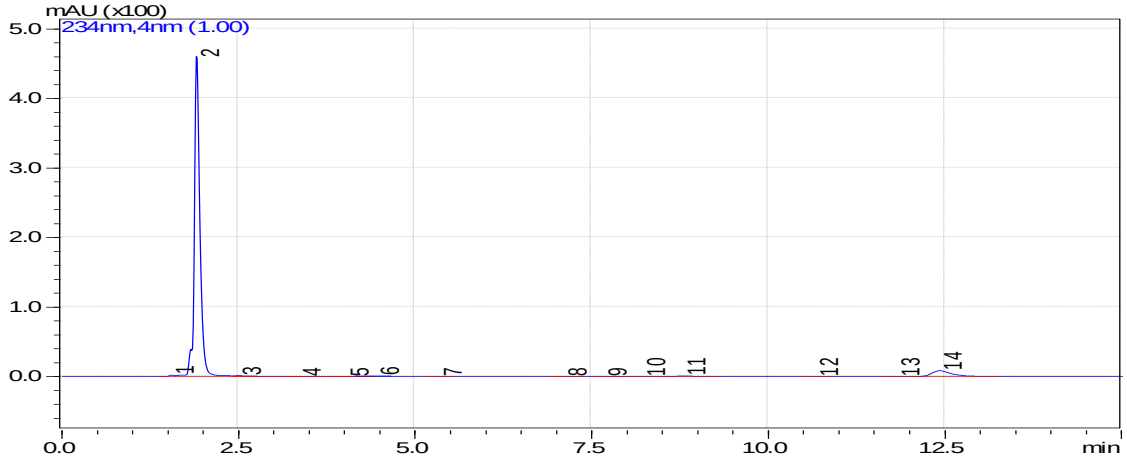

Figure 4.17: Chromatogram of a blank injection (MeOH 85% v/v and H_20 15% v/v) under oxidative stress conditions.

The analysis of the peak purity profile indicated a good correlation of 0.999927 (see Figure 4.18). This finding concluded that there was an absence of impurities within the observed peak. The symmetry of the peak, however, suggested significant tailing.

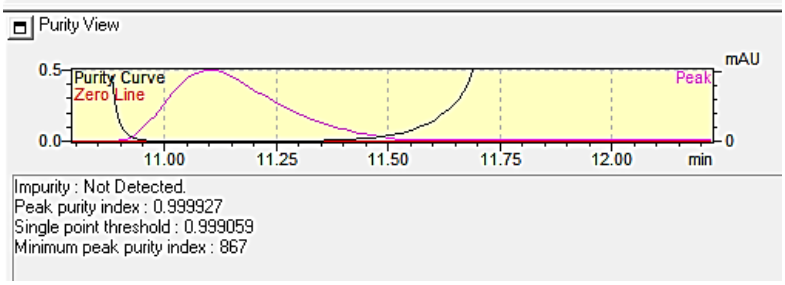

Figure 4.18: Peak purity profile of 0.5 mg/ml miconazole nitrate (MNZ) sample under oxidative stress.

A summary of the oxidative stress results of a 0.5mg/ml MNZ sample is illustrated in Table 4.13. It was observed that MNZ was labile under oxidation when using a 3% H_2O_2 solution, with a slight increase in retention time.

Table 4.13: Summary of oxidative stress results for the assay of a 0.5mg/ml miconazole nitrate (MNZ) sample.

	0.5mg/ml MNZ sample			Blank sample (MeOH 85% v/v:H_2O 15% v/v)		
Sample	**1**	**2**	**3**	**1**	**2**	**3**
Purity profile	0.99995	0.99993	0.99997	-	-	-
Peak area	98230	97657	98823	No peak	No peak	No peak
Mean peak area (*n*=3) + SD	98239.67 ± 0.15			-		
Mean conc.	0.037 mg/ml			-		
Retention factor	11.85	11.60	11.73	-	-	-
Mean retention time	11.73 ± 0.03			-		
% Degradation	92.6%			-		

4.3.7.3 Photolytic degradation

Samples were subjected to photolytic exposure so as to generate chromatographic profiles of MNZ under photolytic stress conditions. Analyte degradation was monitored over a period of seven days. The first reading was taken after 48 hours, then 96 hours and, lastly, after 144 hours. Figure 4.19 illustrates an example of a 0.5 mg/ml sample under photolytic stress after 48 hours. The peak area was slightly smaller than that of the standard solution, which indicated that degradation of MNZ occurred. Additional degradation products, marked 2 to 19 in the figure, were also observed. A slight shift in retention time was also noted.

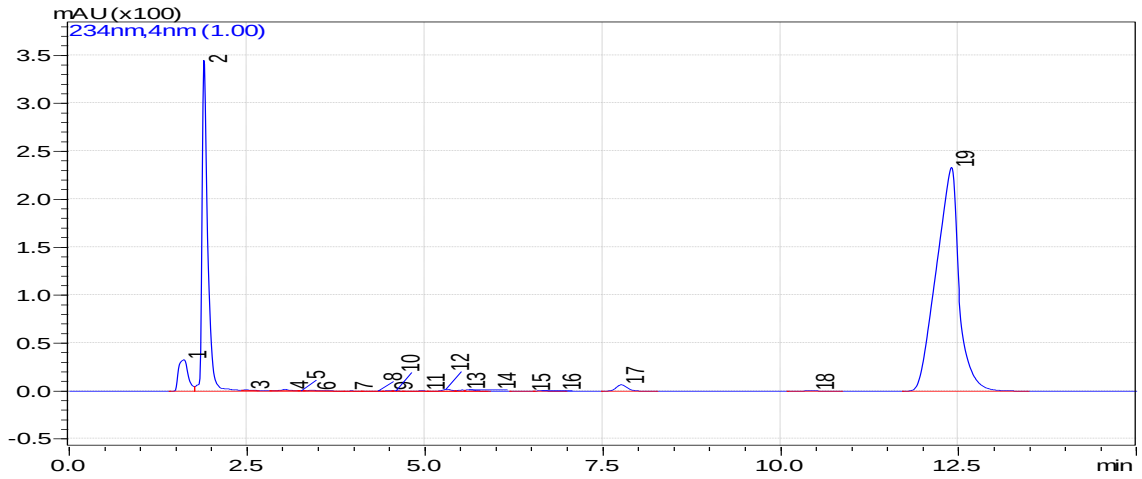

Figure 4.19: Chromatogram of 0.5mg/ml miconazole nitrate (MNZ) sample under photolytic stress at 48 hours.

The assessment of peak purity indicated a good correlation of 0.9999, which suggested the absence of impurities in the observed peak. Good symmetry was also noted (see Figure 4.20).

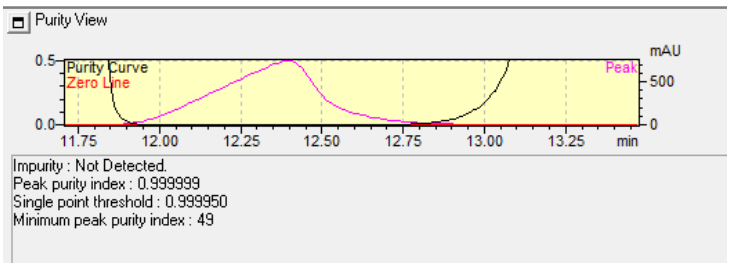

Figure 4.20: Peak purity profile of 0.5 mg/ml miconazole nitrate (MNZ) sample under photolytic stress at 48 hours.

A control test was conducted by placing a 0.5 mg/ml MNZ sample in a dark room. Periodic assays were then conducted at 48, 96 and 144 hours. Figure 4.21 illustrates an example of a chromatogram generated under these conditions at 48 hours. The peak area observed was slightly less than that of the standard sample, which suggested that the analyte had undergone some degradation. Minor degradation products (peaks 2 to 9) were also noted, with an increased retention time.

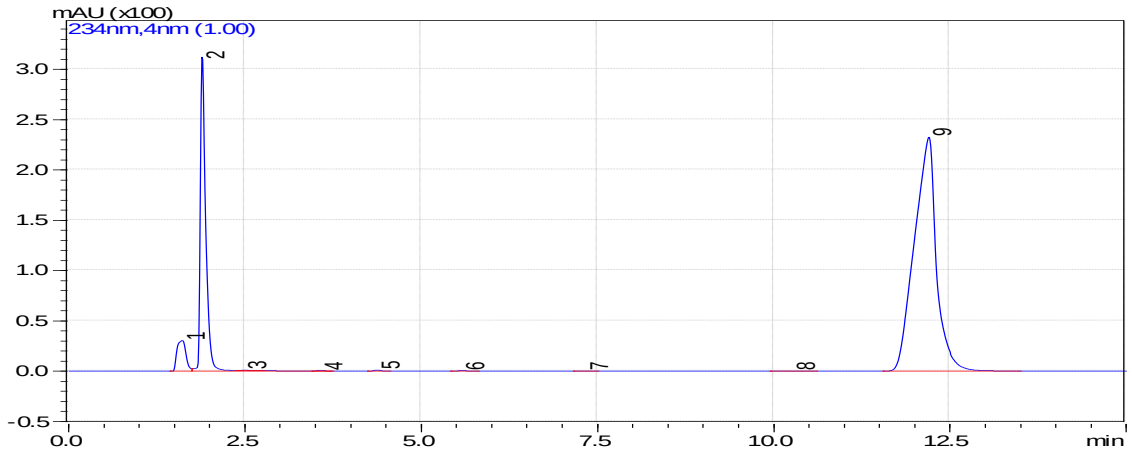

Figure 4.21: Chromatogram of 0.5 mg/ml miconazole nitrate (MNZ) sample stored in a dark room at 48 hours.

The peak purity profile investigation revealed an acceptable index of 0.99999, which suggested the absence of by-products or impurities in the peak.

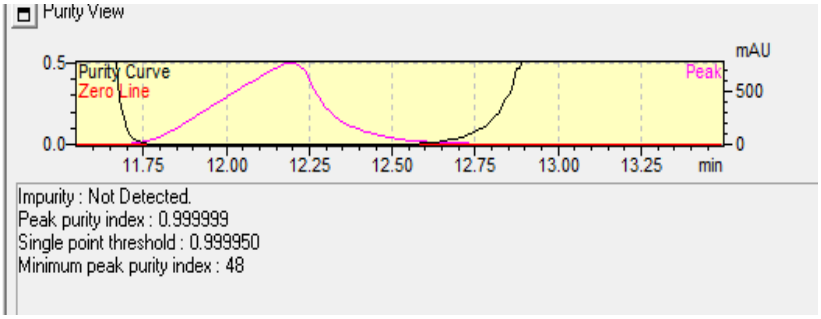

Figure 4.22: Peak purity profile of a 0.5 mg/ml miconazole nitrate (MNZ) sample in a dark room at 48 hours.

A summary of the outcomes from the photolytic stress testing of a 0.5 mg/ml MNZ sample is provided in Table 4.14.

Table 4.14: Summary of photolytic stress testing on a 0.5 mg/ml miconazole nitrate (MNZ) sample.

	Time		
	48 hours	**96 hours**	**144 hours**
1 × ICH photo exposure			
- **R_f**	12.39 min	12.35 min	12.41 min
- **Mean area**	4102433 ± 0.24	2981567 ± 1.02	998756 ± 0.15
- **Mean conc.**	0.48 mg/ml	0.36 mg/ml	0.11 mg/ml
- **Purity profile**	0.99999	0.99997	0.99998
- **% deg.**	4%	28%	77%
Darkroom			
- **R_f**	12.19 min	12.23 min	12.19 min
- **Mean area**	5019559 ± 0.51	3920126 ± 0.13	2005987 ± 0.12
- **Mean conc.**	0.61 mg/ml	0.47 mg/ml	0.24 mg/ml
- **Purity profile**	0.99999	0.99999	0.9999
- **% deg.**	+0.2%	6%	52%

From the information presented in the aforementioned table, MNZ was susceptible to photolytic degradation under both test and control conditions. Light conditions, however, facilitated greater and faster degradation when compared to storage in a dark room. The extent of degradation was greatly increased with prolonged storage and exposure to light. Degradation was also observed in the control sample that was kept in the dark, but this could be attributed to other mechanisms like oxidation upon storage. Moreover, the rate of degradation in the control was relatively high. It should be noted that these tests were conducted at ambient temperature (25 ± 2 °C), which suggested the possibility of MNZ thermal degradation in cases of prolonged storage.

4.3.7.4 Thermal degradation

Freshly-prepared samples were exposed to various temperatures to generate chromatographic profiles of MNZ under thermal stress conditions. The temperatures ranged between four, 25, 60 and 80 °C over a period of 120 hours. Figure 4.23

illustrates an example of a chromatogram of a 0.5 mg/ml MNZ sample under thermal stress at 60 °C after 24 hours. The observed peak area was significantly smaller than that of the standard sample, which indicated that the analyte underwent degradation. Furthermore, additional degradation compounds (marked 2 to 6 in Figure 4.23) were noted.

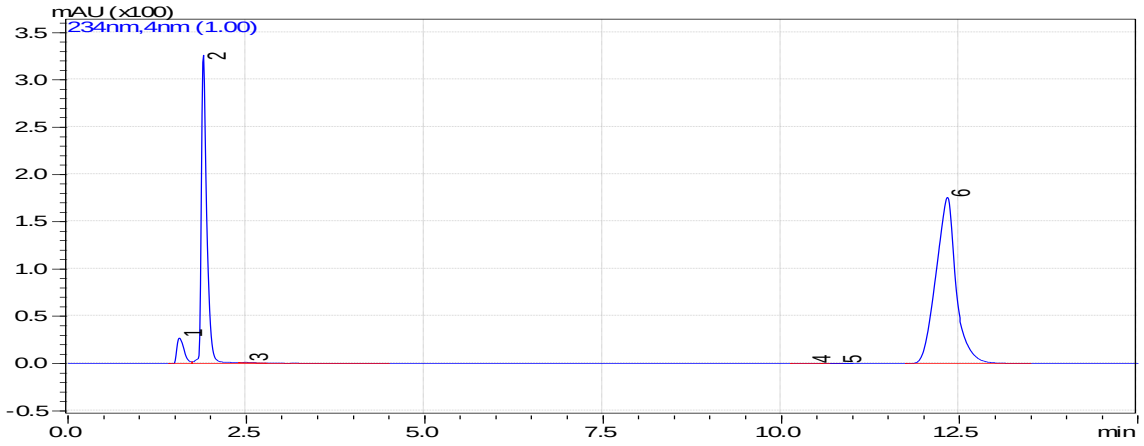

Figure 4.23: Chromatogram of 0.5 mg/ml miconazole nitrate (MNZ) sample at 60°C after 24 hours.

Peak purity profile assessments revealed an acceptable index of 0.99999, which suggested the absence of by-products or impurities in the peak (see Figure 4.24).

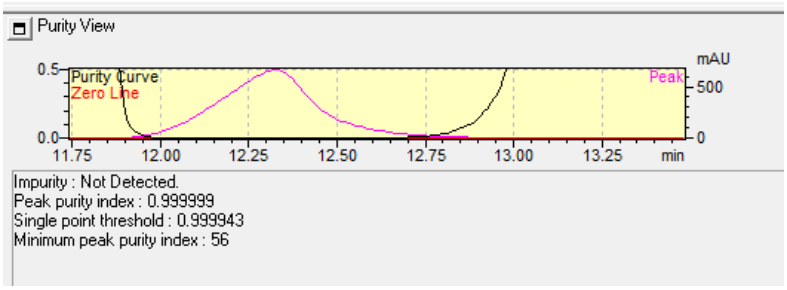

Figure 4.24: Peak purity profile of a 0.5 mg/ml miconazole nitrate (MNZ) sample at 60 °C after 24 hours.

A summary of the chromatographic findings under the respective thermal conditions at each time interval are depicted in Table 4.15.

Table 4.15: Summary of thermal stress testing of a 0.5 mg/ml miconazole nitrate (MNZ) sample(s) over a 24-hour period.

Temperature	Time		
	24 hours	**72 hours**	**120 hours**
4 ± 2°C			
- R_f	12.12 min	12.10 min	12.11 min
- Mean area	4042068 ± 0.21	3825164 ± 0.15	3569817 ± 1.25
- Mean conc.	0.49 mg/ml	0.46 mg/ml	0.43 mg/ml
- Purity profile	0.99999	0.99999	0.99999
- % deg.	3%	8%	14%
25 ± 2°C			
- R_f	12.10 min	12.13 min	12.15 min
- Mean area	3681054 ± 1.54	3109687 ± 1.56	1975264 ± 0.42
- Mean conc.	0.46 mg/ml	0.37 mg/ml	0.24 mg/ml
- Purity profile	0.99999	0.99999	0.99999
- % deg.	8%	26%	52%
60 ± 2°C			
- R_f	12.32 min	12.15 min	12.20 min
- Mean area	3 444 884 ± 2.52	2389675 ± 0.19	1426973 ± 0.52
- Mean conc.	0.41 mg/ml	0.29 mg/ml	0.17 mg/ml
- Purity profile	0.99999	0.99999	0.9999
- % deg.	18%	42%	66%
80 ± 2°C			
- R_f	12.18 min	12.20 min	12.20 min
- Mean area	2765478 ± 1.23	1095231 ± 0.12	862341 ± 1.54
- Mean conc.	0.33 mg/ml	0.13 mg/ml	0.09 mg/ml
- Purity profile	0.99998	0.99999	0.99998
- % deg.	34%	74%	82%

The rate and extent of degradation increased with an increase of temperature and prolonged exposure to thermal conditions. Samples stored at 4 °C were characterised by a larger peak area when compared to the rest, suggesting a slower rate of degradation of the analyte. A shift in retention time was also noted for all samples, which suggested possible oxidative degradation upon storage.

4.3.8. Summary of method validation parameters

An isocratic RP-HPLC stability-indicating method was developed by utilising an octyl stationary phase for the quantification of MNZ in bulk or complex pharmaceutical products. The reliability of the method was statistically validated for linearity, accuracy, precision and specificity within a working range of 0.125 to 1.000 mg/ml. The LoD and LoQ were calculated to be 0.015 and 0.052 mg/ml, respectively. The standard calibration curve was linear within the working range, with a correlation co-efficient of >0.999. A summary of the validation parameters is provided in Table 4.16.

Table 4.16: Summary of method validation parameters.

Parameter	Experimental data
Working range	0.125 to 1.000 mg/ml
Calibration curve	Y = 811214 + 67958
LoD (*n*=3)	0.015 mg/ml
LoQ (*n*=3)	0.052 mg/ml
Accuracy	Recovery = 0.50 ± 2%; % RSD ≤ 2%
Precision - Intra-day - Inter-day	Recovery = 0.50 ± 2%; % RSD ≤ 2%
Specificity	Chromatogram with Gaussian peak Peak purity >0.999 Sufficient degradation under stress conditions

MNZ samples were subjected to stress conditions of hydrolysis, oxidative, thermal and photolytic degradation. The results are summarised in Table 4.17.

Table 4.17: Summary of forced degradation testing parameters.

Parameters	Conditions	Extent of degradation		
Acid/alkali hydrolysis	Acid: in 1M HCl refluxed for 120 min at 80 °C Alkali: in 1M NaOH refluxed for 120 min at 80 °C	Acid: 80.2% Alkali: 90.6%		
Oxidative	In 3% H_2O_2 refluxed for 120min at 80 °C	92.6%		
Photolytic				
Dark room - 48 hrs - 96 hrs - 144 hrs	0.5 mg/ml stored in a dark cupboard; sampling done at periodic intervals at ± 25 °C	 0.2% 6% 52%		
1 × ICH guidelines - 48 hrs - 96 hrs - 144 hrs	0.5 mg/ml samples stored in an incubator, sampling done at periodic intervals at ± 25 °C	 4% 28% 77%		
Thermal	**Conditions**	**24 hrs**	**72 hrs**	**120 hrs**
4 ± 2°C	0.5 mg/ml samples stored in an incubator at the various temperatures	3%	8%	14%
25 ± 2°C		8%	26%	52%
60 ± 2°C		18%	42%	66%
80 ± 2°C		34%	74%	82%

The forced degradation studies proved that MNZ was labile under photolytic, oxidative, hydrolytic and thermal stress. Oxidative stress demonstrated the greatest degradation of 92.6%, whilst thermal stress at 4 °C facilitated the least degradation. Based on these findings it was concluded that, even under extreme stress conditions no degradation products would interefere/interact with the analyte during analysis. Thus deeming the method specific.

4.4 DRUG-EXCIPIENT COMPATIBILITY STUDIES

Simultaneous thermal analysis (SDT) is a highly useful technique for detecting possible incompatibilities between API and excipients in a formulation (Julio *et al.,* 2013) and was, therefore, employed for the determination of drug-excipient compatibility in this study. To that end, bulk materials and binary mixtures of cholesterol and MNZ were investigated.

4.4.1 Thermograms of bulk materials

The thermal behaviour of MNZ (API) in the formulation was investigated. It was observed that MNZ crystalline powder underwent a rapid two-step endothermic degradation. The melting point was recorded at 184.39 °C (see Figure 4.25). Complete degradation occurred by 400 °C with a ± 10% residue.

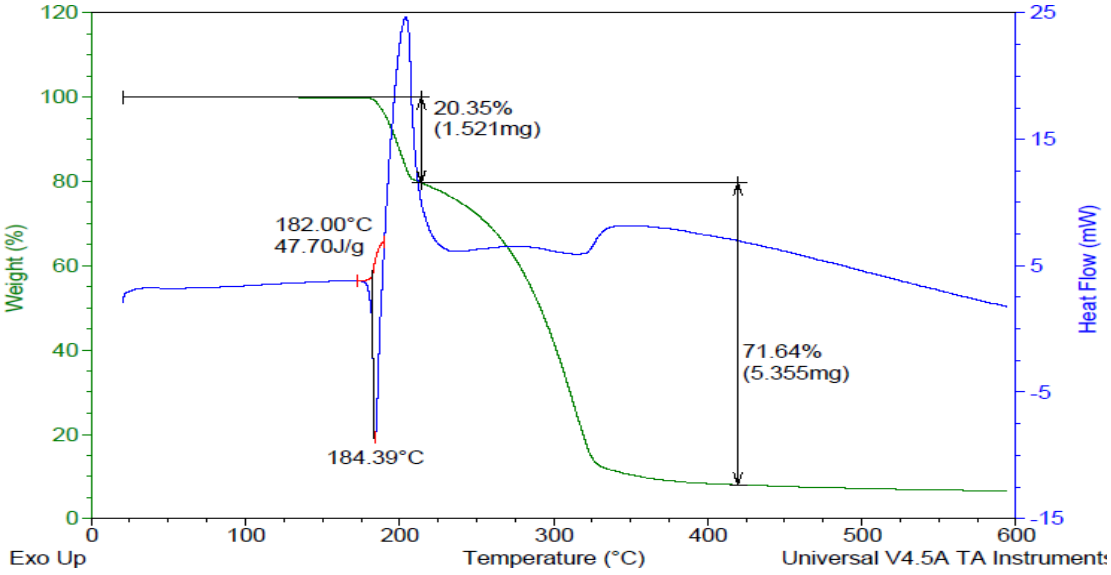

Figure 4.25: Thermogram of bulk miconazole nitrate (MNZ) microcrystalline powder (blue curve indicates the heat flow (mW) as a function of temperature; green curve indicates the % mass of sample as a function of temperature).

For the bulk material of cholesterol, a rapid single-step degradation was observed. The onset of degradation occurred at 143.94 °C with actual melting taking place at 146.7 °C. This melting is indicated by the sharp downward peak in Figure 4.26.

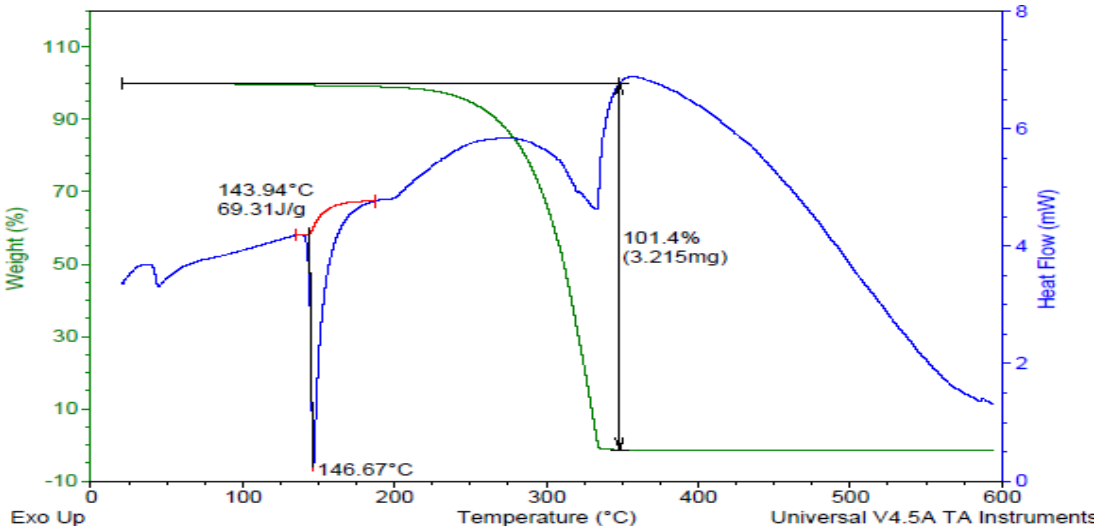

Figure 4.26: Thermogram of bulk cholesterol (blue curve indicates the heat flow (mW) as a function of temperature; green curve indicates the % mass of sample as a function of temperature).

4.4.2 Thermogram of binary mixture

The thermal characteristics of a MNZ and cholesterol binary mixture were investigated in order to determine the possible interaction between the two components. Interactions may be expressed by a shift or broadening of the thermogram. A two-step degradation process was noted for the mixture. The melting range was between 141.6 °C to 155.97 °C, with actual melting taking place at 145.88 °C (see Figure 4.27).

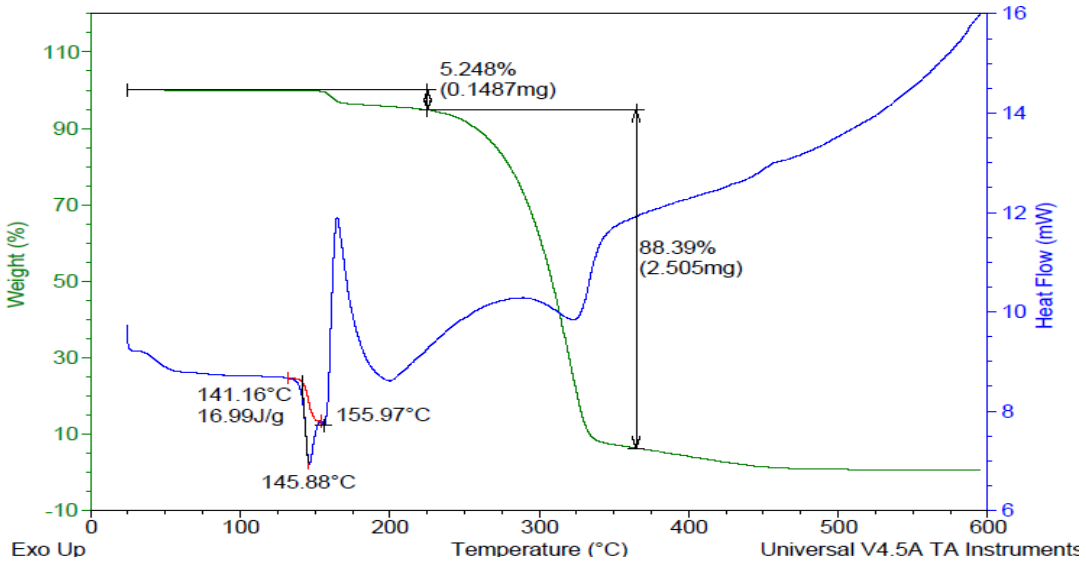

Figure 4.27: Thermogram of dried mixture of miconazole nitrate (MNZ) (35% m/m) and cholesterol (65% m/m).

4.4.3 Summary of drug-excipient compatibility studies

Based on the findings of the SDT, it can be concluded that there is a clear distinction in the thermal behaviours of MNZ and cholesterol, respectively. MNZ demonstrated a much higher melting point (184.39 °C) than cholesterol (146.74 °C). It should be noted that the two-step degradation process observed may have been as a direct result of the dissociation of $N_3O_4^-$ from $C_{18}H_{14}Cl_4^+$ in the MNZ molecule. The molecular mass (M_r) of $N_3O_4^-$ accounted for 22.12% of the total M_r of MNZ (highlighted in Figure 4.28). This number correlates with the 1.52 mg (20.35%) change in mass accounted for in the initial degradation of MNZ.

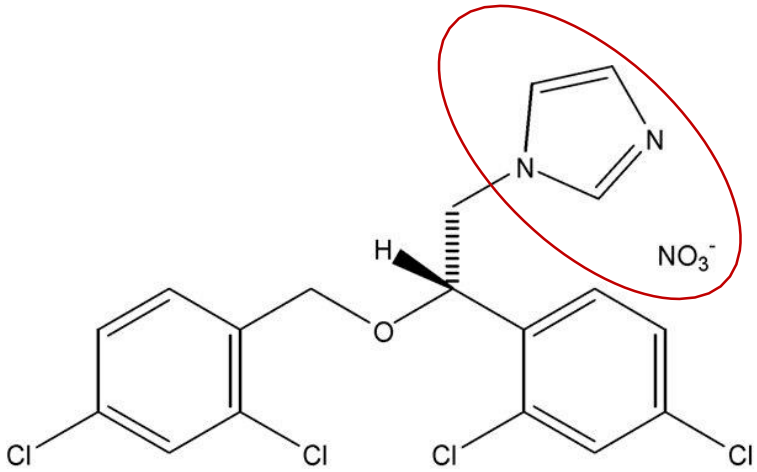

Figure 4.28: Chemical structure of miconazole nitrate (MNZ) demonstrating $N_3O_4^-$ molecule circled in red (De Zan *et al.*, 2009).

A summary of the changes in thermal behaviour of MNZ and cholesterol in bulk and binary mixtures is illustrated in Figure 4.29. The thermogram depicts a shift to a lower temperature from 185 ± 2 °C to 157 ± 2 °C for MNZ in the mixture. The higher melting point of MNZ in the bulk formulation may be indicative of a highly ordered crystal lattice structure. For a less ordered structure, the melting of materials requires less energy than that of highly ordered structures. It is of great importance to note the change in melting point and broadening of the peak as these were associated with lattice defects and the formation of amorphous regions in which a drug can be located. Less order was preferential, as it allowed for greater accommodation of API in the lipid vesicle. Conversely, cholesterol maintained its thermal properties, with negligible shifts in its melting point from 146.06 °C to 146.19 °C.

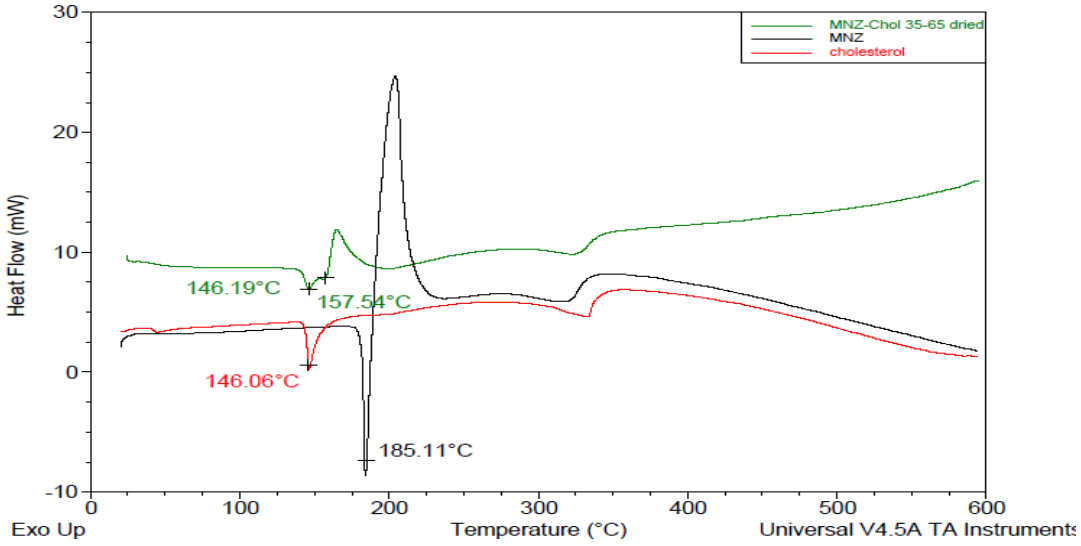

Figure 4.29: Thermogram of cholesterol (red), miconazole nitrate (MNZ) (black) and MNZ (35% v/v) and cholesterol (65% v/v) binary mixture (green).

Figure 4.30 illustrates the thermal degradation of MNZ and cholesterol in bulk and binary mixtures by analysis of % weight as a function of temperature.

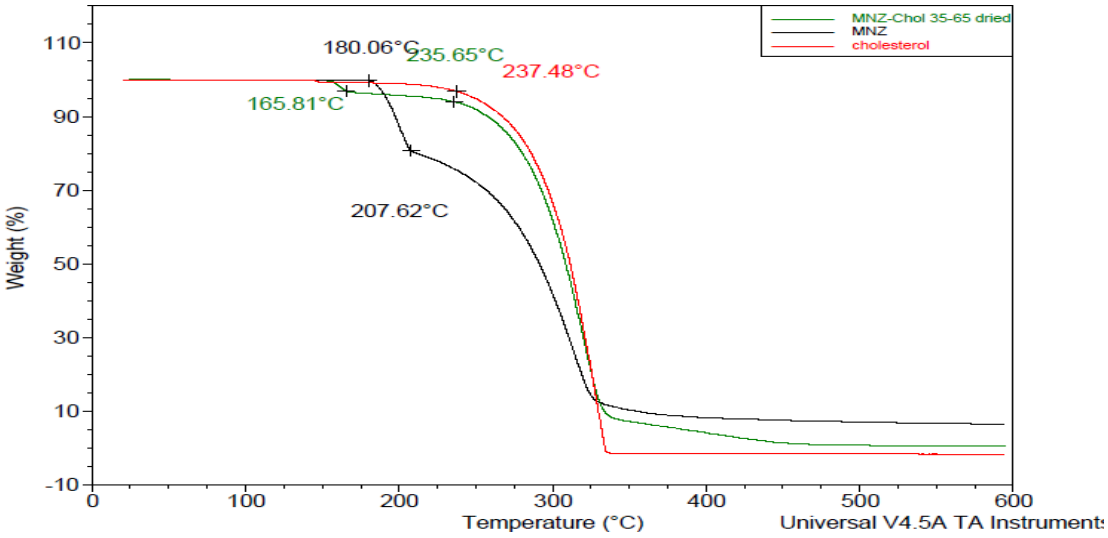

Figure 4.30: Function of % weight versus temperature of miconazole nitrate (MNZ) (black), cholesterol (red) and MNZ (35% v/v) and cholesterol (65% v/v) binary mixture (green).

It was observed that the degradation of cholesterol changed from a single- to a two-step process when placed in a binary mixture, with a shift in melting point from 237.48 °C to 165.81 and 235.65 °C, respectively. This is possibly owing to the presence of the API in the mixture.

Furthermore, the degradation of MNZ followed a two-step process in both the bulk and binary mixture formulations. Its respective melting points went from 180.06 °C and 207.62 °C to 165.81 °C and 235.65 °C, respectively. It was also noted that bulk cholesterol left no residue upon degradation, but MNZ left a residue of 7.0 ± 1%. This residual value of MNZ was, however, decreased to 3.67% when combined in a binary mixture.

MNZ demonstrated satisfactory dissolution with cholesterol and rapid degradation of $N_3O_4^-$ at 165.81°C, thus leaving miconazole alone in the lipid mix. The combination of MNZ and cholesterol resulted in the formation of a distinct chromatogram that assumed the entrapment of the API in the lipid. These findings were deemed favourable as it was expected that cholesterol would modify the thermal behaviour of MNZ so as to facilitate adequate entrapment in the formulation of MNZ-SLNs.

4.5 DEVELOPMENT AND OPTIMISATION OF MNZ LOADED SOLID NANOPARTICLES (MNZ-SLNs)

4.5.1 Preparation of MNZ loaded solid lipid nanoparticles (MNZ-SLNs)

Two techniques, namely bath sonication and PUS, were investigated for the preparation of MNZ-SLNs. A 2% MNZ-SLN formulation was prepared by using a novel melt-emulsification, low-temperature solidification method. The resultant coarse suspension was divided into two equal portions. One portion was subjected to sonication by means of a probe-tip device for four minutes, whilst the other underwent bath sonication for four minutes.

Table 4.18 depicts the respective particle size measurements obtained from PCS analysis of a 2% m/v MNZ-SLN formulation using the two respective techniques.

Table 4.18: Photon correlation spectroscopy (PCS) characteristics of 2% MNZ loaded solid lipid nanoparticles (MNZ- SLNs) formulated via bath and Probe-tip ultrasound sonication (PUS), respectively.

Run	Bath Sonication		PUS	
	z-avg. (d.nm)	PDI	z-avg. (d.nm)	PDI
1	156.90	0.479	51.21	0.191
2	150.23	0.461	52.06	0.193
3	152.60	0.465	52.17	0.193
Mean ± SD	153.24 ± 2.76	0.46 ± 0.01	51.81 ± 0.43	0.192 ± 0.001

Larger particle agglomerates scatter more light, and cause rapid sedimentation when compared to their smaller counterparts (Pradhan *et al.,* 2016). Furthermore, both techniques yielded particles within the nano-size range; however, MNZ-SLN preparation via bath sonication yielded bigger particles with a mean z-avg. value of 153.2 nm. Figure 4.31 illustrates a comparison between observed particle size distributions in nano-dispersions prepared by ultrasonic bath versus PUS.

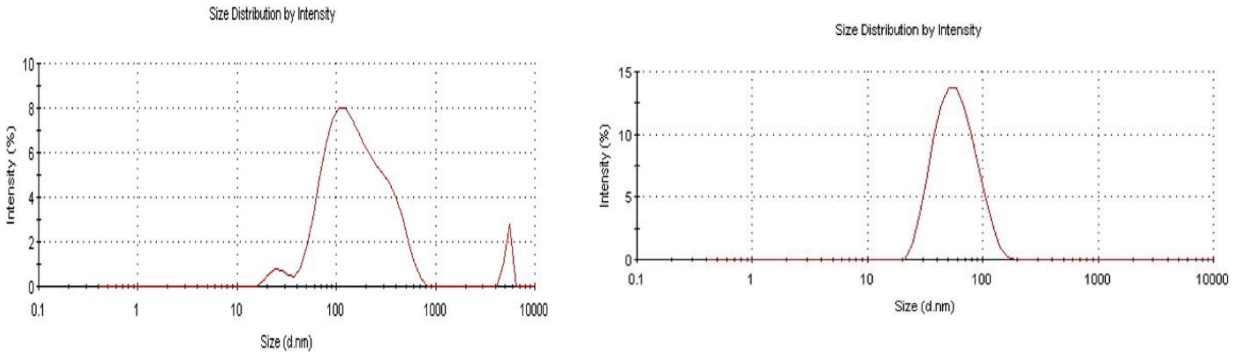

Figure 4.31: Comparison of particle size (z-avg.) distribution in prepared 2% m/v MNZ loaded solid lipid nanoparticles (MNZ-SLNs) via ultrasonic bath device (left) and probe-tip ultrasound sonication PUS (right).

Nanoparticle formation via bath sonication produced an unacceptably high PDI, which suggested sample absorbance and fluorescence due to poor dilution or the presence of large sedimenting particles. PDI values exceeding 0.3 suggest an unstable and non-homogenous suspension that may result in the instability of the final formulation (He *et al.,* 2017). Based on the PCS characterisation results, it can be concluded that the

use of PUS facilitated superior disintegration of particle agglomerates into smaller and mono-dispersed units in the coarse dispersion. These findings motivated PUS as a tool for the preparation of MNZ-SLNs.

4.5.2 Statistical optimisation of prepared MNZ loaded solid lipid nanoparticles (MNZ-SLNs)

DesignExpert® software (v7.0.0. StatEase™. Minneapolis, USA) was used for the statistical optimisation of the prepared MNZ-SLNs. Thirteen experimental runs were generated through a CCRD. These runs were prepared and characterised respectively. An appropriate empirical model was then selected to statistically validate the data input by analysis of variance (ANOVA). A lack-of-fit test was then conducted to evaluate the significance of the chosen model. This process was employed for each measured response. Model desirability was then assessed in order to ascertain optimal conditions that facilitated the maximal entrapment efficiency of MNZ with minimal deviations in particle diameter upon storage.

4.5.2.1 Central composite rotatable design (CCRD)

A CCRD was employed as a RSM tool for the optimisation of particle characteristics of MNZ-SLNs. Thirteen individual nanodispersions were prepared by means of a melt-emulsion, low temperature PUS method in accordance with the specifications of the experimental design sheet (see Table 3.10). Each formulation was divided into two halves, where one half was stored at ambient temperature (25 ± 2 °C) and the other at refrigerated temperatures (4 ± 2 °C). Individual characterisation tests for z-avg., PDI, ZP and %EE were conducted on each formulation at days zero, 14 and 28 of storage.

The overall effects of lipid concentration and sonication time on %EE were assessed by an indirect method. Particle characteristics, such as z-avg., ZP and PDI were determined by means of PCS. The results obtained from these investigations are summarised in Tables 4.19 and 4.20, respectively. Ideal formulations were deemed acceptable if they possessed good uniformity within the nanometre range, and when they had a high ZP value with minimal deviations in characteristics upon storage.

Table 4.19: Characterisation of MNZ loaded solid lipid nanoparticles (MNZ-SLNs) stored at ambient temperature (25 ± 2 °C).

Run	Day 0 (t_0)				Day 14 (t_1)				Day 28 (t_2)			
	Z-avg.	ZP (mV)	%EE	PDI	Z-avg.	ZP (mV)	%EE	PDI	Z-avg.	ZP (mV)	%EE	PDI
1	51.1	28.8	64.8	0.19	51.9	32.3	64.5	0.19	55.8	23.2	62.3	0.25
2	63.3	33.3	70.0	0.31	54.7	31.6	50.2	0.27	49.7	32.2	53.9	0.26
3	72.1	44.9	87.5	0.41	71.7	48.2	85.7	0.31	72.1	33.6	71.5	0.32
4	75.1	42.3	89.5	0.32	72.6	37.1	71.7	0.27	75.1	29.9	71.0	0.28
5	46.1	41.0	76.1	0.26	49.5	38.9	62.2	0.27	57.0	38.7	63.7	0.37
6	40.1	32.2	74.2	0.22	48.7	29.0	69.4	0.26	47.1	28.2	55.2	0.25
7	54.0	35.5	86.2	0.30	53.2	36.1	76.8	0.40	58.5	31.9	76.7	0.45
8	41.1	32.0	40.5	0.27	47.7	31.1	39.6	0.25	47.7	28.3	35.2	0.24
9	55.2	35.0	73.5	0.37	50.1	33.7	68.2	0.29	59.0	31.2	60.2	0.30
10	56.1	32.5	64.9	0.30	58.8	31.7	62.8	0.27	61.5	31.9	42.6	0.31
11	43.8	28.5	92.5	0.38	59.0	29.4	72.6	0.25	62.0	31.7	69.3	0.27
12	51.8	34.6	71.6	0.26	44.4	25.1	69.1	0.18	53.2	35.9	50.2	0.33
13	62.5	32.1	74.0	0.28	68.1	32.7	65.2	0.32	73.8	30.8	64.5	0.26

Table 4.20: Characterisation of MNZ loaded solid lipid nanoparticles (MNZ-SLNs) stored at ambient temperature (25 ± 2 °C).

Run	Day 0 (t_0)				Day 14 (t_1)				Day 28 (t_2)			
	Z-avg.	ZP (mV)	%EE	PDI	Z-avg.	ZP (mV)	%EE	PDI	Z-avg.	ZP (mV)	%EE	PDI
1	51.1	28.8	64.8	0.91	51.4	33.2	64.7	0.17	52.0	31.2	63.9	0.18
2	63.3	33.3	70.0	0.31	55.9	29.1	55.6	0.27	53.4	27.3	52.8	0.28
3	72.1	44.9	87.5	0.41	67.9	41.8	85.7	0.29	68.9	42.4	84.7	0.29
4	75.1	42.3	89.5	0.32	73.1	38.7	87.2	0.28	73.6	38.6	86.9	0.30
5	46.1	41.0	76.1	0.26	47.4	37.2	75.2	0.27	58.4	38.1	63.1	0.34
6	40.1	32.2	74.2	0.22	40.1	32.4	73.8	0.23	40.4	32.6	74.0	0.24
7	54.0	35.5	86.2	0.30	52.8	37.6	85.5	0.32	58.3	37.2	83.2	0.38
8	41.1	32.0	40.5	0.27	44.4	32.2	40.9	0.27	42.1	29.4	41.2	0.29
9	55.2	35.0	73.5	0.37	51.2	33.4	69.5	0.33	52.1	33.8	69.0	0.34
10	56.1	32.5	64.9	0.30	56.4	32.6	62.9	0.29	56.9	33.0	61.0	0.29
11	43.8	28.5	92.5	0.38	54.3	29.1	91.1	0.25	62.3	29.9	91.0	0.26
12	51.8	34.6	71.6	0.26	51.6	34.2	71.9	0.26	50.1	30.2	71.3	0.28
13	62.1	32.1	74.0	0.28	65.4	35.0	70.2	0.29	66.9	35.7	70.2	0.30

All formulations demonstrated desirable characteristics upon analysis at day zero. With prolonged storage, however, changes in particle size and entrapment efficiency were observed in most formulations. From the results tabulated in Table 4.20, changes in particle characteristics (especially PDI and z-avg.) were comparable for samples stored at fridge and ambient temperature. Figure 4.32 depicts the change in particle size of individual formulations under ambient versus fridge conditions over a 28-day period.

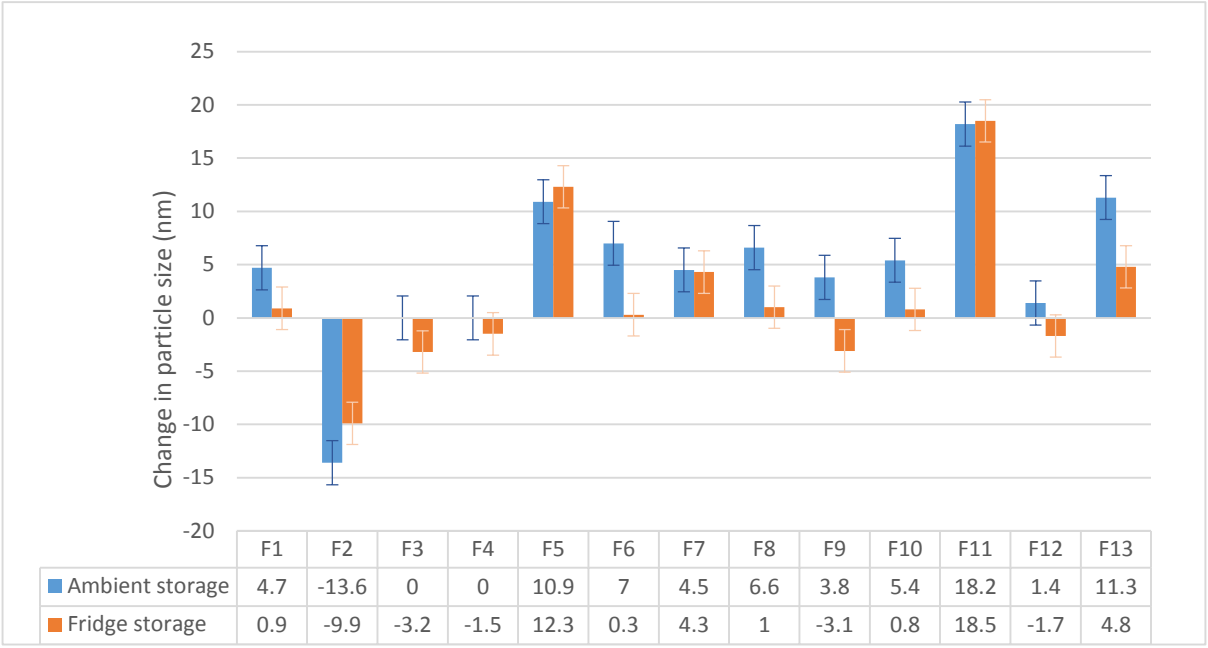

	F1	F2	F3	F4	F5	F6	F7	F8	F9	F10	F11	F12	F13
Ambient storage	4.7	-13.6	0	0	10.9	7	4.5	6.6	3.8	5.4	18.2	1.4	11.3
Fridge storage	0.9	-9.9	-3.2	-1.5	12.3	0.3	4.3	1	-3.1	0.8	18.5	-1.7	4.8

Figure 4.32: Graph depicting the change in particle size (z-avg.) on prepared MNZ solid lipid nanoparticles (MNZ-SLNs) after 28 days at fridge (orange) and ambient (blue) storage.

The majority of formulations demonstrated an increase in particle size over the 28-day period, irrespective of the storage temperature. Only one formulation (F2) demonstrated a decrease in size when stored at ambient temperature. This finding is significantly less than that of the five formulations (F2, F3, F4, F9 and F12) that demonstrated a decrease in particle size upon storage in the fridge. The mean particle size growth was calculated as 6.15 ± 5.04 nm and 5.33 ± 6.23 nm for ambient (*n*=12) and fridge (*n*=8) storage, respectively. The mean particle size shrinkage was calculated as -13.6 ± 00 nm and -3.88 ± 3.09 nm for ambient (*n*=1) and fridge (*n*=5) storage, respectively. Based on these findings, it was concluded that fridge storage facilitated the lowest mean particle growth and shrinkage.

The use of an emulsifier (surfactant) in MNZ-SLN formulations prevents the aggregation of particles through its microviscosity properties (Bynan *et al.,* 2018; Emami *et al.,* 2015). Microviscosity defines the friction experienced by a particle undergoing diffusion due to its interactions with its environment on a microscopic scale (Goins *et al.,* 2008). Higher temperatures, however, induce destabilisation of the colloidal system by reducing the microviscosity of the emulsifier. Furthermore, high temperatures increase the kinetic energy of the colloidal system, which is sufficient for overcoming repulsive forces within the dispersion to form agglomerates (Shah *et al.,*

2014). The consequences of agglomeration include colloidal system instability and drug expulsion. Hence, all forthcoming investigations and assessments were conducted solely on the aforementioned refrigerated samples.

4.5.3 Statistical data analysis

Five output factors (responses), *viz.* ZP, %EE, z-avg., change in z-avg. and %EE upon storage (in a 28-day period) were investigated. The PDI for all formulations were acceptable and, therefore, not investigated further for the purposes of the optimisation studies. Response models were utilised to diagnose and illustrate a relationship(s) between the input variables and the measured responses. Furthermore, statistical data was depicted graphically through the use of 3D plots. Normal plots of residuals were constructed to assess the significance of the proposed model and its suitability in the assumption of normality.

4.5.3.1 Analysis of variance (ANOVA) and normal plots of residuals

ANOVA is a statistical tool used for the prediction of input variable effects on measured responses (Kao and Green, 2008). Where p-values (Prob>F) of less than 0.05 indicate significant model terms, those > 0.1000 are not statistically significant model terms (Ogee *et al.,* 2016). Using ANOVA, normal plots of residuals were generated to determine the data normality. The representation of the generated data by means of these plots allowed for adequate visualisation to discern points that lay close to the straight line, thus confirming that the data were normally distributed. The ideal pattern for distribution points should follow a straight line. However, mild scatter can be expected (Bewick *et al.,* 2005; Schneider *et al.,* 2010).

i. Analysis of variance (ANOVA) and normal plot of residuals for zeta potential (ZP)

An f-value of 0.67 was obtained, which indicated that the model was not significant relative to the noise, with a 65.92% probability that this value would occur due to noise. The lack of a fit p-value of 0.648 was advantageous, as it suggested that there were no significant model terms relative to pure error. Table 4.21 provides a summary of the ANOVA test response for ZP.

Table 4.21: Analysis of variance (ANOVA) test for response surface quadratic model for zeta potential (ZP).

Source	Sum of squares	Degree of freedom	Mean square	f-value	p-value	
Model	96.01	5	19.20	0.67	0.659	**not significant**
Lipid conc. (A)	44.78	1	44.78	1.56	0.2514	
Sonication time (B)	46.02	1	46.02	1.61	0.246	
AB	0.01	1	0.01	0.000349	0.986	
A^2	0.37	1	0.37	0.013	0.9125	
B^2	5.10	1	5.10	0.18	0.686	
Residual	200.56	7	28.65	-	-	
Lack-of-fit	62.34	3	20.78	0.60	0.648	**not significant**
Pure error	138.22	4	34.56	-	-	
Cor. total	296.57	12	-	-	-	

Based on the statistical data provided, it can be concluded that there were no significant model terms that influenced the measured ZP for the prepared formulations. The use of a linear response surface model was recommended for the ANOVA test of ZP because it demonstrated the greatest potential of maximising the predicted and adjusted r^2 values. The normal plot of residuals for ZP, illustrated in Figure 4.33, depicts a fairly linear pattern of the plotted points. This suggests a normal distribution of the points of externally studentised residuals versus normal % probability.

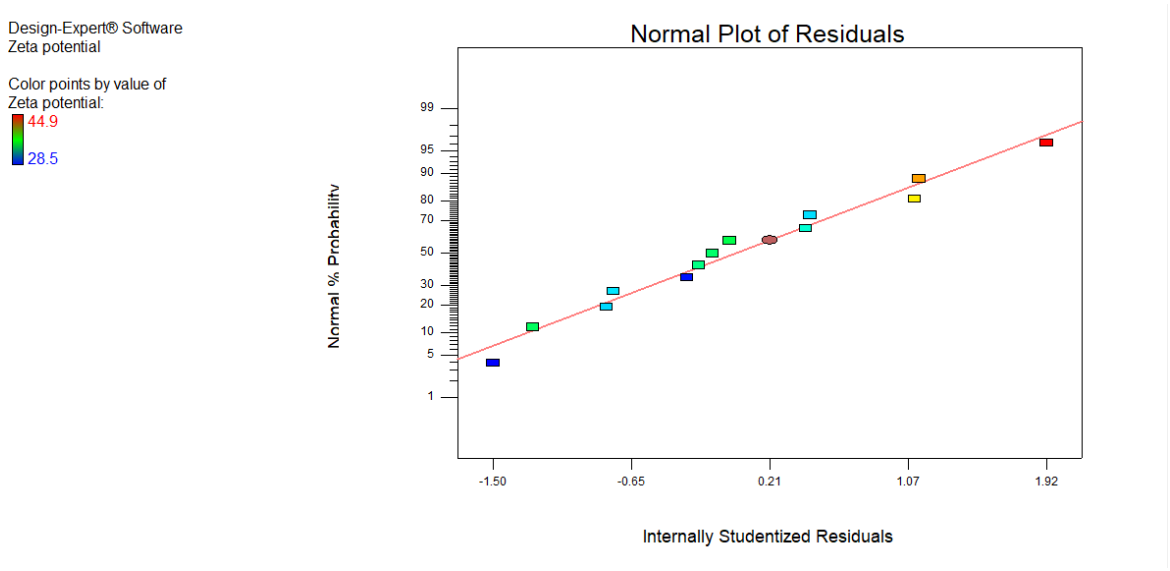

Figure 4.33: Normal probability plot of residuals for zeta potential (ZP) displaying a linear relationship of normal % probability as a function of externally studentised residuals.

The statistical data indicated that there was no relationship between the input variables (i.e. lipid concentration and sonication time) on the measured response (i.e. the ZP). Nanodispersion components that demonstrated the greatest influence on surface charge and particle stability (i.e. surfactants) were kept constant in all formulations; therefore, a significant effect on ZP from the two input variables, respectively, was not anticipated. This phenomenon was supported by the statistical findings and concurs with other findings that the effect of sonication parameters on ZP is negligible (Siddiqui *et al.,* 2014).

ii. Analysis of variance (ANOVA) and normal plot of residuals for entrapment efficiency (%EE)

A series of models were proposed in the ANOVA test of %EE. None were deemed significant; however, the quadratic empirical model resulted in the generation of the highest f-values (0.75) with a high probability that this value would occur due to noise. A lack of f-value of 4.41 with a p-value of 0.0928 favoured a non-significant response, which was ideal. A summary of the ANOVA test response values for %EE is depicted in Table 4.22.

Table 4.22: Analysis of variance (ANOVA) test for response surface quadratic model for entrapment efficiency (%EE).

Source	Sum of squares	Degree of freedom	Mean square	f-value	p-value	
Model	774.36	5	154.87	0.75	0.6133	**not significant**
Lipid conc. (A)	4.55	1	4.55	0.022	0.8865	
Sonication time (B)	169.71	1	169.71	0.82	0.3957	
AB	56.55	1	56.55	0.27	0.6176	
A^2	198.17	1	198.17	0.96	0.3609	
B^2	410.55	1	410.55	1.98	0.2022	
Residual	1451.69	7	207.38	-	-	
Lack-of-fit	1114.72	3	371.57	4.41	0.0928	**not significant**
Pure error	336.97	4	84.24	-	-	
Cor. total	2226.05	12	-	-	-	

The results summarised in Table 4.22 concluded that no significant model terms influenced the measured response (%EE).

The plot of internally studentised residuals versus normal % probability is depicted by Figure 4.34. This figure presents a fairly linear trend of all the plotted data points, thus suggesting a normal distribution.

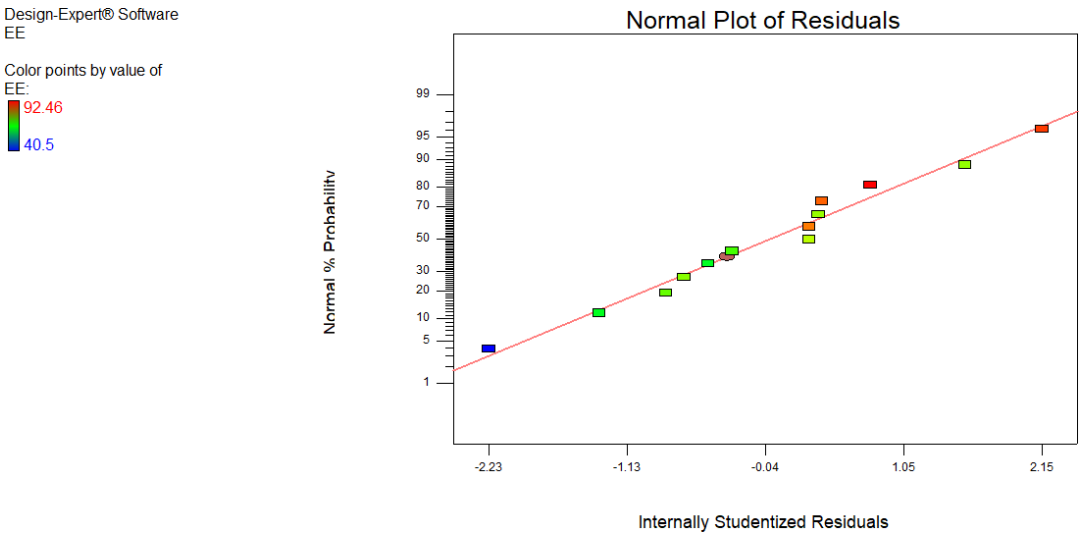

Figure 4.34: Normal probability plot of residuals for entrapment efficiency (%EE) displaying a linear relationship of normal % probability as a function of externally studentised residuals.

The statistical data suggested that no relationship between the input variables on the measured response (%EE) was observed. SLN components that demonstrate the greatest influence on DL and consequently %EE (i.e. lipid type and drug-lipid ratio concentration) were kept constant in all formulations. Generally, changing the drug-lipid ratio allows for the incorporation of more drug into the vesicle until maximal saturation is reached (Emami *et al.,* 2015; Lakshmi *et al.,* 2012). Emami *et al.* (2015) proposed that increasing the amount of lipid concentration can facilitate an improvement of %EE by improving the dissolution of highly lipophilic drugs in vesicles which allows for more space to accommodate the API. Furthermore, Soma and colleagues (2017) noted that lipid concentrations beyond 3% did not facilitate significant increase to %EE. This latter phenomenon was observed in this study, possibly owing to the narrow-working lipid concentration range of 3 to 4% m/v, where no statistically significant changes to %EE were noted.

iii. Analysis of variance (ANOVA) and normal plot of residuals for mean particle size (z-avg.)

Various models were constructed for the ANOVA test of z-avg.; however, none were deemed significant. The use of a quadratic empirical model generated the highest f-values (0.75) but with a high probability that it would occur due to noise. A lack-of-fit value (1.64) with a p-value of 0.3156 favoured a non-significant response, which was

ideal. A summary of the ANOVA test response values for z-avg. are depicted in Table 4.23.

Table 4.23: Analysis of variance (ANOVA) test for response surface quadratic model for mean particle size (z-avg.).

Source	Sum of squares	Degree of freedom	Mean square	f-value	p-value	
Model	508.94	5	101.79	0.75	0.6133	**not significant**
Lipid conc. (A)	64.46	1	64.46	0.47	0.5138	
Sonication time (B)	43.51	1	43.51	0.32	0.5897	
AB	169.00	1	169.00	1.24	0.3022	
A^2	74.41	1	74.41	0.55	0.4840	
B^2	128.14	1	128.14	0.94	0.3645	
Residual	953.97	7	136.28	-	-	
Lack-of-fit	525.56	3	175.19	1.64	0.3156	**not significant**
Pure error	428.41	4	107.10	-	-	
Cor. total	1462.91	12	-	-	-	

The normal plot of residuals for mean particle size (z-avg.) is illustrated by Figure 4.35. A fairly linear trend was observed, with a minor scattering of the points. This suggested a normal distribution of the points of externally studentised residuals versus normal % probability.

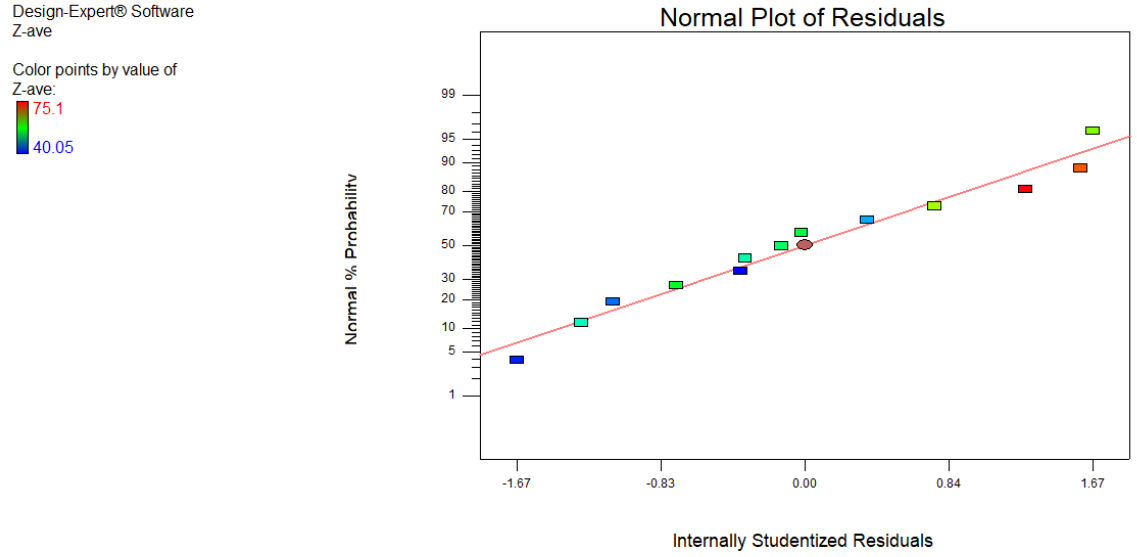

Figure 4.35: Normal probability plot of residuals for mean particle size (z-avg.) displaying a linear relationship of normal % probability as a function of externally studentised residuals.

The statistical data suggest that there was no relationship between the input variables on the measured response (z-avg.) SLN components, which demonstrated an influence on z-avg.; including the likes of surfactant and lipid concentration and method of SLN preparation. The surfactant concentration was kept constant in all formulation and was not expected to have a significant influence on the measured response. Ali and Singh (2018) recommend that an increase in lipid concentration within the formulation has a directly proportional effect on z-avg. This phenomenon was not observed statistically within this study, possibly owing to the narrow-working concentration range used for the statistical investigation.

The effect of sonication time on SLNs z-avg. is complex but can be summarised as an increase in sonication time that results in the reduction of particle size (Gupta *et al.,* 2017). Literature on sonication time effects is conflicting, with some studies suggesting that sonication time increases particle size until a critical point is reached, after which size reduction occurs (Pardhan *et al.,* 2016; Wang *et al.,* 2013). The working range for this study was narrow in order to allow for sufficient observation of this phenomenon. Furthermore, factors such as amplitude, need to be taken into account when sonication effects are investigated. For the purposes of this study, amplitude was kept constant and was, thus, not expected to have a statistically significant effect. This finding was

in agreement with a study conducted by Esmaeilzadeh-Gharedaghi and colleagues 2017.

iv. Analysis of variance (ANOVA) and normal plot of residuals for change in mean particle size (Δ z-avg.)

A modified quadratic model derived from backward elimination regression with and α exit value of 0.100 was used to produce an f-value of 4.72, which indicated a significant model. A p-value of 0.0359 indicated a small probability of 3.59%, where the f-value this vast would occur as a result of noise. A summary of the ANOVA test response values of sonication times with respect to Δ z-avg. over a 28-day period at refrigeration temperature is depicted in Table 4.24. The lack-of-fit p-value of 0.14 was favourable, as it indicated that the lack-of-fit was not significant relative to pure error, with a 98.10% probability that this value would occur due to noise.

Table 4.24: Analysis of variance (ANOVA) test for modified quadratic model for change in mean particle size (Δ z-avg.).

Source	Sum of squares	Degree of freedom	Mean square	f-value	p-value	
Model	299.6	2	149.98	4.72	0.0359	**significant**
B-sonication time	136.42	1	136.42	4.30	0.0649	
B^2	163.54	1	163.54	5.15	0.0466	
Residual	317.43	10	31.74	-	-	
Lack-of-fit	55.95	6	9.33	0.14	0.9810	**not significant**
Pure error	261.48	4	63.37	-	-	
Cor. total	617.40	12	-	-	-	

A normal plot of residuals that depicted a fairly linear trend is illustrated in Figure 4.36. Here, nearly all the points within the minimum and maximum range lie close to the depicted line.

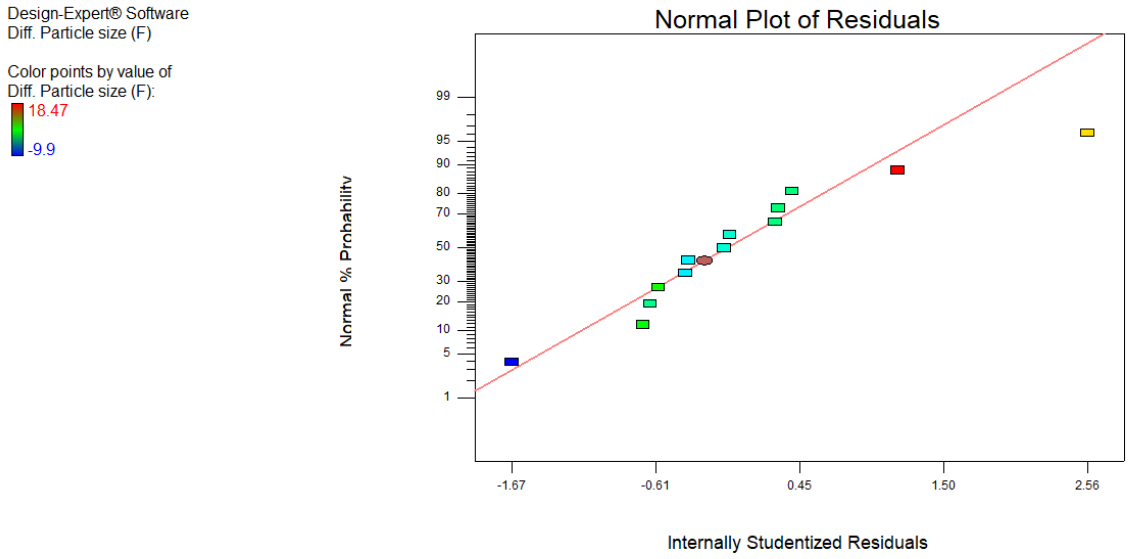

Figure 4.36: Normal probability plot of residuals for change in mean particle size (Δ z-avg.) displaying a linear relationship of normal % probability as a function of externally studentised residuals.

Of the two variables that were investigated, sonication time demonstrated a statistically significant effect with respect to change in particle size upon storage. Therefore, by optimising the sonication parameters effectively, minor changes in MNZ-SLNs z-avg. upon storage could be observed.

v. Analysis of variance (ANOVA) and normal plot of residuals for change in % entrapment efficiency (Δ %EE)

A series of models were constructed for the ANOVA test of the Δ %EE of the formulated MNZ-SLNs upon storage (± 4°C) over a 28-day period. None of the models obtained were deemed significant, and the quadratic model yielded the highest f- and p-values of 0.56 and 0.7259, respectively. Attempts were made to remove insignificant terms with the hope of improving the overall predictor of response. These attempts proved to be unsuccessful.

Table 4.25 summarises the ANOVA test results of lipid concentration and sonication time with respect to the change in SLNs entrapment efficiency upon storage throughout a 28-day period. The lack-of-fit p-value of 0.069 was favourable, which indicated that the lack-of-fit was not significant relative to pure error, with a 97.37% probability that this value would occur due to noise.

Table 4.25: Analysis of variance ANOVA test for response surface quadratic model for change in % entrapment efficiency (Δ %EE.).

Source	Sum of squares	Degree of freedom	Mean square	f-value	p-value	
Model	93.44	5	18.69	0.56	0.7259	**not significant**
Lipid conc. (A)	0.19	1	0.19	5.83E-003	0.9412	
Sonication time (B)	3.85	1	3.85	0.12	0.7430	
AB	7.24	1	7.24	0.22	0.6542	
A^2	29.76	1	29.76	0.90	0.3744	
B^2	62.23	1	62.23	1.88	0.2125	
Residual	231.54	7	33.08	-	-	
Lack-of-fit	11.34	3	3.78	0.069	0.9737	**not significant**
Pure error	220.20	4	55.05	-	-	
Cor. total	324.98	12	-	-	-	

The normal % probability versus internally studentised plot of residuals (illustrated in Figure 4.37) indicated a fairly linear plot for all the distribution points within the minimum and maximum range. This suggested a normal distribution of the generated data.

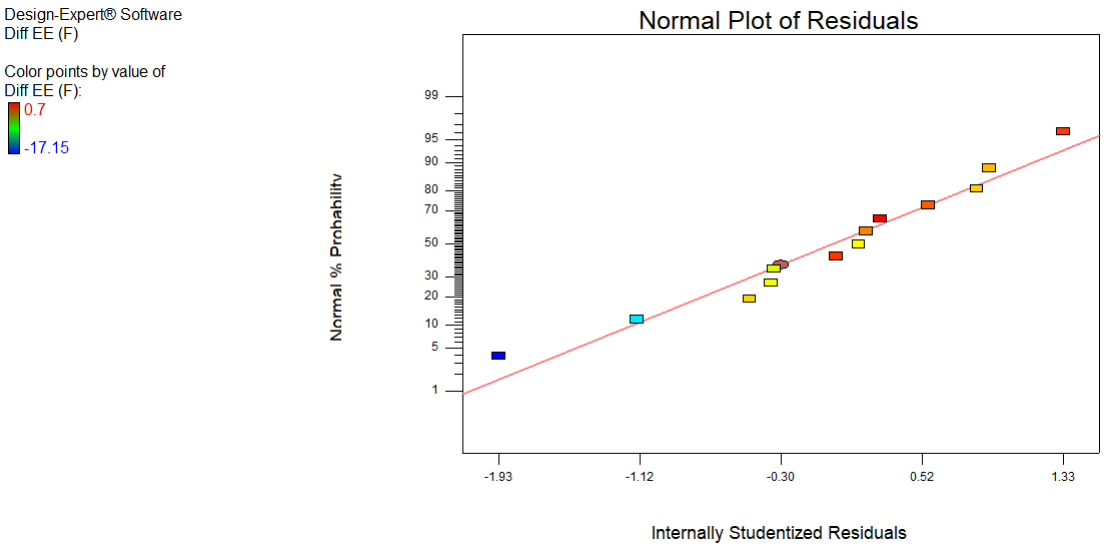

Figure 4.37: Normal probability plot of residuals for change in % entrapment efficiency (Δ %EE) displaying a linear relationship of normal % probability as a function of externally studentised residuals.

The statistical data indicated that there was no relationship between the input variables (i.e. lipid concentration and sonication time) on the measured response (i.e. Δ %EE). Changes in Δ %EE were observed upon storage as a result of configuration changes in the lipid crystalline structure. The period for analysis was kept constant for all formulations tested, but it was not sufficient enough to allow for the observation of statistically significant changes to %EE in the MNZ-SLNs formulations.

vi. Summary of polynomial equations and co-efficient of coded factors

The ultimate empirical model of the coded factors for the responses (Y_1 to Y_5) are depicted by Equations 4.3 to 4.7. The results are based on the analysis of 13 MNZ-SLNs preparations designed in accordance with Table 4.20, stored at 4 ± 2°C for a period of 28 days.

$$Y_1 = 35.70 + 2.37a - 2.40b + 0.050ab - 0.23a^2 - 0.86b^2$$

Equation 4.3: Empirical model for analysis of variance (ANOVA) test of zeta potential.

$$Y_2 = 82.26 - 0.75a - 4.61b + 3.76ab - 5.34a^2 - 7.68b^2$$

Equation 4.4: Empirical model for analysis of variance (ANOVA) test of % entrapment efficiency (%EE).

$$Y_3 = 55.38 + 2.84a + 2.33b - 6.50ab + 3.27a^2 - 4.29b^2$$

Equation 4.5: Empirical model for analysis of variance (ANOVA) test of mean particle size (z-avg.).

$$Y_4 = -1.15 + 14.13b + 4.81b^2$$

Equation 4.6: Empirical model for analysis of variance (ANOVA) test of change in mean particle size (Δ z-avg.).

$$Y_5 = -7.20 + 0.16a + 0.69b - 1.35ab + 2.07a^2 + 2.99b^2$$

Equation 4.7: Empirical model for analysis of variance (ANOVA) test of change in % entrapment efficiency (Δ %EE.).

A summary of the statistics for the evaluated surface response models is presented in Table 4.26.

Table 4.26: Summary statistics for evaluated response surface models (SD = standard deviation, r^2 = regression co-efficient, Adj r^2 = adjusted r^2, Pred r^2 = predicted r^2, Adeq prec = adequate precision, C.V% = co-efficient of variation).

Response	SD	f-value	p-value	r^2	Adj r^2	Pred r^2	Adeq. Prec.	C.V%
Y_1	5.35	0.67	0.66	0.324	-0.159	-1.223	2.620	15.98
Y_2	14.40	0.75	0.6133	0.348	-0.118	-2.798	2.263	19.40
Y_3	11.67	0.75	0.6133	0.348	-0.118	-2.012	2.931	21.32
Y_4	5.63	4.72	0.036	0.485	0.383	0.128	5.71	311.28
Y_5	5.75	0.56	0.726	0.288	-0.224	-0.307	1.782	140.80

ZP (Y_1): The negative value obtained for the predicted r^2 implied that the overall mean would be a better predictor than the current suggested response model. The signal-to-noise ratio indicated by the adequate r^2 is 2.62, which suggested that the model was not sufficient for the navigation of the design space. By removing insignificant model

terms (i.e. AB, A^2, B^2), a linear model was obtained, which was deemed sufficient for the navigation of the design space.

%EE (Y_2): The use of the mean as a predictor of response was likely suitable, due to the negative value of the predicted r^2. This model was unlikely to produce sufficient signal (Adeq. Prec. = 2.263), indicating that this model should not be used in the navigation of the design space.

Z-avg. (Y_3): The negative value obtained for the predicted r^2 implied that the current model was not suitable, and the use of the overall mean would be a better predictor of response. Additionally, a ratio of 2.931 obtained for the adequate precision implied an insufficient signal to allow for the use of this model to navigate the design space.

Δ z-avg. (Y_4): There was a noticeable difference of 0.2553 between the predicted r^2 value and its adjusted value. This was not ideal, and could possibly be explained by the large block effect or a problematic data or model. Possible remedies for correction could come from the transformation of data, model reduction or the exclusion of outliers. The adequate precision value of >4 suggested the sufficiency of the signal for the navigation of the design space.

Δ %EE (Y_5): A negative value obtained for the predicted r^2 implied that the overall mean could be used as a predictor of response. However, the model would not be ideal, since an adequate precision value of 1.78 was obtained.

4.5.3.2 Predicted versus actual plots

Scatter plots of the predicted versus actual response values for each of the measured responses are illustrated in Figure 4.38. These plots serve as an aid to detect values that are not easily predicted by the model (Steyerberg *et al.,* 2010). The actual value is the measured response presented for a particular run and the predicted value was generated by using a prediction equation that included block and centre point corrections, as expressed in Equation 4.8.

$$\hat{y} = X\beta$$

Equation 4.8: Response surface methodology (RSM) prediction value equation.

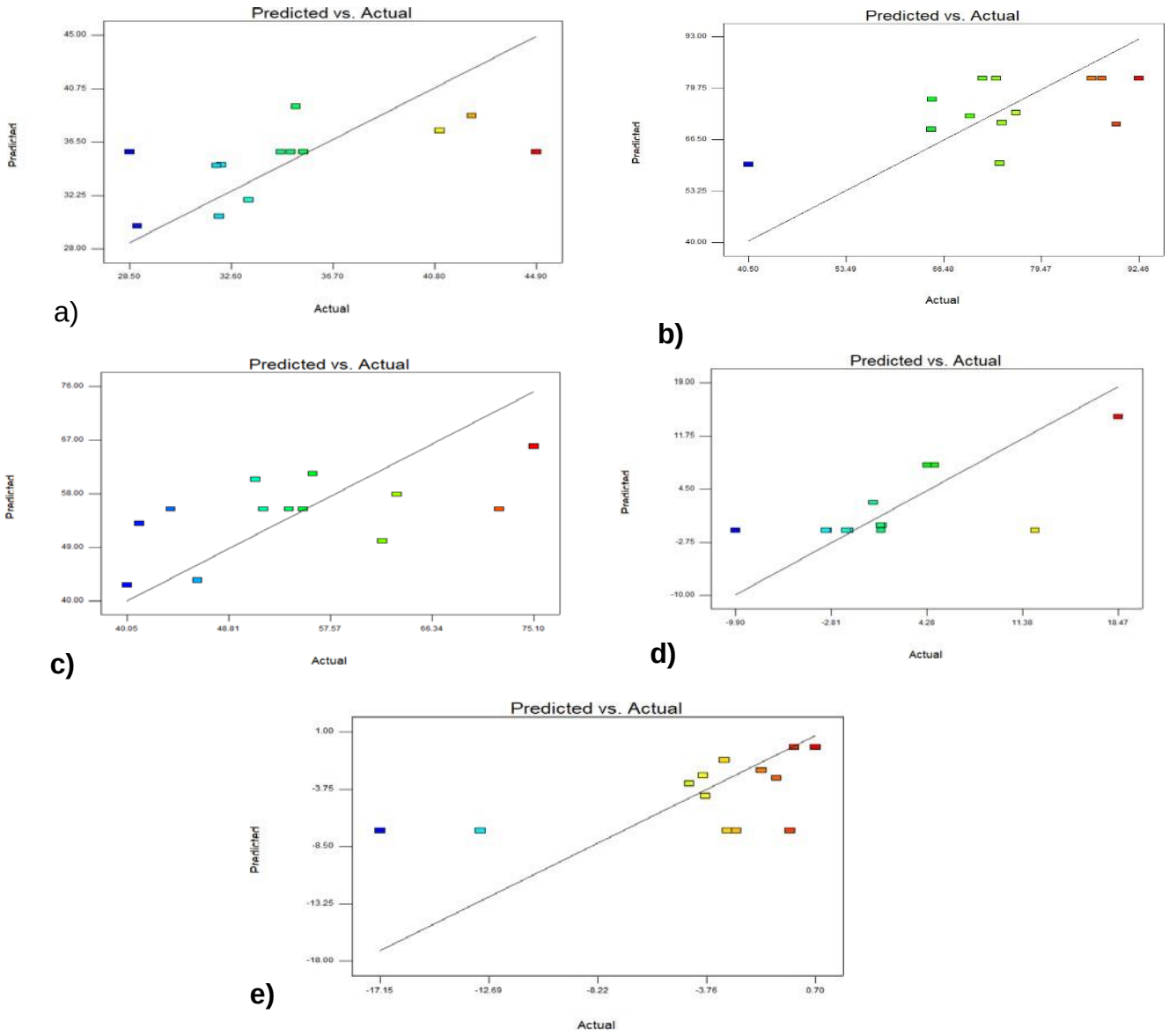

Figure 4.38: Predicted versus actual point prediction plots for (a) zeta potential (ZP) (b) % entrapment efficiency (%EE) (c) mean particle size (z-avg.) (d) change in mean particle size (Δ z-avg.) and (e) change in % entrapment efficiency (Δ %EE).

The distance of a point from an ideal regression line drawn at a 45° angle demonstrates how well or poorly a prediction is performed. Ideally, all the points should lie close to the regressed diagonal line (Field, 2016). A weak correlation between the model prediction and actual results was noted for all the scatter plots in this study. A model possessing a high r^2 value most likely yields points that lie closer to the diagonal line (Steyerberg *et al.,* 2010). Sub-figures a, c and e in Figure 4.38 show a weak correlation, as the points are loosely scattered in specific zones.

4.5.3.3 Residual versus run plots

The residual versus experimental run plots are useful for checking lurking variables that may have affected the response during the experiment. This plot consists of a random scatter (Anderson and Whittcomb, 2003). The trends in this study's plots show a time-related variable lurking in the experiment (see Figure 4.39).

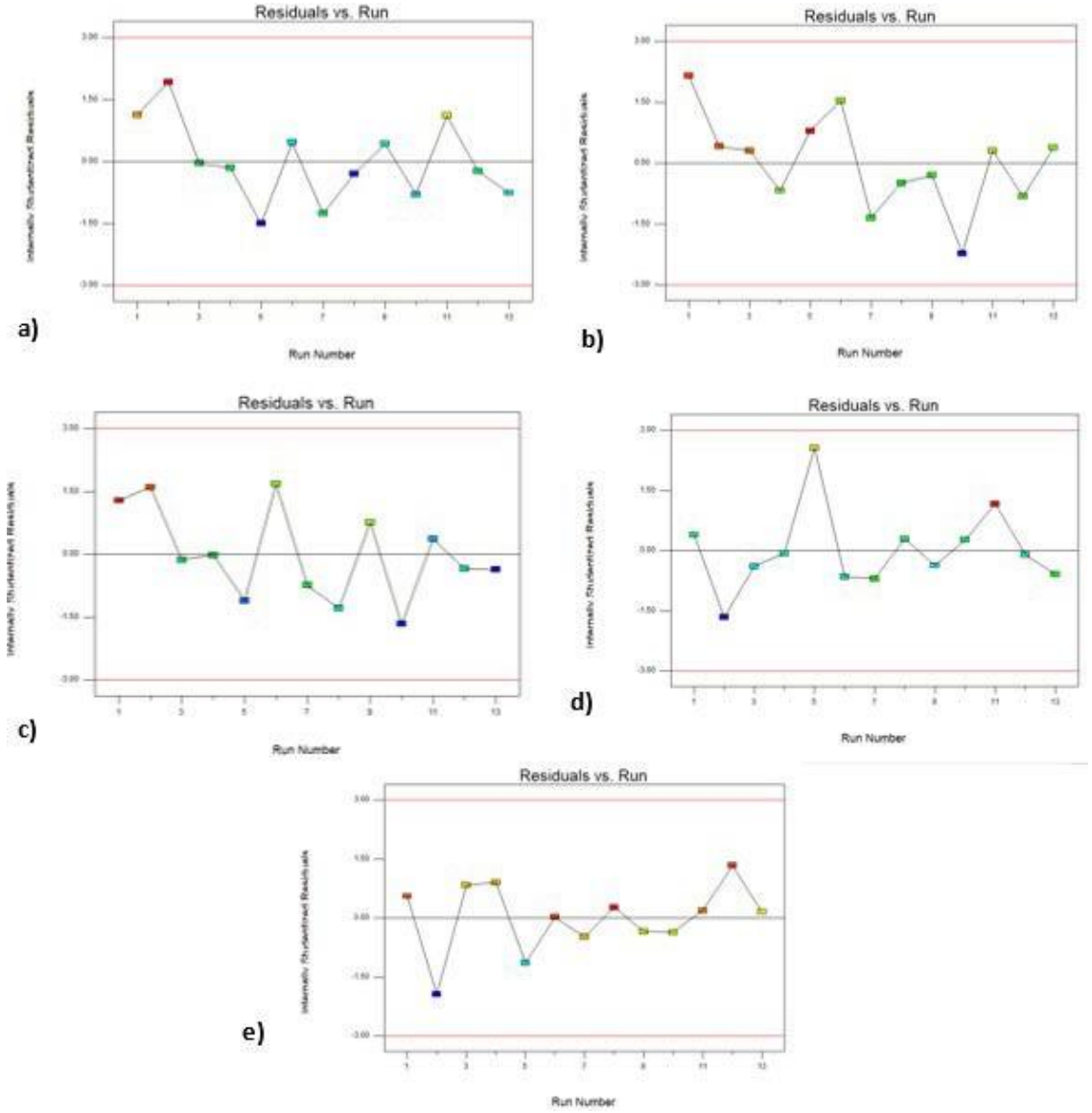

Figure 4.39: Residual versus run plots for (a) zeta potential (ZP) (b) % entrapment efficiency (%EE) (c) mean particle size (z-avg.) (d) change in mean particle size (Δ z-avg.) and (e) change in % entrapment efficiency (Δ %EE).

4.5.3.4 Interaction plots

Interaction plots display average values for the levels of one factor on the x-axis and a separate line for each level of another factor (Anderson and Whittcomb, 2003). Interaction plots are used to demonstrate the relationship between one categorical factor and a continuous response dependent on the value of a second categorical factor. Figure 4.40 illustrates interaction plots for the CCRD used in the optimisation of the prepared MNZ-SLNs.

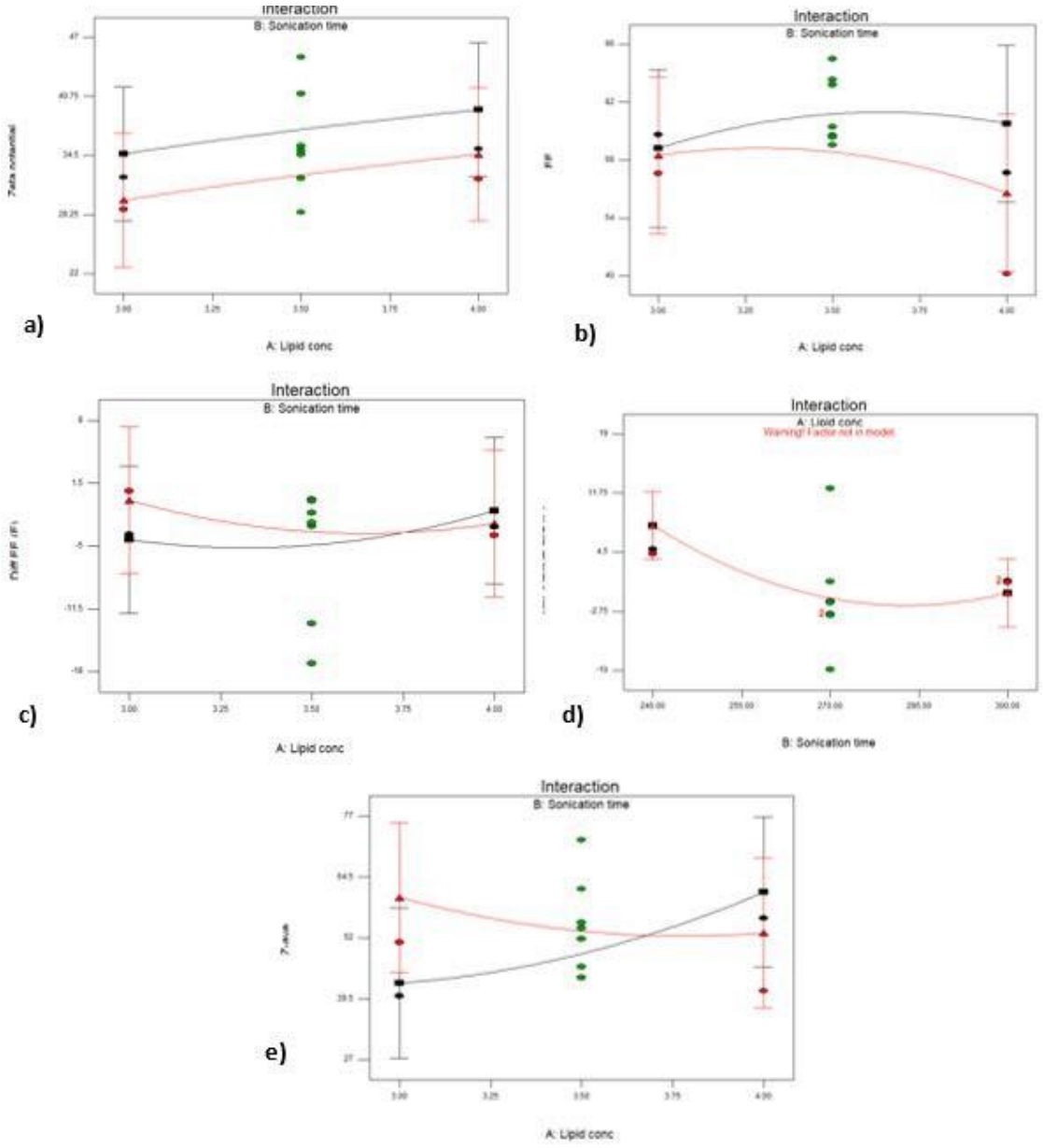

Figure 4.40: Interaction plots for (a) zeta potential (ZP) (b) % entrapment efficiency (%EE) (c) mean particle size (z-avg.) (d) change in mean particle size (Δ z-avg.) (e) change in % entrapment efficiency (Δ %EE).

In order to understand how the interactions affect the relationship between factors and the measured response, the lines of these plots were evaluated. Parallel lines suggest that no interaction occurred, whilst non-parallel lines suggest an interaction between the factors. It was noted that interactions between the input and output variables occurred in all measured responses except for ZP. Although these plots display interactive effects, it was necessary to perform a further evaluation of the statistical significance of these effects. This further evaluation is presented in the following sub-section.

4.5.3.5 Contour and response surface plots

Three dimensional (3D) surface plots were constructed so as to facilitate the understanding of the relationship between the input variables and the measured response(s).

i. Zeta potential (ZP)

Figure 4.41 is a 3D graphical depiction of ZP measurements for 13 experimental runs, as generated by the CCRD. This surface plot was formed by a horizontal axis of lipid concentration (% m/v) and a vertical axis of sonication time (seconds). The lines represent iso-responsive values where no significant interaction in terms of ZP were noted.

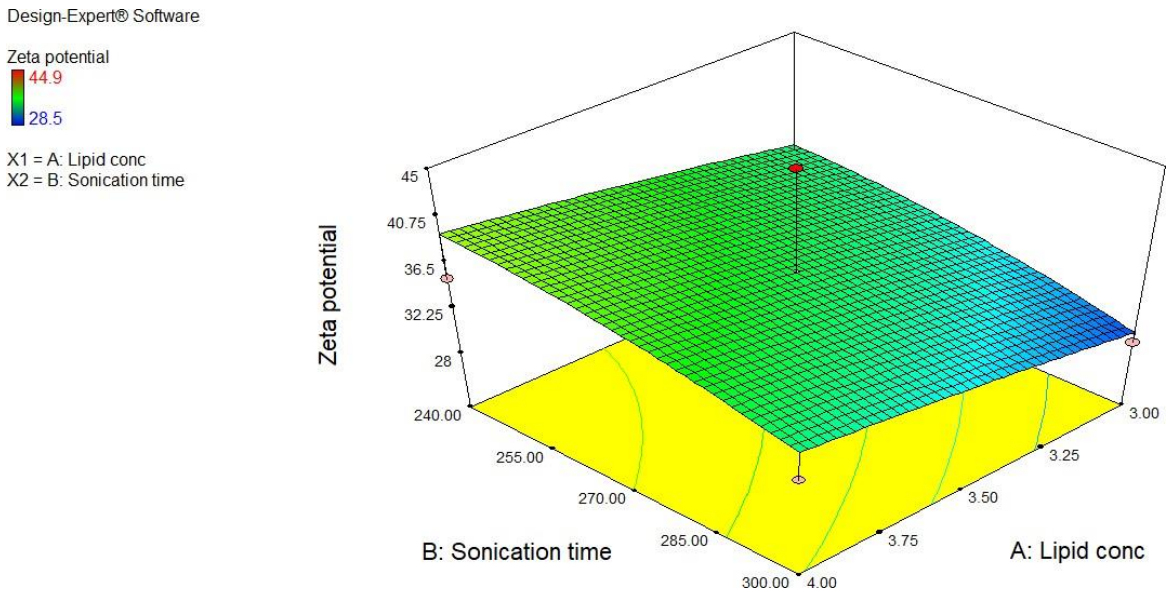

Figure 4.41: 3D response surface plot of lipid concentration (% m/v) and sonication time (seconds) with respect to zeta potential (ZP).

Based on the empirical model quadratic equation, lipid concentration (A) demonstrated a positive effect on ZP, whilst sonication time had a negative effect. This suggests that negative co-efficient values of sonication time result in an indirectly proportional relationship between sonication time and ZP. This effect was, however, not considered to be significant (by the statistical model) for the determination of ZP and, consequently, MNZ-SLNs stability.

ii. % Entrapment efficiency (%EE)

Figure 4.42 provides a 3D graphical depiction of %EE measurements for 13 experimental runs generated by the CCRD. The surface plot was formed by a horizontal axis (lipid concentration % m/v) and a vertical axis (sonication time in seconds). The region of maximal encapsulation was quite large, spanning from 240 to ± 280 seconds in sonication time between 3.5 to 3.8% m/v lipid concentrations.

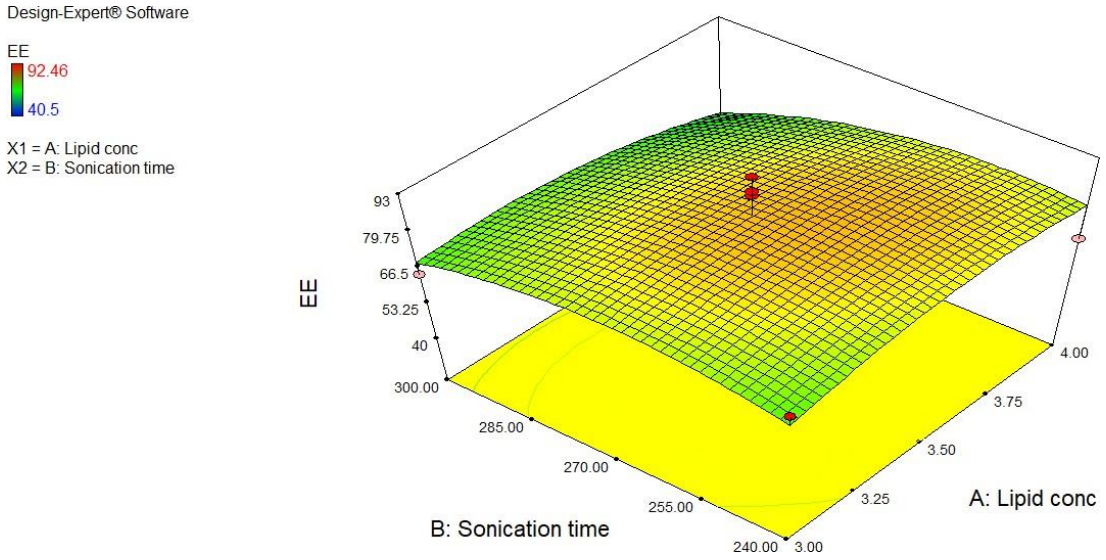

Figure 4.42: 3D response surface plot of lipid concentration (% m/v) and sonication time (seconds) with respect to entrapment efficiency (%EE).

Based on the quadratic model equation for the measured response (%EE), both input variables demonstrated a negative effect on %EE. This suggests that a decrease in lipid concentration and sonication time resulted in increased entrapment of MNZ within the lipid matrix. This effect, however, was not deemed significant by the statistical model.

iii. Mean particle size (z-avg.)

Figure 4.43 offers a 3D graphical depiction of mean particle size (z-avg.) of 13 experimental runs produced by the CCRD. Maximal z-avg. was observed in the region of lower lipid concentration (3% m/v) in the sonication time range of 285 to 300 seconds. Alternatively, maximal particle size was observed with lipid concentrations >3.75 between the sonication time ranges of 240 to 285 seconds.

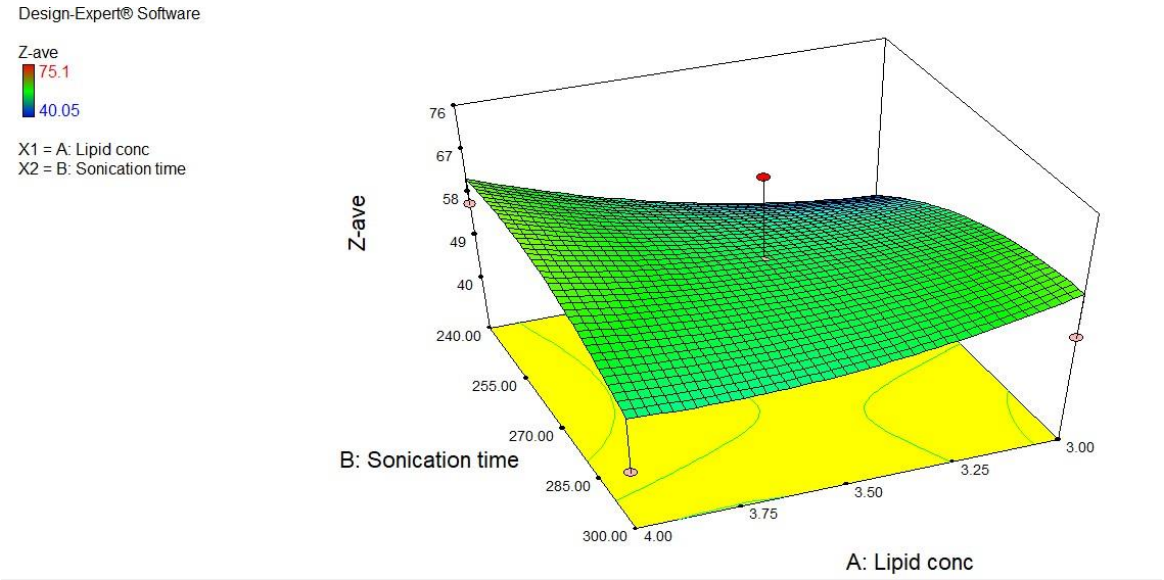

Figure 4.43: 3D response surface plot of lipid concentration (% m/v) and sonication time (seconds) with respect to mean particle size (z-avg.).

Based on the quadratic model equation for the measured response, both input variables demonstrated a positive effect on mean particle size, which suggested that an increase in lipid concentration and sonication time results in increased mean particle size of the developed MNZ-SLNs. This effect, however, was not deemed significant by the statistical model.

iv. Change in particle size (Δ z-avg.)

Figure 4.44 provides a 3D graphical depiction of Δ z-avg. of 13 experimental runs produced by the CCRD. Maximal Δ z-avg. was observed in the regions below 270 seconds of sonication time.

Based on the empirical statistical model for the measured response, lipid concentration did not demonstrate an effect on particle size upon storage. Sonication time does, however, seem to have an inversely proportional relationship with change in particle size, where an increase in sonication time results in statistically significant Δ z-avg. upon storage.

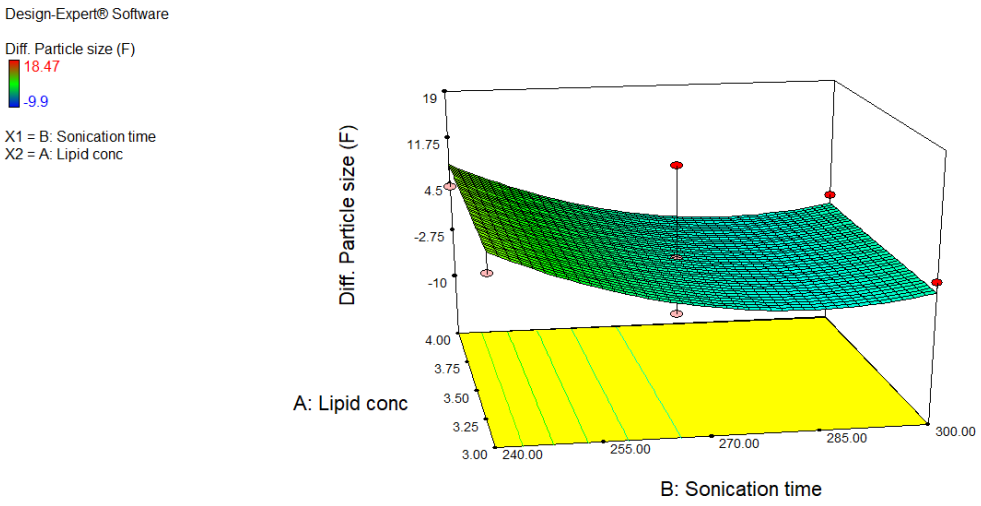

Figure 4.44: 3D response surface plot of lipid concentration (% m/v) and sonication time (seconds) with respect to change in mean particle size (Δ z-avg.) upon storage at fridge temperature (4 ± 2°C).

v. Change in % entrapment efficiency (Δ %EE)

Figure 4.45 provides a graphical depiction of Δ %EE measurements upon storage for 13 experimental runs generated by the CCRD. The surface plot was formed by a horizontal axis (lipid concentration % m/v) and a vertical axis (sonication time in seconds). The region of maximal encapsulation was quite large, spanning from 245 to ± 280 seconds in sonication time between 3.10 to 3.8 % m/v lipid concentrations.

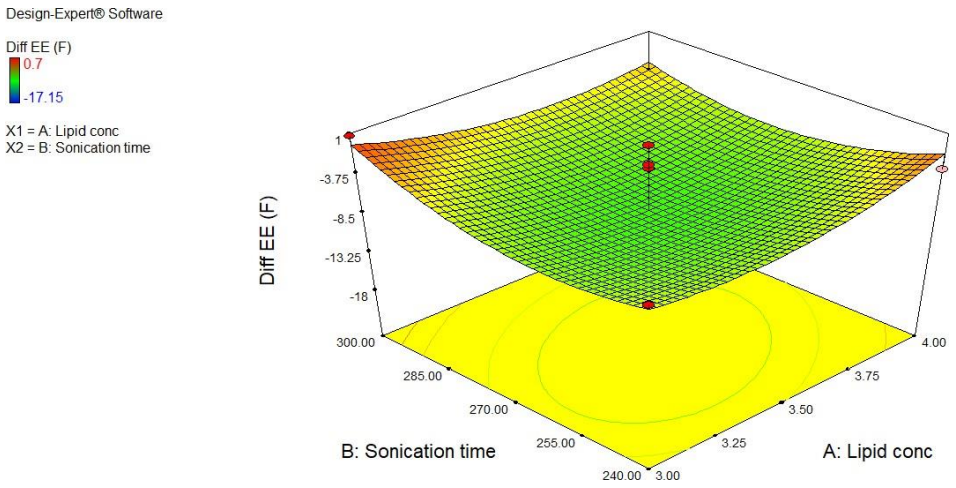

Figure 4.45: 3D response surface plot of lipid concentration (% m/v) and sonication time (seconds) with respect to change in % entrapment efficiency (Δ %EE.) upon storage at fridge temperature (4 ± 2°C).

Based on the quadratic model equation for the measured response, both input variables demonstrated a positive effect on Δ %EE upon storage, which suggested that an increase in lipid concentration and sonication time results in greater changes to particle size in the prepared MNZ-SLNs upon storage. This effect was, however, not deemed significant by the statistical model.

4.5.3.6 Statistical model validation

Table 4.26 provides a summary of the set goals for each response used to generate optimal conditions. From the data gathered by the CCRD and ANOVA testing, the predicted response optimisation parameters were a maximum lipid concentration of 4% m/v with a sonication time of 260.94 seconds.

Table 4.27: Summary of set goals for each measured response, where lipid con = lipid concentration, sonic. = sonication time, ZP = zeta potential, %EE = % entrapment efficiency, z-avg. = mean particle size, diff size = change in particle size upon storage, diff. %EE = change in entrapment efficiency upon storage.

Name	Goal	Lower limit	Upper limit	Lower weight	Upper weight	Importance
Lipid conc.	In range	3.00	4.00	1	1	3
Sonic.	In range	240.00	300.00	1	1	3
ZP	In range	30.00	44.9.0	1	1	1
%EE	Maximise	40.50	92.46	1	1	4
Z-avg.	In range	40.05	75.10	1	1	1
Diff. size	Target = 0	-9.90	18.47	1	1	3
Diff %EE	Target = 0	-17.50	0.70	1	1	4

Three batches of MNZ-SLNs were prepared under the suggested optimisation parameters and characterised in order to validate the predicted response. The predicted response and mean values of the measured response are shown in Table 4.27. In this table, the confidence interval (CI) is defined as a range of values associated with a population parameter. A prediction interval (PI) is a type of CI used in regression analysis, and is defined by the range of values that predicts the value of a new observation, based on an existing model (Pang *et al.,* 2018).

Table 4.28: Predicted response and mean values of measured response (Response ± SD = measured response from validation batches ± standard deviation, Pred. = predicted response, SE mean = mean standard error, CI = confidence intervals, PI = prediction intervals and SE Pred. predicted standard error).

Response	Response ± SD	Pred.	SE Mean	95% CI low	95% CI High	SE Pred.	95% PI Low	95% PI High
ZP	38.43 ± 0.86	38.47	2.88	31.66	45.27	6.08	24.09	52.84
%EE	75.24	77.99	7.75	59.68	96.31	16.35	39.33	116.66
Z-avg.	73.03 ± 0.78	62.36	6.28	47.51	77.20	13.26	31.01	93.70
Diff. size	11.57	0.54	2.01	-3.94	5.01	5.98	-12.79	13.86
Diff %EE	-6.80	-4.51	3.09	-11.82	2.81	6.53	-19.95	10.94

The measured response was compared against the confidence and predicted interval values so as to ascertain the reliability of the model. CI is concerned with the centre of population distribution, whilst PI accounts for the centre as well as the tails of distribution; thus, PI demonstrates greater sensitivity in the assumption of normality (Levin and Robbins, 1981).

The mean values for the ZP, %EE, Z-avg., Δ z-avg. and Δ %EE of the prepared MNZ-SLN formulations were determined as 38.70, 75.24 and 73.03 nm, 11.57 nm and -6.80, respectively, by means of PCS and ultracentrifugation. By employing ANOVA statistical testing, the PI range for the generated model was established between 24.09 and 52.84 for ZP, 39.33 and 116.66 for %EE and 31.10 and 93.70 for z-avg., -2.79 and 13.86 for Δ z-avg and -19.95 and 10.94 Δ %EE (see Table 4.27). Therefore, based on the predicted model, it can be concluded that the measured responses for the validation batched fell within the predicted range of optimised response.

4.6 CHARACTERISATION OF OPTIMISED MNZ LOADED SOLID LIPID NANOPARTICLES (MNZ-SLNS)

Three unloaded and MNZ loaded SLN formulations (*n*=3) were prepared, respectively, under the optimised conditions. Various techniques were then employed for their characterisation. These techniques are discussed in the following sub-sections.

4.6.1 Photon correlation spectroscopy (PCS)

PCS was employed in the determination of z-avg., PDI and ZP characteristics of the prepared formulations.

4.6.1.1 Mean particle size (z-avg.) and polydispersity index (PDI)

Each formulation of (MNZ loaded and unloaded) was analysed in triplicates by means of PCS (Malvern Zetasizer Nano-ZS™, Malvern Instruments™, United Kingdom). Table 4.28 provides an overview of the PCS results for PDI and z-avg. determination.

Table 4.29: Summary of mean particle size (z-avg.) and PDI measurements of optimised unloaded and MNZ loaded solid lipid nanoparticles (MNZ-SLNs) batches.

	Particle size (nm)			PDI		
	Sample 1	**Sample 2**	**Sample 3**	**Sample 1**	**Sample 2**	**Sample 3**
Unloaded SLNs	88.54	89.02	87.90	0.264	0.255	0.266
Mean (*n*=3)	88.49 ± 0.56			0.262 ± 0.005		
2% MNZ-loaded SLNs	72.80	72.40	73.79	0.256	0.253	0.255
Mean (*n*=3)	73.03 ± 0.78			0.254 ± 0.001		

The results obtained from the PCS analysis of 2% MNZ-SLNs demonstrated a mean population size of 73.03 ± 0.78 nm with a narrow size distribution (PDI = 0.254), thus depicting a homogenous dispersion with good size measurements that fall within the acceptable size range for SLNs. It should be noted that the analysis of unloaded SLNs demonstrated a uniform dispersion within an nm range; however, the measured particle size was slightly bigger than that of the 2% MNZ loaded SLN. Under normal circumstances, the incorporation of drugs within SLNs would cause an increase in particle size (Stella *et al.,* 2018). Therefore, it was be expected that the 2% MNZ-loaded SLNs would possess a larger z-avg. value than the unloaded SLNs. This phenomenon was, however, not observed in this study, as the introduction of MNZ

resulted in a subsequent decrease of free lipid content, thereby decreasing the overall z-avg. of the loaded SLNs. These results were in agreement with a study conducted by Shafique and colleagues (2017).

An illustration of the size distribution by intensity for an analysed 2% MNZ loaded SLN formulation is displayed in Figure 4.46. A good correlation between intensity and volume can be noted in this figure by the single distribution peak without additional contaminating peaks. A mean particle hydrodynamic diameter (d.nm) of 73.79 nm was observed, which falls into and acceptable nm range for SLNs.

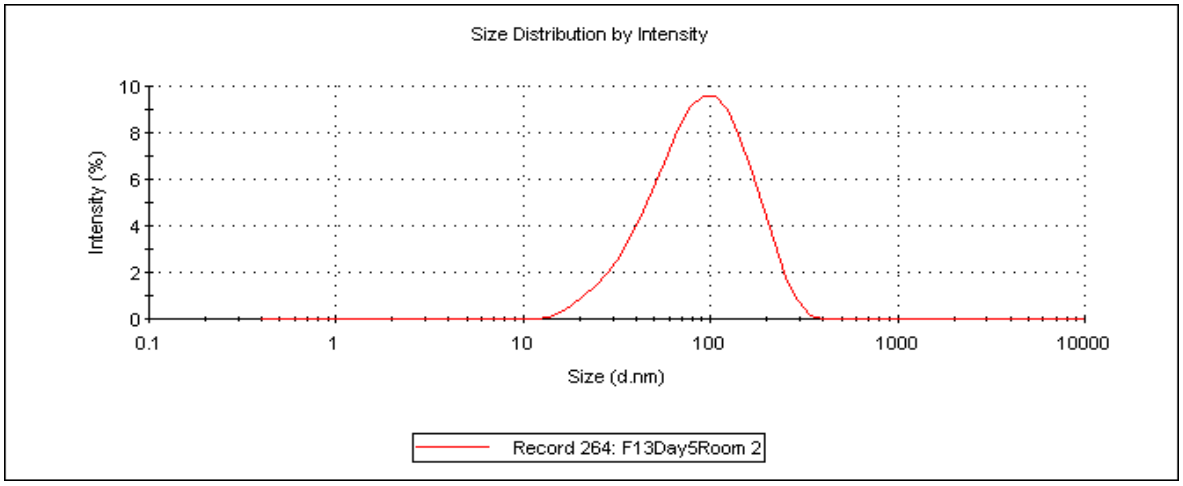

Figure 4.46: Peak of 2% MNZ loaded solid lipid nanoparticle (MNZ-SLN) size distribution by intensity.

4.6.1.2 Zeta potential (ZP)

Each formulation of MNZ loaded and unloaded batches was analysed in triplicates by means of PCS (Malvern Zetasizer Nano-ZS^{TM}, Malvern Instruments^{TM}, United Kingdom). Table 4.30 provides an overview of the PCS results for ZP determination.

Table 4.30: Summary of zeta potential (ZP) measurements of unloaded and optimised MNZ loaded solid lipid nanoparticles (MNZ-SLNs) batches.

	ZP (mV)			
	Sample 1	**Sample 2**	**Sample 3**	**Mean (*n*=3)**
unloaded SLNs	-16.7	-17.7	-16.7	-17.03 ± 0.58
2% MNZ SLNs	37.5	38.6	39.2	38.43 ± 0.86

The mean ZP values for the unloaded SLNs and 2% MNZ-loaded SLNs were -17.03 and 38.43 mV, respectively. The negative surface charge observed on the unloaded SLNs is possibly owing to the chemical nature of the lipid matrix. Naturally, an electrophoretic mobility of less than ± 30 mV would indicate instability (Mendez *et al.,* 2018); however, the use of non-ionic surfactants, such as polysorbate 80 and poloxamer 188, tend to stabilise the nanomolecules, irrespective of the lowered ZP. Surface coverage with these surfactants also lowers ZP by causing a reduction of its electrophoretic mobility; therefore, these molecules rely more on steric stabilisation and less electrostatic stabilisation (Shah *et al.,* 2014).

It should be noted that, in this study, the loading of MNZ into the SLN resulted in a significant increase of ZP. This is possibly due to the presence of cationic nitrogen atoms in the structure of the MNZ moiety, where this charge dominated over the lipids and neutral charge of the surfactants. This finding suggests that the drug molecule coats the surface of the loaded SLN, thus contributing to the reversal of surface charge. This finding was similar to a study by Qushawy *et al.,* 2018 and Shah *et al*., 2016. The magnitude of the mean measured electrophoretic mobility (38.43 ± 0.86 mV) is sufficient for the prevention of particle agglomerates, thus facilitating adequate stability (Mendez *et al.,* 2018). The ZP value fell within the statistically approximated 95% CI value of 38.47 mV and, again, validated the statistical model.

4.6.2 Transmission electron microscopy (TEM)

The microstructure analysis of statistically optimised MNZ-SLNs was undertaken by TEM. The macroscopic appearance of the MNZ-SLN preparation resembled a milky solution immediately after production and upon storage. TEM analysis was then

employed for microscopic visualisation of the preparation. The findings are represented in Figure 4.47.

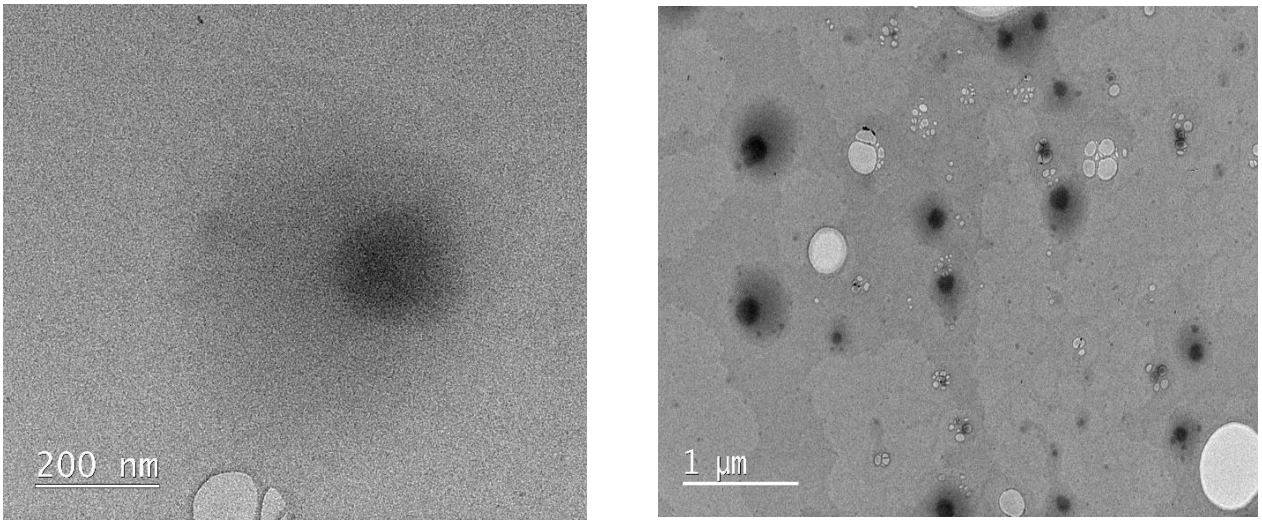

Figure 4.47: Transimission electron microscope (TEM) image of optimised MNZ loaded solid lipid nanoparticles (MNZ-SLNs) preparation.

The size measurements agreed with the data obtained from the PCS analysis of 2% MNZ loaded SLNs. The minor difference between the two measurements may be attributed to the effect of particle dehydration and poor storage conditions prior to analysis resulting in its expansion. Roughly spherical particles were observed and particle size in the nm range (i.e. 10-1000 nm). The periphery of the particles was well-defined, but no clear internal visualisation was possible, which demonstrated the susceptibility of the lipid to the electronic beam. The surface appeared smooth, with no obvious protrusions. No agglomeration of particles was noted, which suggested that the colloidal system was well dispersed. Moreover, TEM analysis served as a size validation tool for the statistically optimised MNZ-SLN preparation, where it fell within the 95% PI range of 31.09 to 93.70 nm.

4.6.3 Calculating % drug entrapment efficiency (%EE)

The %EE of the optimised MNZ-SLN formulation was determined through an indirect method. The dispersion was first centrifuged, after which the quantity of free drug in the supernatant was determined by means of RP-HPLC (see conditions in Section 4.2.4). These results were employed in the calculation of %EE with the aid of Equation 3.15. A summary of the results is provided in Table 4.31

Table 4.31: Summary of calculated % entrapment efficiency (%EE) for optimised 2% MNZ loaded solid lipid nanoparticles (MNZ-SLNs) batches.

Sample	Assayed mass (MNZ-SLN preparation)	Assayed mass (supernatant)	% Entrapment efficiency ± RSD
1	0.27 mg	0.06 mg	76.14
2	0.25 mg	0.07 mg	73.65
3	0.25 mg	0.06 mg	74.32
Mean (*n*=3)	0.26 ± 3.67	0.06 ± 7.44	74.70 ± 1.42

The amount of drug incorporated in a colloidal system is dependent on the physicochemical properties of the drug and its preparation process. The mean %EE for the optimised MNZ-SLNs was relatively high. The overall %EE was reflective of the high solubility of MNZ in the melted lipid. The lipid:drug weight ratio of 2:3 cholesterol to MNZ contributed to an increased DL which, in turn, related to good entrapment of the drug within the lipid. The higher lipid content also provided more space for drug accommodation. Furthermore, the drug:lipid ratio demonstrated an increase in viscosity of the lipid phase, which caused faster solidification of the nano-dispersion and, consequently, entrapping more drug. This phenomenon was in line with previous research that established how solidification prevents the diffusion of drugs to the external aqueous medium and results in the higher entrapment of APIs (Joseprakash *et al.,* 2011; Nandini *et al.,* 2015). The calculated mean %EE fell near the 95% CI of 77.99%, thus validating the statistical model.

4.6.4 Accelerated stability studies

Storage stability tests were conducted to establish a shelf-life profile and label storage instructions applicable to all future batches and batches manufactured under similar conditions. The stability of the prepared MNZ-SLNs was investigated under accelerated storage conditions, as advised by the WHO (2009). Three samples (*n*=3) were kept at ambient temperature and their organoleptic properties, z-avg. and %EE were assessed at predetermined intervals, as was presented in Table 4.32.

ZP is a function of surface coverage by charged species at a specific pH. It is used as an indicator for dispersion stability (Shah *et al.,* 2014). It should be noted, however, that ZP values were not included for the purposes of this study because characterisation assessments by means of PCS revealed sufficient particle stability. Table 4.32 below depicts a summary of MNZ-SLNs characteristics under the accelerated storage conditions.

Table 4.32: Overview of optimised 2% MNZ-solid lipid nanoparticles (MNZ-SLNs) characteristics under accelerated stability storage conditions for WHO zone IVb.

Product name: Optimised 2% MNZ loaded solid lipid nanodispersion. Batch size: 10 ml Date of manufacture: 14 May 2017	Packaging material: 10 ml McCartney glass jars Storage conditions: 40 ± 2 °C/75 ± 5% RH Manufacturer of API: Acros Organics, ThermoFischer Scientific™, Massachusetts, USA.
Date of commencement of stability study	14 May 2017
Specification Limits	Mean particles size <1000 nm

Time intervals (months)	**Sample 1: Z-avg. %EE**	**Sample 2: Z-avg. %EE**	**Sample 3: Z-avg. %EE**	**Mean (*n*=3) Z-avg. %EE**
0	72.80 nm 74.32	72.45 nm 73.65	73.79 nm 76.14	73.01 ± 0.77 nm 74.70 ± 1.41
1	83.81 nm 69.87	83.61 nm 68.51	83.52 nm 70.24	83.65 ± 1.57 nm 69.54 ± 1.07
3	82.65 nm 68.59	83.92 nm 69.02	85.58 nm 70.36	84.13 ± 1.43 nm 69.32 ± 1.09
6	95.21 nm 64.47	94.86 nm 65.41	95.63 nm 65.98	95.23 ± 0.33 nm 65.29 ± 0.95
% Total drug loss	13.25	11.19	13.45	12.63 ± 8.09

The relation between the two measured responses against time are illustrated in Figure 4.48. In this figure, it is evident that as time progressed, the z-avg. (depicted in blue) gradually increased. Simultaneously, the %EE (depicted in orange) gradually decreased upon storage.

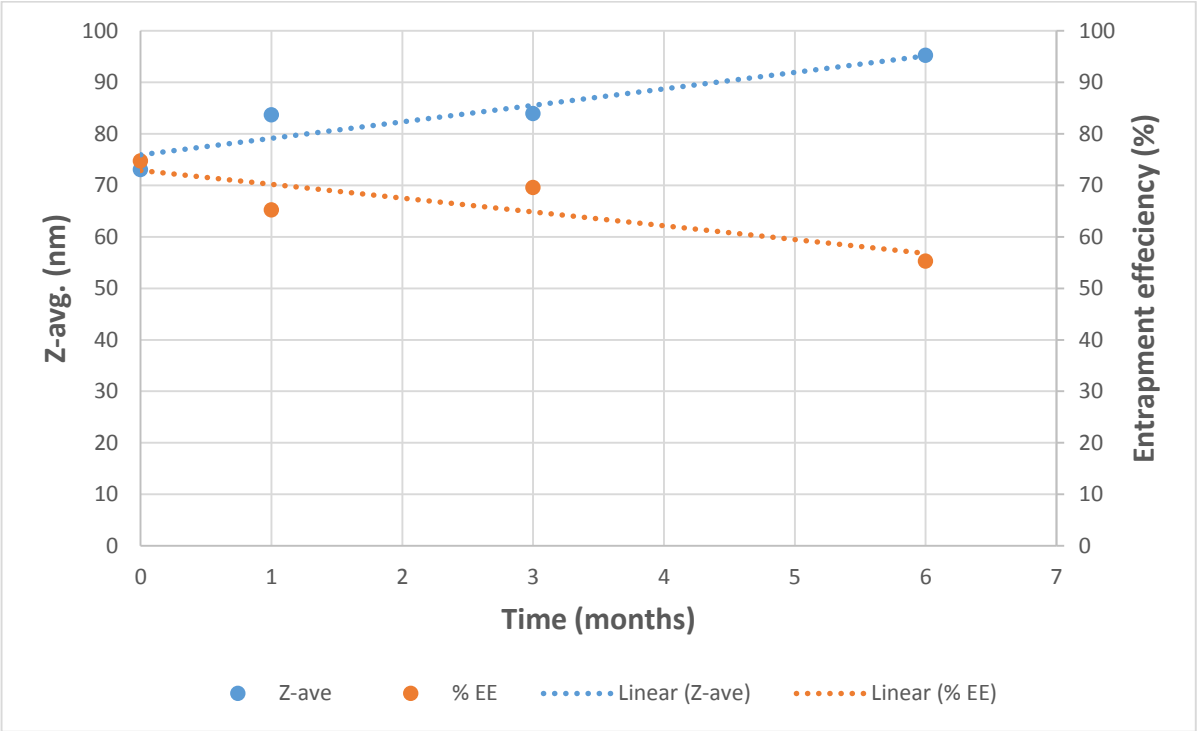

Figure 4.48: Change in particle size (z-avg.) and entrapement efficiency (%EE) under WHO Zone IVb accelerated stability test conditions.

No obvious visual changes to the dispersions were noted over the predefined storage period. However, significant changes to z-avg. were noted upon storage, which were accompanied with a decrease in %EE of the nanoparticles. This phenomenon may be accounted for due to the use of heat in the preparation steps of the nanoparticles. The use of heat during the formulation process causes particle crystallisation in higher energy modifications (α), but upon storage, these modifications are transformed to low-energy and more ordered (β) crystal lattice structure. As a result, this degree of order conferred on the stored nanoparticle can lead to the expulsion of drugs, as less space is available for drug accommodation (Das and Chaudhury, 2010).

These findings imply that, under the accelerated stability conditions, the transition of the optimised SLN dispersions from a high-energy α or β' form to a more stable β form occurred at a slightly rapid rate, which resulted in a mean drug loss of 12.63% over a period of six months under the WHO-accelerated stability storage conditions. A significant change at accelerated storage conditions is defined as 5% loss of potency from the initial assay, degradation exceeding the specification limit, exceeded pH limits and a failure to meet specifications for organoleptic properties (WHO, 2009). Where a significant change is noted under these storage conditions, a minimum of six month's data should be included from an ongoing one-year study at 30 ± 2°C/65% ± 5% RH where the same significance criteria is applied (Hela, 2012). Due to time constraints in this study, such practices were not feasible and, therefore, are discussed in the recommendations section of the next chapter.

Additionally, there are many factors that influence the stability of a pharmaceutical product. A loss in %EE form the SLNs does not necessarily equate to the loss of potency from the product. The API may still be stable in the continuous phase of the lipid dispersion (Harde *et al.,* 2014), and further investigation tests by means of an X-Ray powder diffraction are recommended to determine lipid crystalline phase structures and, consequently, lipid vesicle stability. Moreover, storage conditions need to be taken into account, as the current recommended conditions were not suitable for this novel dosage form. There are also many formulations that require refrigerated conditions due to stability issues; therefore, it is recommended that all prepared MNZ-SLN formulations be stored in a fridge.

4.7 DEVELOPMENT AND CHARACTERISATION OF IN SITU VAGINAL HYDROGELS

Hydrogel formulations of various compositions were prepared and characterised for their organoleptic properties, pH and sol-gel transitioning abilities. The formulation which displayed the most favourable characteristics underwent incorporation with an optimised 2% MNZ-SLN preparation.

4.7.1 Preparation of unloaded hydrogels

The CM of gel production was employed for the preparation of seven hydrogel formulations of various compositions (see Table 3.11). All prepared formulations were transparent and free-flowing at ambient temperature upon production.

The physical appearance of all formulations was aesthetically pleasing, which suggested adequate dissolution of the polymer in the aqueous solvent with no suspending particles.

4.7.2 Determination of optimal hydrogel formulation

Sensory, pH and rheological tests were employed in the determination of the optimal hydrogel formulation that would undergo incorporation with the prepared MNZ-SLNs formulation. These tests are discussed in more detail in the following sub-sections.

4.7.2.1 Organoleptic assessments

Descriptive sensory tests were undertaken to define the organoleptic characteristics of the prepared unloaded hydrogel formulations. The knowledge of product preferences ensured product acceptability. Organoleptic property assessments are critical for determining sensory characteristics of a product, with the aim of improving patient compliance by facilitating dosage form acceptability (Morrow *et al.*, 2014; Joglekar *et al.,* 2008). Formulations FG1 to FG7 were assessed for their physical appearance, colour, homogeneity, texture, skin feel and odour. The results obtained are summarised in Table 4.33.

Table 4.33: Summary of organoleptic evaluations of prepared unloaded hydrogel formulations (FG1 to FG7).

Code	Physical appearance	Colour	Texture	Skin feel	Homogeneity	Odour
FG1	Slightly transparent	Off-yellow	Smooth	Cool, refreshing, moisturising, non-greasy	No phase separation, no particles observed, homogenous	Strong characteristic chemical odour
FG2	Slightly transparent	Off-yellow	Smooth	Cool, refreshing, moisturising, non-greasy	Cool, refreshing, moisturising	Mild characteristic chemical smell
FG3	Slightly transparent	Off-yellow	Smooth	Cool, refreshing, non-greasy	Single phase, homogenous	Mild characteristic chemical odour
FG4	Transparent	Colour-less	Smooth	Cool, light, non-greasy	Single homogenous phase	Odourless
FG5	Slightly transparent	Off-yellow	Smooth	Cool, light, non-greasy	Single homogenous phase	Mild characteristic chemical odour
FG6	Slightly transparent	Off-yellow	Smooth	Cool, non-greasy, refreshing	Single homogenous phase	Characteristic chemical odour
FG7	Transparent	Clear	Smooth	Non-greasy, light, refreshing	Single homogenous phase	Odourless

The findings demonstrate that all formulations displayed cosmetically appealing appearances and a smooth texture, with acceptable homogeneity and no signs of phase separation. Chitosan-containing formulations (FG1, FG2, FG3, FG5 and FG6) had a characteristic chemical odour, which is possibly attributed to the fact that the natural polymer is derived from the marine environment (Muxika et *al.,* 2017). Furthermore, minor concentrations of glacial acetic acid were utilised in the preparation of all chitosan-containing formulations, thus giving them a mild characteristic vinegar smell.

FG4 and FG7 were formulated in the absence of acetic acid and chitosan and were found to possess no characteristic odour or colour. These results are more favourable because many women have indicated their preference towards odourless and colourless products intended for intravaginal use (Plameira-de-Oliveira *et al.,* 2014; Li *et al.,* 2013; Vermani and Garg, 2000).

4.7.2.2 pH measurements

pH is a measure of the acidic or basic nature of a solution. This value can impact the flavour, consistency and stability of a dosage form (Bajaj, 2012). The pH measurements for Day 0 and 84 of the formulated unloaded hydrogel preparations are summarised in Table 4.34.

Table 4.34: Summary of pH measurements of prepared unloaded hydrogel formulations (FG1 to FG7).

	Day 0				Day 84			
	Sample 1	Sample 2	Sample 3	Mean (*n*=3)	Sample 1	Sample 2	Sample 3	Mean (*n*=3)
FG1	4.51	4.51	4.52	4.51 ± 0.01	4.50	4.50	4.51	4.50 ± 0.01
FG2	4.65	4.65	4.65	4.65 ± 0.00	4.62	4.63	4.63	4.63 ± 0.01
FG3	4.51	4.53	4.53	4.52 ± 0.01	4.51	4.52	4.52	4.52 ± 0.01
FG4	6.80	6.81	6.82	6.81 ± 0.01	6.81	6.83	6.83	6.82 ± 0.01
FG5	4.51	4.51	4.50	4.51 ± 0.01	4.51	4.52	4.51	4.52 + 0.01
FG6	4.51	4.51	4.53	4.52 ± 0.01	4.51	4.52	4.52	4.52 ± 0.01
FG7	6.80	6.80	6.81	6.80 ± 0.01	6.81	6.81	6.81	6.81 ± 0.00

Low pH values were noted in all chitosan-containing formulations. This is attributed to the use of small concentrations of glacial acetic acid in the preparation process. The remaining formulations were close-to-neutral in pH. The pH values of hydrogel

formulations containing poloxamer 188 and HPMC, only, were more basic, with an average pH range of 6.82 ± 0.01. Due to the logarithmic nature of the pH scale, even the slightest changes have a significant impact on a formulation (Munhoven, 2013). However, in this study, over a period of 12 weeks, no significant changes in pH for all formulations were noted.

The natural pH of the vaginal environment is in the acidic range (4.5). This low pH acts as a defence mechanism and facilitates a healthy vaginal microflora (Keshwani *et al.,* 2014; Ashok *et al.,* 2014). In order to maintain this environment, the WHO (2012) recommends the use of vaginal lubricating products in a pH of ± 4.5 and osmolality of less than 1200mOsm/kg (Edwards and Panay, 2016).

Furthermore, site-specific drug delivery can be maintained through the creation of an acidic formulation. In such cases, the majority of drug candidates are either weak acids or bases, thereby inferring that drugs can be ionised to a certain extent, depending on their pKa and the pH of the vaginal fluid (Rohan and Sassi, 2009).

The unionised form of a drug with a large pKa is better absorbed from the vagina than its ionised form. Therefore, a slightly acidic vaginal environment favours better pharmacokinetics of acidic formulations, where the pH<pKa of the drug (Kale and Ubgade. 2013). In addition, the likelihood of certain infections (i.e. bacterial vaginosis, in particular) increases with an increase in vaginal pH. Therefore, it is advantageous to use products that maintain the vaginal pH within its physiological range (Haya *et al.,* 2014). Lowered pH (<3) increases the severity of vagina mucosa irritation, whilst higher pH values (>5) compromise the mucosa's natural barrier function, making it feel dry and vulnerable to irritation and infections (Kaminsky and Willigan, 1982). Formulations (i.e. chitosan-based hydrogels) that demonstrated a pH measurement of less than 5 were, therefore, considered ideal for the purposes of this study.

Due to their unfavourable organoleptic characteristics, further manipulation of FG1 and FG8 was also considered. The use of a PBS (pH 4.5 ± 2) to dissolve the respective mucoadhesive polymer was employed as the aqueous phase during the preparation process to reduce the overall pH of the formulation.

4.7.2.3 Viscosity measurements

Viscosity studies of all formulations were conducted to aid with the prediction of their *in situ* gelling behaviour. Flow characteristics of vaginal formulations not only affect their 'spreadability', but also their residence time at the site of application (Almomen *et al.*, 2015). Figure 4.50 depicts a relationship of shear stress versus shear rate for the formulation of FG1 to FG7, with a commercially available vaginal cream as a control.

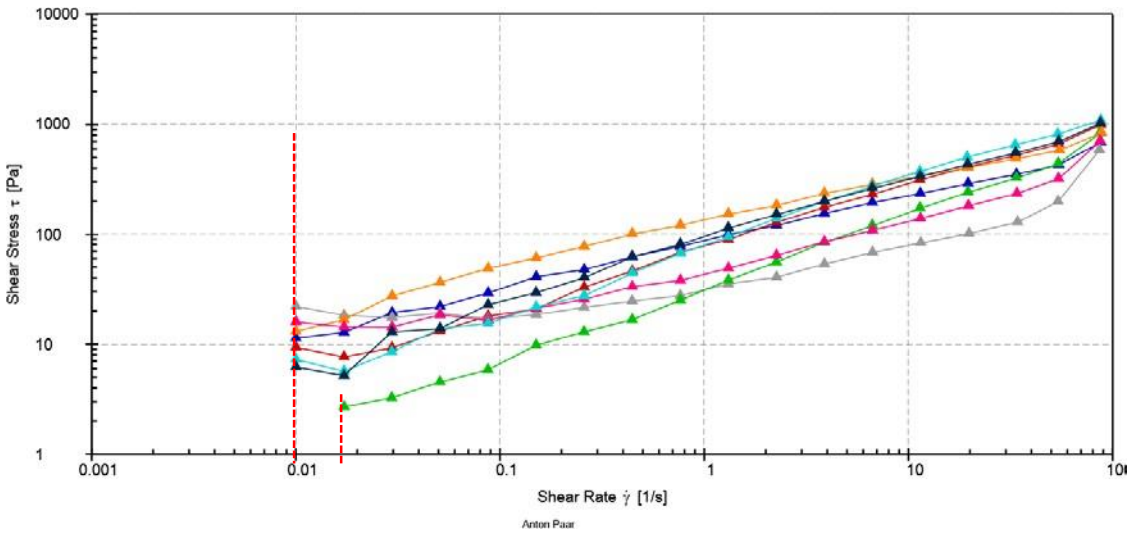

Figure 4.49: Shear stress (Pa) versus shear rate (1/s) of prepared unloaded hydrogels and a commercial vaginal cream, where ▲=FG1, ▲=FG2, ▲=FG 3, ▲=FG4, ▲=FG5, ▲=FG6, ▲=FG7, ▲=control, --- =yield stress at 37 ± 2°C.

A non-Newtonian fluid's flow curve is non-linear and does not cross through the origin. Moreover, its viscosity does not remain constant at a given temperature but is dependent on conditions like shear rate and flow geometry (Chhabra, 2010). Based on this definition, all the tested formulations in this study can be deemed non-Newtonian fluids. The point at which the formulations began to flow was indicated by the yield stress. FG4 possessed a slightly higher yield stress than the other formulations, which suggested that higher shear rates were required to induce flow of the hydrogel.

The flow behaviour of the prepared hydrogels and control were assessed by monitoring the variation of viscosity with respect to the change in their shear rates. A summary of these observations is given in Figure 4.51.

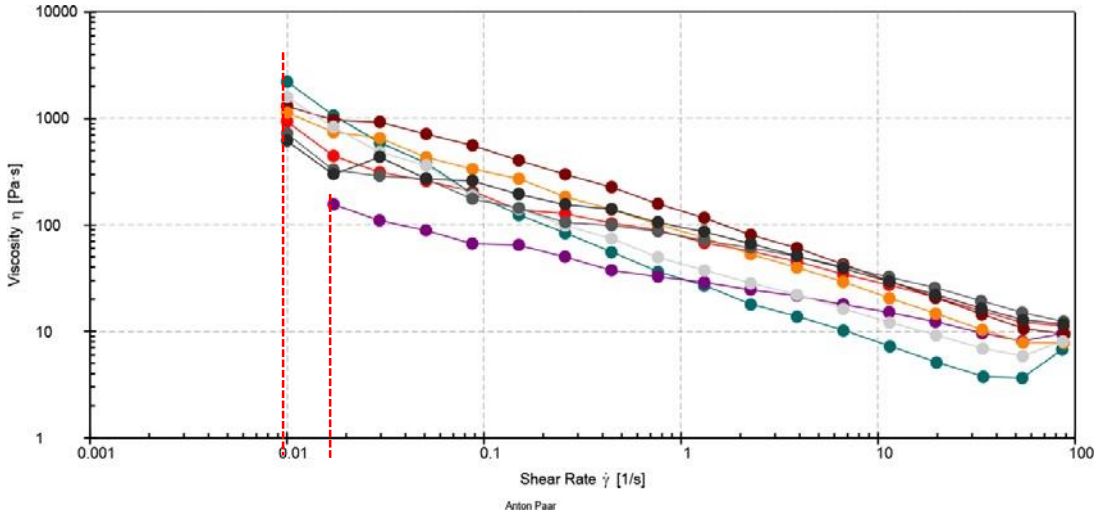

Figure 4.50: Viscosity (Pa·s) versus shear rate (1/s) of prepared unloaded hydrogels and a commercial vaginal cream, where •=FG1, •=FG2, •=FG 3, •=FG4, •=FG5, •=FG6, •=FG7, •=control, ---=yield stress at 37 ± 2°C.

All formulations demonstrated shear thinning behaviour, where a decrease in viscosity was observed when the shear rate increased. In addition, all formulations only began flowing at shear rates ≥0.01 s^{-1}, which suggested that, at body temperature, the formulations displayed Bingham pseudoplastic flow characteristics. Bingham flow principles state that a critical level of stress (yield stress) is required to induce the flow of some liquids (Bjorn *et al.,* 2012). Therefore, below 0.01 s^{-1}, all formulations behaved as solids, absorbing the stress energy without flowing. After the critical stress point was reached, the formulations demonstrated non-Newtonian pseudoplastic flow.

It should be noted that the critical stress level for FG4 was slightly higher (>0.01) when compared to the other formulations. This suggests that more energy was required to induce its flow. Ideally, an operator should strive to compare dosage formulations of similar physiochemical properties. However, at the time of the study there were no MNZ-containing gels on the South African market, which necessitated the use of a cream for the control. The control demonstrated similar rheological properties to the rest of the formulations.

The low yield stress values for the preparation inferred easy pourability of the dosage form. This was deemed advantageous for facilitating easy extrusion from the packaging and spreading within the vaginal tract (Andrews *et al.,* 2009). Together with

its mucoadhesive properties, the hydrogel preparations maintained intimate contact at the site of application.

Additional assessment of the temperature-dependent characteristics of the formulations was investigated in this study in order to define the thermo-responsive nature of the formulations. Figure 4.52 illustrates a graph of temperature-dependent viscosity for the investigated formulations. A formulation was deemed thermoresponsive if it demonstrated an increase in viscosity over a temperature of interest (25 to 38 °C).

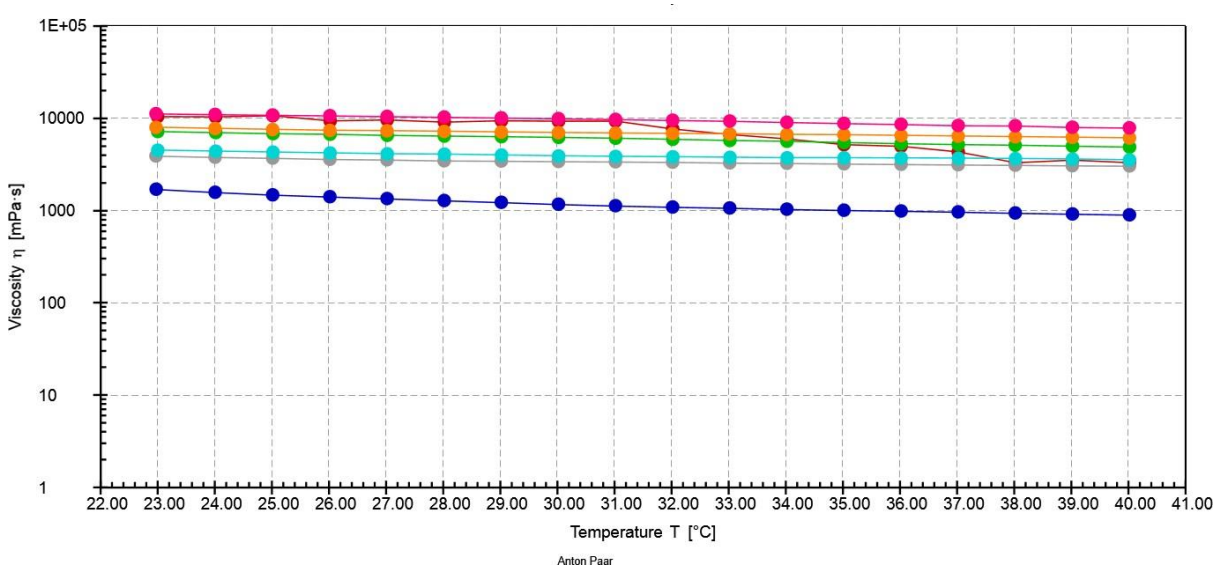

Figure 4.51: Graph of viscosity (mPa·s) as a function of temperature (°C) for prepared unloaded hydrogels and a commercial vaginal cream, where •=FG1, •=FG2, •=FG 3, •=FG4, •=FG5, •=FG6, •=FG7, •=control.

Nearly all formulations displayed similar temperature-dependent viscosity behaviour. At a constant shear rate, most formulations displayed uniform viscosity irrespective of a gradual increase in temperature. These findings impacted the study negatively by demonstrating that the prepared formulations were not thermo-responsive. No significant viscosity changes were observed for most formulations, with the exception of FG4. The temperature-dependent viscosity of the various formulations is presented in Figure 4.53.

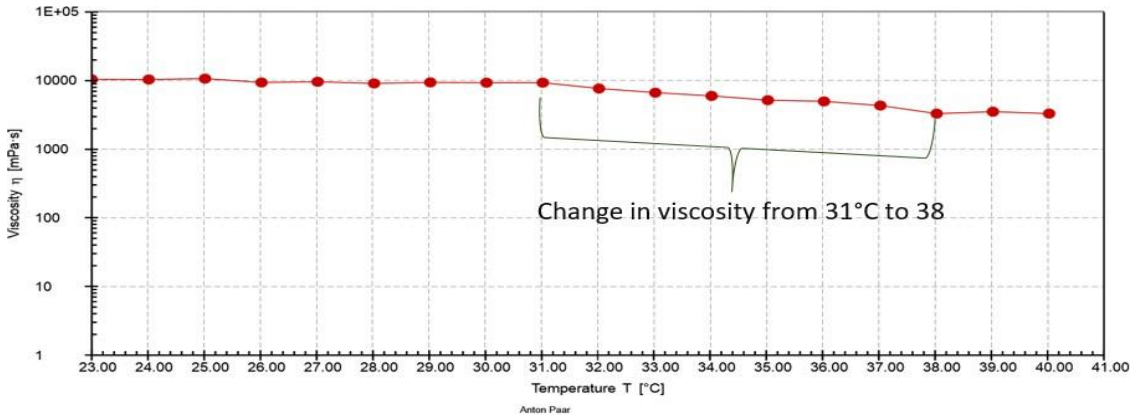

Figure 4.52: Graph of viscosity (mPa·s) as a function of temperature (°C) for FG7 containing poloxamer 188 18% m/v and hydroxyypropyl methylcellulose (HPMC) 1.5% v/v.

It was noted that over the temperature range of 31 to 38 °C, the viscosity of FG7 decreased gradually. This minimal viscosity change was not anticipated because both poloxamer 188 and HPMC display positive thermoresponsive behaviour (i.e. an increase in temperature causes an increase in viscosity) around this temperature range (Baloglu *et al.,* 2011; Pal *et al.,* 2013). Formulation FG7 demonstarted great potential for thermoresponsiveness. It was subjected to further manipulation by varying polymer concentrations to yield idead thermoresponsive characteristics for vaginal drug delivery. The results of this step are presented in Section 4.7.3.

4.7.2.4 Summary of optimal hydrogel formulation determination

Organoleptic assessments revealed that chitosan-containing formulations possessed unfavourable characteristics, such as bad odour. This was problematic, as formulations with bad odour are closely linked to poor patient compliance that can result in unfavourable therapeutic outcomes. It was resolved that chitosan would not be used for formulation purposes onwards. However, pH investigations of the various formulations revealed that all chitosan-containing formulations possessed ideal characteristics suitable for intravaginal drug delivery. As a result, and due to their undesirable sensory characteristics, the use of a PBS (pH 4.5) for the dissolution of the mucoadhesive polymer was proposed for future formulation purposes.

All rheological findings were unsatisfactory, thus declaring all such formulations unsuitable for MNZ-SLNs incorporation. However, the temperature-dependent

viscosity of FG7 prompted a brief investigation into the effect of polymer types and concentration on the overall thermal behaviour of future formulations. Hence, blank and loaded formulations were developed for further investigation and are discussed in the following section (see 4.7.3).

4.7.3 Incorporation of MNZ solid lipid nanoparticles (MNZ-SLNs) into optimal hydrogel formulation

In order to obtain an optimal hydrogel formulation for the incorporation of optimised 2% m/v MNZ-SLNs, four blank formulations were prepared and characterised for their pH, organoleptic and sol-gel transitioning abilities by means of a pH meter, sensory organs and test tube inversion methods. This investigation was prompted by the rheological findings of FG7. Table 4.35 provides an overview of the prepared hydrogel compositions and characteristics.

Table 4.35: Overview of hydrogel composition and characteristics for F-Gel 1 to 4, where P188 = poloxamer 188, HPMC = hydroxypropyl methylcellulose and MC450. = methylcellulose 450.

Sample code	Thermopolymer	Mucoadhesive polymer	pH	Organoleptic properties at 25 ± 2°C	Sol-gel transition
F-Gel 1	P188 (18% m/v)	HPMC (1.5% m/v)	4.55 ± 0.01	Transparent, colourless, odourless	No
F-Gel 2	P188 (18% m/v)	MC450 (1.5% m/v)	4.53 ± 0.01	Transparent, colourless, odourless	Yes
F-Gel 3	P188 (6% m/v)	HPMC (1.5% m/v)	4.55 ± 0.01	Transparent, colourless, odourless	No
F-Gel 4	P188 (6% m/v)	MC450 (1.5% m/v)	4.55 ± 0.01	Transparent, colourless, odourless	No

The effect of the P188 concentration was investigated at two levels, *viz*. six and 18% m/v. Generally, T_{sol} decreases with an increase in polymer concentration (Gandra, 2013). Hence, it was envisioned that through the alteration of polymer concentrations

the desired sol-gel transition temperature (T_{sol}) could be achieved. Furthermore, the gelling ability of hydrogel formulation is altered by the presence of APIs and other excipients (Dumortier *et al.,* 2006). Therefore, to improve the gelling potential, HPMC was substituted with methylcellulose (MC) 450 to facilitate adequate sol-gel transition. The four formulations were prepared through the CM of gel production and their pH was adjusted by using PBS for the dissolution of the mucoadhesive polymers.

As seen in Table 4.35, pH and organoleptic properties for all formulations were satisfactory for intravaginal drug delivery. F-Gel 2 demonstrated sufficient sol-gel transition at 34 ± 2 °C and was, therefore, deemed ideal for MNZ-SLN incorporation.

The reduction of P188 concentration did not have a significant effect on T_{sol} because neither F-Gel 3 nor F-Gel 4 transitioned to form a gel. However, the substitution of HPMC with MC450 did have a significant effect on the formulation, because a sol-gel transition occurred at 34 ± 2 °C.

This phenomenon is possibly explained by the reduction of the hydroxypropyl molar substitution in HPMC. Under normal circumstances, HMPC displays a T_{sol} of 75 to 90 °C, which is not ideal for intravaginal drug delivery because the dosage form will remain in its sol state upon application and potentially result in leakage (Almomen *et al.,* 2015). The high occurrence of hydroxyl groups provides HPMC with extremely strong intermolecular interactions, resulting in its poor solubility in water and most organic solvents (Otoni *et al.,* 2018). By reducing the hydroxypropyl molar substitution, MC450 can interact with H_2O more freely and gelation is due to the intermolecular association of hydrophobic methoxy groups on the polymer chains that are a function of temperature. At ambient temperature and below, H_2O molecules form enclosed structures around the hydrophobic groups, causing MC450 to be more water soluble. Upon temperature increments, these structures fragment and reveal the hydrophobic groups, thus inducing the formation of hydrophobic aggregates where gelation occurs (Karoyo and Wilson, 2017). MC gels are completely thermoreversible and liquefy upon cooling. Furthermore, they undergo swelling and erosion *in vivo;* therefore, not warranting the removal of the dosage form after complete drug release (Bain *et al.,* 2010).

The respective physical characteristics of F-Gel 1 to 4 are depicted in Figure 4.54.

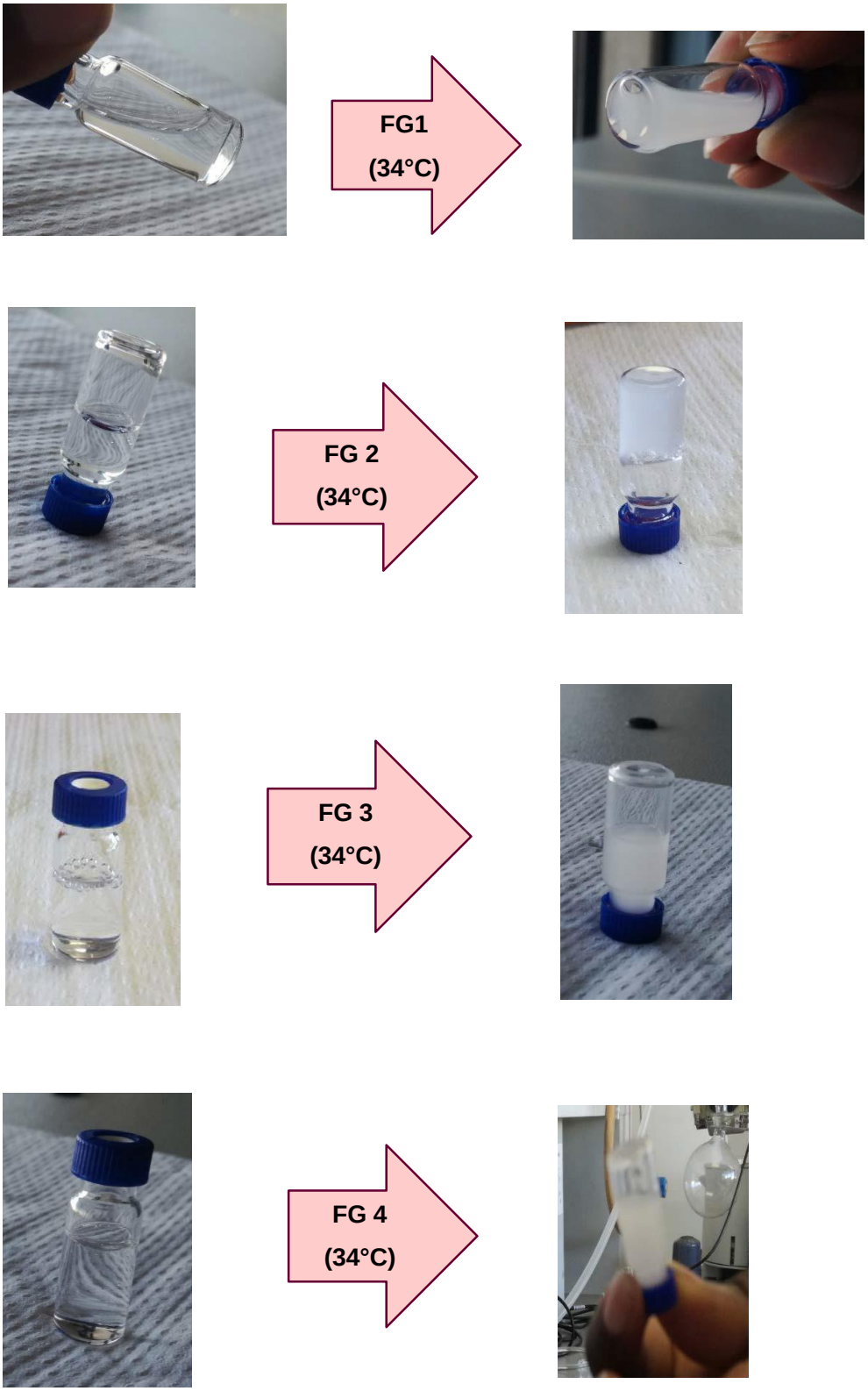

Figure 4.53: Physical characteristics of (a) F-Gel 1, (b) F-Gel 2, (c) F-Gel 3 and (d) F-Gel 4 at ambient and elevated (34 ± 2 °C) temperature.

At room temperature, all formulations were transparent and colourless, which demonstrated favourable organoleptic characteristics. Distinct changes in physical appearance were noted upon gradual temperature increments. At elevated temperatures, F-Gel 1 and 3 remained free-flowing, transparent and colourless liquids. F-Gel 2 solidified quickly at elevated temperatures to form an opaque, white non-flowing mass capable of supporting its own weight. However, F-Gel 4 did not solidify at elevated temperature but rather turned into a white opaque solution incapable of supporting its own weight. With continuous stirring and gradual temperature increments, F-Gel 4 solidified at 72 ± 2 °C; however, it was not deemed thermoresponsive for the purposes of this study because it did not transition at the body temperature of interest.

4.7.4 Characterisation of hydrogel incorporated with MNZ-solid lipid nanoparticles (MNZ-SLNs).

Three optimised 2% MNZ-SLN formulations were incorporated into three respective F-Gel 2 preparations by means of the CM of gel preparation. These formulations were referred to as MNZ-hydrogel(s), where they were characterised for their T_{sol} and drug content uniformity release, respectively.

4.7.4.1 Measurement of sol-gel transition temperature (T_{sol})

T_{sol} is the temperature at which a liquid or sol phase makes a transition to a gel phase (Tsao *et al.,* 2014). To facilitate satisfactory intravaginal drug delivery, the transition should occur in the range of 28 to 35 °C. T_{sol} >37 °C results in a liquefied formulation upon insertion at physiological temperature. This, in turn, causes leakage, messiness and rapid clearance of the dosage form at the site of application (Mei *et al.,* 2017). Conversely, T_{sol} <25 °C results in gel formation at ambient temperature, which can cause difficulty in dosage form extrusion from the packaging, with minimal spreading of the dosage form in the vaginal tract (Soliman *et al.,* 2016).

Due to limitations of available rheometers, a test tube inversion method was employed for the determination of MNZ-hydrogel T_{sol} in this study. The test tube inversion is a qualitative method that offers the operator a simple and rapid means of determining T_{sol}. All assessments were conducted in triplicates, allowing sufficient time for the

formulation to cool down to ambient temperature before re-testing. A summary of the test findings is given in Table 4.36.

Table 4.36: Summary of sol-gel transition determination of prepared MNZ-hydrogels using the test tube inversion method.

	MNZ-hydrogel 1	MNZ-hydrogel 2	MNZ-hydrogel 3	Mean (*n*=3)
T_{sol} (°C)	34	32	34	33.33 ± 2.82

The mean T_{sol} was calculated as 33.33 ± 2.82 °C. This is within the range for appropriate intravaginal drug delivery (Mei *et al.,* 2017). This dosage form exhibits great promise for convenient delivery of MNZ, whilst providing adequate spreading. Furthermore, the use of a mucoadhesive polymer aims to prolong dosage form retention at the site of application.

4.7.4.2 Drug content uniformity testing

In order to determine MNZ homogeneity in each formulation, drug content was established by means of RP-HPLC under optimised chromatographic conditions (see Section 4.2.4). Drug content was determined by assessing the area under the peak against the standard calibration curve of MNZ. Sampling of the three prepared MNZ-hydrogel formulations was done from the top, middle and bottom of the containers. A summary of the assay results is provided in Table 4.37.

Table 4.37: Summary of RP-HPLC assay results of prepared MNZ-hydrogels at 234 nm, MP (MeOH 85% v.v:H_2O 15% v/v), flow rate 1 ml/min.

	MNZ-hydrogel 1 (peak area)	MNZ-hydrogel 2 (peak area)	MNZ-hydrogel 3 (peak area)	Mean (*n*=3) (peak area)
Top sample	1 805 978	1 752 852	1 800 316	1 786 382 ± 23821.70
Middle sample	1 816 784	1 721 375	1 711 295	1 749 818 ± 47530.59
Bottom sample	1 802 713	1 712 359	1 705 623	1 740 232 ± 44266.47
Mean peak area	1 808 492	1 728 862	1 739 078	1 758 811 ± 35376.71
Concentration (mg/ml)	0.21 mg/ml	0.20 mg/ml	0.21 mg/ml	0.21 mg/ml
% recovery	105%	100%	105%	103.33 ± 2.36%

MNZ was well-distributed within each respective MNZ-hydrogel formulation. This was demonstrated by minimal deviations in peak response from the top, middle and bottom sample in each formulation. The mean % recovery was determined to be 103.33 ± 33%, which is a statistically significant deviation. Ideally, the % recovery should be found in the range of 98 to 102% (Ueda *et al.,* 2009). The deviation may be accounted for by human error during any of the preparatory steps when working with minute sample amounts.

4.8 *IN VITRO* DRUG RELEASE TESTING (IVDRT)

IVDRT plays a key role in pharmaceutical formulation development and quality control by monitoring the consistency and stability of dosage forms and facilitating the prediction of *in vivo* drug absorption (Stillhart *et al.,* 2017). FVDC was used to perform IVDRT on an optimised 2% MNZ-SLN preparation and a MNZ-hydrogel, respectively. Intravaginal conditions were replicated by means of a PBS (pH 4.5) at 37 °C. The drug release profiles of the respective formulations were determined using a plot of cumulative drug release as a function of time with the aid of Microsoft Excel® (2016)

(see Figure 4.55). The mean cumulative amount was calculated with the aid of Equation 3.18, from the mean (*n*=3) drug released at each sampling point.

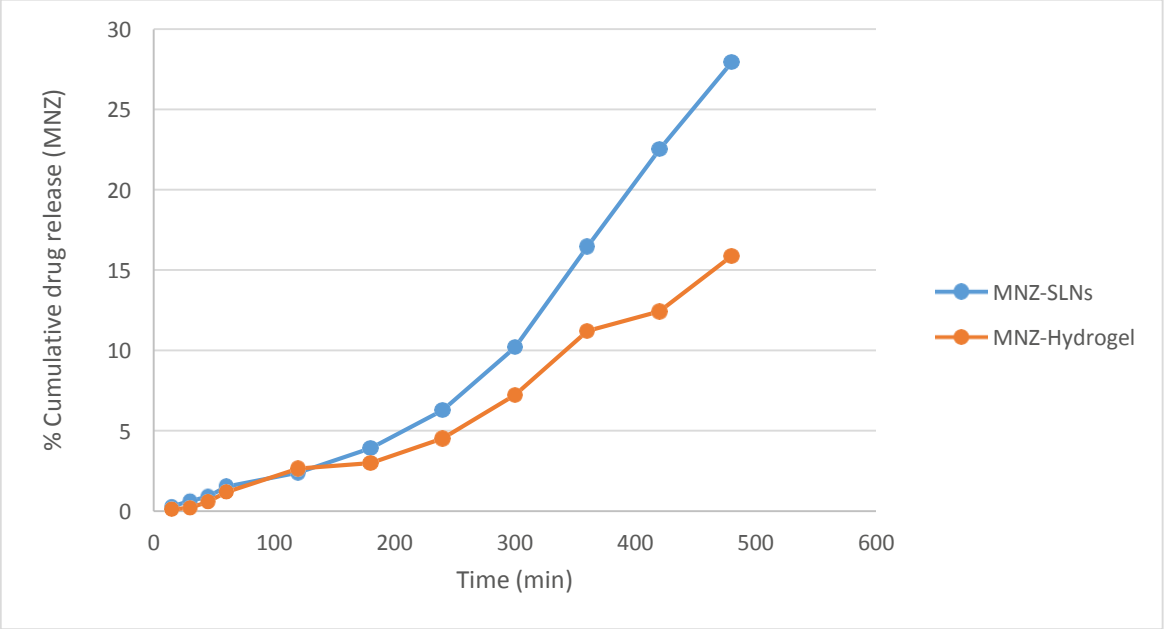

Figure 4.54: Plot of cumulative % drug release of miconazole nitrate (MNZ) as a function of time (min), where orange = MNZ-hydrogel and blue = MNZ-solid lipid nanoparticles (MNZ-SLNs).

IVDRT tests were conducted over a period of 480 minutes (i.e. eight hours). During this period, both formulations showed very similar release kinetics. The MNZ-hydrogel preparation exhibited a slower rate of drug release, with a total of 15.87% of MNZ released in an eight-hour period. This was in comparison to the 27.94% MNZ released from the optimised MNZ-SLN preparation in the same period.

The slow release kinetics of the MNZ-SLN preparation may be attributed to the solubilised drug in the lipid core which is released through dissolution or diffusion methods (Aljaed and Hosny, 2016). The drug rate was further extended by the incorporation of MNZ-SLNs into the hydrogel polymer network, possibly owing to the slower rate of drug diffusion through the hydrogel matrix or due to erosion. The IVDRT results gathered were used to generate non-linear mathematical models in order to assess MNZ drug release from the prepared dosage forms. Generally, the mechanism of drug release from hydrophilic polymeric matrices involves solvent penetration, hydration and swelling of the polymer, diffusion of the dissolved drug in the matrix and erosion of the gel layer (Chaterjee, 2011).

4.8.1 Non-Linear Mathematical modelling

Mathematical models play a significant role in establishing the mechanism of drug release and providing a guideline for NDDS (Nabatchian *et al.,* 2014). Data for this study were plotted and analysed with the aid of DDSolver™ (Microsoft Excel® add-ins, 2016). Various models including Zero-order, First-order, Kosmeyer-Peppas, Hixon and Crowell, Higuchi, Bakers and Lonsdale were investigated. To test the best-fitting model, the acquired r^2 value from each model was compared, and the one which demonstrated the highest numerical value was chosen as the best fit. This statistical analysis was conducted on the MNZ-SLNs and MNZ-hydrogel preparations, respectively (see Table 4.38).

Table 4.38: Correlation coefficients (r^2) for non-linear mathematical models for an optimised MNZ-solid lipid nanoparticles (MNZ-SLN) and MNZ-hydrogel.

Mathematical model	MNZ-SLNs (r^2)	MNZ-hydrogel (r^2)
Zero-order	0.8708	0.9351
First-order	0.8474	0.9250
Korsmeyer-Peppas	**0.9941**	**0.9945**
Hixson-Crowell	0.8552	0.9284
Higuchi	0.6175	0.7026
Higuchi with T_{lag}	0.9582	0.9338
Higuchi with F_0	0.7995	0.9457
Bakers and Lonsdale	0.6067	0.6960

The optimised MNZ-SLNs formulation that attained the highest r^2 of 0.9941 came from the Korsmeyer-Peppas model. The MNZ-hydrogel preparation that achieved the highest r^2 of 0.9945 also came through the Korsmeyer-Peppas mathematical model. Therefore, the Korsmeyer-Peppas model was deemed the best fit for both formulations.

4.8.2 Miconazole nitrate (MNZ) drug release models

Plots of % cumulative drug release profiles for the Korsmeyer-Peppas model are depicted in Figures 4.56 and Figure 4.57 for the optimised MNZ-SLNs formulation and MNZ-hydrogel, respectively.

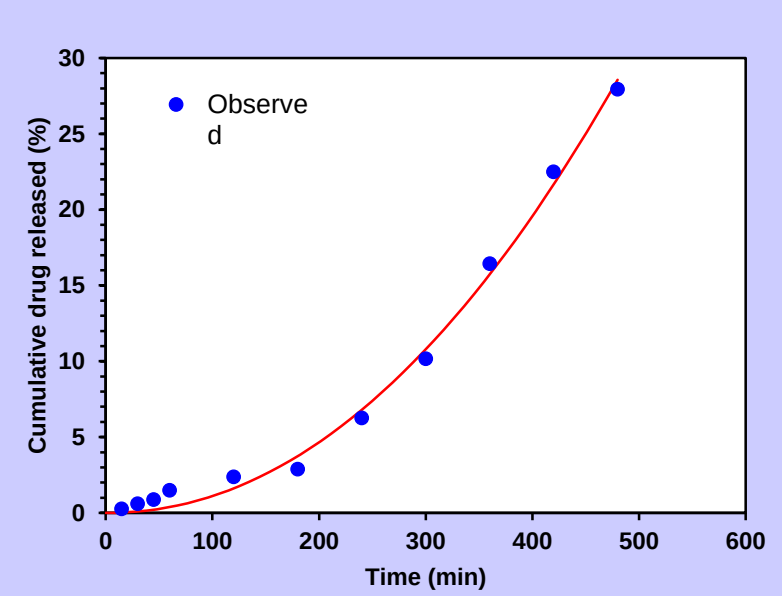

Figure 4.55: Plot of % cumulative drug release of an optimised MNZ loaded solid lipid nanoparticles (MNZ-SLNs) depicting the Kosmeyer-Peppas mathematical model fit.

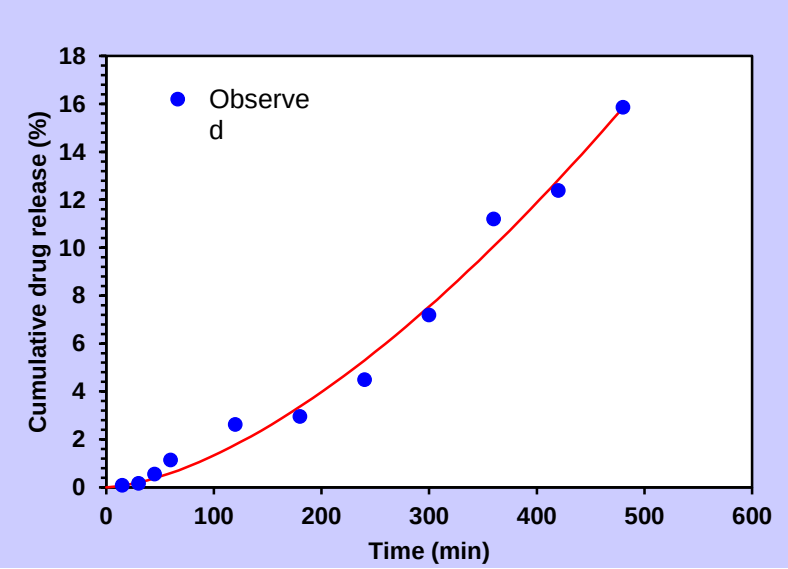

Figure 4.56: Plot of % cumulative drug release of a MNZ-hydrogel depicting the Korsmeyer-Peppas mathematical model fit.

The mechanism of drug release from matrices of swellable polymers is a complex phenomenon. Some systems display diffusion or erosion, whilst others exhibit a combination of both to facilitate controlled drug release (Grassi and Grassi, 2005). The Korsmeyer-Peppas model takes into account simultaneous processes, such as gel formation and the dissolution of polymers to model drug release, making it useful for describing drug release from several MR dosage forms (Shaikh *et al.,* 2015).

From the results presented earlier, it was observed that all formulations showed good correlation to the Kosmeyer-Peppas model. The release rate constant (*kKP*) and diffusional exponent (*n*) were key parameters which were governed by the release mechanism. *n* indicates the mechanism of drug release when more than one phenomenon is involved, where an *n* value of <0.43 indicates Fickian diffusion, 0.43<*n*<0.85 indicates non-Fickian diffusion which combines erosion and diffusion mechanisms, 0.89<*n*<1 suggests the case II transport and *n*>1 suggests a super case II transport mechanism (Fu and Kao, 2011). The *n* value for MNZ-SLNs and MNZ-hydrogel in this study were determined as 2.071 and 1.580, respectively. This finding suggested a super case II drug release mechanism that involves the erosion of lipid or polymer matrix where applicable, as per Lee (1985) and Abbas and colleagues' (2013) earlier findings. *kKP* values for MNZ-SLNs and MNZ-hydrogel were determined as 0.000 and 0.001, respectively. The slightly higher *kKP* value of the hydrogel suggests faster discharge of the drug from the thermoresponsive gel upon insertion. This corresponds with Zhang *et al.*'s (2011) assertions.

4.8.3 Statistical significance

The statistical significance of drug release data from the two respective formulations were evaluated by means of a paired sample t-test (Microsoft Excel®, 2016). A t-test is conducted to ascertain if the means of two populations are equal so as to either accept or reject a null hypothesis (Kao and Green, 2008). The results of the test are depicted in Table 4.39.

Table 4.39: Results of t-test: Paired two sample for means where variable 1=% cumulative drug release from MNZ-solid lipid nanoparticles (MNZ-SLNs) and Variable 2=% cumulative drug release from MNZ-hydrogel.

	Variable 1	Variable 2
Mean	8.355455	5.339091
Variance	95.04205	30.69337
Observations	11	11
Pearson correlation	0.990048	
Hypothesised mean difference	0	
df	10	
t Stat	2.307963	
P(T<=t) one-tail	0.021829	
t Critical one-tail	1.812461	
P(T<=t) two-tail	0.043659	
t Critical two-tail	2.228139	

The test yielded a value of 0.021829 which means that the test was statistically significant when a p-value <0.05 is considered as statistically significant. Therefore, the test proved that there was a significant difference between MNZ release data for the MNZ-SLNs formulation and MNZ-hydrogel. Concluding that the difference did not occur simply because the data sets were atypical.

4.8.4 Summary of *in vitro* drug release testing (IVDRT)

IVDRT of the two prepared formulations indicated that they followed very similar release kinetics via the Korsmeyer-Peppas model. After a period of eight hours, only 27.94% of the API had been released from the MNZ-SLNs, which was significantly higher than the 15.87% of the hydrogel formulation. This finding suggests that the prepared hydrogel showed great potential as a vehicle in the delivery of MNZ, whilst facilitating controlled drug release.

4.9 ANTIMICROBIAL SUSCEPTIBILITY TESTING (AST)

The anti-fungal efficacies of MNZ-SLNs and the MNZ-hydrogel against *Candida albicans* species were investigated by means of a modified Kirby-Bauer disc diffusion assay. A commercially available cream and unloaded SLN and hydrogel preparations were used as controls. The respective mean (*n*=3) zones of inhibitions for each formulation is depicted in Figure 4.58.

A blank hydrogel and nanodispersion were used as positive test controls to determine whether or not the presence of excipients within the formulation contributed to the antifungal activity of the final dosage form. It was noted that the blank hydrogel had no activity against *Candida albicans spp*. since it did not inhibit its growth on the agar. This result was anticipated, as none of the excipients used in the formulation of the hydrogel possessed known antifungal activities. The blank nanodispersion, however, appeared to possess weak antifungal activity, as indicated by a mean zone of inhibition of 7.67 mm. It was recommended that further investigations be done to determine the influence of excipients in the SLN preparation, as time and resource constraints in this study hindered further investigation. .

Furthermore, a titanium metal PUS was used in the fabrication of the MNZ-SLNs formulation. Titanium is known to possess some antifungal properties (Betts *et al.,* 2013). One of the biggest concerns with SLNs formulated by means of PUS is possible dispersion contamination by eroding metal (Pooja *et al.,* 2015). Therefore, the resultant formulation was recommended for titanium or metal testing. A negative control by means of a blank segment of the agar was evaluated to determine whether or not any constituents within the MHA possessed any antifungal activity against *Candida albicans.* Complete growth was observed in that segment with a zone of inhibition of 0mm. This indicates that the storage conditions and agar were suitable for the germination of the fungi species.

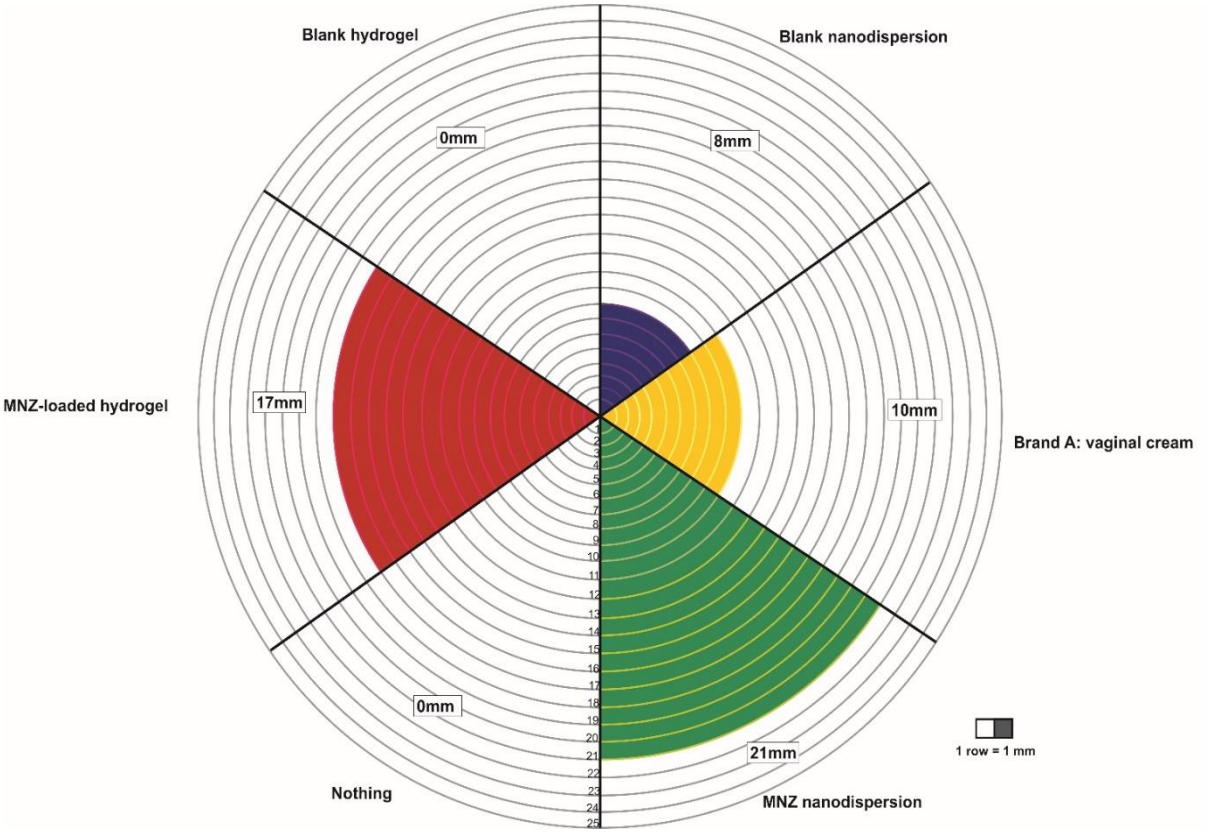

Figure 4.57: Mean zone of inhibition (mm) for various test formulations, where MNZ = miconazole nitrate.

The results indicate that the MNZ-SLNs, MNZ-hydrogel and a commercial antifungal cream demonstrated some activity against the *Candida albicans spp*. The antifungal activity of both the MNZ-SLNs and MNZ-hydrogel proved to be superior to the commercially available cream. This enhancement in antifungal activity could possibly be attributed to the reduction in particle size of the API by means of drug encapsulation within solid lipid nano-particles, thus enhancing the formulations' permeation through the agar. Additionally, the AST results correlated with the *in vivo* behaviour of the dosage from, which suggested that the prepared novel dosage forms show great potential in improving the therapeutic outcome of VVC as a result of *Candida albicans*.

4.10 CONCLUSION

This chapter comprised experimental results of the analytical method development and validation of MNZ, followed by its thermal analysis. These investigations allowed for the quantification of MNZ in bulk and complex formulations as well as the determination of drug-excipient compatibilities for the preparation of MNZ-SLNs.

MNZ-SLNs were prepared by means of a novel melt-emulsification sonication and low temperature solidification method. The resultant formulation was optimised statistically through the use of a CCRD, where a lipid concentration of 4% m/v and a sonication time of 260.94 seconds were deemed ideal. The optimised MNZ-SLNs were then characterised for particle characteristics, surface morphology, drug entrapment efficiency and stability. A thermo-responsive hydrogel formulation was developed and characterised for its organoleptic properties, pH, T_{sol} and drug content uniformity, where the organoleptic, pH and drug content uniformity were deemed favourable. The hydrogel T_{sol} was determined qualitatively by means of a test tube inversion method. This T_{sol} came to 33.33 ± 2.82 °C, which was deemed favourable for intravaginal drug delivery.

IVDRT were then undertaken to define the release kinetics of the optimised MNZ-SLNs and MNZ-hydrogel preparations. Both formulations suggested release mechanisms with the aid of the Korsmeyer-Peppas mathematical model. Finally, the superiority of the two formulations against a commercially available formulation against *Candida albicans* species was established through a modified Kirby-Bauer disc diffusion assay.

The final chapter of this study provides concluding remarks. An overview of the study's success, its limitations and prospective research suggestions will be discussed briefly.

CHAPTER 5

CONCLUSIONS AND RECOMMENDATIONS

This developmental study led to the formulation of a novel pharmaceutical dosage form. In chapter four, the experimental findings were presented. The focus of chapter five is to present a summary of the findings and draw subsequent conclusions.

5.1 CONCLUSIONS

Locally-acting imidazole creams were identified as first line agents in the treatment of uncomplicated VVC, but owing to poor patient adherence these dosage forms have been implicated in the high incidence of antifungal resistance and the subsequent reoccurrence of VVC infection. MNZ and imidazole antifungals were chosen as the model drugs for the purposes of this study, due to their lengthy treatment periods and frequent need for re-application. MNZ has also been associated with poor clinical outcomes. Therefore, it was necessary to conduct an investigation into ways of optimising this drug's delivery through the use of NDDS in the treatment of VVC. With the aid of reviewed literature, the physiochemical properties of MNZ *viz*. pKa and BCS were established. These characteristics suggested a highly lipophilic compound with poor aqueous solubility that made it an ideal candidate for solid lipid nanoparticle encapsulation. MNZ-SLNs were then developed and incorporated into a thermoresponsive mucoadhesive hydrogel for the intended treatment of VVC.

An analytical method was developed for the quantification of MNZ in bulk and complex pharmaceutical products by means of RP-HPLC by using an octyl stationary phase at 234 nm with an injection volume of 10 µL, a flow rate of 1.0 ml/min and a MP composition of MeOH:H_2O (85:15). The developed method was determined as suitable for its intended use with a peak symmetry value of 0.94 and a linear equation of y = 811214x + 67958 within a working range of 0.125 to 1.00 mg/ml. LoD and LoQ were determined to be 0.015 and 0.052 mg/ml, respectively. All calculated % RSD values for accuracy and precision were within the acceptable limit of ± 2%. Forced degradation studies established that MNZ was labile under photolytic, oxidative, hydrolytic and thermal stress. As part of this study's pre-formulation studies, SDT investigations were undertaken to determine drug-excipient compatibility. MNZ demonstrated satisfactory

dissolution in cholesterol with the promise of facilitating high drug entrapment within the lipid vesicle.

A thirteen-run two-factor CCRD was employed as the RSM statistical tool in order to optimise the developed MNZ-SLNs for ZP, particle size (z-avg.), %EE, change in z-avg. and %EE upon storage. The predicted optimisation parameters were 4% m/v for lipid concentration and 260.94 seconds for sonication time. The mean %EE for the optimised MNZ-SLNs was 75.24%, with a mean z-avg. of 73.03 nm and a narrow PDI. The stability of the optimised MNZ-SLNs was monitored under accelerated conditions over a period of six months. A mean ZP value of 38.43 mV suggested a well-stabilised formulation. Minor z-avg. increments were observed over a period of six months, with a total drug loss of 12.63% from the lipid vesicles.

Unloaded hydrogels were formulated and characterised for their pH, organoleptic properties and rheology. The most promising formulation underwent further manipulation to a cosmetically pleasing thermoresponsive hydrogel with a T_{sol} of 33.33 ± 2.82 °C. An optimised MNZ-SLNs formulation was then incorporated into the hydrogel by means of simple mixing below the T_{sol}. The MNZ-SLNs hydrogel displayed uniform drug content within each assayed sample.

A FVDC was used to perform *in vitro* drug release studies from the MNZ-SLNs and MNZ-hydrogel. A plot of % cumulative drug release as a function of time showed slow release kinetics for MNZ over an eight-hour period. A % cumulative drug release value of 27.94% was obtained for MNZ-SLNs and a slightly lower 15.87% was obtained for the MNZ-hydrogel. These findings implied that the hydrogel retarded the release of MNZ to a greater extent than the SLN formulation. This data was fitted into various kinetic models with the aid of DDSolver™ (Microsoft Excel® add-ins, 2016). Both formulations attained the highest r^2 of 0.9941 and 0.9945, respectively, following the Korsmeyer-Peppas mathematical model. The Korsmeyer-Peppas model has been used to describe drug release from various MR dosage forms. A high diffusional exponent of >1 in both formulations suggest a super case II drug release mechanism facilitated through lipid or polymer matrix erosion.

A modified Kirby-Bauer disc diffusion assay was used to determine *Candida albicans* susceptibility to the developed formulations. Controls, in the form of unloaded

preparations and a commercially available cream, were used. MNZ-SLNs and a MNZ-hydrogel demonstrated superior antifungal activities when compared to the commercially available cream.

Based on these experimental findings, it can be concluded that the primary aim and objectives were achieved through the development, optimisation and characterisation of MNZ-SLNs which were incorporated into a mucoadhesive thermoresponsive system intended for localised intravaginal drug delivery.

5.2 RECOMMENDATIONS

The concept of nanomaterials and 'smart' drug delivery shows great promise in addressing the current global issue of microbial resistance by advising on new strategies that improve therapeutic outcomes. One manner of achieving this is through target-specific dosage forms that promote high patient acceptability.

This study achieved the set aims and objectives by successfully developing and characterising a novel formulation of MNZ-SLN-loaded *in situ* vaginal hydrogel. The study design utilised a quantitative approach, in which data was generated and analysed through experimental and computational techniques. Due to time and resource constraints further investigations were not feasible. Therefore based on the current study findings, recommendations for future works are proposed below:

- To conduct further studies into the possible release mechanisms of the prepared dosage forms. By extending the IVDRT time, a better release profile may be generated for mathematical modelling.
- To expand the range of input variables in the CCRD in order to gain a better understanding of the interactive effects between the input variables and measured responses.
- To further investigate the rate of MNZ decomposition under accelerated conditions in order to explain the interaction that results in such rapid degradation even at room temperature.
- To conduct long-term stability studies on MNZ-hydrogel so as to determine its ideal storage conditions.

- To perform histological analysis of mucosal tissue to determine the effects of lipid and surfactant concentration on *in vivo* toxicity.
- To investigate patient acceptability of applicator devices used to apply this dosage form.
- Propose additional strategies for antimicrobial stewardship in an effort to combat resistance of microbial species.

REFERENCES

ARTICLES

Abbas S, Ahmad B, Ali J, Bashir S, Hassan S, Mohammad S & Mateen A (2013) To Evaluate and Study the Swelling and Drug Release Behavior of Poly (N-Vinyl-2-Pyrrolidone) Gel. *World Applied Sciences Journal,* 26: 333-344.

Abegunrin OA, Okhuevbie SO & Animasaun IL (2016) Comparison between the flow of two non-Newtonian fluids over an upper horizontal surface of paraboloid of revolution: Boundary layer analysis. *Alexandria Engineering Journal,* 55: 1915-1920.

Ačanski MM, Perišić-Janjić NU & Dimova V (2003) Normal and reversed phase high performance liquid chromatography of some new 1,2,4-triazole derivatives. *Acta Periodica Technologica,* 34: 1–14

Acarturk F (2009) Mucoadhesive vaginal drug delivery systems. *Recent Patents on Drug Delivery and Formulation,* 3: 193-205.

Adolfsson A, Hagander A, Mahjourbipour F & Larsson P (2016) How vaginal infections impact women's everyday life – women's lived experiences of bacterial vaginosis and recurrent vulvovaginal candidiasis. *Advances in Sexual Medicine*, 7: 1-19.

Ahmad SAR, Patil L, Usman MRM, Imran & Akhtar R (2018) Analytical Method Development and Validation for the Simultaneous Estimation of Abacavir and Lamivudine by Reversed-phase High-performance Liquid Chromatography in Bulk and Tablet Dosage Forms. *Pharmacognosy Research,* 10: 92-97.

Ahn SK, Kasi R, Kim SC, Sharma N & Zhou Y (2007) Stimuli-responsive polymer gels. *Soft Matter,* 4: 1151-1157.

Akbari B, Tavandashti MP & Zandrahimi M (2010) Particle size characterization of nanoparticles – a practical approach. *Iranian Journal of Materials Science and Engineering,* 8: 48-57.

Akhtar MF, Hanif M & Ranjha NM (2016) Methods of synthesis of hydrogels … A review. *Saudi Pharmaceutical Journal*, 24: 554-559.

Akpabio EA (2012) *Formulation and evaluation of drug delivery systems for the administration of ciprofloxacin hydrochloride to the female genital tract*, PhD, University of Nigeria, Nsukka Nigeria: 11.

Alexander NJ, Baker E, Kaptein M, Karck U, Miller L & Zampaglione E (2004) Why consider vaginal drug administration? *Fertility and Sterility,* 82: 1-12.

Ali H & Singh SK (2018) Preparation and characterization of solid lipid nanoparticles of furosemide using quality by design. *Particulate Science and Technology,* 36: 695-709.

Aljaed BM & Hosny KM (2016) Miconazole-loaded solid lipid nanoparticles: formulation and evaluation of a novel formula with high bioavailability and antifungal activity. *International Journal of Nanomedicine*, 44: 441-447.

Almeida H, Amaral MH & Lobao P (2012) Temperature and pH stimuli-responsive polymers and their applications in controlled and selfregulated drug delivery. *Journal of Applied Pharmaceutical Science,* 2: 01-10.

Almeida M, Magalhaes M, Veiga F & Figueiras A (2018) Poloxamers, poloxamines and polymeric micelles: Definition, structure and therapeutic applications in cancer. *Journal of Polymer Research,* 25: 1-14.

Almomen A, Cho S, Yang CH, Li Z, Jarboe EA, Peterson CM, Huh KM & Janat-Amsbury MM. (2015) Thermosensitive Progesterone Hydrogel: A Safe and Effective New Formulation for Vaginal Application. *Pharmaceutical Research,* 32: 2266-2279.

Alomar MJ (2014) Factors affecting the development of adverse drug reactions (Review article). *Saudi Pharmaceutical Journal,* 22: 83-94.

Alves T, Souza J, Rebelo M, Pontes K, Santos C, Lima R, Jozala A, Grotto D, Severino P, Rai M & Chaud M (2018) Formulation and evaluation of thermoresponsive polymeric blend as a vaginal controlled delivery system. *Journal of Sol-Gel Science and Technology,* 86: 536-552.

Amanolahi F, Mohammadi A, Oskuee RK, Nassirli H & Malaekeh-Nikouei B (2017) A simple, sensitive and rapid isocratic reversed-phase high-performance liquid chromatography method for determination and stability study of curcumin in pharmaceutical samples. *Avicenna Journal of Phytomedicine*, 7: 444-453.

Amati GD, di Gioia CRT, Proietti Pannunzi L, Pistili D, Carosa E, Lenzi A & Jannini EA (2003) Functional anatomy of the human vagina. *Journal of Endocrinological Investigation,* 26: 92-96.

Anacleto SD, Borges MMC, de Oliveira HL, Vicente A, Fugueiredo EC, de Oliveria MAL, Borges BJP, de Oliveria MA, Borges W & Borges KB (2018) Evaluation of physicochemical properties as supporting information on quality control of raw materials and veterinary pharmaceutical formulations. *Journal of Pharmaceutical Analysis,* 8: 168-175.

Anderson DJ, Marathe J & Pudney J (2014) The Structure of the Human Vaginal Stratum Corneum and its Role in Immune Defense. *American Journal of Reproductive Immunology,* 71: 618-623.

Anderson MJ & Whittcomb PJ (2003) How to Use Graphs to Diagnose and Deal with Bad Experimental Data. *Annual Quality Congress,* Kansas City, MI, 57.

Andonova V & Peneva P (2017) Characterization Methods for Solid Lipid Nanoparticles (SLN) and Nanostructured Lipid Carriers (NLC). *Current Pharmaceutical Design,* 23: 6630-6642.

Andrade AO, Parente ME & Ares G (2014) Screening of mucoadhesive vaginal gel formulations. *Brazilian Journal of Pharmaceutical Sciences,* 50: 931-941.

Andrews GP, Donnelly L, Jones DS, Curran RM, Morrow RJ, Woolfson D & Malcom RK (2009) Characterization of the Rheological, Mucoadhesive, and Drug Release Properties of Highly Structured Gel Platforms for Intravaginal Drug Delivery. *Biomacromolecules,* 10: 2427-2435.

Angotti LB, Lambert LC & Soper DE (2007) Vaginitis: Making Sense of Over-the-Counter Treatment Options. *Infectious Diseases in Obstetrics and Gynecology,* 2007:97424.

Apalata T, Carr WH, Sturm WA, Longo-Mbenza B & Moodley P (2014) Determinants of Symptomatic Vulvovaginal Candidiasis among Human Immunodeficiency Virus Type 1 Infected Women in Rural KwaZulu-Natal, South Africa. *Infectious Diseases in Obstetrics and Gynecology,* 2014: 1-10.

Armbruster DA & Pry T (2008) Limit of Blank, Limit of Detection and Limit of Quantitation. *Clinical Biochemist Reviews,* 29: 49-52.

Arun RJ, Elwin J, Jyoti H & Sreerekha S (2016) Formulation and evaluation of ketoprofen solid dispersion incorporated topical gels. *European Journal of Biomedical and Pharmaceutical Sciences,* 3: 156-164.

Arunachalam A & Shankar M (2013) Stability studies: A review. *Asian Journal of Pharmaceutical Analysis and Medicinal Chemistry,* 1: 184-195.

Ashok V, Kumar RM, Murali D & Chatterjee A (2014) A review on vaginal route as a systemic drug delivery. *Critical review in Pharmaceutical Sciences,* 1: 1-20.

Astefanei A, Dapic I & Camenzuli M (2016) Different Stationary Phase Selectivities and Morphologies for Intact Protein Separations. *Chromatographia,* 80: 665-687.

Attama AA, Schicke BC, Paepenmuller T & Muller-Goymann CC (2007) Solid lipid nanodispersions containing mixed lipid core and a polar heterolipid: characterisation. *European Journal of Pharmaceutics and Biopharmaceutics,* 67: 48-57.

Bagul U, Pisal VV, Solanki NV & Karnavat A (2018) Current Status of Solid Lipid Nanoparticles: A Review. *Modern Application of Bioequivalence & Bioavailability,* 3: 001-010.

Bahari LAS & Hamishehkar H (2016) The Impact of Variables on Particle Size of Solid Lipid Nanoparticles and Nanostructured Lipid Carriers; A Comparative Literature Review. *Advanced Pharmaceutical Bulletin,* 6: 143-151.

Bain MK, Bhowmik M, Maity D, Bera NM, Ghosh S & Chattopadhyah D (2010) Control of thermo reversible gelation of methylcellulose using polyethylene glycol and sodium chloride for sustained delivery of ophthalmic drug. *Journal of Applied Polymer Science,* 118:631-637.

Bajaj S, Singla D & Sakhuja N (2012) Stability Testing of Pharmaceutical Products. *Journal of Applied Pharmaceutical Science,* 2: 129-138.

Bakshi P, Korey A, Fowler W & Banga AK (2018) Development and validation of an HPLC-UV method for analysis of methylphenidate hydrochloride and loxapine succinate in an activated carbon disposal system. *Journal of Pharmaceutical Analysis,* 8: 349-356.

Baloglu E, Karavana SY, Senyigit ZA & Guneri T (2011) Rheological and mechanical properties of poloxamer mixtures as a mucoadhesive gel base. *Pharmaceutical Development and Technology,* 16: 627-639.

Baloglu E, Senyigit ZA, Karavana SY & Bernkop-Schnurch A (2009) Strategies to Prolong the Intravaginal Residence Time of Drug Delivery Systems. *Journal of Pharmaceutical Sciences,* 12: 312-336.

Balouiri M, Sadiki M & Ibnsouda SK (2016) Methods for in vitro evaluating antimicrobial activity: A review. *Journal of Pharmaceutical Analysis,* 6: 71-79.

Ban. E, Park M, Jeong S, Kwon T, Kim EU, Jung K & Kim. A. (2017) Poloxamer-Based Thermoreversible Gel for Topical Delivery of Emodin: Influence of P407 and P188 on Solubility of Emodin and Its Application in Cellular Activity Screening. *Molecules,* 22: 246.

Barnes HA (1999) The yield stress—a review or 'panta roi'—everything flows? *Journal of Non-Newtonian Fluid Mechanics,* 81: 133-178.

Bates RG (1948) Definitions of pH Scales. *Chemical Reviews,* 42: 1-61.

Battaglia L, Gallarate M, Panciani PP, Ugazio E, Sapino S, Peira E & Chirio D (2014). 'Techniques for the preparation of solid lipid nano and microparticles'. Sezer AD (ed.) *Application of Nanotechnology in Drug Delivery,* InTech Open: 51.

Beher SK, Meena H, Chakraborty S & Meikap BC (2018) Application of response surface methodology (RSM) for optimization of leaching parameters for ash reduction from low-grade coal. *International Journal of Mining Science and Technology,* 28: 621-629.

Belal TS & Haggag RS (2012) Gradient HPLC-DAD Stability Indicating Determination of Miconazole Nitrate and Lidocaine Hydrochloride in their Combined Oral Gel Dosage Form. *Journal of Chromatographic Science,* 50: 401-409.

Betts J, Johnson M, Rygiewics P, King G & Andersen C (2013) Potential for metal contamination by direct sonication of nanoparticle suspensions. *Environmental Toxicology and Chemistry,* 32: 889-893.

Betz JM, Brown PN & Roman MC (2011) Accuracy, Precision, and Reliability of Chemical Measurements in Natural Products Research. *Fitoterapia,* 82: 44-52.

Bewick V, Cheek L & Ball J (2005) Statistics review 14: Logistic regression. *Critical Care (London, England),* 9: 112-118.

Bezerra MA, Santelli RE, Oliveira EP, Villar LS & Escaleira LA (2008) Response surface methodology (RSM) as a tool for optimization in analytical chemistry. *Talanta,* 75: 965-977.

Bharat P, Paresh M, Sharma RK, Tekade BW, Thakre VM & Patil VR (2011) A Review: Novel Advances in Semisolid Dosage Forms & Patented Technology in Semisolid Dosage Forms. *International Journal of PharmTech Research,* 3: 420-430.

Bhardwaj A & Kumar L (2011) Colloidal drug delivery systems: A future prospective treatment of tuberculosis. *American Journal of PharmTech Research,* 1: 102-123.

Bhardwaj SA, Dwivedi K & Agarwal DD (2015) A Review: HPLC Method Development and Validation. *International Journal of Analytical and Bioanalytical Chemistry*, 5: 76-81.

Bhat SR & Shivakumar HG (2010) Bioadhesive controlled release clotrimazole vaginal tablets. *Tropical Journal of Pharmaceutical Research,* 9: 339-346.

Bhattacharjee S (2016) DLS and zeta potential – what they are and what they are not? *Journal of Controlled release,* 235: 337-351.

Bhowmik D, Gopinath H, Kumar BP, Duraivel S & Sampath Kumar KP (2012) Controlled Release Drug Delivery Systems. *The Pharma Innovation,* 1: 24-33.

Bhoyar N, Giri TK, Tripathi DK, Alexander A & Ajazuddin A (2012) Recent Advances in Novel Drug Delivery System through Gels: Review. *Journal of Pharmacy and Allied Health Sciences,* 2: 21-39.

Biju SS, Talegaonkar S, Mishra PR & Khar RK (2006) Vesicular systems: An overview. *Indian Journal of Pharmaceutical Sciences,* 68: 141-153.

Bisht R, Rupenthal ID, Sreebhavan S & Jaiswal JK (2017) Development of a novel stability indicating RP-HPLC method for quantification of Connexin43 mimetic peptide and determination of its degradation kinetics in biological fluids. *Journal of Pharmaceutical Analysis,* 7: 365-373.

Bisschop MPL, Merkus JMW, Scheygrond H, Van Cutsem J & Van de Kuy A (1979) Treatment of vaginal candidiasis with ketoconazole a new orally active antimycotic. *European Journal of Obstretics, Gynaecology, Reproduction Biology*, 9: 253-259.

Bitew A & Abebaw Y (2018) Vulvovaginal candidiasis: species distribution of Candida and their antifungal susceptibility pattern. *BioMed Central Women's Health*, 18: 94-104.

Bjorn A, de La Monja PS, Karlsson A, Ejlertson J & Svensson BH (2012) 'Chapter 2'. *Rheological Characterization*. InTech Open Access Publisher.

Blessy M, Patel RD, Prajapati PN & Agrawal YK (2014) Development of forced degradation and stability indicating studies of drugs—A review. *Journal of Pharmaceutical Analysis,* 4: 159-165.

Boddupalli BM, Mohammed ZNK, Nath RA & Banji D (2010) Mucoadhesive drug delivery system: An overview. *Journal of Advanced Pharmaceutical Technology and Research,* 1: 381-387.

Bodratti AM & Alexandridis P (2018) Formulation of poloxamers for drug delivery. *Journal of Functional Biomaterials,* 9: 1-24.

Bondaryk M, Kurzatkowski W & Staniszewsk M (2013) Antifungal agents commonly used in the superficial and mucosal candidiasis treatment: mode of action and resistance development. *Advances in Dermatology and Allergology,* 30: 293–301.

Bongomin F, Gago S, Oladele RO & Denning DW (2017) Global and Multi-National Prevalence of Fungal Diseases—Estimate Precision. *Journal of Fungi,* 3: 57-86.

Boonen J, D'hondt M, Veryser L, Peremans K, Burvenich C & de Spiegeleer B (2013) A critical quality parameter in quantitative fused-core chromatography: The injection volume. *Journal of Pharmaceutical Analysis,* 3: 330-334.

Bora A, Deshmunk S & Swain K (2014) Recent advances in semisolid dosage form. *International Journal of Pharmaceutical Sciences and Research,* 5: 3954-3608.

Brahmbhatt D (2017) Bioadhesive drug delivery systems: Overview and recent advances. *International Journal of Chemical and Life Sciences*, 6: 2016-2024.

Brar SK & Verma M (2011) Measurement of nanoparticles by light-scattering techniques. *Trends in Analytical Chemistry,* 30: 4-18.

Bratolli M, de Gennaro G, de Pinto V, Loiotille AD, Lovascio S, Penza M (2011) Odour detection methods: olfactometry and chemical sensors. *Sensors,* 11: 5290-5322.

British Pharmacopeia Commission (2014) [CD-ROM] *The British Pharmacopeia* 2014. London United Kingdom, The Stationary Office.

Brockel U, Meier W & Wagner G (2013) 'Experimental methods of rheology'. *Product Design and Engineering: Formulation of Gels and Pastes,* Wiley and Sons: 251.

Brown CK, Friedel HD, Barker AR, Buhse LF, Keitel S, Cecil TI, Kraemer J, Michael Morris J, Reppas C, Stickelmeyer P, Yomota C & Shah VP (2011) *Indian Journal of Pharmaceutical Sciences,* 73: 338-353.

Bynan R, Khan I, Ehtezazi T, Saleem I & Gordon S (2018) Surfactant Effects on Lipid-Based Vesicles Properties. *Journal of Pharmaceutical Sciences,* 107: 1237-1246.

Cabral ME, Ramos AN, Caberra CA, Valdez JC & Gonzalez SN (2014) Equipment and method for in vitro release measurements on topical dosage forms. *Pharmaceutical Development and Technology,* 20: 1-7.

Caramella CM, Rossi S, Ferrari F, Bonferoni MC & Sandri G (2015) Mucoadhesive and thermogelling systems for vaginal drug delivery. *Advanced Drug Delivery Reviews,* 92: 39-52.

Cardot JM, Chaumont C, Dubray C, Costantini D & Aiache JM (2004) Comparison of the pharmacokinetics of miconazole after administration via a bioadhesive slow release tablet and an oral gel to healthy male and female subjects*. British Journal of Clinical Pharmacology,* 58: 345-351.

Carley KM, Kamneva NY & Reminga J (2004) Response Surface Methodology - CASOS Technical Report. *Standard Form,* 298: 8-95.

Carr PW, Doherty RM, Kamlet MJ, Taft RW, Melander W & Horvath C (1986) Study of temperature and mobile-phase effects in reversed-phase high-performance liquid chromatography by the use of the solvatochromic comparison method. *Analytical Chemistry,* 58: 264-2680.

Carr PW, wang X & Stoll DR (2009) The Effect of Pressure, Particle Size and Time on Optimizing Performance in LC. *Analytical Chemistry,* 81: 5342-5353.

Cavrini V, Pietra AM & Gatti R (1989) Analysis of miconazole and econazole in pharmaceutical formulations by derivative UV spectroscopy and liquid

chromatography (HPLC). *Journal of Pharmaceutical and Biomedical Analysis,* 1989: 1535-1543.

Centres for Disease Control and Prevention (2015) Vulvovaginal Candidiasis. *Sexually Transmitted Diseases Treatment Guidelines,* 2015: 1-137.

Chakraborty T, Saini V, Sharma S, Kaur B & Dhingra G (2014) Antifungal gel: for different routes of administration and different drug delivery system. *International Journal of Biopharmaceutics,* 5: 230-240.

Challener. C. (2018) Selecting Excipients for Controlled Release. *Pharmaceutical Technology,* 42: 24-26.

Chambin O, Champion D, Debray C, Rochat-Gonthier MH, Le Meste M & Pourcelot Y (2004) Effects of different cellulose derivatives on drug release mechanism studied at a preformulation stage. *Journal of Controlled Drug release,* 20: 101-108.

Chashoo G, Singh SK, Qazi NA & Saxena AK (2012) Nanoparticle Based Drug Delivery System: Milestone for Cancer Therapy. *Journal of Biomedical and Pharmaceutical Research,* 1: 1-6.

Chaterji S, Kwon IK & Park K (2008) Smart Polymeric Gels: Redefining the Limits of Biomedical Devices. *Progress in Polymer Science,* 32: 1083-1122.

Chatterjee A, Bhowmik BB & Kumar L (2008) An overview of intra-vaginal drug delivery system. *Journal of Pharmacy Research,* 2: 698-700.

Chatterjee B, Amalina N, Sengupta P & Mandal UK. (2017) Mucoadhesive Polymers and Their Mode of Action: A Recent Update. *Journal of Applied Pharmaceutical Science,* 7: 195-203.

Chauhan A, Mittu B & Chauhan P (2015) Analytical Method Development and Validation: A Concise Review. *Journal of Analytical & Bioanalytical Techniques,* 6: 233-244.

Chen DTN, Wen Q, Janmey PA, Crocker JC & Yodh AG (2010) Rheology of Soft Materials. *Annual Reviews,* 2010: 301-322.

Chen MX, Alexander KS & Baki G (2016) Formulation and Evaluation of Antibacterial Creams and Gels Containing Metal Ions for Topical Application. *Journal of Pharmaceutics,* 2016: 10-20.

Chhabra A & Singh G (2011) The Framework for Performance Modeling and Evaluation of Parallel Job Scheduling Algorithms. *International Journal of Computer Applications,* 34: 30-39.

Chhabra RP (2010) Non-Newtonian fluids: An introduction. *SERC School-cum-Symposium on Rheology of Complex Fluids,* Kanpar, Indian Institute of Technology: 4.

Chillistone S & Hardman JG (2017) Factors affecting drug absorption and distribution. *Anaesthesia & Intensive Care Medicine*, 18: 335-339.

Chirani N, Yahia L, Gritsch L, Motta FL, Chirani S & Fare S (2015) history and Applications of Hydrogels. *Journal of Biomedical Sciences,* 4: 1-25.

Claessens HA (1999) 'Chapter 2: Synthesis, Retention Properties and Characterization of Reversed-Phase Stationary Phases'. *Characterization of Stationary Phases for Reversed-phase Liquid Chromatography: Column Testing, Classification and Chemical Stability,* Eindhoven: Technische Universiteit: 7-27.

Cledera-Castro M, Santos-Montes A, Izquierdo-Hornillos R & Gonzalo-Lumbreras R (2007) Comparison of the performance of different reversed-phase columns for liquid chromatography separation of 11 pollutant phenols. *Journal of Separation Science,* 30: 699-707.

Cope JE (1980) Mode of action of Miconazole on Candida albicans: Effect on Growth, Viability and K^+ release. *Journal of General Microbiology,* 119: 245-251.

Coskun O (2016) Separation techniques: Chromatography. *Northern Clinics of Istanbul,* 3: 156-160.

Crawford Scientific (2017) Reversed Phase Chromatography. *LCGC's ChromAcademy*: 12.

Curcio M, Pouci F, Spizzirri UC, Iemma F, Cirillo G, Parisi OI & Picci N (2010) Negative Thermo-responsive Microspheres Based on Hydrolyzed Gelatin as Drug Delivery Device. *AAPS PharmSciTech,* 1: 652-662.

Czaplicki J (2013) 'Chapter 4: Chromatography in Bioactivity Analysis of Compounds'. *Column Chromatography,* InTech Open: 102.

D'Souza S (2014) A Review of In Vitro Drug Release Test Methods for Nano-Sized Dosage Forms. *Advances in Pharmaceutics,* 2014: 304757.

Danaei M, Dehghankhold M, Ataei S, Hasanzadeh Davarani F, Javanmard R, Dokhani A, Khorasani S & Mozafari MR (2018) Impact of Particle Size and Polydispersity Index on the Clinical Applications of Lipidic Nanocarrier Systems. *Pharmaceutics,* 10: 1-17.

Dandamudi S (2017) In Vitro Bioequivalence Data for a Topical Product: Bioequivalence Review Perspective. *FDA Public Workshop Topical*

Dermatological Generic Drug Products: Overcoming Barriers to Development and Improving Patient Access, 2017: 1-37.

Daneshmend TK (1986) Systemic absorption of miconazole from the vagina. *The Journal of Antimicrobial Chemotherapy,* 18: 507-511.

Das S & Chaudhury A (2010) Recent Advances in Lipid Nanoparticle Formulations with Solid Matrix for Oral Drug Delivery. *America Association of Pharmaceutical Sciences PharmSciTech,* 12: 62-79.

Dash S, Narasimha P, Nath L & Chowdhury P (2010) Kinetic modelling on drug release from controlled drug delivery systems. *Acta Poloniae Pharmaceutica,* 67: 217-223.

Dayyih WA, Al Saadi N, Hamad M, Mallah E, Matalka K & Arafat T (2012) Development and validation of hplc method for some azoles in pharmaceutical preparation. *International Journal of Pharmaceutical Sciences and Research,* 3: 3686-3692.

de Campos ML, Padilha EC & Peccinini RG (2014) A review of pharmacokinetic parameters of metabolites and prodrugs. *Drug Metabolism Letters,* 7: 105-116.

de Souza-Ferreira SB, Moco TD, Borghi-Pangoni FB, Junqueira MN & Bruschi ML (2015) Rheological, mucoadhesive and textural properties of thermoresponsive polymer blends for biomedical applications. *Journal of the Mechanical Behaviour of Biomedical Materials,* 55: 164-178.

de Zan MM, Camara MS, Robles JC, Kergaravat SV & Goicoechea. HC (2009) Development and validation of a simple stability-indicating high performance. *Talanta*, 79: 762-767.

Deangelis NJ & Papariello GJ (1968) Differential Scanning Calorimetry: Advantages and Limitations for Absolute Purity Determinations. *Journal of Pharmaceutical Sciences,* 57: 1868-1873.

Denning DW, Kneale M, Sobel JD & Rautemaa-Richardson R (2018) Global burden of recurrent vulvovaginal candidiasis: a systematic review. *The Lancet Infectious Diseases,* 18: 339-347.

Desai MP, Labhasetwar V, Walter E, Levy RJ & Amidon GL (1997) The mechanism of uptake of biodegradable microparticles in Caco-2 cells is size dependent. *Pharmaceutical Research,* 14: 1568-1573.

Desbrieres J, Hirrien M & Ross-Murphy SB (2000) Thermogelation of methylcellulose: Rheological considerations. *Polymer,* 41: 2451-2461.

Deshkar SS, Patil AT & Poddar SS (2015) Development of thermosensitive gel of fluconazole for vaginal candidiasis. *International Journal of Pharmacy and Pharmaceutical Sciences,* 8: 391-398.

Devi DR, Sandhya P & Hari V (2013) Poloxamer: A Novel Functional Molecule for Drug Delivery And Gene Therapy. *Journal of Pharmaceutical Sciences and Research,* 5: 159-165.

Dobaria N, Mashru R & Vadia NH (2007) Vaginal drug delivery systems*. East and Central African Journal of Pharmaceutical sciences,* 3: 3-13.

Dodou K (2018) 'Chapter 41. 'Rectal and vaginal drug delivery'. Aulton ME & Taylor KMG (ed.) *Aulton's Pharmaceutics: The Design and Manufacture of Medicines,* 5ed, Elsevier: 750.

Dong MW & Guillarme D (2017) UHPLC, Part II: Benefits. *LCGC North America,* 35: 486-495.

Dorraj G & Moghimi HR (2015) Preparation of SLN-containing Thermoresponsive In-situ Forming Gel as a Controlled Nanoparticle Delivery System and Investigating its Rheological, Thermal and Erosion Behavior. *Iranian Journal of Pharmaceutical Research,* 14: 347-358.

Dresser LD & Brown TR (2014) 'Chapter 98. Superficial Fungal Infections'. DiPiro JT (ed.) *Pharmacotherapy: A pathophysiologic Approach,* 9ed, New York, McGraw-Hill.

Dumortier G, Grossiord JL & Agnely F (2006) A Review of Poloxamer 407 Pharmaceutical and Pharmacological Characteristics. *Pharmaceutical Research,* 23: 2709-2728.

Dutka M, Dataranto M & Lovas T (2015) Application of a Central Composite Design for the Study of NOx Emission Performance of a Low NOx Burner. *Energies,* 2015: 3606-3627.

Echeverria C, Fernandes S, Godinho MH, Borges JP & Soares PL (2018) Functional stimuli-responsive gels: hydrogels and microgels. *Gels,* 4: 1-37.

Edwards D & Panay N (2016) Treating vulvovaginal atrophy/genitourinary syndrome of menopause: how important is vaginal lubricant and moisturizer composition? *Climacteric,* 19: 151-161.

Ekambaram P, Sathali AH & Priyanka K (2011) Solid lipid nanoparticles: A review. *Journal of Scientific Reviews and Chemical communications,* 2: 80-102.

El-Garhy OH (2013) Investigating the potential of polyethylene glycols in solubilization of imidazole drugs of interest. *International Journal of Pharmacy and Pharmaceutical Sciences,* 5: 266-272.

Emami J, Mohiti H, Hamishehkar H & Varshosaz J (2015) Formulation and optimization of solid lipid nanoparticle formulation for pulmonary delivery of budesonide using Taguchi and Box-Behnken design. *Research in Pharmaceutical Sciences,* 10:17-33.

Emeribe A, Abdullahi NI, Onyia J & Ifunanya AL (2015) Prevalence of vulvovaginal candidiasis among non-pregnant women attending a tertiary health care facility in Abuja, Nigeria. *Dove Press Journal: Research and Reports in Tropical medicine*, 2015: 37-42.

Ensign LM, Hoen T, Maisel K, Cone R & Hanes J (2013) Enhanced vaginal drug delivery through the use of hypotonic formulations that induce fluid uptake. *Biomaterials,* 34: 6922-6929.

Esmaeilzadeh-Gharedaghi E, Faramarzi MA, Amini MA, Rouholamini Najafabadi A, Rezayat SM & Amani A (2012) Effects of processing parameters on particle size of ultrasound prepared chitosan nanoparticles: an Artificial Neural Networks Study. *Pharmaceutical Development and Technology,* 17: 636-647.

Fan MD, Kramzer LF, Hillier SL, Chang JC, Meyn LA & Rohan LC (2016) Preferred Physical Characteristics of Vaginal Film Microbicides for HIV Prevention in Pittsburgh Women. *Archive of Sexual behaviour,* 46: 1111-1119.

Faro S (1994) Systemic vs. Topical Therapy for the Treatment of Vulvovaginal Candidiasis. *Infectious Diseases in Obstetrics and Gynecology,* 1: 202-208.

Faro S, Apuzzio J, Bohannon N, Elliot K, Martens MG, Mou SM, Phillipis-Smith LE, Soper DE, Strayer A & Young RL (1997) Treatment Considerations in Vulvovaginal Candidiasis. *The Female Patient,* 22: 1-17.

Fetih D (2010) Meloxicam formulations for transdermal delivery: hydrogels versus organogels. *Journal of Drug Delivery, Science and Technology,* 20: 451-456.

Field A (2016) Linear Model: Looking for bias. *Discovering Statistics,* 2016: 1-17.

Franck A (2016) Understanding Rheology of Structured Fluids. *TA Instruments™,* AAN106, 1-11.

Francois IEJA, Cammue BOA, Borgers M, Ausma J, Dispersyn GD & Thevissen K (2006) Azoles: mode of antifungal action and resistance development effect of miconazole on endogenous reactive oxygen species production in candida albicans. *Anti-Infective Agents in Medicinal Chemistry,* 2006: 1-39.

Fromtling RA (1988) Overview of medically important antifungal azole derivatives. *Clinical Microbiology Reviews,* 1: 187-217.

Fu Y & Kao WJ (2011) Drug Release Kinetics and Transport Mechanisms of Non-degradable and Degradable Polymeric Delivery Systems. *Expert Opinion on Drug Delivery,* 7: 429-444.

Galindo-Rosales FJ, Alves MA & Oliveira MSN (2012) Microdevices for extensional rheometry of low viscosity elastic liquids: a review. *Microfluid Nanofluid,* 14: 1-19.

Gandra S (2013) *The Preparation and Characterization of Poloxamer-Based Temperature-Sensitive Hydrogels for Topical Drug Delivery*, MSc, University of Toledo, United States: 6.

Ganesan P & Narayanasamy D (2017) Lipid nanoparticles: Different preparation techniques, characterization, hurdles, and strategies for the production of solid lipid nanoparticles and nanostructured lipid carriers for oral drug delivery. *Sustainable Chemistry and Pharmacy,* 6: 37-56.

Garg RK & Singhvi I (2015) Optimization techniques: an overview for formulation development. *Asian Journal of Pharmaceutical Research,* 5: 217-221.

Garud A, Singh D & Garud N (2012) Solid Lipid Nanoparticles (SLN): Method, Characterization and Applications. *International Current Pharmaceutical Journal,* 1: 384-393.

Gaumet M, Vargas A, Gurny R, Delie F (2008) Nanoparticles for drug delivery: the need for precision in reporting particle size parameters. *European Journal of Pharmaceutics and Biopharmaceutics,* 69: 1-9.

Gelperina S, Kisich K, Iseman MD & Heifets L (2005) The Potential Advantages of Nanoparticle Drug Delivery Systems in Chemotherapy of Tuberculosis. *American Journal of Respiratory and Critical Care Medicine,* 172: 1487-1490.

Gerk MP, Yu ABC & Shargel L (2016) 'Physiologic Factors related to drug absorption', Geric PM, Shargel L & Yu ABC (ed.) *Applied Biopharmaceutics & Pharmacokinetics,* 7ed, New York, McGraw-Hill.

Ghannoum MA & Rice LB (1999) Antifungal Agents: Mode of Action, Mechanisms of Resistance, and Correlation of These Mechanisms with Bacterial Resistance. *Clinical Microbiology Reviews,* 12: 501-517.

Ghasemi A & Zahediasi S (2012) Normality Tests for Statistical Analysis: A Guide for Non-Statisticians. *International Journal of Endocrinology and Metabolism,* 102: 486-489.

Gigg RH (2018) ‘Lipid’. In *AccessScience,* Chicago, McGraw-Hill Education.

Gill P, Moghadam TT & Ranjbar B (2010) Differential Scanning Calorimetry Techniques: Applications in Biology and Nanoscience. *Journal of Biomolecular Techniques*, 21:167–193.

Gillar M, Jaworski A, McDonald TS (2014) Solvent selectivity and strength in reversed-phase liquid chromatography separation of peptides. *Journal of Chromatography A,* 1337: 140-146.

Giuliano E, Paolino D, Fresta M & Cosco D (2018) Mucosal Applications of Poloxamer 407-Based Hydrogels: An Overview. *Pharmaceutics,* 10: 1-26.

Goins AB, Sanabria H & Waxham MN (2008) Macromolecular Crowding and Size Effects on Probe Microviscosity. *Biophysical Journal,* 95: 5362-5373.

Gong C, Qi T, Wei X, Qu Y, Wu Q, Luo F& Qian Z (2013) Thermosensitive polymeric hydrogels as drug delivery systems. *Journal of Current Medicinal Chemistry*, 20: 79-94.

Good D & Wu Y (2017) ‘Excipient characterisation’. Koo OMY (ed.) *Pharmaceutical excipients: Properties, Functionality, and Applications in Research and Industry,* New Jersey, John Wiley and Sons: 13.

Govind C (2016) Vulvovaginal Candidiasis. *Pathologists Lancet Laboratories,* 2016: 1-2.

Graham NB & McNeill ME (1984) Hydrogels for controlled drug delivery. *Biomaterials,* 5: 27-36.

Granstrom M (2009) *Cellulose Derivatives: Synthesis, Properties and Applications*, MSc, University of Helsinki, Finland: 13.

Grassi M & Grassi G (2005) Mathematical modelling and controlled drug delivery: matrix systems. *Current Drug Delivery,* 2: 97-116.

Grodowska K & Parczewski A (2010) Organic solvents in the pharmaceutical industry. *Acta Poloniae Pharmaceutica,* 67: 3-12.

Groll AH, Piscitelli SC & Walsh TJ (1998). Clinical Pharmacology of Systemic Antifungal agents: A Comprehensive Review of Agents in Clinical Use, Current Investigational Compounds, and Putative Targets for Antifungal Drug Development., *Advances in Pharmacology*, 44: 343-500.

Guillarme D, Ruta J, Rudaz S & Veuthey JL (2010) New trends in fast and high-resolution liquid chromatography: a critical comparison of existing approaches. *Analytical and Bioanalytical Chemistry,* 397: 1069-1082.

Guillaume YC & Peyrin E (2000) Optimising mobile phase composition, its flow-rate and column temperature in HPLC using taboo search. *Talanta,* 51: 576-586.

Gunasekaran T, Haile T, Nigusse T & Dhanaraju MD (2014) Nanotechnology: an effective tool for enhancing bioavailability and bioactivity of phytomedicine. *Asian Pacific Journal of Tropical Biomedicine,* 1: 1-7.

Gupta S, Kesarla R, Chotai N & Omri A (2017) Development and validation of reversed-phase HPLC gradient method for the estimation of efavirenz in plasma. *Plos One,* 2017: 1-12.

Hainer BL & Gibson MV (2011) Vaginitis: Diagnosis and Treatment. *American Family Physician,* 83: 807-815.

Hamm LL, Nakhoul N & Hering-Smith KS (2015) Acid-Base Homeostasis. *Clinical Journal of the American Society of Nephrology,* 10: 2232-2242.

Hao J, Fang X, Zhou Y, wang J, Guo F, Li F & Peng X (2011) Development and optimization of solid lipid nanoparticle formulation for ophthalmic delivery of chloramphenicol using a Box-Behnken design. *International Journal of Nanomedicine,* 2011: 683-692.

Harde H, Das M & Jain S (2014) Solid lipid nanoparticles: an oral bioavailability enhancer vehicle. *Expert Opinion on Drug Delivery,* 8: 1407-1424.

Hassan BAR (2012) HPLC Uses and Importance in the Pharmaceutical Analysis and Industrial Field. *Pharmaceutica Analytica Acta,* 3: 9.

Haya J, Garcia A, Lopez-Manzanara C, Balawi M & Haya L (2014) Importance of Lactic Acid in Maintaining Vaginal Health: A Review of Vaginitis and Vaginosis Etiopathogenic Bases and a Proposal for a New Treatment. *Open Journal of Obstetrics and Gynecology,* 4: 787-799.

Haywood A & Glass BD (2011) Pharmaceutical excipients – where do we begin? *Australian Prescriber,* 34: 112-114.

He J, Han Y, Xu G, Yin L, Neubi N, Zhou J & Ding Y (2017) Preparation and evaluation of celecoxib nanosuspensions for bioavailability enhancement. *Royal Chemistry Society Advances,* 2017: 13053–13064.

He X, Kadomura S, Takekuma Y, Sugawara M & Miyazaki K (2003) A new system for the prediction of drug absorption using a pH-controlled Caco-2 model: Evaluation

of pH-dependent soluble drug absorption and pH-related changes in absorption. *Journal of Pharmaceutical Sciences,* 93: 71-78.

Heinisch R & Rocca JL (2004) Effect of mobile phase composition, pH and buffer type on the retention of ionizable compounds in reversed-phase liquid chromatography: application to method development. *Journal of Chromatography A,* 1048: 183-193.

Hela M (2012) 'Stability'. *Registration of Medicines,* South Africa, Medicines Control Council: 3.

Hermawan D, Sulaeman SU, Istiqomah A & Aboul-Enein HY (2017) Development of high performance liquid chromatography method for miconazole analysis in powder sample. *IOP Conference Series: Materials Science and Engineering,* 172: 1-7.

Hicks SRJ (2012) Forced degradation to develop stability indicating methods. *Pharmaceutical Outsourcing,* 13: 1.

Hildago JA & Vazquez JA (2018) Candidiasis Treatment & Management. *WebMD Medical Reference,* 2018.

Hirai M, Kimura R, Takeuchi K, Hagiwara Y, Kawai-Hira R, Ohta N, Igarashi N & Shimuzu N (2013) Structure of liposome encapsulating proteins characterized by X-ray scattering and shell-modelling. *Journal of Synchroton radiation,* 20: 869-874.

Ho DX & Kim KH (2011) Effect of HPLC binary mobile phase composition on the analysis of carbonyls. *Environmental Monitoring and Assessment,* 180: 163-176.

Huber L (2007) *Validation of Analytical Methods: Validation and Qualification in Analytical Laboratories,* 2nd Edition, New York, InformaHealthcare: 125. ,

Hurler J, Engesland A & Kermany P (2012) Improved texture analysis for hydrogel characterisation: Gel cohesiveness, adhesiveness and hardness. *Journal of Applied Polymer Sciences,* 125: 180-188.

Hussain A & Ahsan F (2005) The vaginal as a route for systemic drug delivery. *Journal of Controlled Release,* 103: 301-313.

ICH Harmonised Tripartite Guideline Q1A(R2) (2003) 'Stability testing of new drug substances and products'. *International Conference on Harmonisation (ICH) of Technical Requirements for Registration of Pharmaceuticals for Human Use,* 2003.

ICH Harmonised Tripartite Guideline Q1B (1996) 'Stability testing: Photostability testing of new drug substances and products'. *International Conference on*

Harmonisation (ICH) of Technical Requirements for Registration of Pharmaceuticals for Human Use, 1996.

ICH Harmonised Tripartite Guideline Q2(R1) (1994), 'Validation of Analytical Procedures: Text and Methodology', *International Conference on Harmonisation (ICH) of Technical Requirements for Registration of Pharmaceuticals for Human Use,* 2005.

Iram F, Iram H, Iqbal A & Hussain A (2016) Force degradation studies. *Journal of Analytical and Pharmaceutical Research,* 3: 1-5.

IUPAC (1997) 'Solubility'. McNaught AD & Wilkison A (ed.) *Compendium of Chemical Terminology,* Oxford, Blackwell Scientific Publications: 2214.

Jadhav SM, Morey P, Karpe M & Kadam V (2011) Novel vesicular system: An overview. *Journal of Applied Pharmaceutical Science*, 2: 193-202.

Jain S, Jain S, Khare P, Gulbake A, Bansal D & Jain S (2009) Design and development of solid lipid nanoparticles for topical delivery of an anti-fungal agent. *Drug Delivery,* 17: 443-451.

Jain S, Jain V & Mahajan SC (2014) Lipid based vesicular drug delivery systems. *Advances in Pharmaceutics,* 2014: 1-12.

Jalwal P, Singh B * Singh S (2018) A comprehensive review on sustained release drug delivery systems. *The Pharma Innovation,* 7: 349-352.

Jandera P & Hajek T (2017) Mobile phase effects on the retention on polar columns with special attention to the dual hydrophilic interaction–reversed-phase liquid chromatography mechanism - a review. *Journal of Separation Science,* 41: 145-162.

Jandera P (2002) Comparison of reversed-phase and normal-phase column liquid chromatographic techniques for the separation of low and high molecular weight compounds. *Journal of Liquid Chromatography & Related Technologies,* 25: 2901-2931.

Janmey PA & Schilwa M (2010) Rheology. *Current Biology,* 18: 639-641.

Jawahar N & Meyyanathan SN (2012) Polymeric nanoparticles for drug delivery and targeting: A comprehensive review. *International Journal of Health & Allied Sciences,* 1: 217-223.

Jian. S, Sandhu PS, Malvi R & Gupta B (2013) Cellulose Derivatives as Thermoresponsive Polymer: An Overview. *Journal of Applied Pharmaceutical Science,* 3: 139-144.

Jin J, Sklar GE, Oh VMS & Li SC (2008) Factors affecting therapeutic compliance: A review from the patient's perspective. *Therapeutics and Clinical Risk Management,* 4: 269-286.

Joglekar A, Rhodes CT & Danish M (2008) Preferences of Women for Use of Intravaginal Medications. *Drug Development and Industrial Pharmacy,* 17: 2103-2114.

Johal HS, Garg T, Rath G & Goyal AK (2016) Advanced topical drug delivery system for the management of vaginal candidiasis. *Drug delivery: oral and transdermal drug delivery,* 23: 550-563.

Johari O (1968) Comparison of Transmission Electron Microscopy and Scanning Electron Microscopy of Fracture Surfaces. *Journal of Minerals,* 6: 26-32.

Johnson TC (2018) Is OTC Treatment OK for a Vaginal Yeast Infection? *WebMD Medical Reference,* 2018.

Jorgensen JH & Ferraro MJ (1998) Antimicrobial Susceptibility Testing: General Principles and Contemporary Practices. *Clinical Infectious Diseases*, 26: 973-980.

Jorgensen JH, Redding JS, Maher LA & Howell AW (1987) Improved Medium for Antimicrobial Susceptibility Testing of Haemophilus influenza. *Journal of Clinical Microbiology,* 1978: 2015-2113.

Joseprakash D, Somasundaram I, .Ravichandiran V, Kausalya J, Rupenagunta A & Senthilnathan B (2011) Preparation and characterization of solid lipid nanoparticles loaded with imadapril. *Journal of Pharmacy Research,* 4: 1620-1625.

Joshi VS, Kumar V & Rathore AS (2015) Role of Organic Modifier and Gradient Shape in RP-HPLC Separation: Analysis of GCSF Variants. *Journal of Chromatographic Science,* 53: 417-423.

Jug M, Hafner A, Lovric J, Kregar ML, Pepic I, Vanic Z, Cetina-Cizmek B & Filipovic-Grcic J (2017) In vitro dissolution/release methods for mucosal delivery systems. *ADMET & DMPK,* 5: 173-183.

Julio TA, Zamara IG, Garcia JS & Trevisan MG (2014) Compatibility of sildenafil citrate and pharmaceutical excipients by thermal analysis and lc-uv. *Journal of Thermal Analysis and Calorimetry,* 49: 645-652.

Kadam SV, Shinkar DM & Saudagar RB (2013) Review on solubility enhancement techniques. *International Journal of Pharmacy and Biological Sciences,* 3: 462-475.

Kadjo AF, Liao H & Dasgupta PK (2017) Width Based Characterization of Chromatographic Peaks: Beyond Height and Area. *Analytical Chemistry,* 89: 3893-3900.

Kah M & Brown CD (2008) LogD: lipophilicity for ionisable compounds. *Chemosphere,* 72: 1401-1408.

Kakar S, Singh R & Semwal A (2014) Drug release characteristics from dosage forms: a review. *Journal of Coastal Life Medicine,* 2: 332-336.

Kale VV & Ubgade A (2013) Vaginal Mucosa – A Promising Site for Drug Therapy. *British Journal of Pharmaceutical Research,* 3: 983-1000.

Kaminsky M & Willigan DA (1982) pH and the potential irritancy of douche formulations to the vaginal mucosa of the albino rabbit and rat. *Food and Chemical Toxicology,* 20: 193-196.

Kanfer I, Rath S, Purazi P &.Mudyahoto N (2017) In vitro release testing of semi-solid dosage forms. *Dissolution Technologies,* 24: 52-60.

Kankala RK, Zhang YS, Wang SB, Lee CH & Chen AZ (2017) Supercritical fluid technology: an emphasis on drug delivery and related biomedical application. *Advanced Health Care Materials,* 2017: 1-31.

Kao LS & Green CE (2008) Analysis of Variance: Is There a Difference in Means and What Does It Mean? *Journal of Surgical Research,* 144: 158-170.

Kaplan YC, Koren G & Bozzo P (2015) Fluconazole exposure during pregnancy. *Canadian Family Physician,* 61: 685-686.

Karoyo AH & Wilson LD (2017) Physicochemical Properties and the Gelation Process of Supramolecular Hydrogels: A Review. *Gels,* 3: 1-18.

Kasongo KW, Pardeike J, Muller RH & Walker RB (2011) Selection and characterisation of suitable lipid excipients for use in the manufacture of didanosine-loaded solid lipid nanoparticles and nanostructured lipid carriers. *Journal of Pharmaceutical Sciences,* 100: 5158-5196.

Kaul N, Agrawal H, Paradkar AR & Mahadik KR (2005) The ICH Guidance in Practice: Stress Degradation Studies on Stavudine and Development of a Validated Specific Stability-Indicating HPTLC Assay Method. *Journal of Chromatographic Science,* 43: 406-415.

Kaur A, Kaur R, Jaiswal S & Gupta GD (2016) Mucoadhesive vaginal drug delivery system: An overview. *Indo American Journal of Pharmaceutical Research,* 6: 6325-6333.

Kazakevich Y & Lobrutto R (2007) '3: Stationary Phases'. Kazakevich Y & Lobrutto R (ed.) *HPLC for Pharmaceutical Scientists,* John Wiley and Sons: 76.

Kazemian S, Prasad A & Huat BBK (2012) Review of Newtonian and non-Newtonian fluids behaviour in the context of grouts. Viggiani (ed.) *Geotechnical Aspects of Underground Construction in Soft Ground,* London, Taylor and Francis Group, 321-325.

Kazusaki M, Ueda S, Takeuchi N & Ohgami Y (2012) Validation of analytical procedures by high−performance liquid chromatography for pharmaceutical analysis. *Chromatography,* 33: 65-74.

Kenechukwu FC, Attama AA, Ibezim EC, Nnamani PO, Umeyor CE, Uronnachi EM, Momoh A, Akpa PA & Ozioko AC (2018) Novel Intravaginal Drug Delivery System Based on Molecularly PEGylated Lipid Matrices for Improved Antifungal Activity of Miconazole Nitrate. *BioMed Research International,* 2018: 1-18.

Kesharwani R, Nair SK & Patel D (2013) Solid Lipid Nanoparticle (SLN): A Modern Approach for Drug Delivery. *Journal of Pharma Research,* 239: 121-128.

Keshwani B,, Sharma D, Chaterjee A, Jamini M & Arora P (2014) Novel Concepts in Vaginal Drug Delivery. *Journal of Pharma Research,* 3: 184-187.

Keunchkarian S, Reta M, Romero L & Castells C (2006) Effect of sample solvent on the chromatographic peak shape of analytes eluted under reversed phase liquid chromatographic conditions. *Journal of Chromatography A,* 1119: 20-28.

Khadka P, Ro J, Kim H, Kim I, Kim JT, Cho JM, Yun G & Lee J (2014) Pharmaceutical particle technologies: An approach to improve drug solubility, dissolution and bioavailability. *Asian Journal of Pharmaceutical Sciences,* 9: 304-316.

Khan AB & Saha C (2015) A review on vaginal drug delivery system. *Journal of Pharmaceutical Sciences,* 4: 142-147.

Khan AU, Mahmood N & Bazmi AA (2009) Direct comparison between rotational and extrusion rheometers. *Materials Research,* 12: 477-481.

Khatak S & Dureja H (2015) Recent Techniques and Patents on Solid Lipid Nanoparticles as Novel Carrier for Drug Delivery. *Recent Patents on Nanotechnology,* 9:15-177.

Khoshkam R & Afshar M (2014) Validation of a Stability-Indicating RP-HPLC Method for Determination of L-Carnitine in Tablets. *International Scholarly Research Notes,* 2014: 1-7.

Khoshnevisan K & Barkhi M (2015) Information about Zeta Potential. *Zeta Potential,* 2015: 1-9.

Khoza S, Moyo I & Ncube D (2017) Comparative hepatotoxicity of Fuconazole, Ketoconazole, Itraconazole, Terbinafine and Griseofulvin in Rats. *Journal of Toxicology,* 2017: 1-9.

Kim YJ & Matsunaga YT (2017) Thermo-responsive polymers and their application as smart biomaterials. *Journal of Materials Chemistry B,* 5: 4307-4321.

Kirkland JJ, Henderson JW, DeStefano JJ, van Straten MA & Claessens HA (1997) Stability of silica-based, endcapped columns with pH 7 and 11 mobile phases for reversed-phase high-performance liquid chromatography. *Journal of Chromatography A,* 762: 97-112.

Klouda L & Mikos AG (2011) Thermoresponsive hydrogels in biomedical applications - a review. *European Journal of Pharmaceutics and Biopharmaceutics,* 68: 34-45.

Kocen R, Gasik M, Gantar A & Novak S (2017) Viscoelastic behaviour of hydrogel-based composites for tissue engineering under mechanical load. *Biomedical Materials,* 12: 025004.

Kokardekar RR & Mody HR (2011) Solid lipid nanoparticles: A drug carrier system. *Chronicles of Young Scientists,* 2: 26-28.

Korolczuk-Hejnak M (2014) Determination of flow curves on selected steel grades in their liquid state. *Archives of Metallurgy and Materials,* 59: 1553-1559.

Krapf JM (2018) Vulvovaginitis Treatment & Management. *WebMD Medical Reference,* 2018.

Kumar K, Dhawan N, Sharma H, Vaidya S & Vaidya B (2013) Bioadhesive polymers: novel tool for drug delivery. *International Journal of Artificial cells, Nanomedicine and Biotechnology,* 42: 274-283.

Kunin R & McGarvey FX (1962) Ion Exchange Chromatography. *Analytical Chemistry,* 34: 48-50.

Lakshmi DP, Nair R, Chakrapani M & Venkatkrishnakiran P (2012) Solid lipid nanoparticle systems for delivery of drugs to the brain. *International Journal of Biopharmaceutics,* 3: 70-77.

Lalitha MK (2004) *Manual on Antimicrobial Susceptibility Testing.* Indian Association of Medical Microbiologists, Tamil Nadu, India: 5.

Laouini A, Jaafar-Maalej C, Limayem-Blouza I, Sfar S, Charcosset C & Fessi H (2012) Preparation, Characterization and Applications of Liposomes: State of the Art. *Colloid Science and Biotechnology,* 1: 147-168.

Lason E & Ogonowski J (2011) Solid lipid nanoparticles – characteristics, application and obtaining. *Chemik,* 65: 960-967.

Lebherz TB, Goldman L, Wiesmeier E, Mason D & Ford LC (1983) A comparison of the efficacy of two vaginal creams for vulvovaginal candidiasis, and correlations with the presence of Candida species in the perianal area and oral contraceptive use. *Clinical Therapeutics,* 5: 409-416.

Lecaroz C, Gamazo C, Renedo MJ & Blanco-Prieto MJ (2006) Biodegradable micro- and nanoparticles as long-term delivery vehicles for gentamicin. *Journal of Microencapsulation,* 23: 782-792.

Lee PI (1985) Kinetics of drug release from hydrogel matrices. *Journal of Controlled Release,* 2: 277-288.

Levin B & Robbins H (1981) Selecting the highest probability in binomial or multinomial trials. *Proceedings of the National Academy Sciences USA,* 78: 4663-4666.

Li B, Zaveri T, Ziegler GR & Hayes JE (2013) User Preferences in a Carrageenan-Based Vaginal Drug Delivery System. *Plos One*, 8: 54975.

Li Q, Cai T, Huang Y, Xia X, Cole SPC & Cai Y (2017) A Review of the Structure, Preparation, and Application of NLCs, PNPs, and PLNs. *Nanomaterials,* 1: 1-25.

Liebenberg W, Englebrecht E, Wessels A, Devarakonda B, Yang W & De Villiers MM (2003) A Comparative Study of the Release of Active Ingredients from Semisolid Cosmeceuticals Measured with Franz, Enhancer or Flow-Through Cell Diffusion Apparatus. *Journal of Food and Drug Analysis,* 11: 90-102.

Likavcan L, Kosik M, Bilik J & Martinkovic M (2014) Determination of Apparent Viscosity as Function of Shear Rate and Fibres Fraction in Polypropylene. *International Journal of Engineering and Innovative Technology,* 4: 23-26.

Lim CK (1988) Sample preparation for high-performance liquid chromatography in the clinical laboratory. *TrAC Trends in Analytical Chemistry,* 7: 340-345.

Lin CH, Chen CH, Lin ZC & Fang JY (2017) Recent advances in oral delivery of drugs and bioactive natural products using solid lipid nanoparticles as the carriers. *Journal of Food and Drug Analysis,* 25: 219-234.

Liu J (2005) Physical Characterization of Pharmaceutical Formulations in Frozen and Freeze-Dried Solid States: Techniques and Applications in Freeze-Drying Development. *Pharmaceutical Development and Technology,* 11: 3-28.

Luc M, Butler-Wu S & Abbott (2015) *A Comparison of Disc Diffusion and Microbroth Dilution Methods for the Detection of Antibiotic Resistant Subpopulations in Gram Negative Bacilli,* MSc, University of Washington, USA: 20.

Lupo S & Kahler T (2017) New Advice on an Old Topic: Buffers in Reversed-Phase HPLC. *LCGC North America,* 35: 424-433.

Machado RM, Palmeira-de-Oliveira A, Martinez-de-Oliveira J & Palmeira-de-Oliveira R (2013) Vaginal films for drug delivery. *Journal of Pharmaceutical Sciences,* 102: 2069-2081.

Mah E & Ghosh R (2013) Thermo-Responsive Hydrogels for Stimuli-Responsive Membranes. *Processes,* 2013: 283-262.

Maitra. J & Shukla VK (2014) Cross-linking in Hydrogels - A Review. *American Journal of Polymer Science,* 4: 25-31.

Majekodunmi SO (2015) A Review on Centrifugation in the Pharmaceutical Industry. *American Journal of Biomedical Engineering,* 5: 67-78.

Majumdar S and Devi PS (2010) Synthesis of Nanoparticles Using Ultrasonication. *AIP Conference Proceedings,* 1276: 1.

Malakar J, Nayak AK & Goswami S (2012) Use of Response Surface Methodology in the Formulation and Optimization of Bisoprolol Fumarate Matrix Tablets for Sustained Drug Release. *ISRN Pharmaceutics,* 2012: 730624.

Malkin AY & Isayev AI (2017) 'Rheometry *Experimental Methods'. Rheology: Concepts, Methods and Applications,* 3ed, Elsevier: 288.

Malvern Instruments™ (2018) *Automated Protein Characterization with The MPT-2 Autotitrator,* Pharmaceutical Online, 2018.

Mao SR, Wang YZ, Ji HY & Bi DZ (2003) Preparation of solid lipid nanoparticles by microemulsion technique. *Acta Pharmaceutica Sinica,* 38: 624-626.

Marks JA (2015) *Synthesis and Applications of Cellulose Derivatives for Drug Delivery,* PhD, Virginia Polytechnic Institute and State University, United States of America: 7.

Marques-Marinho FD & Vianna-Soares CD (2014) 'Chapter 8: Cellulose and Its Derivatives Use in the Pharmaceutical Compounding Practice'. *Cellulose,* InTech Open: 8.

Martino JL & Vermun SH (2002) Vaginal Douching: Evidence for Risks or Benefits to Women's Health. *Epidemiologic reviews,* 24: 109-124.

Martono S, Febriani I & Rohman A (2017) Application of Liquid Chromatography-Photodiode Array Detector for Analysis of Whitening Agents in Cream Cosmetics. *Journal of Applied Pharmaceutical Science,* 8: 143-147.

Mayrhofer S, Domig KJ, Mair C, Zitz U, Huys G & Kneifel W (2008) Comparison of Broth Microdilution, Etest, and Agar Disk Diffusion Methods for Antimicrobial Susceptibility Testing of *Lactobacillus acidophilus* Group Members. *Applied and Environmental Microbiology,* 2008: 3745-3748.

Mazurek-Wadolkowska E, Winnicka K, Czajkowska-Kosnik A, Czyzewska U & Miltyk W (2013) Application of differential scanning calorimetry in evaluation of solid state interactions in tablets containing acetaminophen. *Acta Poloniae Pharmaceutica – Drug Research,* 70: 787-793.

McCalley DV (2000) Effect of temperature and flow-rate on analysis of basic compounds in high-performance liquid chromatography using a reversed-phase column. *Journal of Chromatography A,* 902: 311-321.

McPollin O (2009) 'Validation Characteristics'. *Validation of Analytical Methods for Pharmaceutical Analysis,* Warrenpoint, Mourne Training Services: 10.

Mei L, Chen J, Yu S, Huang Y, Xie Y &Wang H, Pan X & Wu C (2017) Expansible thermal gelling foam aerosol for vaginal drug delivery. *Drug Delivery,* 24: 1325-1337.

Mendez JP, Garcia FP, Gonzalez NT, Santilllan YM & Sandoval OAA (2018) Zeta potential and electrophoretic mobility for the recovery of a saline soil with organic amendments. *Ciência e Agrotecnologia,* 42: 420-430.

Mendez PRD, Alicke AA & Thompson RL (2009) Parallel plate geometry correction for transient rheometric experiments. *Applied Rheology,* 24: 1-11.

Mendoza JA (1998) *A study of the rheological properties of some of the gels commonly used in the pharmaceutical, food and cosmetic industries and their influence on microbial growth,* MSc, University of Rhode Island, USA: 47.

Merkatz RB, Simmons K, Kumar N, Variano B, Plagianos M, Roberts K, Han L & Creasy G (2017) Effects of coadministration of vaginal miconazole nitrate on the pharmacokinetics andabsorption of the nestorone and ethinyl estradiol contraceptive vaginal ring. *Fertility and Sterility,* 108: 10-11.

Meyboom RH, Havinga JS, Lastdrager CJ & de Koning GH (1995) Damage to condoms caused by vaginally administered drug. *Nederlands Tijdschrift voor Geneeskunde,* 139: 1602-1605.

MicrobeWiki (2008) Vagina. *Kenyon College Department of Biology*, 2008.

Mirza MO, Panda AK, Asif A, Verma D, Talegaonkar S, Manzoor N, Khan A, Ahmed FJ, Dudeja M & Iqbal Z (2016) A Vaginal drug delivery model. *Drug delivery,* 23: 3123-3134.

Modi PB & Shah NJ (2016) A review article: in vitro release techniques for topical formulations. *Indo American Journal of Pharmaceutical Research,* 6: 1-7.

Moldoveanu SC (2004) Solutions and Challenges in Sample Preparation for Chromatography. *Journal of Chromatographic Science,* 42: 1-14.

Moller PCF, Mewis J & Bonn D (2005) Yield stress and thixotropy: on the difficulty of measuring yield stresses in practice. *Soft Matter,* 2: 274–283

Montemurro M, de Zan MM & Robles JC (2016) Optimized high performance liquid chromatography–ultraviolet detection method using core-shell particles for the therapeutic monitoring of methotrexate. *Journal of Pharmaceutical Analysis,* 6: 103-111.

Morgan M, McInerney F, Rumbold J & Liamputtong P (2009) Drawing the experience of chronic vaginal thrush and complementary and alternative medicine. *International Journal of Social Research Methodologies,* 12: 127-146.

Morrow KM, Underhill K, van den Berg J, Vargas S, Rosen R & Katz DF (2015) User-Identified Gel Characteristics: A Qualitative Exploration of Perceived Product Efficacy of Topical Vaginal Microbicides. *Archives of Sexual Behaviour,* 43: 1459-1467.

Moustafa YM & Morsi RE (2013) 'Chapter 1: Ion Exchange Chromatography - An Overview'. *Column Chromatography,* Intech Open: 2.

Mudshinge SR, Deore AB, Patil S & Bhalgat CM (2011) Nanoparticles: Emerging carriers for drug delivery. *Saudi Pharmaceutical Journal,* 19: 129-141.

Mukherjee S, Ray S & Thakur RS (2009) Solid lipid nanoparticles: a modern formulation approach in drug delivery system*. Indian Journal of Pharmaceutical Sciences,* 71: 349-358.

Munhoven G (2013) Mathematics of the total alkalinity–pH equation – pathway to robust and universal solution algorithms: the SolveSAPHE package v1.0.1. *Geoscientific Model Development,* 6: 1367-1388.

Muriithi DK, Arap Koske JK & Gathungu GK (2017) Application of Central Composite Design Based Response Surface Methodology in Parameter Optimization of Watermelon Fruit Weight Using Organic Manure. *American Journal of Theoretical and Applied Statistics,* 6: 108-116.

Muxika A, Etxabide A, Uranga J, Guerrero P & de la Caba K (2017) Chitosan as a bioactive polymer: Processing, properties and applications. *International Journal of Biological Macromolecules,* 105: 1358-1368.

Myers RH, Montgomery DC & Anderson-Cook CM (2009) 'Building Empirical Models'. *Response Surface Methodology: Process and Product Optimization Using Designed Experiments,* New Jersey, John Wiley and Sons: 14.

Nabatchian MR, Shahriari H & Shahriari M (2014) Introduction of a mathematical model for optimizing the drug release in the patient's body. *DARU: Journal of faulty of Pharmacy, Tehran University of Medical Sciences,* 22: 1.

Nagy K & Vekey K (2008) 'Chapter 5- Separation methods'. Vekey K, Telekes A & Vertes A (ed.). *Medical Applications of Mass Spectrometry,* Elsevier Sceince: 61-92

Naik P, Shah S, Heaney J, Hanson R & Nagarsenker MS (2016) Influence of Test Parameters on Release Rate of Hydrocortisone from Cream: Study Using Vertical Diffusion Cell. *Dissolution Technologies,* 23: 14-20.

Nalungwe S & Kilian G (2016) *Development of a liposomal acyclovir mucoadhesive film,* MSc (General Health Sciences), Nelson Mandela Metropolitan University, Port Elizabeth South Africa: 4.

Nandini PT, Doijad RC, Shivakumar HN & Dandagi PM (2015) Formulation and evaluation of gemcitabine-loaded solid lipid nanoparticles. *Drug Delivery,* 22: 647-651.

Naseri N, Valizadeh H & Zakeri-Milani P (2015) Solid Lipid Nanoparticles and Nanostructured Lipid Carriers: Structure, Preparation and Application. *Advanced Pharmaceutical Bulletin,* 5: 305-313.

Navarra MA, Dal Bosco C, Moreno JS, Vitucci FM, Paolone A & Panero S (2015) Synthesis and Characterization of Cellulose-Based Hydrogels to be used as Gel Electrolytes. *Membranes,* 27: 810-823.

Navratilova N, Dermek P, Drienovský M, Čička R & Náplava A (2014) The usage of differential scanning calorimetry and thermogravimetric analysis for optimization of plastics processing. *Tehnički vjesnik,* 21: 1235-1238.

Ncube S, Poliwoda A, Cukrowska E, Wieczorek P & Chimuka L (2016) Comparative Study of Different Column Types for the Separation of Polar Basic Hallucinogenic Alkaloids. *South African Journal of Chemistry,* 69:189-195.

Ndesendo VMK, Pillay V & Buchmann E (2009) *A novel controlled release intravaginal bioadhesive polymeric device,* PhD, University of the Witwatersrand, Johannesburg.

Ndesendo VMK, Pillay V, Choonara YE, Buchmann E, Bayever DN & Meyer LCR (2008) A Review of Current Intravaginal Drug Delivery Approaches Employed for the Prophylaxis of HIV/AIDS and Prevention of Sexually Transmitted Infections. *American Association of Pharmaceutical Sciences PharmSciTech,* 9: 505-520.

Nelson M, Wanjiru W & Muturi WM (2013) Prevalence of vaginal candidiasis and determination of the occurrence of candida species in pregnant women attending the antenatal clinic of Thika District Hospital, Kenya. *Open Journal of Medical Microbiology,* 3: 264-272.

Nguyen L, Laurent A, Raplor S, Carbonnel F, Trouillet R, Bourrel G & Ninot G (2016) Defining a Collaborative Ontology for Non-Pharmacological Interventions (NPIs). *International Behavioural Trials Network,* 2016.

Nikalje APG (2015) Nanotechnology and its application in medicine. *Medicinal Chemistry,* 5: 81-89.

Nounou MM, Gui LKE, Khalafallah N & Khalil SA (2006) In vitro release of hydrophilic and hydrophobic drugs from liposomal dispersions and gels. *Acta Pharm,* 56: 311-324.

Noyori R (1999) Supercritical Fluids: Introduction. *Chemical Reviews,* 99: 353-354.

Nurbhai M, Grimshaw J, Watson M, Bond CM, Mollison JA & Ludbrook A (2009) Oral versus intravaginal imidazole and triazole anti-fungal treatment of uncomplicated vulvovaginal candidiasis (thrush). *Cochrane Database of Systemic Reviews,* 2007: 1-57.

Ornaf RM & Dong MW (2015) 'HPLC in Pharmaceutical analysis'. Ahuja S & Dong M (eds.) *Handbook of Pharmaceutical Analysis by HPLC,* Elsevier, p29.

Ostolska I & Wiśniewska M (2014) Application of the zeta potential measurements to explanation of colloidal Cr_2O_3 stability mechanism in the presence of the ionic polyamino acids. *Colloid and Polymer Science,* 292: 2453-2464.

Otoni CG, Lorevice M, de Moura MR & Mattoso LHC. (2018) On the effects of hydroxyl substitution degree and molecular weight on mechanical and water barrier properties of hydroxypropyl methylcellulose films. *Carbohydrate Polymers,* 185: 105-111.

Owen MK & Clenney TL (2004) Management of vaginitis. *American Family Physician*, 70: 2125-2132.

Ozioko C (2017) Preformulation Studies: Drug-Excipient Compatibility Studies. *Pharmapproach.com.*

Paczkowska M, Zalewski P, Garbacki P, Talaczyńska A, Krause A & Cielecka-Piontek J (2014) The Development and Validation of a Stability-Indicating UHPLC-DAD Method for Determination of Perindopril l-Arginine in Bulk Substance and Pharmaceutical Dosage Form. *Chromatographia,* 77: 1497-1501.

Paithankar H (2013) HPLC method validation for pharmaceuticals: a review. *International Journal of Universal Pharmacy and Bio Sciences,* 2: 229-242.

Pal K, Paulson AT & Rousseau D (2013) Biopolymers in Controlled-Release Delivery Systems. Ebnesajjad S (ed.). *Handbook of Biopolymers and Biodegradable Plastics,* Willam Andrews Publishers.

Palmeira-de-Oliveira R, Duarte P, Palmeira-de-Oliveria A, das Neves J, Amaral MH, Breitenfeld L & Matrinez-de-Oliveira J (2014) What do Portuguese Women Prefer Regarding Vaginal Products? Results from a Cross-Sectional Web-Based Survey. *Pharmaceutics,* 6: 543-556.

Pang J, Liu D, Peng Y & Peng X (2018) Optimize the Coverage Probability of Prediction Interval for Anomaly Detection of Sensor-Based Monitoring Series. *Sensors (Basel),* 18: 967.

Papai ZS & Pap TL (2002) Analysis of peak asymmetry in chromatography. *Journal of Chromatography A,* 953: 31-38.

Pappas PG, Rex JH, Sobel JD, Filler SG, Dismukes WE, Walsh TJ & Edwards JE (2004) Guidelines for Treatment of Candidiasis. *Clinical Infectious Diseases,* 38: 161-189.

Pardeshi C, Rajput P, Belgamwar V, Tekade A, Patil G, Chaudhary K & Sonje A (2012) Solid lipid nanocarriers: An overview. *Acta Pharm,* 62:433-472.

Pardhan S, Hedberg J, Blomberrg E, Wold S & Wallinder IO (2016) Effect of sonication on particle dispersion, administered dose and metal release of non-functionalized, non-inert metal nanoparticles. *Journal of Nanoparticle Research,* 18: 285.

Parhi R & Suresh P (2012) Supercritical fluid technology: A review. *Journal of Advanced Pharmaceutical Science and Technology,* 1: 13-36.

Parhi. R. (2017) Cross-Linked Hydrogel for Pharmaceutical Applications: A Review. *Advanced Pharmaceutical Bulletin,* 7: 515-530.

Parsapure R, Rahimiforushani A, Majlessi F, Montazeri A, Sadeghi R & Garmarudi G (2016) Impact of Health-Promoting Educational Intervention on Lifestyle (Nutrition Behaviors, Physical Activity and Mental Health) Related to Vaginal Health Among Reproductive-Aged Women With Vaginitis. *Iranian Red Crescent Medical Journal*, 18: 37698.

Patel D, Kesharwani R & Nair S (2013) Solid Lipid Nanoparticle (SLN): A Modern Approach for Drug Delivery. *Asian Journal of Pharmaceutical Research and Development,* 3: 1-17.

Patel GM & Patel AP (2010) A novel effervescent bioadhesive vaginal tablet of ketoconazole: formulation and in vitro evaluation. *International journal of PharmTech Research,* 2: 656-667.

Patel HR, Patel RP & Patel MM (2009) Poloxamers: A pharmaceutical excipients with therapeutic behaviours. *International Journal of PharmTech Research*, 1: 299-303.

Patel KG, Shah PM, Shah P & Gandhi TR (2016) Validated high-performance thin-layer chromatographic (HPTLC) method for simultaneous determination of nadifloxacin, mometasone furoate, and miconazole nitrate cream using fractional factorial design. *Journal of Food and Drug Analysis,* 24: 610-619.

Patel P, Ahir K, Patel V, Manani L & Patel C (2015) Drug-Excipient compatibility studies: First step for dosage form development. *The Pharma Innovation,* 4: 14-20.

Patil A, Bhide S, Bookwala M, Soneta B, Shankar V, Almotairy A, Almutairi M & Murthy SN (2017) Stability of Organoleptic Agents in Pharmaceuticals and Cosmetics. *American Association of Pharmaceutical Sciences,* 19: 1-13.

Pearsura P (2015) Application of Response Surface Methodology for Modelling of Postweld Heat Treatment Process in a Pressure Vessel Steel ASTM A516 Grade 70. *The Scientific World Journal,* 2015: 318475.

Pennsylvania State University (2018) *Central Composite Designs.* Pennsylvania State University Department of Statistics, 2018.

Pershing LK, Corlett J & Jorgensen C (1994) In vivo pharmacokinetics and pharmacodynamics of topical ketoconazole and miconazole in human stratum corneum. *Antimicrobial Agents and Chemotherapy,* 38: 90-95.

Piano TC & Moore AD (1999) Determination of the LOD and LOQ of an HPLC method using Four Different Techniques. *Pharmaceutical Technology,* 23: 86-90.

Pierce Biotechnology™ (2005) Technical Resource: Convert between times gravity (× g) and centrifuge rotor speed (RPM), PierceTM USA.

Politis NS, Colombo P, Colombo G & Rekkas MD (2017) Design of experiments (DoE) in pharmaceutical development. *Drug Development and Industrial Pharmacy,* 43: 889-901.

Pollard C (2005) Menstrual Tampons and Pads: Information for Premarket Notification Submissions (510(k)s) - Guidance for Industry and FDA Staff. *US Food and Drug Administration,* 2018. New Hampshire.

Ponton A, Barboux-Doeuff & Sanchez C (2005) Physico-chemical control of sol–gel transition of titanium alkoxide-based materials studied by rheology. *Journal of Non-crystalline Solids,* 351: 45-53.

Pooja D, Tunki L, Kulhari H, Reddy BB & Sistla R (2015) Optimization of solid lipid nanoparticles prepared by a single emulsification-solvent evaporation method. *Data in Brief,* 25: 15-19.

Powell K (2010) Vaginal thrush: quality of life and treatments. *British Journal of Nursing,* 19: 1106-1111.

Prathap GM & Nishat A (2013) Ultra performance liquid chromatography: a chromatography technique. *International Journal of Pharmacy,* 3: 251-260.

Punitha E, Anbazhagan S, Sathya B & Vilamson DC (2018) Recent approaches in vaginal drug delivery systems. International Journal of Research in Pharmacy and Pharmaceutical Sciences, 3: 97-106.

Quijano CD (2017) A Multifunctional Mineral Excipient. *Pharmaceutical Technology,* 4: 24-26.

Qushway M, Nasr A, Abd-Alhaseeb M & Swidan S (2018) Design, Optimization and Characterization of a Transfersomal Gel Using Miconazole Nitrate for the Treatment of Candida Skin Infections. *Pharmaceutics,* 10: 1-22.

Radic DB, Stanojevic MM, Obradovic MO & Jovovic AM (2017) Thermal analysis of physical and chemical changes occuring during regeneration of activated carbon. *Thermal Science,* 21: 1067-1081.

Rafferty JL, Siepmann JI & Schure MR (2011) Mobile phase effects in reversed-phase liquid chromatography: A comparison of acetonitrile/water and methanol/water solvents as studied by molecular simulation. *Journal of Chromatography A,* 1218: 2203-2213.

Rahman SS & Ahmed AB (2016) Vaginal Drug Delivery System a Promising Approach for Antiretroviral Drug in the Prevention of HIV Infection: A Review. *Journal of Pharmaceutical Sciences and Research,* 8: 1330-1338.

Raissi S and Eslami-Farsani R (2009) Statistical Process Optimization through Multi-Response Surface Methodology. *World Academy of Science, Engineering and Technology,* 51: 267-272.

Ramteke KH, Joshi SA & Dhole SN (2012) Solid Lipid Nanoparticle: A Review. *International Organisation of Scientific Research Journal of Pharmacy,* 2: 34-44.

Rana S, Chaudhary H, Aroa V, Kholi K & Kumar V (2013) Effect of Physicochemical Properties of Biodegradable Polymers on Nano Drug Delivery. *Polymer Reviews,* 53: 546-567.

Rane S (2005) Polydispersity Index: How Accurately Does It Measure the Breadth of the Molecular Weight Distribution? *Chemistry of Materials,* 17: 926-926.

Rangasamy M & Parthiban KG (2010) Recent advances in novel drug delivery systems. *International Journal of Research in Ayurveda & Pharmacy,* 1: 316-326.

Rao BV, Sowjanya GN, Ajitha A & Rao VUM (2015) A review on stability indicating hplc method development. *World Journal of Pharmacy and Pharmaceutical Sciences, 4: 405-424.*

Rao NM, Bagyalakshmi J & Ravi TK (2010) Development and validation of UV-spectroscopic method for estimation of Voglibose in bulk and tablets. *Journal of Chemical and Pharmaceutical Research,* 2: 350-356.

Rathod SD & Buffler PA (2014) Highly-cited estimates of the cumulative incidence and recurrence of vulvovaginal candidiasis are inadequately documented. *BioMed Central Women's Health,* 2014: 43.

Rathod SD, Klausner JD, Krupp K, Reingold AL & Madhivanan P (2012) Epidemiologic Features of Vulvovaginal Candidiasis among Reproductive-Age Women in India. *Infectious Diseases in Obstetrics and Gynecology,* 2012: 1-8.

Ravisankar P, Navya CN, Pravallika D & Sri DN (2015) A Review on Step-by-Step Analytical Method Validation. *International Organisation of Scientific Research Journal of Pharmacy,* 5: 07-19.

Rawat T & Pandey IP (2015) Forced degradation studies for Drug Substances and Drug Products- Scientific and Regulatory Considerations. *Journal of Pharmaceutical Sciences and Research,* 7: 238-241.

Reller LB, Weinstein M, Jorgensen JH & Ferraro MJ (2009) Antimicrobial Susceptibility Testing: A Review of General Principles and Contemporary Practices. *Clinical Infectious Diseases,* 49: 1749–1755.

Ren DB, Yang ZH, Liang YZ, Fan W & Ding Q (2013) Effects of injection volume on chromatographic features and resolution in the process of counter-current chromatography. *Journal of Chromatography A,* 1277: 7-14.

Rencber S, Karavana SY, Senyigit ZA, Erac B, Limoncu MH & Baloglu E (2016) Mucoadhesive in situ gel formulation for vaginal delivery of clotrimazole: formulation, preparation, and in vitro/in vivo evaluation. *Pharmaceutical Development and Technology,* 2016: 1-13.

Reynolds DW, Facchine KL, Mulley JF, Alsante KM, Hatajik TD & Motto MG (2000) Available G=guidance and best practices for conducting forced degradation studies. *Pharmaceutical Technology,* 2002: 48-57.

Ringdahl EN (2000) Treatment of Recurrent Vulvovaginal Candidiasis. *American Family Physician,* 61: 3306-3312.

Rizvi SAA & Saleh AM (2018) Applications of nanoparticle systems in drug delivery technology. *Saudi Pharmaceutical Journal,* 26: 64-70.

Roberts T, Smith M & Roberts B (1999) Observations on Centrifugation: Application to Centrifuge Development. *Clinical Chemistry,* 45: 1889–1897.

Rogovina LZ, Vasil'ev VG & Braudo EE (2008) Definition of the concept of polymer gel. *Polymer Science Series C,* 50: 85-92.

Rohan LC & Sassi AB (2009) Vaginal Drug Delivery Systems for HIV Prevention. *American Association of Pharmaceutical Sciences,* 11: 78-87.

Roose P (2009) Compliance: the impact of adverse events and tolerability on the physician's treatment decisions. *European Neuropsychopharmacology*, 13: 85-92.

Rosen RK, van den Berg J, Vargas SE, Senocak N, Shaw JG, Buckheit RM, Smith KA & Guthrie KM (2015) Meaning-making matter sin product design: users' sensory perceptions and experience evaluations of long-acting vaginal gels and intravaginal rings. *Contraception,* 92: 596-601.

Roses M, Canals I, Alleman H, Siigur K & Bosch E (1996) Retention of Ionizable Compounds on HPLC. 2. Effect of pH, Ionic Strength, and Mobile Phase Composition on the Retention of Weak Acids. *Analytical Chemistry,* 68: 4094-4100.

Rossiter D (2016) 'Genitourinary system and sex hormones', in Rossiter D (ed*.) South African Medicines Formulary,* 12ed, Pretoria, Health and Medical Publishing Group: 218.

Roy S, Pal K, Pramanik K & Prabhakar B (2009) Polymers in mucoadhesive drug-delivery systems: A brief note. *Designed Monomers and Polymers,* 12: 483-495.

Rueda MM, Auscher MC, Fulchiron R, Perie T, Martin G, Sonntag P & Cassagnau P (2017) Rheology and applications of highly filled polymers: A review of current understanding. *Progress in Polymer Science,* 66: 22-53.

Sabir N, Moloy M & Bhasin PS (2013) HPLC method development and validation: a review. *International Research Journal of Pharmacy,* 4: 39-46.

Sahoo CK, Nayak PK, Sarangi DK & Sahoo TK (2013) Intra vaginal drug delivery system: An Overview. *American Journal of Advanced Drug Delivery,* 1: 43-55.

Sahoo DR & Jain S (2016) A Rapid and Validated RP-HPLC Method for the Simultaneous Quantification of Benzoic Acid, Metronidazole and Miconazole Nitrate in Vaginal Formulations. *Journal of Chromatographic Science,* 54: 1613-1618.

Sailaja A, Ghosh S, Reddy TPK, Deepthi PN & Banji D (2016) A Review on Trouble Shooting In HPLC and its Solutions. *International Journal of Pharmaceutical and Chemical Sciences,* 3: 625-636.

Saini R, Saini S & Sharma S (2010) Nanotechnology: The Future Medicine. *Journal of Cutaneous and Aesthetic Surgery,* 3: 32-33.

Salamanca CH, Barrera-Ocampo A, Lasso JC, Camacho N & Yarce CJ (2018) Franz Diffusion Cell Approach for Pre-Formulation Characterisation of Ketoprofen Semi-Solid Dosage Forms. *Pharmaceutics,* 10: 148-158.

Salehi MB, Sefti MV, Moghadam AM & Koohi A (2012) Study of Salinity and pH Effects on Gelation Time of a Polymer Gel Using Central Composite Design Method. *Journal of Macromolecular Science Part B,* 51: 438-451.

Sanii Y, Torkamandi H, Gholami K, Havavand N & Javadi M (2016) Role of pharmacist counselling in pharmacotherapy quality improvement. *Journal of Research in Pharmacy Practice,* 5: 132-137.

Santo IE, Pedro AS, Fialho R & Cabral-Albuquerque EC (2013) Characteristics of lipid micro- and nanoparticles based on supercritical formation for potential pharmaceutical application. *Nanoscale Research Letters,* 8: 386.

Sawant B and Khan T (2017) Recent advances in delivery of antifungal agents for therapeutic management of candidiasis. *Biomed & Pharmacotherapy,* 96: 1478-1490.

Schellinger A & Carr PW (2006) Isocratic and gradient elution chromatography: A comparison in terms of speed, retention reproducibility and quantitation. *Journal of Chromatography A,* 1109: 253-266.

Schneider A, Hommel G & Blettner M (2010) Linear Regression Analysis: Part 14 of a Series on Evaluation of Scientific Publications. *Deutsches Arzteblatt International,* 107: 776-782.

Schneider CR, Moles R & El-Den S (2018) Thrush: detection and management in community pharmacy. *The Pharmaceutical Journal: A Royal Pharmaceutical Society Publication*, 2018: 1-10.

Schoenitz M, Joseph S, Nitz A, Bunjes H & Scholl S (2014) Controlled polymorphic transformation of continuously crystallized solid lipid nanoparticles in a microstructured device: a feasibility study. *European Journal of Pharmaceutics and Biopharmaceutics,* 86: 324-331.

Schwarz C, Mehnert W, Lucks JS & Muller RH (1994) Solid lipid nanoparticles (SLN) for controlled drug delivery. I. Production, characterization and sterilization. *Journal of Controlled Release,* 30: 83-96.

Sengul U (2016) Comparing determination methods of detection and quantification limits for aflatoxin analysis in hazelnut. *Journal of Food and Drug Analysis,* 24: 56-62.

Shafaat K, Hussain A, Kumar B, Hasan R, Prabhat P & Yadav VK (2013) An overview: storage of pharmaceutical products. *World Journal of Pharmacy and Pharmaceutical Sciences,* 2: 2499-2515.

Shafique M, Khan MA, Khan WS, Rehman M, Ahmad W & Khan S (2017) Fabrication, Characterization, and In Vivo Evaluation of Famotidine Loaded Solid Lipid Nanoparticles for Boosting Oral Bioavailability. *Journal of Nanomaterials,* 2017: 7357150.

Shah KA, Date AA, Joshi MD & Patravale VB (2007) Solid lipid nanoparticles (SLN) of tretinoin: potential in topical delivery. *International Journal of Pharmaceutics,* 345: 163-171.

Shah R, Eldridge D, Palombo E & Harding I (2015) 'Chapter 2: Composition and Structure', in *Lipid nanoparticles: Production, Characterisation and Stability,* Berlin, Springer: 11.

Shah RM, Bryant G, Taylor M, Eldridge DS, Palombo EA and Harding (2016) Structure of solid lipid nanoparticles produced by a microwave-assisted microemulsion technique. *Royal Chemistry Society Advances,* 6: 36803 –36810.

Shah SM, Jain AS, Kaushik R, Nagarsenker MS & Nerurkar MJ (2014) Preclinical Formulations: Insight, Strategies, and Practical Considerations. *American Association of Pharmaceutical Sciences PharmSciTech,* 15: 1307-1323.

Shahtaheri SJ, Ghamari F, Golbabaoi, Rahimi-Froushani A & Abdollahi M (2005) Sample Preparation Followed by High Performance Liquid Chromatographic (HPLC) Analysis for Monitoring Muconic Acid as a Biomarker of Occupational Exposure to Benzene. *International Journal of Occupational Safety and Ergonomic,* 11: 377-388.

Shaikh HK, Kshirsagar RV & Patil SG (2015) Mathematical models for drug release characterisation: A review. *World Journal of Pharmacy and Pharmaceutical Sciences,* 4: 324-338.

Shaikh R, Singh TRR, Garland MJ, Woolfson AD & Donnelly R (2011) Mucoadhesive drug delivery systems. *Journal of Pharmacy and BioAllied Sciences,* 3: 89-100.

Shalliker RA & Guichon G (2009) Understanding the importance of the viscosity contrast between the sample solvent plug and the mobile phase and its potential consequence in two-dimensional high-performance liquid chromatography. *Journal of Chromatography A,* 30: 787-793.

Sharma J. Klara S, Sharma A & Rani S (2009) Colloidal drug carrier. *The internet Journal of Family Practice,* 9: 1-6.

Sharma MK & Murugesan M (2017) Forced Degradation Study an Essential Approach to Develop Stability Indicating Method. *Journal of Chromatography & Separation Techniques,* 8: 1-3.

Shen J & Burgess DJ (2013) In Vitro Dissolution Testing Strategies for Nanoparticulate Drug Delivery Systems: Recent Developments and Challenges. *Drug Delivery and Translational Research,* 3: 409-415.

Shi L, Li Z, Yu L, Jia H & Zheng L (2011) Effects of surfactants and lipids on the preparation of solid lipid nanoparticles using double emulsion method. *Journal of Dispersion Science and Technology,* 32: 254-259.

Shinde NG, Bangar BN, Deshmukh SM, Sulake SP & Sherekar DP (2013) Pharmaceutical Forced Degradation Studies with Regulatory Consideration*. Asian Journal of Research in Pharmaceutical Sciences,* 3: 178-188.

Shrivastava A & Gupta V (2011) Methods for the determination of limit of detection and limit of quantitation of the analytical methods. *Chronicles of Young Scientists,* 2: 21-25.

Shubhra QTH, Toth J, Gyenis J & Feczko T (2014) Poloxamers for surface modification of hydrophobic drug carriers and their effects on drug delivery. *Journal of Polymer Review,* 54: 112-138.

Siddiqui A, Alayoubi A, El-Malah Y & Nazzal S (2014) Modeling the effect of sonication parameters on size and dispersion temperature of solid lipid nanoparticles (SLNs) by response surface methodology (RSM). *Pharmaceutical Development and Technology,* 19: 342-346.

Siegel RA & Rathbone MJ (2012) 'Chapter 2: Overview of Controlled Release Mechanisms'. Siepmann J, Siegel RA & Rathbone MJ (eds.) *Fundamentals and Applications of Controlled Release Drug Delivery,* Springer: 20.

Siepmann J & Peppas NA (2011) Higuchi equation: derivation, applications, use and misuse. *International Journal of Pharmaceutics,* 418: 6-12.

Silicycle (2018) Ideal injection volume vs column dimension, SiliCycle™ Inc, Quebec Canada.

Singh K, Malviya R & Sharma P (2014) Solubility Enhancement of Miconazole Nitrate for Formulation and Evaluation of Mucoadhesive Gel. *Global Journal of Pharmacology,* 8: 518-524.

Singh N (2001) Trends in the epidemiology of opportunistic fungal infections: predisposing factors and the impact of antimicrobial use practices. *Clinical Infectious Diseases*, 10: 1692–1696.

Singh R & Lillard JW (2009) Nanoparticle-based targeted drug delivery. *Experimental and Molecular Pathology,* 86: 215-223.

Sivaraman A & Banga AK (2015) Quality by design approaches for topical dermatological dosage form. *Research and Reports in Transdermal Drug Delivery,* 2015: 9-21.

SixSigma (2018) *Design of Experiments Planning.* SixSigma.net

Slew A (2018) Analyzing Content Uniformity. *Pharmaceutical technology,* 42: 16-21.

Smith C (2011) Optimizing HPLC Sample Preparation. *Biocompare,* 2011: 1-2.

Sobel DJ (2017b) 'Candida vulvovaginitis', in Barbieri RL, Kaufmann CA & Eckler K (ed.) *UpToDate*, Alphen aan den Rijn, Netherlands, Wolters Kluwer: 1.

Sobel JD & Sobel R (2018) Current treatment options for vulvovaginal candidiasis caused by azole-resistant Candida species. *Expert Opinion on Pharmacotherapy*, 19: 971-977.

Sobel JD (2017a) Vulvovaginal candidosis. *The Lancet,* 9577: 1961-1971.

Sobel JD, Faro S, Force RW, Foxman B, Ledger WJ, Nyirjesy PR, Reed BD & Summers PR (1998) Vulvovaginal candidiasis: epidemiologic, diagnostic, and therapeutic considerations. *American Journal of Obstetrics and Gynecology*, 178: 203-211.

Soliman GM, Fetih G, Abbas AM.(2016) Thermosensitive bioadhesive gels for the vaginal delivery of sildenafil citrate: in vitro characterization and clinical evaluation in women using clomiphene citrate for induction of ovulation. *Drug development and Industrial Pharmacy,* 43: 399-408.

Soma D, Attari Z, Reddy MS, Damodaram A & Koteshwara KBG (2017) Solid lipid nanoparticles of irbesartan: preparation, characterisation, optimisation and pharmacokinetic studies. *Brazilian Journal of Pharmaceutical Sciences,* 55: 1-10.

Sosnik A & Seremeta KP (2017) Polymeric Hydrogels as Technology Platform for Drug Delivery Applications. *Gels,* 3: 25-37.

South African National Department of Health (SA DoH) (2017) *Standard Treatment Guidelines and Essential Medicines List for South Africa: Hospital Level Paediatrics*, SA DoH, Pretoria: 227.

Spall JC (2010) Factorial Design for Efficient Experimentation*. IEEE Control Systems Magazine,* 2010: 38-54.

Srikrishna S & Cardozo L (2013) The vagina as a route for drug delivery: a review. *International Urogynecology Journal,* 24: 537-543.

Stadtlander CTKH (2007) Scanning Electron Microscopy and Transmission Electron Microscopy of Mollicutes: Challenges and Opportunities. Mendez-Vilas A & Diaz J (ed.) *Modern Research and Educational Topics in Microscopy, Minnesota,* Formatex: 127.

Steinmann W, Walter S, Beckers M, Seide G & Gries T (2013) 'Chapter 12: Thermal Analysis of Phase Transitions and Crystallization in Polymeric Fibers'*. Applications of Calorimetry in a Wide Context – Differential Scanning Calorimetry, Isothermal Titration Calorimetry and Microcalorimetry,* InTech Open: 279

Stella B, Peira E, Dianzani C, Gallarate M, Battagalia L, Gigliotti CL, Boggio E, Dianzani U & Dosio F (2018) Development and Characterization of Solid Lipid Nanoparticles Loaded with a Highly Active Doxorubicin Derivative. *Nanomaterials,* 2018: 110-126.

Stevens RE, Konsil J, Verrill SS, Roy P, Desai PB, Upmalis DH & Cone FL (2013) Bioavailability Study of a 1200 mg Miconazole Nitrate Vaginal Ovule in Healthy Female Adults. *The Journal of Clinical Pharmacology,* 42: 52-60.

Steyeberg EW, Vickers AJ, Cook NR, Gerds T, Gonen M, Obuchowski N, Pencina MJ & Kattan MW (2010) Assessing the performance of prediction models: a framework for some traditional and novel measures. *Epidemiology (Cambridge Mass),* 21: 128-138.

Stillhart C, Parrott NJ, Lindenberg M, Chalus P, Bentley D & Szepes A (2017) haracterising Drug Release from Immediate-Release Formulations of a Poorly Soluble Compound, Basmisanil, Through Absorption Modelling and Dissolution Testing. *American Association of Pharmaceutical Sciences PharmSciTech,* 19: 827-836.

Stoll DR, Li X, Wang X, Carr PW, Porter SEG &Rutan SC (2007) Fast, comprehensive two-dimensional liquid chromatography. *Journal of Chromatography A,* 1168: 3-43.

Sud IJ & Feingold DS (1981) Mechanisms of Action of the Antimycotic Imidazoles. *Dermatology,* 76: 438-441.

Sun C, Shen Y, Sun D, Hang T & Tu J (2012) Method Development and Validation for the Determination of Indiquinoline Tartrate, a Novel Kappa Opioid Agonist, and its Related Substances by High-Performance Liquid Chromatography. *Journal of Chromatographic Science,* 50: 343-348.

Swain S & Babu SM (2015) Solid Lipid Nanoparticle: An Overview. *Pharmaceutical Regulatory Affairs: Open Access,* 4: 154.

Swartz M (2006) A guide to analytical method validation. *LCGC North America,* 26: 110-117.

Swartz M (2010) HPLC detectors: a brief review. *Journal of Liquid Chromatography and Related Technologies,* 33: 1130-1150.

Swati R, Ankaj K & Vinay P (2014) Organogels: A novel drug delivery systems. *World Journal of Pharmacy and Pharmaceutical Sciences,* 4: 455-471.

Tamilselvan C, Joseph SJ, Mugunthan G & Ahamed SSM (2014) Validation of HPLC Method for Quantitative Determination of Pirimiphos methyl. *International Letters of Chemistry, Physics and Astronomy,* 28: 93-102.

Taurin S Almomen AA, Pollak T, Kim SJ, Maxwell J, Peterson CM, Owen SC & Janat-Amsbury MM (2018) Thermosensitive hydrogels a versatile concept adapted to vaginal drug delivery. *Journal of Drug Targeting,* 26: 533-550.

Taylor MJ, Tomlins P & Sahota TS (2017) Thermoresponsive gels. *Gels,* 3: 1-31.

Taylor T (2016) Column Selection for HPLC Method Development. *LCGC North America,* 32: 87-98.

Thakker KD & Chern WH (2003) Development and Validation of In Vitro Release Tests for Semisolid Dosage Forms—Case Study. *Dissolution Technologies,* 2003: 10-15.

Thammana M (2016) A Review on High Performance Liquid Chromatography (HPLC). *Research & Reviews: Journal of Pharmaceutical Analysis,* 5: 22-29.

The Pharmaceutical Society of Great Britain (1979) 'Miconazole'. *The Pharmaceutical Codex,* 11ed, London, The Pharmaceutical Press: 569.

Tindall GW & Dolan JW (2003) Mobile-phase buffers, part III - Preparation of buffers. *LCGC Europe*, 21: 28-32.

Tiwari G & Tiwari R (2010) Bioanalytical method validation: An updated review. *Pharmaceutical Methods,* 1: 25-38.

Tiwari G, Tiwari R, Sriwastawa B, Bhati L, Pandey S, Pandey P & Bannerjee SK (2012) Drug delivery systems: An updated review. *International Journal of Pharmaceutical Investigation,* 2: 2-11.

Tsao CT, Hsiao MH, Zhang M, Levengood SL & Zhang M (2014) Chitosan-PEG Hydrogel with Sol–Gel Transition Triggerable by Multiple External Stimuli. *Macromolecular Rapid communications,* 36: 332-338.

Tscharnuter W (2000) 'Photon Correlation Spectroscopy in Particle Sizing'. Meyers RA (ed.) *Encyclopaedia of Analytical Chemistry*, Chichester, John Wiley & Sons Ltd: 5469.

Turner SA & Butler G (2014) The Candida Pathogenic Species Complex. *Cold Spring Harbor Perspectives in Medicine,* 4: 1-17.

Ueda CT, Shah VP, Derdzinski K, Ewing D, Flynn G, Maibach H, Marques M, Rytting H, Shaw S, Thakker K & Yacobi A (2009) Topical and Transdermal Drug Products. *Pharmacopeial Forum,* 35: 750-765.

Ummadi S, Shravani B, Rao NGR, Reddy MS, & Nayak BS (2013) Overview on Controlled Release Dosage Form. *International Journal of Pharma Sciences,* 3: 258-269.

Uner M (2006) Preparation, characterization and physico-chemical properties of solid lipid nanoparticles (SLN) and nanostructured lipid carriers (NLC): their benefits as colloidal drug carrier systems. *Die Pharmazie,* 61: 375-386.

Uner M, Wissing SA, Yener G & Muller RH (2004) Influence of surfactants on the physical stability of solid lipid nanoparticle (SLN) formulations. *Die Pharmazie,* 59: 331-332.

United States Pharmacopeial Convention (2013) Topical and transdermal drug products – product quality tests. *Interim Revision Announcement,* 1: 3.

Upadhyay RK (2014) Drug Delivery Systems, CNS Protection, and the Blood Brain Barrier. *BioMed Research International*, 2014: 1-37.

Vail JG, Cohen JA & Kelly KL (2004) Improving Topical Microbicide Applicators for Use in Resource-Poor Settings. *American Public Health Association,* 94: 1089-1092.

Vakilinezhad MA, Tanha S, Montaseri H, Dinarvand R, Azadi A & Javar A (2018) Application of Response Surface Method for Preparation, Optimization, and Characterization of Nicotinamide Loaded Solid Lipid Nanoparticles. *Advanced Pharmaceutical Bulletin,* 8: 245-256.

Varshosaz J, Emami J, Tavakoli N, Minaiyan M, Rahmani N, Ahmadi F & Dorkoosh F (2011) Development and validation of a rapid HPLC method for simultaneous analysis of budesonide and its novel synthesized hemiesters in colon specific formulations. *Research in Pharmaceutical Sciences,* 6: 107-116.

Varshosaz J, Tabbakhian M & Salmani Z (2008) Designing of a Thermosensitive Chitosan/Poloxamer In Situ Gel for Ocular Delivery of Ciprofloxacin. *The Open Drug Delivery Journal,* 2: 61-70.

Venkataraman S & Manasa M (2018) Forced degradation studies: Regulatory guidance, characterization of drugs, and their degradation products - a review. *Drug Invention Today,* 10: 137-147.

Verma P, Thakur AS, Deshmukh K, Jha AK & Verma S (2010) Routes of drug administration. *International Journal of Pharmaceutical Studies and Research,* 1: 54-59.

Vermani K & Garg S (2000) The scope and potential of vaginal drug delivery. *PSTT Research Focus,* 3: 359-364.

Vintiloiu A & Leroux JC (2008) Organogels and their use in drug delivery — A review. *Journal of Controlled Release,* 125: 179-192.

Voutou B & Stefanaki EC (2008) Electron Microscopy: The Basics. *Physics of Advanced Materials Winter School,* 2008: 1-11.

Wahab F, Patel DC & Armstrong DW (2017) Peak Shapes and Their Measurements: The Need and the Concept Behind Total Peak Shape Analysis. *LCGC North America,* 35: 846-853.

Wang H, Li Q, Reyes S, Zhang J, Xie L, Melendez V, Hickman M & Kozar MP (2013) Formulation and Particle Size Reduction Improve Bioavailability of Poorly Water-Soluble Compounds with Antimalarial Activity. *Malaria Research and Treatment*, 2013: 769234.

Wani TA, Ahmad A, Zargar S, Khalil NY & Darwish IA (2012) Use of response surface methodology for development of new microwell-based spectrophotometric method for determination of atrovastatin calcium in tablets. *Chemistry Central Journal,* 6: 134.

Weissman SA & Anderson NG (2015) Design of Experiments (DoE) and Process Optimization. A Review of Recent Publications. *Organic Process Research and Development,* 19: 1605-1633.

Welton T (2015) Solvents and sustainable chemistry. *Proceedings. Mathematical, Physical, and Engineering sciences,* 471: 1-26.

Wen H, Jung H & Li X (2015) Drug Delivery Approaches in Addressing Clinical Pharmacology-Related Issues: Opportunities and Challenges. *American Association of Pharmaceutical Sciences PharmSciTech,* 17: 1327-1340.

Whaley SG, Berkow EL, Rybak JM, Nishimoto AT, Barker KS & Rogers PD (2017) Azole antifungal resistance in Candida albicans and emerging non-albicans species. *Frontiers in Microbiology,* 7: 2173-2185.

Wheat P (2001) History and development of antimicrobial susceptibility testing methodology. *Journal of Antimicrobial Chemotherapy,* 48: 1-4.

White DJ & Vanthuyne A (2006) Vulvovaginal candidiasis. *Sexually Transmitted Infection,* 82: 28-30.

Winey M, Meehl JB, O'Toole ET & Giddings Jr TH (2014) Conventional transmission electron microscopy. *Molecular Biology of the Cell,* 25: 319-323.

Wittrig B (2003) HPLC Method Development. *Restek Corporation,* 2003: 1-68.

World Health Organisation Expert Committee (1997) *Quality assurance of pharmaceuticals: A compendium of guidelines and related materials,* Geneva Switzerland: 37.

World Health Organisation Expert Committee (2009) 'Annex 2: Stability testing of active pharmaceutical ingredients and finished pharmaceutical products' *WHO Technical Report Series,* 953: 90.

World Health Organisation Expert Committee (2017) WHO Model List of Essential Medicines, 20th edition: 35.

Xia D, Shrestha N, van de Streek J, Mu H & Yang M (2016) Spray drying of fenofibrate loaded nanostructured lipid carriers. *Asian Journal of Pharmaceutical Sciences,* 11: 507-515.

Xie HY, Feng D, Wei DM, Chen H, Mei L, Wang X & Fang F (2013) Probiotics for vulvovaginal candidiasis in non-pregnant women (Protocol). *Cochrane Database of Systematic Reviews,* 2013: 1-18.

Yadav V, Mahor A, Prajapati S, Alok S, Verma A, Kumar A, Gupta N & Kumar S (2014) Solid lipid nanoparticles (SLN): Formulation by high pressure homogenisation. *World Journal of Pharmacy and Pharmaceutical Sciences,* 3: 1200-1213.

Yahia LH, Chirani N, Gritsch L, Motta FL, Chirani S & Fare S (2015) History and applications of hydrogels. *In Journal of Biomedical Sciences,* 4: 1-15.

Yang T (2012) *Mechanical and swelling properties of hydrogels,* PhD, Uppsala University, Stockholm, Sweden: p 9.

Yapar EA & Inal O (2012) Poly(ethylene oxide)–Poly(propylene oxide)-Based Copolymers for Transdermal Drug Delivery: An Overview. *Tropical Journal of Pharmaceutical Research,* 11: 855-866.

Young CS & Weigand RJ (2002) An efficient approach to column selection in HPLC method development. *LCGC North America,* 20: 465-472.

Young G & Jewell D (2001). Topical treatment for vaginal candidiasis (thrush) in pregnancy. *Cochrane Database of Systematic Reviews*, 2001: 1-20.

Zeng X, Zhang Y, Zhang T, Xue Y, Xu H & An R (2018) Risk Factors of Vulvovaginal Candidiasis among Women of Reproductive Age in Xi'an: A Cross-Sectional Study. *BioMed Research International,* 2018: 1-8.

Zhang Y, Huo M, Zhou J, Zou A, Li W, Yao C & Xie S (2011) DDSolver: An Add-In Program for Modeling and Comparison of Drug Dissolution Profiles. *American Association of Pharmaceutical Sciences PharmSciTech,* 12: 263-271.

APPENDIX A: RESEARCH OUTPUTS

A.1. ABSTRACT SUBMITTED AND ACCEPTED FOR ORAL PRESENTATION AT THE FIRST CONFERENCE OF BIOMEDICAL AND NATURAL SCIENCES AND THERAPEUTICS (CoBNeST)

Entry: Young scientist award: Basic Pharmacology

Venue: Spier Estate, Stellenbosch (7-10 October)

Development, optimisation and characterisation of miconazole nitrate-loaded solid lipid nanoparticles for vaginal muco-adhesion.

W.A Gwimo, G. Kilian, Y.E Kadernani

Department of Pharmacy, Faculty of Health Sciences, P.O. Box 77000, Nelson Mandela University, Port Elizabeth, 6031, RSA

Corresponding author: W.A Gwimo (s212243314@mandela.ac.za).

Abstract

Objective: To develop and optimize miconazole nitrate loaded solid lipid nanoparticles (MNZ-SLNs) for vaginal mucoadhesion, for the intended treatment of vulvovaginal candidiasis (VVC).

Methodology: MNZ-SLNs were developed by means of a novel low-temperature solidification and melt-emulsion ultrasonication method, a CCD was later employed for formulation optimisation. The resultant MNZ-SLN formulation was characterized for surface morphology, particle size, ZP and drug entrapment efficiency by means of TEM, PCS and high-performance liquid chromatography respectively. Finally, the optimal formulation was incorporated into a stimuli sensitive mucoadhesive hydrogel through the cold mechanical method of gel production. Which was characterized for anti-fungal activity, rheological and organoleptic properties.

Results: Response surface methodology statistical optimisation suggested that input variables of 4% m/v lipid concentration and 260.24 seconds sonication time would yield a stable formulation with high drug entrapment. Particle characteristics of the optimum formulation revealed a stable colloidal system with a mean particle size of 73.03 ± 0.78 nm and a high entrapment efficiency. The final formulation, which was comprised of

MNZ-SLN-loaded thermo-sensitive hydrogel displayed promising antifungal activity against *Candida albicans* species when compared to a commercially available cream. Further characterisation tests of the hydrogel displayed a sol/gel transition above 34°C with a modified drug release supported by the Korsmeyer-Peppas mathematical model.

Conclusion: A novel dosage form was developed with promising controlled release characteristics. Controlled release dosage forms assist in the promotion of patient compliance by decreasing the dosage requirements in the treatment of VVC.

Keywords: solid lipid nanoparticles, miconazole nitrate, mucoadhesive, thermo-sensitive hydrogels, controlled drug release.

A.2. ABSTRACT SUBMITTED AND ACCEPTED FOR POSTER PRESENTATION AT THE FIRST CONFERENCE OF BIOMEDICAL AND NATURAL SCIENCES AND THERAPEUTICS (CoBNeST)

Entry: Young scientist award: Basic Pharmacology

Venue: Spier Estate, Stellenbosch (7-10 October)

Development and validation of a RP-HPLC method for the quantification of miconazole nitrate in bulk or complex pharmaceutical products.

W.A Gwimo, G. Kilian, Y.E Kadernani

Department of Pharmacy, Faculty of Health Sciences, P.O. Box 77000, Nelson Mandela University, Port Elizabeth, 6031, RSA

Corresponding author: W.A Gwimo (s212243314@mandela.ac.za).

Abstract

Objective: To develop and validate a simple reverse phase high performance liquid chromatography (RP-HPLC) method for the quantification of miconazole nitrate (MNZ), a lipophilic antifungal drug, in pharmaceutical formulations.

Methodology: An isocratic RP-HPLC stability-indicating method was developed and optimised by means of an octyl (C_8) stationary phase with a mobile phase composition of methanol: water (85:15% v/v). Under the following chromatographic conditions, temperature of 40 °C, flow rate of 1ml/min and PDA detection of 234 nm.

Results: A linear calibration curve with a correlation co-efficient of 0.9998 was obtained within the working range of 0.125 to 1.00 mg/ml. The respective LoQ and LoD were 0.052 mg/ml and 0.015 mg/ml. Validation parameters were all deemed satisfactory for specificity, accuracy, precision and intermediate precision. Force degradation studies conducted under oxidative, hydrolytic, thermal and photolytic stress revealed MNZ was labile. Oxidative stress demonstrated the greatest degradation of 92.6% whilst thermal stress at 4°C facilitated the least degradation.

Conclusion: A simple, rapid and highly sensitive stability-indicating method was developed and validated for MNZ in bulk or complex pharmaceutical preparations.

Keywords: analytical method development, miconazole nitrate, high performance liquid chromatography, validation, force degradation studies.

APPENDIX B: LETTER FROM THE LANGUAGE PRACTITIONER

One Stop Solution
24 Firenze Gardens
Warbler Road
Cotswold Ext
Port Elizabeth
6045
www.onestopsolution.co.za

TO WHOM IT MAY CONCERN

I, Debby Dewes, declare that I have proofread and edited the language (spelling, grammar, punctuation, consistency) of the dissertation by:

WIMANA ALEXIS GWIMO

entitled:

DEVELOPMENT AND CHARACTERISATION OF MICONAZOLE NITRATE LOADED SOLID LIPID NANOPARTICLES FOR INCORPORATION INTO A VAGINAL MUCOADHESIVE SYSTEM

Submitted in fulfilment of the requirements for the degree of Master of Science in the Faculty of Health Sciences at the Nelson Mandela University.

I cannot guarantee that the changes that I have suggested have been implemented nor do I take responsibility for any other changes or additions that may have been made subsequently.

Any other queries related to the language and technical editing of this treatise may be directed to me at 076 481 8341.

Dated at Port Elizabeth on 24 November 2018

D.K. Dewes